# PERFORMANCE AND EMISSION CHARACTERISTICS OF

# A GAS-DIESEL ENGINE

by

YINCHU TAO

B. Eng., Jiangsu Institute of Technology (P. R. China), 1983

A THESIS SUBMITTED IN PARTIAL FULFILMENT OF

THE REQUIREMENTS FOR THE DEGREE OF

MASTER OF APPLIED SCIENCE

in

THE FACULTY OF GRADUATE STUDIES

Mechanical Engineering Department

We accept this thesis as conforming

to the required standard

THE UNIVERSITY OF BRITISH COLUMBIA

August 1993

In presenting this thesis in partial fulfilment of the requirements for an advanced degree at the University of British Columbia, I agree that the Library shall make it freely available for reference and study. I further agree that permission for extensive copying of this thesis for scholarly purposes may be granted by the head of my department or by his or her representatives. It is understood that copying or publication of this thesis for financial gain shall not be allowed without my written permission.

(Signature)

Department of _Mechanical Engineering_

The University of British Columbia
Vancouver, Canada

Date _August 23, 1993_

ABSTRACT

The performance and emission characteristics of high pressure injection of natural gas with liquid pilot-diesel fuel (ie. gas-diesel operation) was investigated in a single-cylinder, two-stroke compression-ignition engine with a poppet-valve gas-diesel injector.

The investigated injector geometries and engine operating parameters included: fuel injection angle, fuel jet interruption ratio, engine speed, load, beginning of injection timing, natural gas injection pressure, pilot-diesel to total-fuel energy ratio and pilot-diesel cetane number. These parameters were found to have very strong effects on thermal efficiency and exhaust emissions (ie. $NO_x$, THC, $CH_4$, CO, $CO_2$ and BOSCH smoke index). The thermal efficiency and exhaust emissions were determined as a function of load (ie. BMEP).

The thermal efficiency of the optimum gas-diesel operation was shown to exceed that of the conventional diesel operation at full load, but was lower at low load.

With this gas-diesel injector configuration, it was found that the pilot-diesel fuel was not mixed well enough to burn completely. A new gas-diesel injector designed to overcome this drawback is in process.

A three-zone combustion and exhaust emission analysis model was established to deduce ignition delay from cylinder pressure data with crank angle. At low loads, it was found that the ignition

delay of natural gas was excessive with very late burning and consequently low thermal efficiency. At high loads, the ignition delay of natural gas was considerably longer than that of diesel fuelling, but not so long as to affect the thermal efficiency.

The three-zone model was also used to deduce maximum burned-gas temperature. It was found that equilibrium NO concentration calculated from this temperature and cylinder pressure can be used to correlate the exhaust NO measured from engine exhaust pipe.

# TABLE OF CONTENTS

# LIST OF SYMBOLS

| | |
|---|---|
| A | area |
| $bs_e$ | brake specific emissions |
| B | diameter of the cylinder bore |
| BMEP | brake mean effective pressure |
| $c_1$ | constant |
| $c_2$ | constant |
| $c_3$ | constant |
| $c_4$ | constant |
| CFK | correction factor |
| $CH_{1.8}$ | diesel |
| $CH_2$ | diesel |
| $CH_4$ | methane (or natural gas) |
| $CH_y$ | combined fuel |
| CN62 | cetane number 62 diesel fuel |
| CO | carbon monoxide |
| $CO_2$ | carbon dioxide |
| $C_P$ | constant-pressure specific heat |
| $C_V$ | constant-volume specific heat |
| DF1 | diesel fuel grade 1 |
| DF2 | diesel fuel grade 2 |
| DP | degree of purity of the charge |
| E | total internal energy |
| $f_{corr}$ | power correction factor |
| f | molal fraction |

$F_{dw}$      conversion factor of dry-to-wet basis emissions

$F_G$      geometric function

$F_{res}$      residual molal (or mass)fraction

$F_\epsilon$      emissivity function

$F/A$      fuel-air ratio

$F/A_{CNG}$      CNG fuel-air ratio

$F/A_{DSL}$      diesel fuel-air ratio

h      specific enthalpy

H      specific humidity

         enthalpy of the system

HC      hydrocarbon

$H_2O$      water

k      specific heat ratio

         thermal conductivity

$K_{dw1}$      correction factor

$K_{dw2}$      correction factor

LHV      lower heating value

m      mass per cycle

$m_a$      mass of dry air

$m_{atrap}$      mass of air trapped in the cylinder

$m_{trap}$      mass of the cylinder contents at inlet port closure

$m_w$      mass of water vapour in air

$\dot{m}$      mass flow rate

$\dot{m}_i$      mass flow rate of emission component "i"

$\dot{m}_{fuel}$     total fuel mass flow rate

M         number of moles

$MW_i$      molecular weight of a component "i"

n         polytropic constant

$n_R$        number of crank revolutions for each power stroke per
          cylinder

$n_T$        total moles of the combustion products

N         speed

          number of moles

$N_2$        nitrogen

NMHC      non-methane hydrocarbon

NO        nitric oxide

$NO_2$       nitrogen dioxide

$NO_x$       nitrogen oxides

$O_2$        oxygen

$O_3$        ozone

OH        hydroxyl group

P         pressure

$P_a$        partial pressure of dry air

$P_b$        brake power

          barometric pressure

PM        particulate matter

Pr        Prandal number

$P_s$        saturated pressure of water vapour

$P_w$        partial pressure of water vapour in air

| | |
|---|---|
| q | heat transfer per unit mass |
| Q | heat transfer to the system |
| r | residual-air molal ratio |
| $r_m$ | pilot-diesel fuel to CNG fuel mass ratio |
| R | gas constant |
| $R_a$ | gas constant of dry air |
| Re | Reynolds number |
| $R_w$ | gas constant of water vapour |
| RFASTOIC | equivalent stoichiometric fuel-air ratio |
| t | time |
| $T_0$ | standard temperature |
| T | temperature |
| $T_b$ | engine torque |
| $T_d$ | dry bulb temperature |
| THC | total hydrocarbon |
| u | specific energy |
| U | internal energy of the system |
| UFRAT | unburned fuel mass ratio in exhaust |
| v | specific volume |
| V | volume |
| $V_d$ | cylinder displacement volume |
| $V_{pis}$ | piston velocity |
| W | work done on the piston |
| $W_c$ | engine shaft work per cycle |
| $x_1$ | burned-gas mass fraction |
| x | fuel mass-burned fraction |

$X_i$    molal fraction of a component "i" in exhaust emissions

$y$    atomic hydrogen to carbon ratio

$yCNG$    atomic hydrogen to carbon ratio of CNG

$Y_{DSL}$    atomic hydrogen to carbon ratio of diesel

$Y_i$    signal-output voltage of the span gas "i"

$Z_i$    concentration of the span gas "i"


Greek Letters:

$\gamma$    specific heat ratio

$\eta_b$    scavenged-blower efficiency

$\eta_{th}$    thermal efficiency

$\lambda$    relative air-fuel ratio

$\Lambda$    delivery ratio

$\mu$    dynamic viscosity

$\rho$    density

$\sigma$    Stefan-Boltzmann constant

$\phi$    relative humidity


Subscript:

abox    air box

air    trapped fresh air

AVG    average

bg    burned gas

bulk    bulk

charge    cylinder content at intake port closure

$CH_2$    diesel

$CH_4$     methane

$CH_y$     combined fuel

CNG     compressed natural gas

CO     carbon monoxide

$CO_2$     carbon dioxide

CONV     convection

dry     dry-basis data

DSL     diesel

exh     exhaust gas

EQUIL     equilibrium

fbmax     fuel burned at maximum temperature

fuel     fuel

HC     hydrocarbon

ipc     intake port closure

$N_2$     nitrogen

NMHC     non-methane hydrocarbon

NO     nitric oxide

$NO_x$     nitrogen oxides

$O_2$     oxygen

res     trapped residual gas

RAD     radiation

surf     surface

tot     total mass of the cylinder content

THC     total hydrocarbon

ub     unburned gas

uf     unburned fuel

WALL    wall

wet    wet-basis data


Abbreviations:

ABDC    after bottom dead centre

ATDC    after top dead centre

BDC    bottom dead centre

BOI    beginning of injection

BTDC    before top dead centre

CA    crank angle

CHEMI    chemiluminescence

CI    compression ignition

CNG    compression natural gas

EGR    exhaust gas recycling

EPA    environmental protection agency

FID    flame ionization detector

IPC    intake port closure

NDIR    non-dispersive infrared

ppm    parts per million

PW    pulse width of injection

RPM    revolution per minute

TDC    top dead centre

# LIST OF TABLES

LIST OF FIGURES

## ACKNOWLEDGEMENTS

# 1. INTRODUCTION

## 1.1 Introduction

One of the key symbols that represents human civilization is transportation. Our present transportation systems are mainly powered by internal combustion engines, which use petroleum-based liquid fuels. From the so-called "oil-crisis" of the 1970's, when crude oil supplies seemed to become uncertain and prices increased significantly, people realized that for energy security it was time to research and utilize alternative fuels. Since then many alternative fuel research projects have emerged, as well as many new theories and new techniques.

Exhaust emission control for environmental protection is the latest and the most important motivation which reinforces the necessity of alternative-fuel research and utilization. According to the "Journal of Air Pollution Control Association", automobile engine exhaust emissions contributed about 50% of pollutants from all air pollution sources from 1960's to 1980's in the United States (USA). This clearly indicates the importance of automobile engine exhaust emission control. [1]

## 1.2 The History of Federally Enacted Laws

From the beginning of this century, with the rapid increase in the number of automobiles, air quality declined and smog frequently occurred in large city such as Los Angeles, New York, Chicago,

Mexico City and Tokyo. Based on this situation, some governments and Congress began to establish national laws to protect the global environment. The following is a brief summary of the history of USA national air pollution control laws which relate to automobile exhaust emissions. [2]

The first air pollution control act was developed by the USA Congress in 1955 (Public Law 84-159, July 14,1955). It was narrow in scope and potential and did not regulate exhaust emissions of automobile IC engines. An important amendment to the 1955 act was passed by the USA Congress in 1960. In the face of worsening conditions in urban areas caused by mobile sources, Congress directed the Surgeon General to conduct a thorough study of the effects of motor vehicle exhaust emissions on human health.

The first Clean Air Act was passed by the USA Congress in 1963. Item 6 of this act, encouraged "efforts on the part of automotive companies and the fuel industries to prevent pollution". For the first time, this act provided for federal financial aid for research and technical assistance as well as a formal process for reviewing the status of the motor vehicle pollution problem.

The Motor Vehicle Air Pollution Control Act was passed by the USA Congress in 1965. This act formally recognized the technical and economic feasibility of setting automotive emission standards, and the national standards should be set for automotive emissions. Finally it stipulated that controls would be tightened as technological advances became available in conjunction with reasonable costs.

The Environmental Protection Agency (EPA) established in 1971 is a US national administrative agency which is responsible for implementing of the requirements of the Clean Air Act.

## 1.3   The Diesel Engine Exhaust Emission Problem

The most recent EPA Clean Air Act Amendments (CAAA) extend to 1998 and include the emission standards for urban bus heavy-duty engines shown in Table 1.1. In this table, $NO_x$ refers to oxides of nitrogen (NO or $NO_2$ expressed as NO equivalent), HC designates unburned non-methane hydrocarbon in gaseous form, CO denotes carbon monoxide, and PM denotes particulate matter.

Table 1.1: EPA CAAA Emission Standards for Urban Bus Engines.

------------------------------------------------------------------

URBAN BUS HEAVY-DUTY ENGINE EMISSION STANDARDS

(g/bhp-hr measured during EPA heavy-duty engine test)

| Year | $NO_x$ | HC | CO | PM |
|------|------|-----|------|------|
| 1990 | 6.0 | 1.3 | 15.5 | 0.60 |
| 1991 | 5.0 | 1.3 | 15.5 | 0.25 |
| 1993 | 5.0 | 1.3 | 15.5 | 0.10 |
| 1994 | 5.0 | 1.3 | 15.5 | 0.05 |
| 1998 | 4.0 | 1.3 | 15.5 | 0.05 |

------------------------------------------------------------------

With electronic controls, present production diesel engines can meet the restrictions of HC and CO on the 1993/94 EPA standards

when they operate with conventional liquid diesel fuel. But to meet the $NO_x$ and soot particulates standards is difficult, as shown in Figure 1.1.
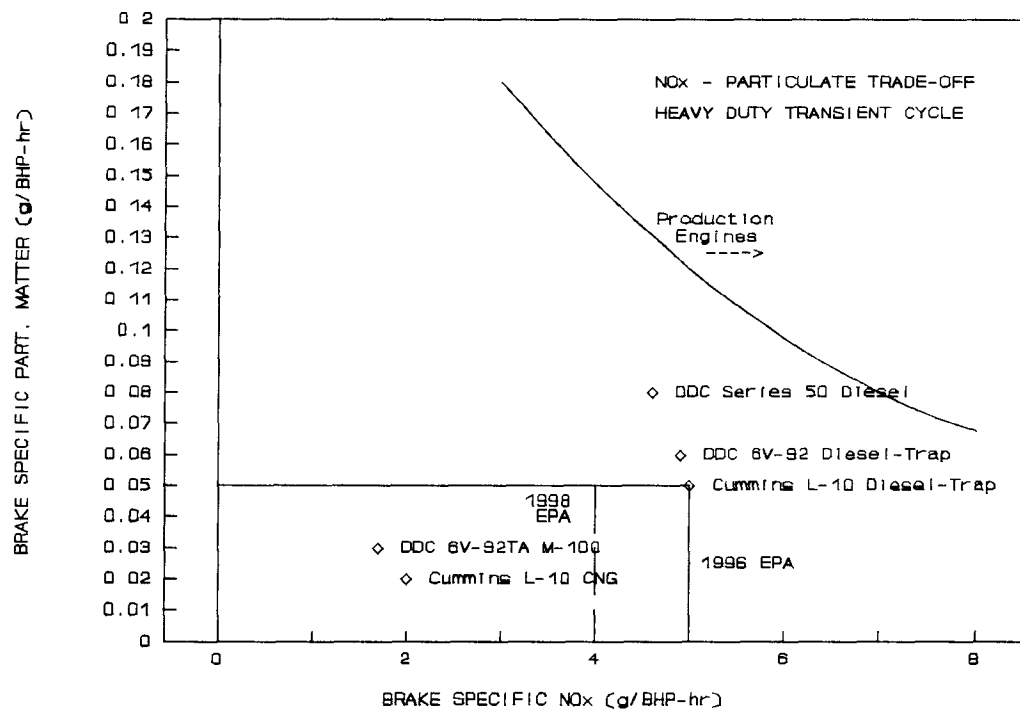


Figure 1.1: 1996 and 1998 EPA Standards as well as $NO_x$ and Soot Particulates Emission Level of Present Engines.

Figure 1.1 shows how far the 1996 and 1998 EPA standards for $NO_x$ and soot particulates are below the $NO_x$ and particulates emission ranges of the most production engines. These are the major problems for diesel engines operating with conventional liquid diesel fuel. As shown, the $NO_x$ and soot particulates emissions of

DDC 6V-92 and Cummins L-10 diesel engines equipped with particulates trap are close to the 1996 EPA standards; the $NO_x$ and soot particulates emissions of methanol fuelled DDC 6V-92TA M-100 (compression-ignition engine) and CNG fuelled Cummins L-10 CNG (spark-ignition engine) meet the 1998 EPA standards.

In order to solve $NO_x$ and soot particulate emission problems while maintaining the high thermal efficiency of diesel engine operation, natural gas has been considered as an alternative fuel for engines. [3]

## 1.4 Natural Gas as an Alternative Fuel

Natural gas consists mainly of methane. The conclusions of previous research indicate that natural gas is a promising alternative fuel for internal combustion engines [4]. It produces less soot particulates and $NO_x$ emissions than conventional diesel liquid fuels and is thus considered to be a potentially clean burning fuel.

Because natural gas is already a widely utilized fuel in North America, existing natural gas extraction and processing techniques make it ready to use at low cost.

Natural gas has a high autoignition temperature [5]. Since it would not autoignite inside a diesel engine of the highest feasible compression ratio, a supplemental ignition device is needed to ignite the natural gas. In a compression ignition engine (ie. diesel engine), a quantity of liquid diesel fuel (called pilot-diesel fuel) can be injected with natural gas to provide

temperature high enough for subsequent autoignition of the natural gas. Thus a gas-diesel fuel injector and its electronic control module are needed to be designed to achieve this concept. Pilot-diesel fuel is defined as a small quantity of liquid diesel fuel injected with (or before) natural gas and burns before natural gas for heating the cylinder environment, thereby igniting the natural gas. The gas-diesel fuel injector is defined as an injector that can inject pilot-diesel and CNG fuels at a desired timing. A gas-diesel engine is defined as a compression-ignition engine operating with natural gas and pilot-diesel fuel.

## 1.5 Objectives of This Research

Based on environmental, economic and energy security concerns, the Alternative Fuels Laboratory of UBC is presently developing a gas-diesel injection system for gas-diesel engines. The objectives of my research are the following:

1. To investigate the influences of injector geometry and engine operating parameters on engine performance and exhaust emissions (ie. $NO_x$, HC, CO etc.).

2. To correlate engine experimental NO emission data with equilibrium calculations and results of numerical simulation of combustion.

3. To provide fundamental information to assist in the design of gas-diesel fuel injectors.

## 1.6 Method

The research program is mainly experimental, and utilizes an existing two-stroke diesel engine whose design is the characteristic of the engines most widely used for urban buses in North America. The engine is equipped with a dynamometer and instrumentation for processing the engine performance and emission measurements. A gas-diesel fuel injector with an electronic controller is supplied for fuelling the engine. The principal variables of concern are:

Injector geometrical parameters:

-- Fuel injection angles.

-- Fuel jet sheet configuration.

Engine operating parameters:

-- Engine load.

-- Engine speed.

-- Injection timing.

-- Compression natural gas (CNG) injection pressure.

-- Pilot-diesel/total fuel energy ratio.

-- Pilot-diesel cetane number.

The effects of these principal variables on the engine performance and emissions are investigated and discussed in the subsequent chapters.

# 2.  LITERATURE REVIEW

## 2.1  Introduction

A compression-ignition (CI) engine is defined as an engine in which the fuel is directly injected into the cylinder (or combustion chamber), and autoignites in compressed air. A diesel engine may be defined as a CI engine operating with liquid fuel. We may define a natural gas engine as a CI engine operating with natural gas fuel and a gas-diesel engine as a CI engine operating with natural gas and pilot-diesel fuels.

In this chapter, the combustion characteristics of natural gas and the methodology of gas-diesel engine operation are discussed first. This is followed by a review of the theory of pollutant formation in diesel engines. The final section describes previous experimental studies of exhaust emissions from compression-ignition engines.

## 2.2  Combustion Characteristics of Natural Gas

Methane (the main component of natural gas ) is the simplest and the most stable member of the hydrocarbon family of fuels. It is a potentially clean burning fuel which can provide superior exhaust emission characteristics under most operating conditions [6] [7] [8]. Exhaust emissions include soot, particulates and NO.

Previous experimental studies [9] [10] [11] [12] of the shock tube ignition of methane-ethane-air mixtures, and Westbrook and

Pitz's modelling study [13] of the autoignition of premixed natural gas at typical compression-ignition (CI) engine condition (10-30 atm, 1000-1100 K) have shown that fuel composition and gas/environment temperature are the most important parameters affecting the autoignition delay time; the initial environmental pressure is less important. The autoignition delay time of the fuel can be considered an index to indicate ignitability of the fuel. An acceptable value for liquid diesel fuel used in a diesel engine is about 2 milliseconds, which corresponds to 12 crank angle degrees at 1000 rpm.

The low pressures (typically 1-4 atm) and high temperatures (1300-2100 K) of shock tube data may not be representative of CI engine environments, and Westbrook and Pitz's premixed natural gas autoignition may differ from the diffusion mixing in CI engines. However, the conclusions drawn from the above studies are consistent with recent results of Fraser, Siebers and Edwards [5] who studied the autoignition delay time characteristics of direct-injected methane and natural gas under simulated CI engine condition (5-55 atm, 600-1700 K). They found that a compression temperature of between 1200 to 1300 K is needed to operate a CI engine with natural gas (ie. achieve autoignition delay time less than 2 ms) in the absence of a supplementary ignition source and without a chemical ignition improver. This implies that in a naturally aspirated CI engine with a bottom-dead-centre (BDC) temperature of 325 K and pressure 1 atm, the compression ratio required to reach the 1250 K top-dead-centre (TDC) temperature

isentropically would be in excess of 29:1. In contrast, about 800 K (compression ratio of 10:1) is needed to autoignite cetane in 2 ms [14].

The reason for the methane having such high autoignition temperature is that the first-broken C-H bond in methane needs more energy than the others and certainly more than the C-H bonds in longer-chain hydrocarbons [15].

In order to convert diesel engines into natural gas engines, several methods have been proposed to raise the end-of-compression temperature. The first method is to raise the compression ratio over 29:1; but this is impractical because of design difficulties (for example, the minimum clearance for valve lift, and the mechanical loading associated with higher cylinder pressure). The second method is to supercharge the intake air or to recirculate part of the exhaust gas. The third method is to use a supplemental ignition source.

There are two supplemental ignition methods recommended by previous work [4]: spark ignition and pilot-diesel-fuel-injection ignition. If the gas and air are mixed before entering the engine, the spark-ignition method (with throttling to control the fuel-air ratio) is more suitable than the pilot-diesel-fuel method. This is because the air-fuel mixture is uniform inside the cylinder and can be ignited easily with a spark plug (regardless of the location) if the spark timing can be controlled closely. The thermal efficiency however, is lower because of the requirement to reduce compression ratio to avoid compression knock, and because of throttling losses.

Pilot-diesel-fuel-injection ignition is used together with direct injection of high pressure natural gas into the cylinder, as discussed by Beck [16]. This will be discussed in the next section.

## 2.3  Gas-Diesel Engine Operation

There are three main approaches for utilizing natural gas in gas-diesel engines. They are natural fumigation method, timed-port injection method, and direct-injection method (ie. direct injection of high pressure natural gas into the cylinder). The schematics of these three methods are shown in Figure 2.1. Natural fumigation is the original method to utilize natural gas fuel, and direct injection is the latest method.

Natural Fumigation Method:

A schematic of the natural fumigation method is shown in Figure 2.1 (A). Natural gas as the main fuel is injected into the air-gas mixer upstream of the inlet manifold. In the mixer and the manifold, the incoming air and the natural gas are premixed. Then the premixture is introduced into the cylinder of the gas-diesel engine. A throttle is placed upstream of the mixer to control the air-fuel ratio of the mixture according to the load. A certain amount of pilot-diesel fuel is injected into the cylinder to initiate combustion of the natural gas.

Detailed experimental investigations of the characteristics of gas-diesel operation with the natural fumigation method have been made by Simonson [17], Moore and Mitchell [18] in a single-
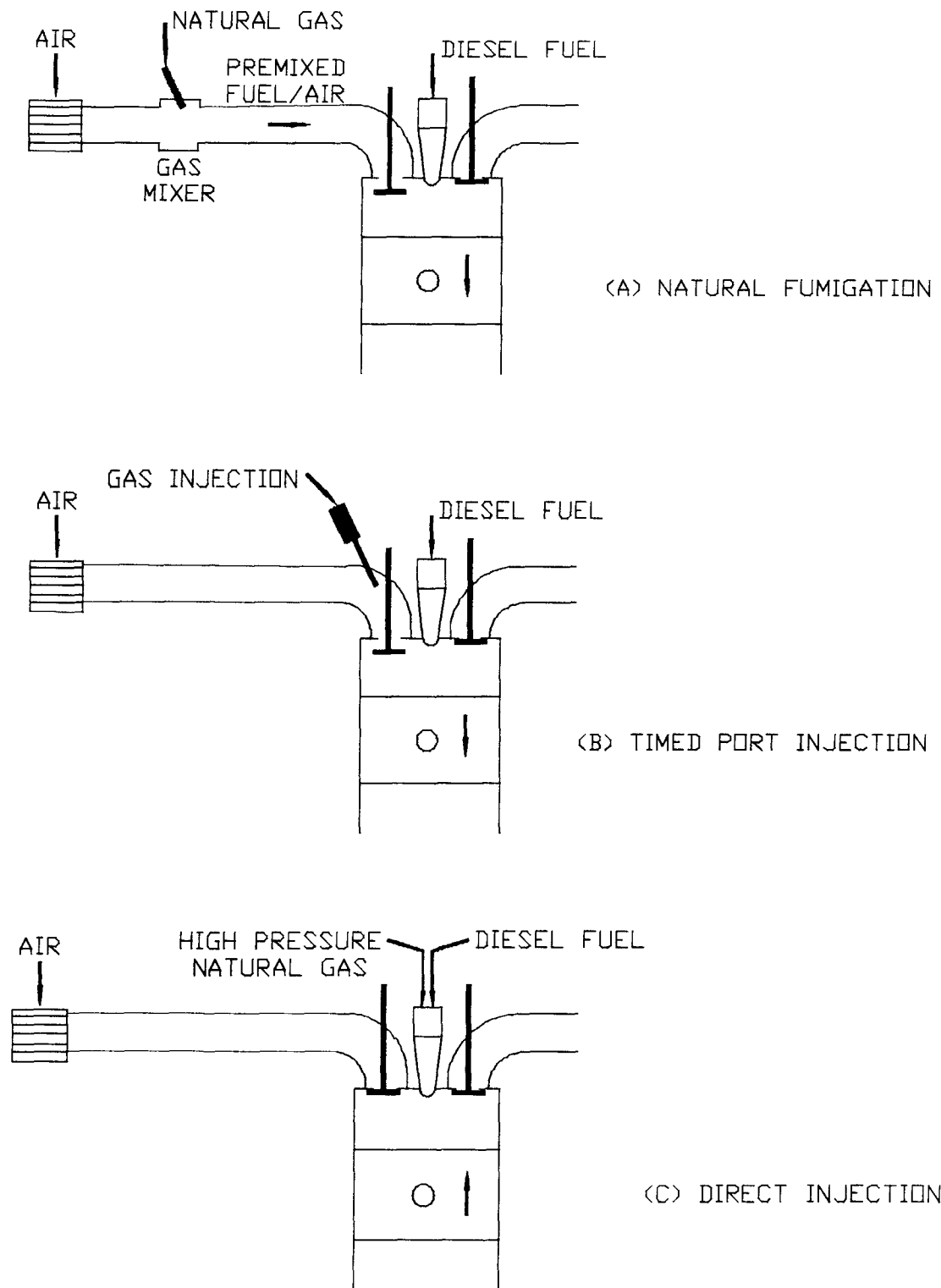
Figure 2.1: Methods of Using Natural Gas in Gas-Diesel Engine.

cylinder compression ignition engine with natural aspiration, and later by Wong [19] in a twelve-cylinder two-stroke diesel engine (Detroit Diesel 12V-149T) as well as by Ding and Hill [20] in a four-cylinder pre-chamber turbocharged diesel engine (Caterpillar 3304). One of the main findings of these studies is that gas engines using natural gas premixed with intake air (natural fumigation method) have lower engine thermal efficiency than that of straight diesel operation, especially at part load. This is caused by throttling losses or poor combustion of the fuel.

Although this method has poor part-load performance, it is still used in stationary and mining engines for driving power generators, compressors and pumps. In these applications, however, the engines are usually operated at full-load and constant speed with fully opened throttle.

Timed-Port Injection Method:

A schematic of the timed-port injection method is shown in Figure 2.1 (B); the natural gas injector in this method is set at the inlet manifold close to the intake valve. Low-pressure natural gas is injected into the inlet manifold a short time before the intake valve closes. A throttling valve may be placed upstream of the inlet manifold to restrict the air entry for controlling air-fuel ratio. A certain amount of diesel fuel is injected directly into the cylinder to initiate combustion of the natural gas.

In order to achieve the same thermal efficiency with diesel operation as with gas-diesel operation, Beck and Johnson used the

timed-port injection method on a OM-352 engine [16] and a Belarus D-144 diesel engine (for truck and bus applications) [21]. Theoretically, partial stratification of the gas-air mixture may improve the part-load thermal efficiency. But experimental results indicate that the timed-port injection method does not fully overcome the disadvantages of the natural fumigation method. One of the reasons might be that, within the time period from the gas injection to the beginning of combustion, the mixing is such that the advantages of stratified charge are lost.

Direct Injection Method:

Figure 2.1 (C) shows the schematic of the direct injection method. A gas-diesel fuel injector replaces the conventional diesel injector. Pilot diesel is injected into the cylinder with (or before) high pressure natural gas (CNG). The combustion of pilot diesel raises the local temperature high enough to ignite the natural gas. The appropriate relative injection timing of pilot diesel and natural gas, however, still needs to be determined experimentally. The gas-diesel fuel injector is the key element for this method.

Miyake and his coworkers [22] have successfully studied the fundamental behaviour of the high pressure gas spray jet and found that it is similar to the liquid fuel (ie. diesel) spray jet. They also found that the higher the natural gas injection pressure, the higher the indicated thermal efficiency. A combined gas-diesel fuel injector was designed by Miyake and his coworkers [23]. They used

a pilot-diesel fuel supply system to control the injection timing and duration of natural gas. A medium speed large marine diesel engine (L35MC engine) was converted into a gas-diesel engine to perform the test. Their experimental results show that direct injection of natural gas with pilot diesel quantities as low as 5% can be achieved while high thermal efficiency and low emissions can be obtained.

Similar work has been done by Wakenell, O'Neal and Baker on a two-stroke medium-speed locomotive diesel engine. They found that the pilot diesel fuel quantities can be reduced to 1.8% without knock and that a low emission level can be achieved while keeping good thermal efficiency [24].

A comparison study has been conducted by Lom and Ly [25] on a DDC 8V92TA engine. Three methods were evaluated: 1) post-pilot in-cylinder injection; 2) early in-cylinder injection; 3) timed-port injection. The post-pilot in-cylinder injection method is the same as the direct injection method, but the natural gas is controlled to inject after the pilot diesel. The early in-cylinder injection method is to inject natural gas into the cylinder just after exhaust valve closure. In principle, this is similar to the natural fumigation method. Experimental results indicated that the post-pilot in-cylinder injection method (ie. direct inject method) is potentially the best method for fuelling the engine with natural gas. It can rival the diesel operation in all aspects of efficiency, peak pressure and cylinder pressure rate of increase and also match closely the diesel operation on HC emission.

As concluded by Beck [16], the direct injection method has the following advantages:

1.  Uses basic diesel cycle with compression ignition of pilot fuel followed by high pressure gas injection.

2.  No detonation limit if gas injection is simultaneous with liquid fuel pilot injection.

3.  Unthrottled.

4.  Lean burn, requiring no mixture ratio control.

5.  Diesel cycle efficiency.

## 2.4  Pollutant Formation in Diesel Engines

Oxides of nitrogen (nitric oxide, NO, and small amounts of nitrogen dioxide, $NO_2$, collectively known as $NO_x$), carbon monoxide (CO), unburned or partially burned hydrocarbons (HC) and particulates are the main pollutants from the exhaust gas of the internal combustion engine.

In the diesel engine, the fuel is injected into the cylinder just before combustion starts, so throughout most of the burning period the fuel distribution is nonuniform. The pollutant formation processes are strongly dependent on fuel distribution and how that distribution changes with time due to mixing as well as combustion temperature. The mechanisms of the formation of the above pollutant species can be explained as following [26].

Nitric Oxide (NO):

Because NO and $NO_2$ are usually grouped together as $NO_x$

emission, NO is the predominant oxide of nitrogen produced inside an engine cylinder, so only NO formation will be discussed in this subsection.

In principle, the formation and destruction processes of NO are not part of the fuel combustion process, but they take place in an environment created by the combustion reactions. NO forms throughout the high-temperature burned gases behind the flame through chemical reactions involving nitrogen and oxygen atoms and molecules, which may not attain chemical equilibrium. The principal chemical reaction equations are the following:

$$O+N_2=NO+N$$
$$N+O_2=NO+O \qquad\qquad (2.1)$$
$$N+OH=NO+H$$

Starting from these three equations, the initial NO formation rate can be derived and expressed by the following formula (referring to Appendix A and [27] for the detailed derivation of initial NO formation rate):

$$\frac{d[NO]}{dt}=\frac{6\times10^{16}}{T^{1/2}}\exp(\frac{-69,090}{T})\,[O_2]_e^{1/2}\,[N_2]_e \qquad\qquad (2.2)$$

where the unit of d[NO]/dt is mol/cm$^3$s and [ ]$_e$ denotes the equilibrium concentration. From the exponential term of this formula, we see that the NO formation rate has very strong dependence on temperature.

As described by Heywood [26], the NO formation process in the cylinder is as follows. When the burned gas temperature inside the

engine cylinder increases during the combustion reaction, the NO formation rate stays at a low level until the temperature reaches a threshold value. Above the threshold temperature, the NO formation rate increases sharply with temperature. Also, the formation rates are highest in the regions close to stoichiometric. Then, as the burned gas cools during the expansion stroke, the NO reaction suddenly freezes (ie. both forward and backward reactions freeze). It leaves the NO concentration at a level that is much higher than the level corresponding to equilibrium at exhaust condition.

As shown in Eq. (2.2), the concentrations of $O_2$ and $N_2$ also affect the NO formation rate (ie. reducing air concentration in the cylinder will also decrease the NO formation rate). This indicates that exhaust gas recycling (EGR) and residual gas kept in the cylinder are the methods to reduce NO formation.


Soot and Particulates:

Diesel particulates consist principally of combustion generated soot on which some organic compounds are absorbed. Most particulate material result from incomplete combustion of fuel hydrocarbons; some result from burning the lubricating oil.

The results of fundamental studies of soot formation in simple premixed and diffusion flames, stirred reactors, shock tubes and constant-volume combustion bombs are available in a recent review [28]. As quoted by Heywood [26], soot particles form primarily from carbon in diesel fuel ($C_{12}H_{26}$). The formation process starts with a

fuel molecule containing 12 to 22 carbon atoms and an H/C ratio of approximately 2, and ends with particles typically a few hundred nanometres in diameter, composed of spherules 20 to 30 nm in diameter, each containing about 105 carbon atoms and having an H/C ratio of about 0.1. Although the results of these fundamental studies of soot formation may not fully apply to the diesel engine environment (which has high gas temperatures and pressures, complex fuel composition, and turbulent mixing), they imply that natural gas fuel jets ($CH_4$) will likely form much less soot than diesel fuel sprays.

Experimental studies of the soot formation in diesel engines have been conducted by Whitehouse and his coworkers [29] on a large direct-injection engine (30.5 cm bore and 38.1 cm stroke), by Aoyagi and his coworkers [30] on a small direct-injection engine with swirl, as well as by Duggal and his coworkers [31] on a IDI swirl chamber engine. They found that soot forms in the rich unburned core of a fuel spray at high temperature and in low oxygen concentration. In such regions, the fuel (including unvaporized liquid diesel droplets and diesel vapour) is heated by burned gas but with insufficient oxygen to oxidize it. Therefore, pyrolysis of the fuel takes place, and thereby soot is produced. As the soot contacts oxygen in the flame zone, it is then oxidized. Approximately 90% of soot is oxidized before exhaust [26]. Swirl speeds soot mixing with air and tends to reduce soot concentration [30].

## Gaseous Hydrocarbons (HC):

Gaseous hydrocarbons (HC) originate mainly from incomplete combustion of fuel. Fuel that vaporizes from the nozzle sac volume during the later stages of combustion is also a source of HC [26].

After injection into a cylinder in the diesel engine, some of the fuel will have rapidly mixed with air to equivalence ratios lower than the lean limit of combustion (called locally over-lean mixture); some will be within the combustible range; and some will have mixed more slowly and be too rich to burn (called locally over-rich mixture). Slow reaction of the mixture, or even no autoignition and no flame propagation, caused by locally overlean or overrich mixtures is one source of the HC emissions. The overrich mixture may burn later by mixing with air or already-burned gases within the time available before rapid expansion and cooling occurs. The overlean mixture can be oxidized only by relatively slow thermal-oxidation reactions which are incomplete, and is believed to be an important part of HC emissions.

At the end of the fuel-injection process, the injector sac volume (the small volume left in the tip of the injector after the needle seats) is filled with fuel. As the combustion and expansion processes proceed, this fuel is heated and vaporized, and enters the cylinder at low velocity through the nozzle holes. This fuel vapour mixes relatively slowly with air and may escape the primary combustion process, thereby becoming another source of HC emissions.

Carbon Monoxide (CO):

Carbon monoxide (CO) also forms during the fuel combustion process, depending on the fuel/air equivalence ratio. Usually CO forms in the locally fuel-rich mixture regions because of insufficient oxygen to oxidize all the carbon atoms in the fuel to $CO_2$. High-temperature dissociation is another source of CO emission. Diesel engines, however, always operate well on the lean fuel-air mixture side of stoichiometric, so diesel engine CO emission is generally insufficient to be significant [26].

## 2.5 Exhaust Emission Studies in Compression-ignition (CI) Engines

For diesel engines, one of the main concerns is NO (or $NO_x$) emission. It is well established in theory that NO is frozen at equilibrium levels corresponding to the local maximum flame temperature. This indicates that a reduction in maximum flame temperature will reduce the NO formation.

Emission Studies in the Diesel Engines:

An experimental investigation was made by Torpey, Whitehead and Wright [32] on both direct-injection (DI) and swirl-chamber (IDI) versions of the engine (Ricardo E16 single-cylinder research engine with 140-mm stroke and 121-mm bore). The purpose of their work was to study the effects of injection timing, exhaust recirculation (hot and cold), water injection into the inlet manifold, compression ratios, and combustion chamber configurations

on exhaust emissions ($NO_x$, HC and CO). Their major findings are as follows:

1.  Retarding the injection timing from optimum performance injection timing significantly reduces the NO emission (with a decrease of 55% at 8° retard), while neither HC nor CO emission show any significant changes. But, the thermal efficiency suffers.

2.  Recycling of 15% cold exhaust gases (to constitute 15% of the intake charge) reduces NO in half with 10% power penalty. 10% hot gas recycling reduces NO by 25% with 10% power loss.

3.  Inducing water into the intake system reduce NO by half with little effect on performance.

4.  Redesigning the combustion chamber and varying the compression ratio have very little effect on emissions.

A similar study was made by Khan and Wang [33] on a DI diesel engine. Their results confirm that retarding injection timing can cause a significant reduction in NO emission. They also found that an increase in the rate of injection or air swirl reduces the exhaust smoke emission.

Herzog, Burgler and Winklhofer [34] suggested that controlling in-cylinder $NO_x$ formation requires the control of both the mixing and the combustion process with respect to local oxygen-nitrogen concentrations, local temperature, and their temporal development. Their latest experimental investigations were focused on the following aspects:

1.  In-cylinder charge conditions (charge temperature, pressure

and rotation).

2. Fuel injection system parameters.

3. Exhaust gas recirculation (cooled and uncooled EGR).

4. fuel formulation.

Their conclusion is, in order to meet US 1998 (49 states) HD/MD Standard (ie. EPA 1998 Heavy-Duty/Medium-Duty Diesel Engine Emission Regulations); CAL 1995 MD-TLEV Standard (California 1995 Medium-Duty, Transitional-Low-Emission Vehicle Emission Regulations); and CAL 1998 MD-LEV/MD-ULEV Standard (California 1998 Medium-Duty Low-Emission Vehicle/Medium-Duty Ultra-Low-Emission Vehicle Emission Regulations), optimized combustion system and reformulated fuels with higher cetane-numbers have to be used as well as additional elements such as EGR (uncooled or cooled), injection rate control, and DENO$_x$-catalyst have to be added.

## Emission Studies in Gas-Diesel Engines:

An experimental study of the exhaust emission characteristics of gas-diesel operation with the natural fumigation method was made by Ding and Hill [20] in a four-cylinder pre-chamber turbocharged diesel engine (Caterpillar 3304). The variables of their study included pilot diesel fuel proportion, intake air restriction, engine speed, and pilot diesel injection timing. Their conclusions are as follows:

1. Generally speaking, gas-diesel operation (with natural fumigation) produces higher HC and CO emission than straight diesel operation, especially at low loads. This is caused by

poor combustion.

2.  At low loads, air restriction increases the mixture strength, leading to improvement of combustion and reduction of unburned hydrocarbon emission.

3.  Advancing injection timing at low loads can reduce HC emission with little influence on CO and $NO_x$ emissions. Retarding injection timing at high loads can reduce $NO_x$ emission to a great extent with little effect on HC emission.

Beck and Johnson [21] studied the exhaust emission characteristics of gas-diesel operation with the timed-port injection method. Their experimental results show that HC and $NO_x$ emissions with gas-diesel operation are higher than those with straight diesel operation.

A study by Lom and Ly [25] on a DDC 8V92TA engine, as mentioned before in this chapter, evaluated three methods: post-pilot in-cylinder injection, early in-cylinder injection and timed-port injection. Unfortunately, only HC emission was measured in this study. The results indicate that the potentially best method for fuelling an engine with natural gas is the post-pilot in-cylinder injection method. It can closely match the straight diesel operation on HC emission.

# 3. EXPERIMENTAL APPARATUS

## 3.1 Introduction

This chapter describes the experimental apparatus used in this research for this thesis. The test engine and its control and the data acquisition system are described first. followed by the specifications of the exhaust emission analysis systems.

Two exhaust emission analysis systems (EEAS), EEAS-A and EEAS-B will be explained in this chapter. EEAS-A was established in 1985 and was used until August, 1992. EEAS-B is an updated system. A description of both systems is necessary, because the experimental results discussed in subsequent chapters are acquired from these two systems.

## 3.2 Test Engine and Test Control System

A schematic diagram of experimental apparatus and instrumentation is shown on Figure 3.1. Intake air, compressed natural gas (CNG) and pilot diesel are measured and introduced into the fully instrumented test engine. Compressed natural gas and pilot diesel fuels are supplied by the natural gas and diesel fuelling systems which will be explained in Subsection 3.2.3. Figure 3.1 also shows that the water-brake dynamometer with speed and load sensors is used to measure torque. An exhaust emission analysis system and a BOSCH smoke sampling pump are connected to the engine exhaust pipe. The engine dynamometer control console is
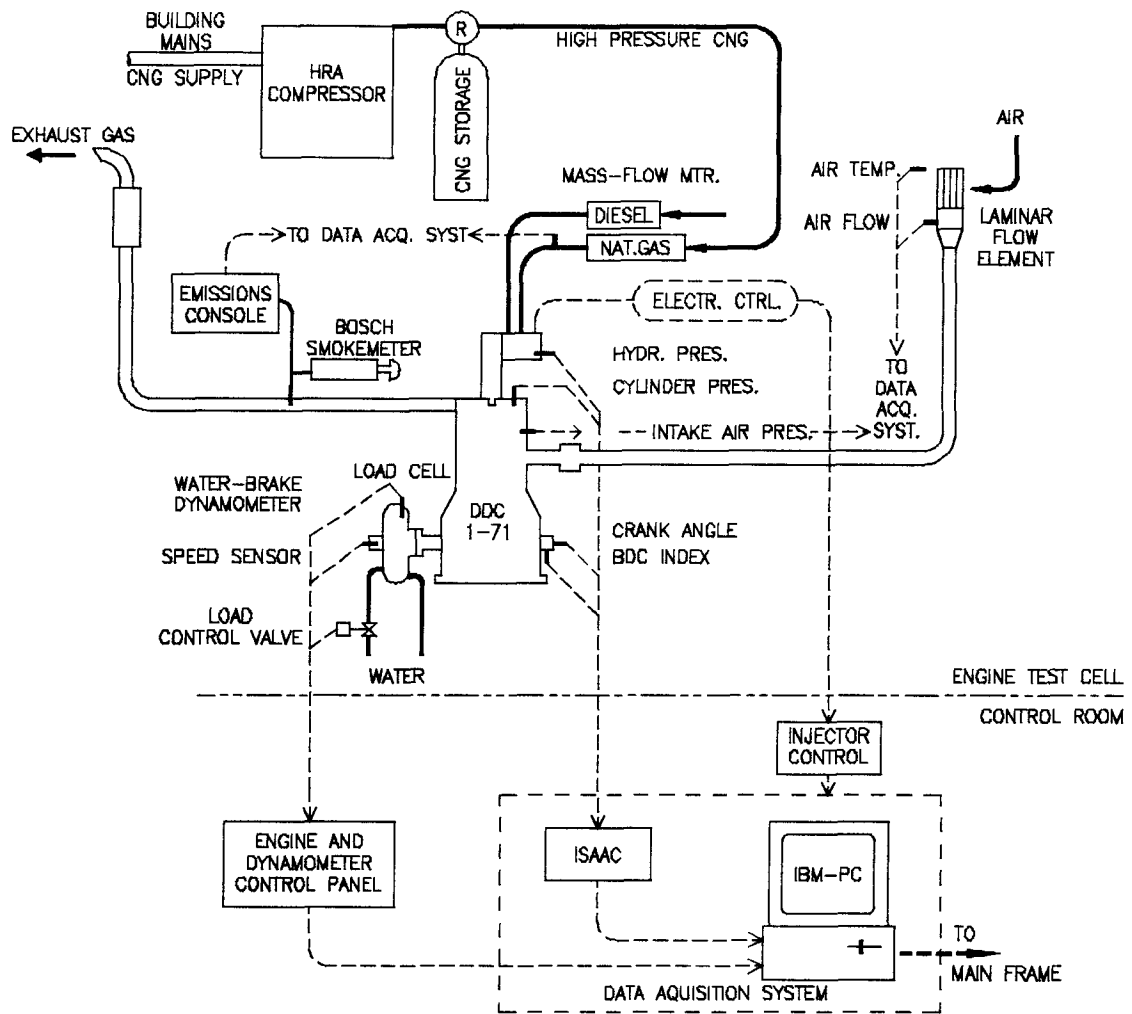
Figure 3.1: Schematic of Experimental Apparatus and
Instrumentation.

used to control engine operation. A PC-based and monitored data
acquisition system is used to obtain and to record engine
performance, exhaust emission, and pressure data.

3.2.1  Test Engine

A Detroit Diesel Series 71 single-cylinder diesel engine was

Table 3.1: General Specifications of 1-71 Diesel Engine.

-----------------------------------------------------------------

Bore & Stroke:                    4.25 in.(108 mm) & 5.0 in.(127 mm)

Displacement:                     70.93 cu. in. (1.162 litres)

Compression ratio:                16 to 1

Maximum operating speed:          1600 RPM

Rated speed:                      1200 RPM

Idle speed:                       500 RPM

Rated output:                     10 kW

Maximum bmep (break mean

  effective pressure):            5 bar

Scavenging type:                  Uniflow

-----------------------------------------------------------------
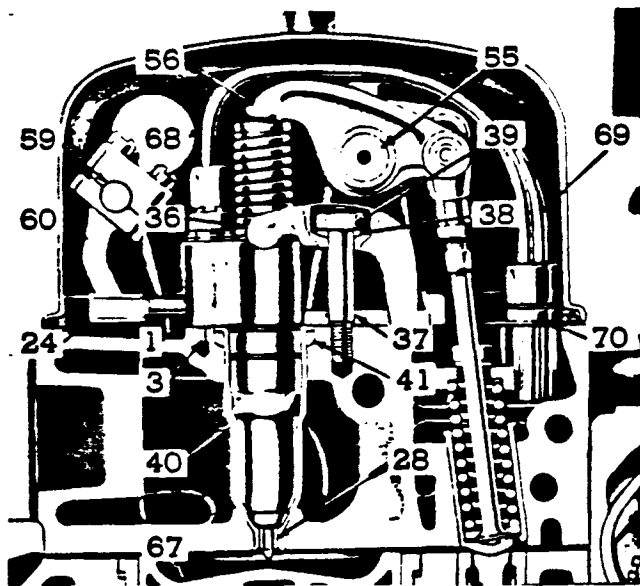


1. Injector-Fuel.
3. Pin-Dowel.
24. Rock-Control.
28. Tip-Spray.
36. Clamp-Injector.
37. Stud-Injector Clamp.
38. Washer.
39. Nut.
40. Tube-Injector.
41. Ring-Seal.
55. Shaft-Rocker.
56. Arm-Injector Rocker.
59. Shaft-Injector Control.
60. Lever-Rock Control.
67. Chamber-Combustion.
68. Pipe-Fuel Inlet.
69. Pipe-Fuel Outlet.
70. Connector-Fuel Pipe.

Figure 3.2: The Combustion Chamber Geometry and Injector
Mounting of the 1-71 Diesel Engine.

used of this study. This engine is a 71 cubic inch displacement, two-stroke, direct-injection diesel engine with forced air aspiration and scavenging by a blower. The engine specification characteristics are shown in Table 3.1.

Figure 3.2 shows the geometry of the combustion chamber and the injector mounting. A shallow bowl-shaped combustion chamber (67) was formed on the top of the piston. A mechanically-controlled fuel unit injector (1) was originally mounted on this engine, but it was replaced with an electronically-controlled unit injector to control the injection timing depending on the temperature, load, and speed [35] [36]. Electronic control was based on the Detroit Diesel Electronic Control Module (ECM) shown in Figure 3.4.
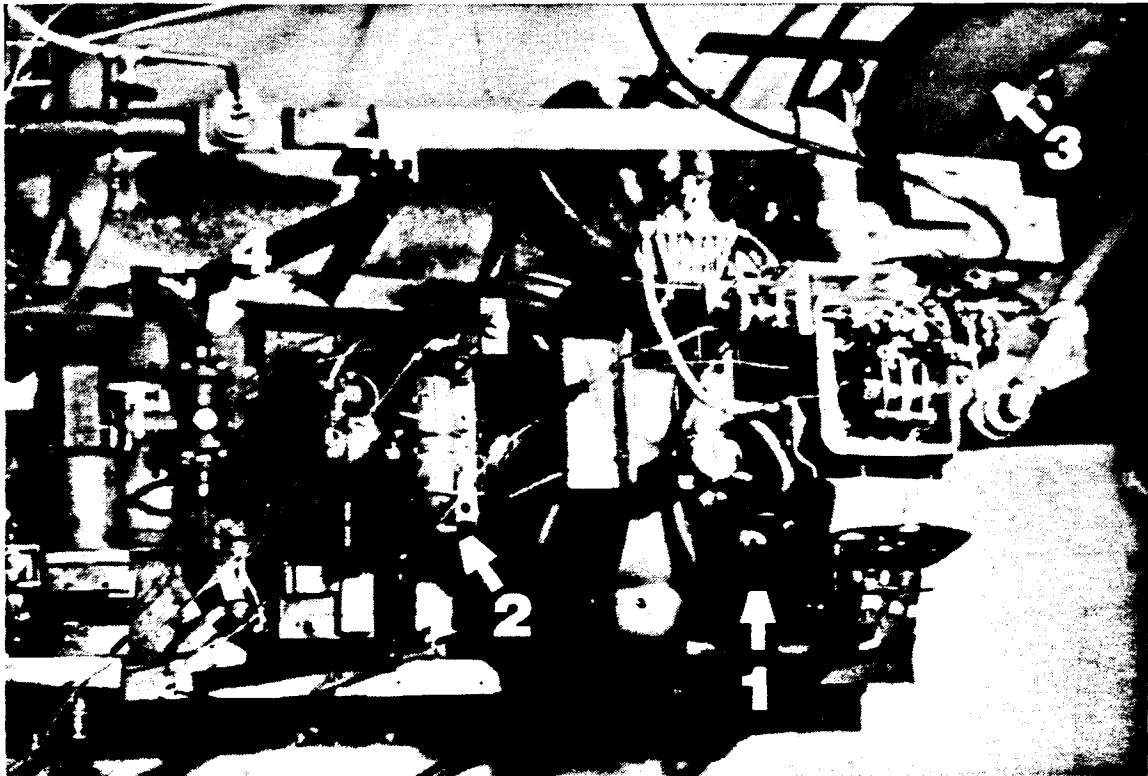


Figure 3.3: The Arrangement of the Test Engine Cell.
(1) Test Engine, (2) Dynamometer, (3) Cooling Tower.

## 3.2.2 Dynamometer, DCM and DDM

Figure 3.3 shows the arrangement of the test engine cell. The test engine (1) was coupled to a 600 hp water-brake dynamometer (2) (GO-Power Model DA-316) which converts the rotating engine torque to stationary torque that can be precisely measured. A cooling tower (3) has been installed to replace the radiator to control the engine cooling-water temperature.
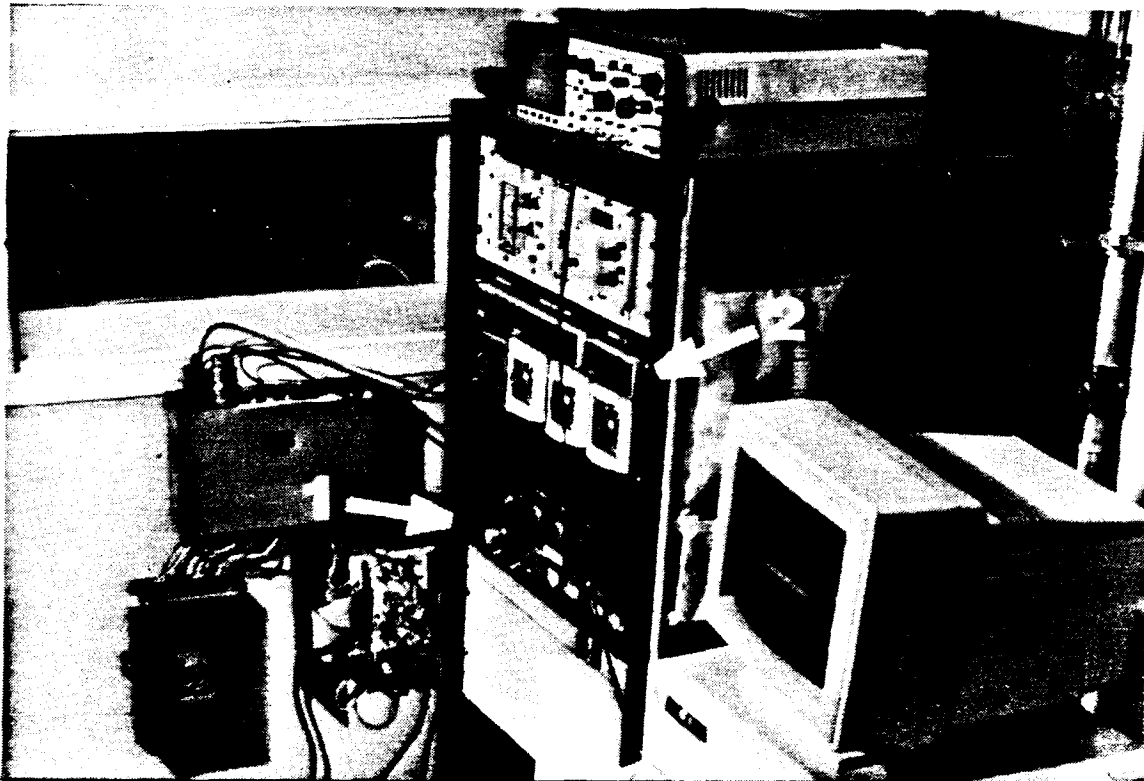


Figure 3.4: The Engine Control Console.
(1) Dynamometer Control Module (DCM), (2) Data Display Module (DDM), (3) Electronic Control Module (ECM).

As shown in Figure 3.4, a Dynamometer Control Module (DCM) (1) and a Data Display Module (DDM) (2) are both located on the engine control console in the control room. The engine speed and load, which are controlled through the throttle and load control dial on

the DCM front panel, are detected by the tachometer and the load cell, and then displayed on the DDM. The DDM also provides displays of engine cooling water temperature, lubrication oil temperature and pressure, and provides fault-mode automatic shutdown.

## 3.2.3 Engine Fuelling System
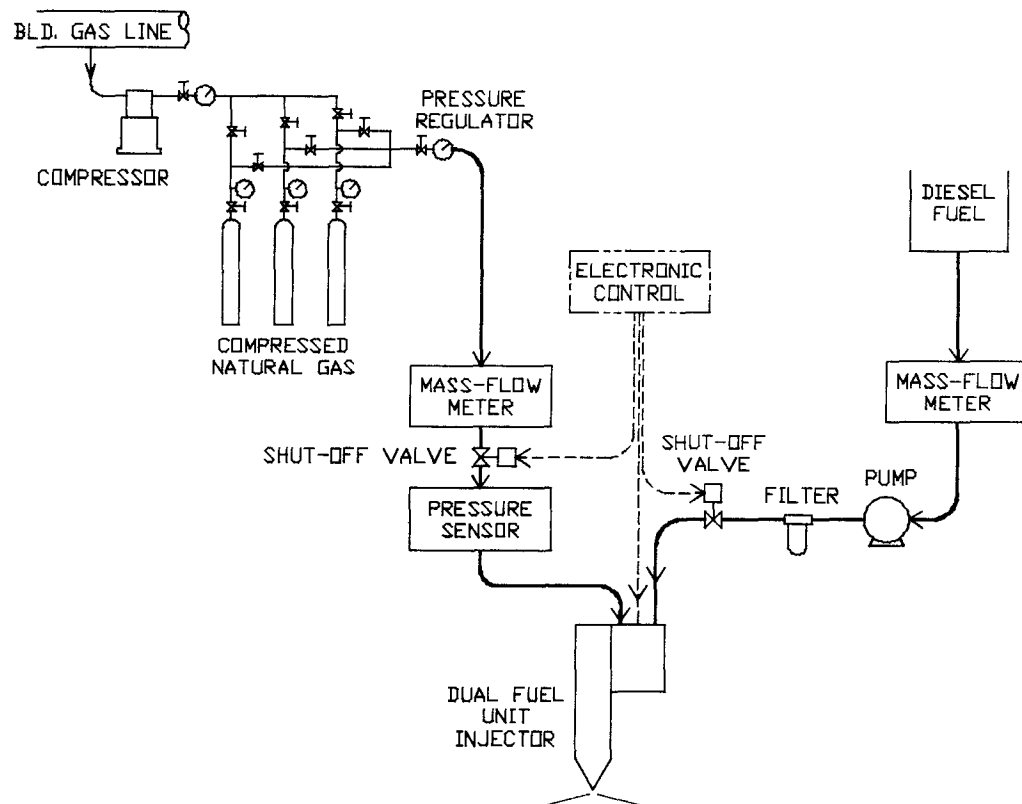


Figure 3.5: Schematic of Engine Fuelling System.

As natural gas (the principal fuel) has a high autoignition temperature, a small amount of pilot-diesel is injected into the cylinder to initiate the combustion of natural gas. Two independent fuel supply systems, for diesel and natural gas, were established to achieve gas-diesel operation. Figure 3.5 shows the schematic of

the engine fuelling system.

Diesel Fuelling System:

Commercial grade 1 and grade 2 diesel as well as cetane number 62 diesel were used in straight diesel operation. But only cetane number 62 diesel was used in gas-diesel operation because it has better ignition quality (ie. shorter ignition delay time) and is more effective than the others in igniting the natural gas. The properties of these diesel fuels are listed in Table 3.2.

Table 3.2: Properties of Diesel Fuels.

|  | Grade 1 (Shell) | Grade 2 (Chevron) | Cetane No.62 (Shell) |
|---|---|---|---|
| Higher Heating Value (kJ/kg): | 45,094 | 45,220 | 45,220 |
| Density (kg/m³): |  | 860 | 836 |
| Cetane Number: | ≈45 | ≈45 | 62.2 |

As shown in Figure 3.5, in the diesel fuelling system diesel flows by gravity from the fuel tank to the AVL730 Dynamic Fuel Meter (AVL). After leaving the AVL, the diesel is pumped to the inlet of the gas-diesel injector through the filter and the emergency shut-off valve. Then a small amount of returned diesel is sent back to the AVL directly from the outlet of the injector. With this closed-loop connection, the AVL can measure the net

consumption of diesel fuel.

## Natural Gas Fuelling System:

The natural gas obtained from B.C. GAS through the city gas pipe line was the main fuel. Table 3.3 shows the typical composition of B.C. natural gas, the properties of which are listed in Table 3.4.

Table 3.3: Composition of the B.C. Natural Gas.

----------------------------------------------------------------

| | |
|---|---|
| Methane ($CH_4$) | 95.50 (Volume %) |
| Ethane ($C_2H_6$) | 3.00 |
| Propane ($C_3H_8$) | 0.50 |
| Iso-Butane | 0.05 |
| N-Butane | 0.10 |
| Carbon Dioxide ($CO_2$) | 0.20 |
| Nitrogen ($N_2$) | 0.60 |
| Pentanes | 0.04 |
| Hexanes | 0.01 |

----------------------------------------------------------------

Figure 3.5 (page 30) shows that the commercial oil-free 4-cylinder 4-stage Residential Refuelling Appliance (RRA) is connected to the city gas pipe line. It compresses the natural gas from the pipe line pressure (5 psi) to about 3000 psi high pressure. The compressed natural gas (CNG) is stored in 3 gas

storage bottles.


Table 3.4: Properties of the B.C. Natural Gas.

```
----------------------------------------------------------------
Molecular Weight (kg/kmol):         16.689

Density (kg/m³):                    0.6903 (at 20°C, 101.325 Kpa)

                                    0.7023 (at 15°C, 101.325 Kpa)

Lower heating value (kJ/kg):        49,098 (at 15°C, 101.325 kPa)
----------------------------------------------------------------
```


The mass-flow meter (Micro Motion Model DH012), the solenoid shut-off valve, and the pressure sensor are installed on the pipe line between the gas storage bottles and the gas inlet of the gas-diesel injector, as shown in Figure 3.5. A regulator unit is mounted directly on the outlet of gas storage bottle to adjust the CNG back pressure of the injector.

Both diesel and CNG shut-off valves are connected to DCM for fault-mode automatic shutdown.


Gas-Diesel Fuel Injection System:

This system consists mainly of a gas-diesel electronic unit injector (EUI) (ie. gas-diesel fuel injector) and a modified Electronic Control Module (ECM).

Figure 3.6 shows the schematic of the gas-diesel electronic unit injector. The gas-diesel fuel injector uses the hydraulic actuation of the original configuration of the Detroit Diesel EUI,
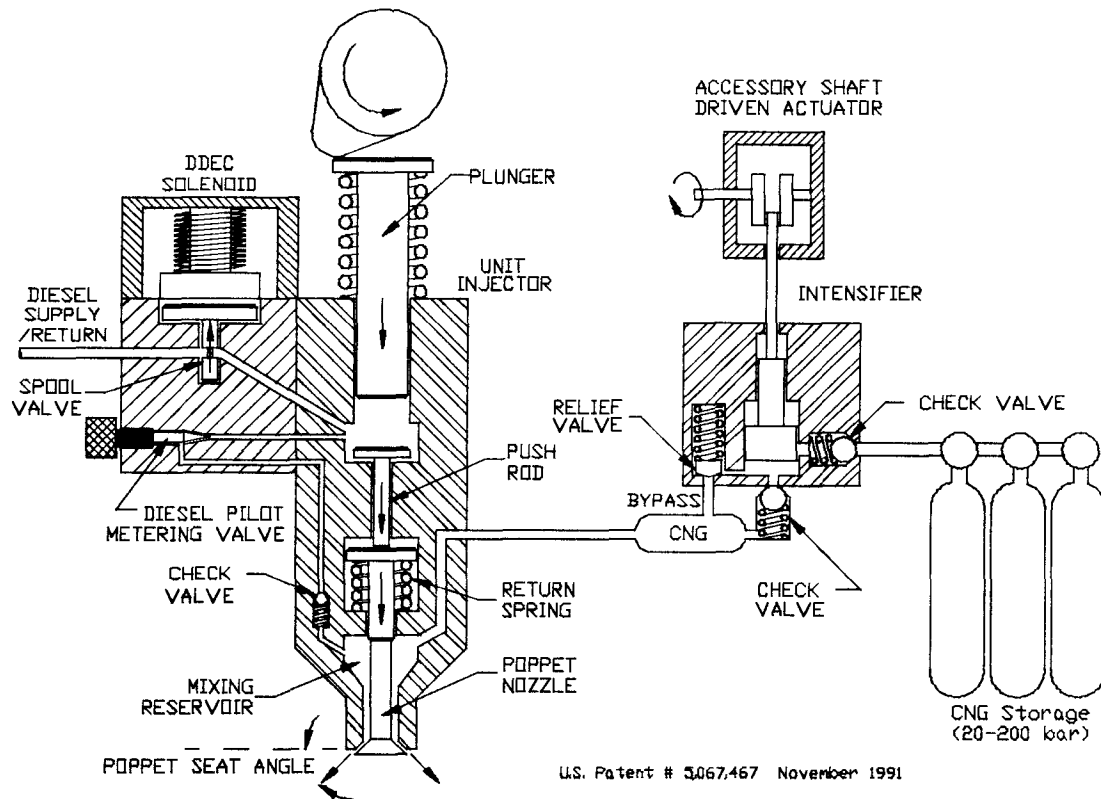
Figure 3.6: Schematic of Gas-Diesel Electronic Unit Injector.

which is the electronic solenoid valve controlling injection timing and the cam-driven, and the plunger-bush pressurized device. A CNG passage, a diesel hydraulic actuated poppet nozzle, a pressure check valve and a pilot-diesel metering valve were introduced to provide gas-diesel injection.

The modified ECM is used to control the beginning of injection (BOI) and the duration of injection (or pulse width, PW) of the gas-diesel injector through the solenoid valve. The BOI, the PW and the pilot-diesel metering valve opening (to control the amount of pilot diesel injected into the engine) can be set and adjusted from the front panel of the engine control console.

## 3.2.4 Engine Cooling System

To keep the engine operating at the same temperature so that reliable and repeatable performance and emission data can be obtained, a cooling tower was used (as shown in Figure 3.3, page 28). An thermostatic valve was installed at the water inlet of the cooling tower to keep the engine cooling water temperature between 80 and 95 °C and the lubrication oil temperature between 70 and 110 °C.

## 3.2.5 Instrumentation

Engine speed, torque, inlet air flow rate, CNG mass-flow rate and diesel mass-flow rate are the raw data which can be measured directly by the instruments and used to calculate the other engine performance data. The other raw data, such as intake temperature and pressure, ambient temperature and pressure as well as relative humidity, are measured for correcting engine performance data to standard ambient conditions. Cylinder pressure is measured for calculating the mass burned fraction and emission simulation computation. The following is the description of the instruments used to measure the raw data.

## Engine Speed:

A speed sensor mounted on the end of the dynamometer was used to measure the engine speed. This magnetic pickup type sensor consisted of a 60-tooth gear and magnetic pickup (sensor). This sensor assembly developed a frequency signal that was directly

proportional to RPM (ie. 1 RPM corresponds to 1 cycle per second). The frequency signals were displayed on the front panel of the engine control console (ie. on an digital instrument) as well as run through a digital-to-analog converter (DAC) and sent to the data acquisition system. This instrument was calibrated by a hand digital tachometer (Shimpo Model DT-205).

Torque:

A strain gauge load cell mounted on the trunnion support of the dynamometer was used to measure load (ie. rotating torque) applied on the engine. The low level analog load signals were amplified and sent to the data acquisition system as well as to the display of engine control console through a analog-to-digital converter (ADC). This instrument was calibrated by applying weights to the torque arm.

Flow Rate:

A laminar flow element (Meriam Instrument Model 50MC2) mounted after the air filter was used to measure air flow rate. Pressure drop across the element was transmitted by a transducer and then sent to the data acquisition system.

A mass-flow sensor (Micro Motion Model DH012) installed on the CNG intake line between the gas storage bottle and the inlet of the gas-diesel injector was used to measure the CNG mass flow rate. This instrument worked on the Coriolis acceleration principle. The signal from the mass-flow sensor was sent to the remote flow

transmitter (Micro Motion Model RFT9712) and converted to 4-20 mA current signal which was then sent to the data acquisition system. The mass-flow sensor, in conjunction with a remote flow transmitter, formed a complete mass flowmeter system.

An AVL 730 Dynamic Fuel Consumption Measuring Equipment was used to measure the diesel mass-flow rate. This instrument worked on a gravimetric measuring principle. The analog signal was sent to the data acquisition system and displayed on the evaluation module through an analog-to-digital converter (ADC).

## Ambient Conditions:

Ambient temperature, pressure, and relative humidity were read from the digital gauges and recorded manually. Ambient temperature and relative humidity were used to determine the humidity ratio. Humidity ratio and ambient pressure data were used by the data acquisition system to calculate the correction factor for engine performance data.

## Cylinder Pressure:

A PCB piezo-electric pressure transducer was installed in a sleeve in the cylinder head. The signal from the transducer was transmitted to a Model 5004 Kistler Charge Amplifier and then to the data acquisition system. A dead-weight tester was used to check the linear slope of the calibration and quality of the transducer.

## 3.2.6  Data Acquisition System
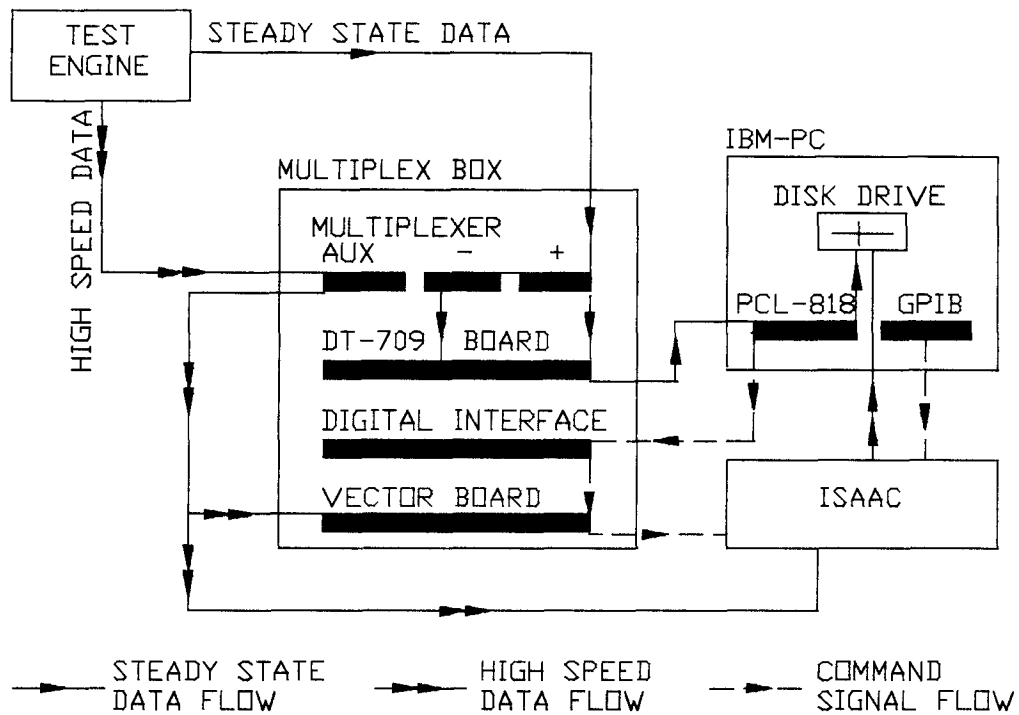


Figure 3.7: Schematic of Data Flow in Data Acquisition System.

An IBM-PC-based data acquisition system was used to acquire steady-state data and high-speed data from the test engine [37]. Table 3.5 lists the names of the steady-state data and high-speed data as well as their corresponding channel numbers. The data acquisition system consisted of hardware and software. Figure 3.7 shows the general diagram of the data flow in the data acquisition system.

The hardware of the data acquisition system included a multiplex box which functioned as a multiswitch, an IBM-PC and an ISAAC which functioned as a computer to acquire high speed pressure data. The multiplex box contained a multiplexer board, a screw terminal board (DT-709), a digital interface board and a vector

trigger board. The IBM-PC was equipped with a data acquisition board (PC Lab PCL-818) and a general purpose interface board (GPIB, IEEE-488).

Table 3.5: List of Steady State Data and High Speed Data.

---

| Name | Channel | Type |
| --- | --- | --- |
| Natural gas mass flow: | No. 0 | Steady state data |
| Beginning of injection: | No. 1 | Steady state data |
| Ambient temperature: | No. 2 | Steady state data |
| Pulse width: | No. 3 | Steady state data |
| Torque: | No. 4 | Steady state data |
| Speed: | No. 5 | Steady state data |
| Intake pressure: | No. 6 | Steady state data |
| Diesel mass flow: | No. 7 | Steady state data |
| Air flow (delta P): | No. 8 | Steady state data |
| Natural gas pressure: | No. 9 | Steady state data |
| $CH_4$ emission: | No. 10 | Steady state data |
| $O_2$ emission: | No. 11 | Steady state data |
| $CO_2$ emission: | No. 12 | Steady state data |
| CO emission: | No. 13 | Steady state data |
| Total HC emission: | No. 14 | Steady state data |
| $NO_x$ emission: | No. 15 | Steady state data |
| Crank angle & BDC index: | | High speed data |
| Cylinder pressure: | | High speed data |
| Injection hydraulic pressure: | | High speed data |

---

As shown in Figure 3.7, the steady-state-data analog signals (total 16 channels) are directed by the multiplexer to the DT-709 screw terminal board. From the board, the signals are sent to the PCL-818 data acquisition board in which they are converted from an analog voltage to a 12 bit digital number. The digital numbers are then saved on a specified floppy disk.

The high-speed data flow is more complicated than the steady-state data flow as one can see from Figure 3.7. When commanded to acquire high-speed data, the GPIB initiates the ISAAC and gives the command to take a specified number of data points, and the PCL-818 then sends a digital signal to the vector trigger board which prepares a trigger for the ISAAC to begin taking high-speed data. Using the next BDC signal as a trigger and the crank angle signal as an external clock, the ISAAC then starts taking data. After the completion of data taking, the ISAAC sends a signal to the GPIB that data acquisition is completed, and the data is transferred to the designated drive in binary form.

A menu-driven program, ENGDATA, controls the data acquisition system. It allows the user to tailor the data acquisition system to his specific needs. i.e. allows the building of configuration and calibration files, directs data flow, does calculations with data, converts binary pressure data to ASCII, and allows data to be saved to disk.

## 3.3 The Exhaust Emission Analysis System A, (EEAS-A)

The exhaust emission analysis system A (EEAS-A) was established in 1985 at the Alternative Fuels Laboratory of UBC [20]. The EEAS-A has a Model 951 Chemiluminescent $NO/NO_x$ Analyzer, a Model 400 Flame Ionization Detection (FID) Hydrocarbon Analyzer, and a Model 865 Non-Dispersive Infrared Analyzer (for CO). After the 1990 modification [38], a Model 880 Non-Dispersive Infrared Analyzer (for $CO_2$), a Model 1054 $O_2$ Analyzer and a sample-gas chiller were added into this system. This system was used until August, 1992. The Model 865 Non-Dispersive Infrared Analyzer (for CO), the Model 880 Non-Dispersive Infrared Analyzer (for $CO_2$) and the sample-gas chiller were re-equipped in EEAS-B.

### 3.3.1 Arrangement of the EEAS-A

Figure 3.8 shows the schematic diagram of the exhaust emission analysis system A (EEAS-A). The exhaust sample gas is taken by a sampling probe which is mounted downstream on the exhaust pipe about 2 meters away from engine exhaust manifold outlet flange. After entering the sampling line, the sample gas is pumped first through a coarse filter to eliminate soot and particulates, then through a chiller to remove water, and then through fine filters and a relief valve before separating into two tubes. In one tube, the sample gas goes directly to HC, CO, $CO_2$ and $O_2$ analyzers. In the other tube, the sample gas is heated and sent to the $NO_x$ analyzer. The flowmeter and valve after the analyzer are used to adjust the sample gas flow rate passing through the analyzer. Zero and span

SAMPLING PROBE

COARSE FILTER   PUMP   CHILLER (CONDENSER)   FINE FILTER   RELIFE VALVE   FINE FILTER HEATER

MAIN BYPASS

OUTLET

Model 400 HC Analyzer   Model 865 CO Analyzer   Model 880 CO2 Analyzer   Model 1054 O2 Analyzer   Model 951 NOx Analyzer

AIR   40% H2 + 60% He   CH4 (+N2)   N2   CO (+N2)   CO2 (+N2)   NO (+N2)   O2
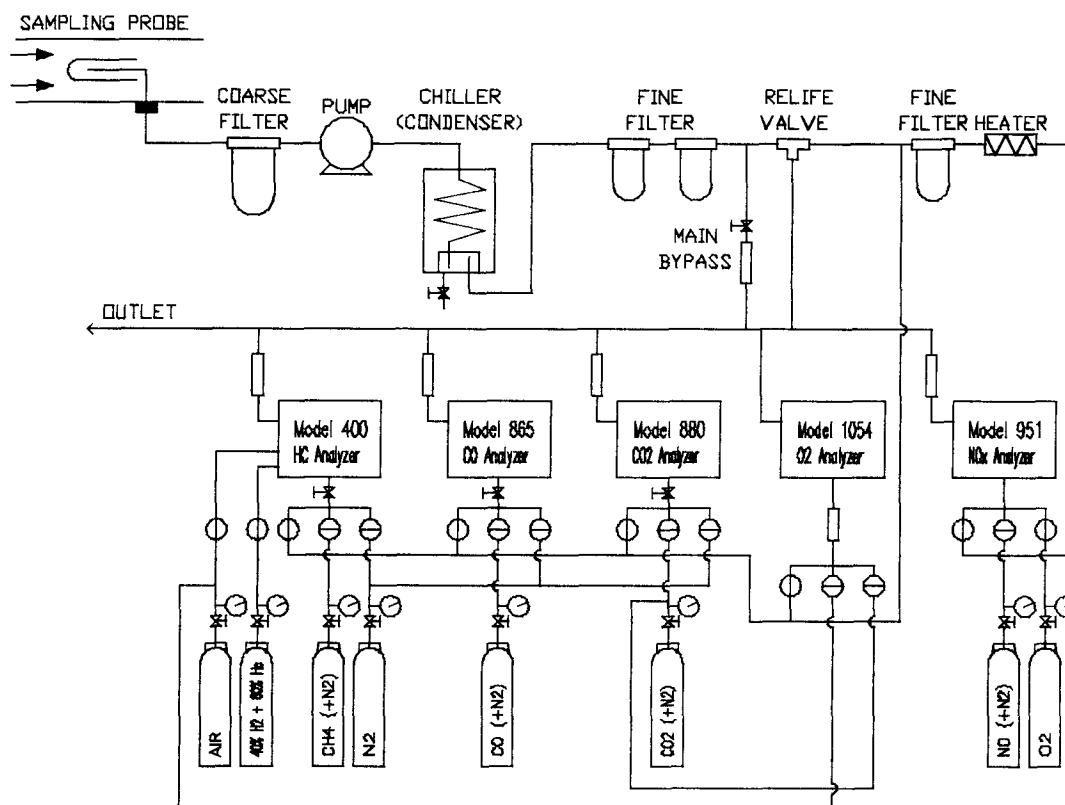
Figure 3.8: Schematic of Exhaust Emission Analysis System A.

gas cylinders are connected to the analyzer. Pressure regulators are used to set the right flow rate for zero and span gases flowing into the analyzer. Zero and span gases are used to calibrate the analyzer before tests. The best span gas concentration range is between 75% and 100% of full operating scale; the full operating scale is determined by maximum engine experimental emission data. The output signals from this system are sent to the data acquisition system and recorded on discs continuously by a IBM PC.

## 3.3.2  Principle of the Analyzers in the EEAS-A

The following summarizes the principles of the major analyzers which were in the EEAS-A.

Nitric Oxide Determination (Model 951):
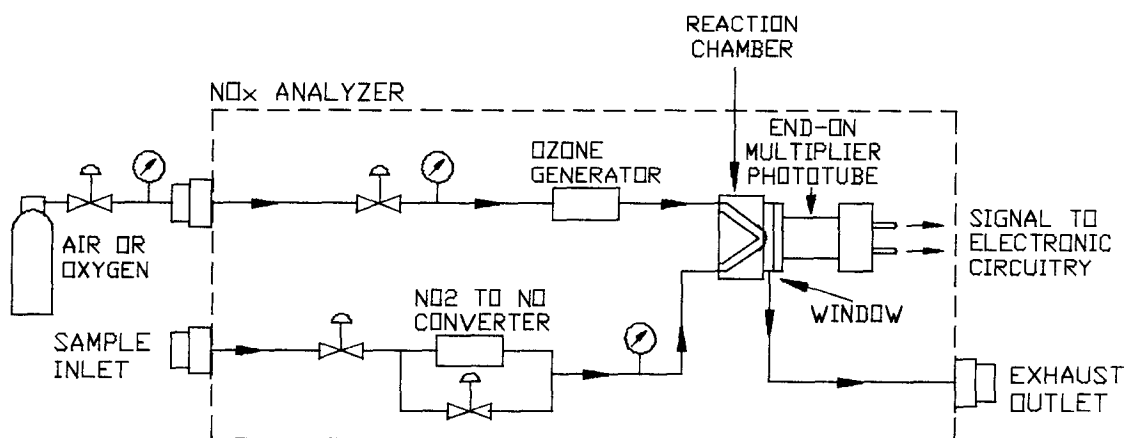
Figure 3.9: Schematic Flow Diagram of NO/NO$_x$ Analyzer.

Figure 3.9 shows the schematic flow diagram of the NO/NO$_x$ analyzer and the chemiluminescent method. The chemiluminescent method for detection of nitric oxide (NO) is based on its reaction with ozone (O$_3$) to produce nitrogen dioxide (NO$_2$) and oxygen (O$_2$). Some of the nitrogen dioxide molecules thus produced are initially in an electronically excited state (NO$_2^*$). These revert immediately to ground state with emission of photons. The reactions involved are

$$NO + O_3 \dashrightarrow NO_2^* + O_2$$

$$NO_2^* \dashrightarrow NO_2 + h\nu$$
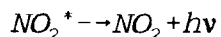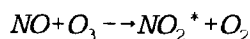
where:  h = Planck's constant;  $\nu$ = frequency, Hz

As shown in Figure 3.9, after flowing into the analyzer in the lower tube, the sample gas first passes to a $NO_2$-to-NO converter where all $NO_2$ in the sample gas will be convert to NO. Then, the sample gas passes to the reaction chamber. In the upper tube, the air flows into a ozone generator to produce $O_3$ which is then sent to the reaction chamber of the analyzer. As NO and $O_3$ mix in the reaction chamber, the chemiluminescent reaction produces light emission that is directly proportional to the concentration of NO. This emission is measured by a photomultiplier tube and associated electronic circuitry. The $NO_x$ concentration is then known since it is equal to the NO concentration.

Hydrocarbon Determination (model 400):

The Model 400A Hydrocarbon Analyzer utilizes the flame ionization method of detection. The sensor is a burner in which a regulated flow of sample gas passes through a flame sustained by regulated flows of air and a fuel gas (hydrogen or a hydrogen-diluent mixture). Within the flame, the hydrocarbon components of the sample stream undergo a complex ionization that produces electrons and positive ions. Polarized electrodes collect these ions, causing current to flow through electronic measuring

MODEL 400 HYDROCARBON ANALYZER
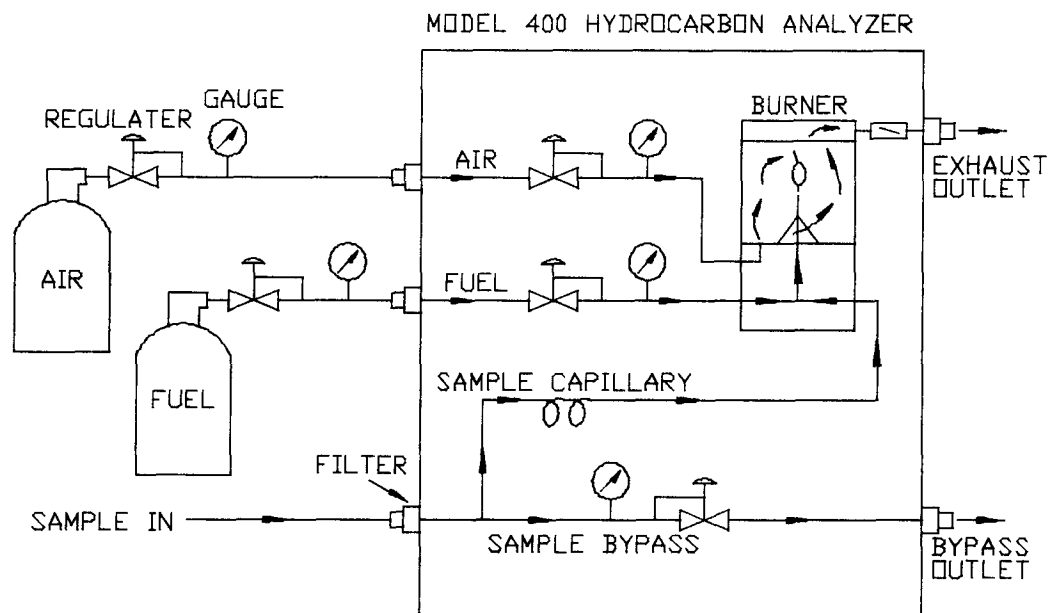


Figure 3.10: Schematic Flow Diagram of HC Analyzer.

circuitry. Current flow is proportional to the rate at which carbon atoms enter the burner. Figure 3.10 shows the schematic flow diagram of HC analyzer.

## Non-Dispersive Infrared Detection Method (Model 865 and 880):

As shown in Figure 3.11, in the analyzer, infrared radiation is produced by two separate energy sources. Once produced, this radiation is beamed separately through a chopper which interrupts it at a certain frequency. Depending on the application, the radiation may then pass through optical filters to reduce background interference from other infrared-absorbing components.

The infrared beams pass through two cells: one is a reference cell containing a non-absorbing background gas, and the other is a sample cell containing a continuously flowing sample.
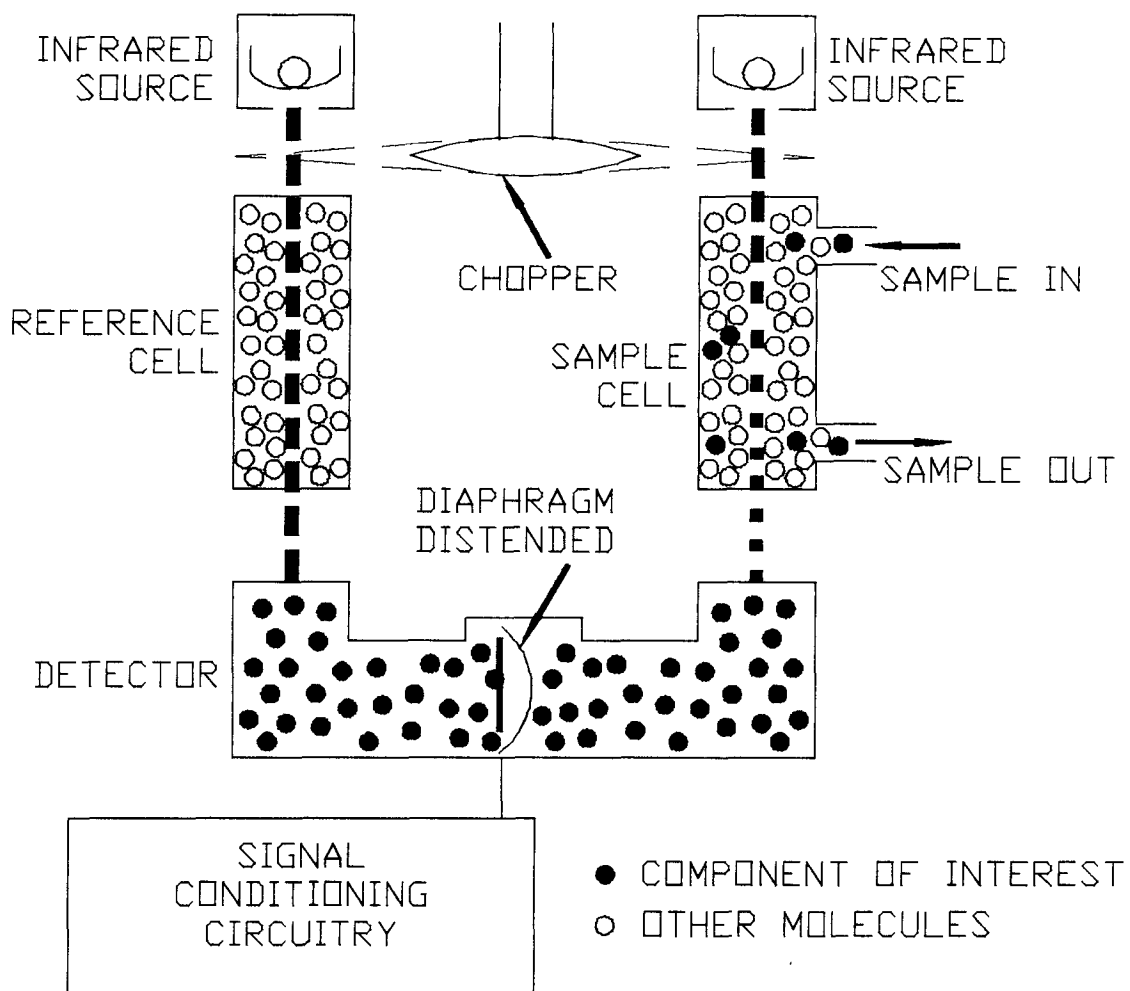
Figure 3.11: Schematic of Non-Dispersive Infrared Detection
System with Double-Beam Method.

During operation, a portion of the infrared radiation is
absorbed by the component of interest in the sample such as CO and
$CO_2$, with the percentage of infrared radiation absorbed being
proportional to the component concentration. The detector is a "gas
microphone" operating on the Luft principle. It converts the

difference in energy between sample and reference cells to a capacitance change. This capacitance change, equivalent to component concentration, is amplified and indicated on a meter.

### 3.3.3  Drawback of the EEAS-A

The major drawback of this system was that precise results of total hydrocarbon (HC) and nitric oxides ($NO_x$) could not be obtained. The reason for that is the following. The sampling pipe, the filters, and the hydrocarbon analyzer were not heated, so water condensed from the sample gas on the way to the analyzers. A sample-gas chiller was used to protect analyzers from water corrosion. But the sample-gas chiller also condensed some hydrocarbons which are heavier than methane and some nitrogen dioxides ($NO_2$). This caused the readout of the hydrocarbon and nitric oxides analyzers lower than the true concentration. To overcome this drawback, a new system, EEAS-B, has been established since September, 1992.

## 3.4  The Exhaust Emission Analysis System B, (EEAS-B)

The major advantage of this new system is that it provides a precise measurement for total hydrocarbon (THC) and nitric oxides ($NO_x$). In contrast to the EEAS-A, the EEAS-B has a heated sample-gas sampling system which includes heated sample-gas tubes, heated filters, heated pump and heated valves. The new instruments installed on the EEAS-B are the heated total hydrocarbon (THC) analyzer (RATFISCH Model RS-55), the oxygen analyzer (SIEMENS

OXYMAT 5E), the $CH_4$ and $NO_x$ analyzer (SIEMENS ULTRAMAT 22P), and heated $NO_2$ to NO converter. The instruments transferred from the EEAS-A to the EEAS-B are the carbon monoxide, the carbon dioxide analyzers, and the sample-gas chiller.

## 3.4.1   Arrangement of the EEAS-B
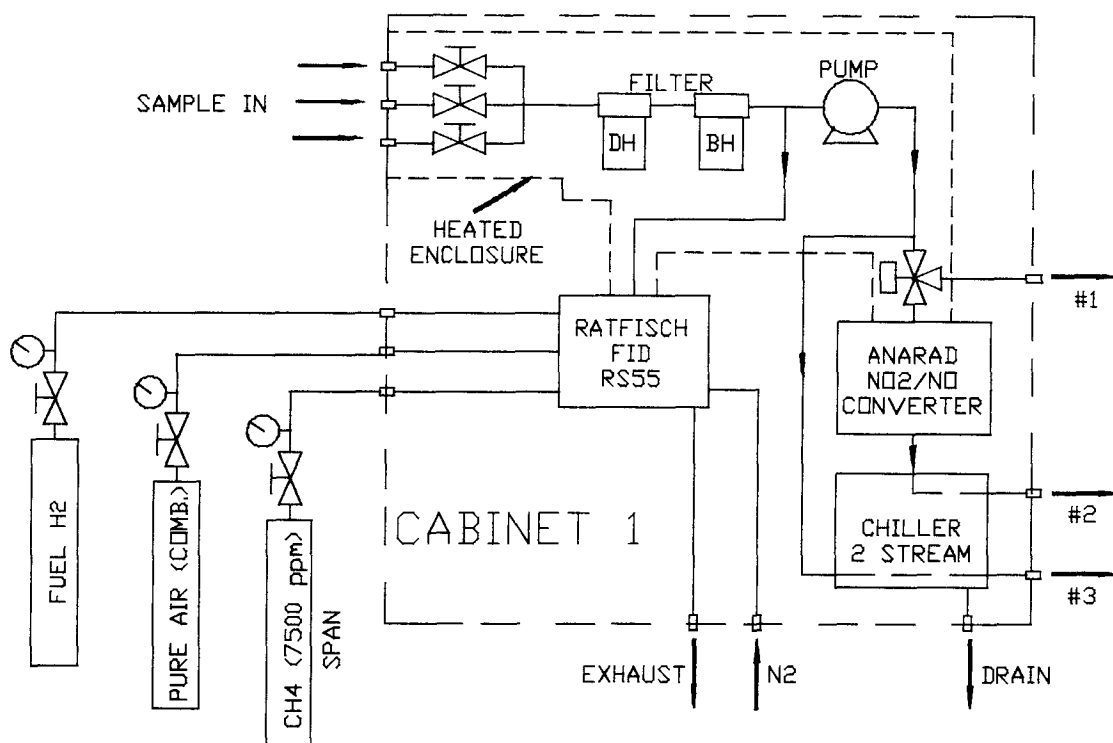


Figure 3.12: Schematic Flow Diagram of the First Cabinet of Exhaust Emission Analysis System B (EEAS-B).

Generally, the EEAS-B consists of two cabinets of instruments. Figures 3.12 and 3.13 show the schematic flow diagrams of the first

and the second cabinets of the EEAS-B. Cabinet 1 comprises all the heated instruments and the heated auxiliary as well as the sample-gas chiller; Cabinet 2 consists of all the "cool" instruments.
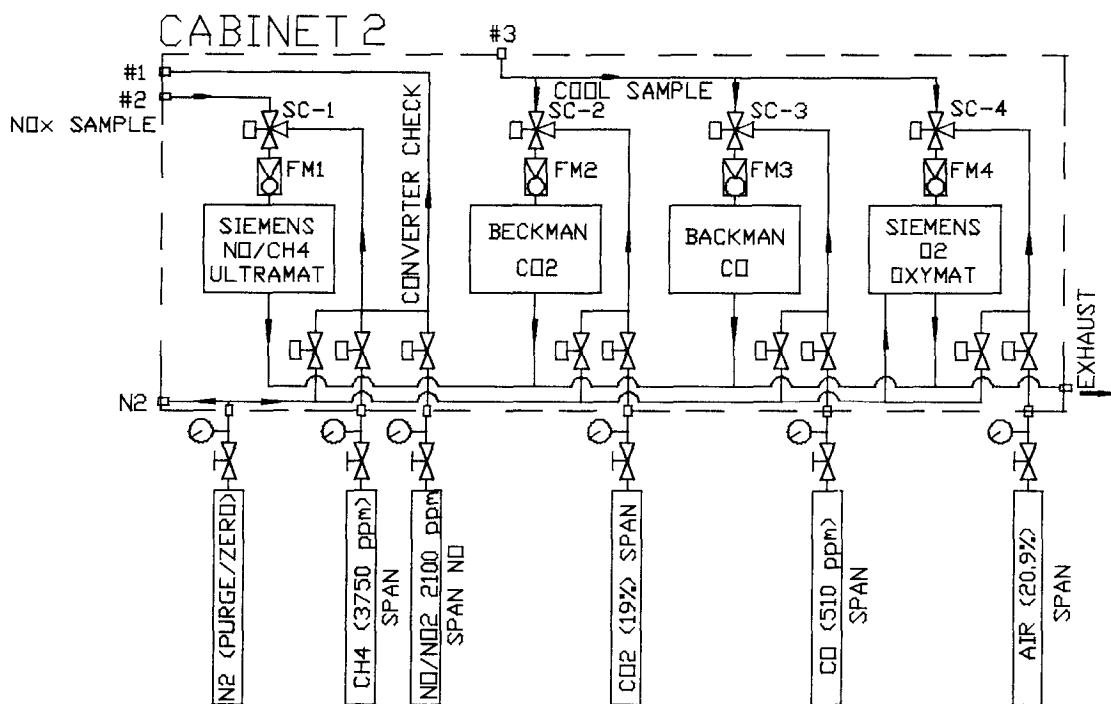


Figure 5.13: Schematic Flow Diagram of the Second Cabinet of Exhaust Emission Analysis System B (EEAS-B).

As shown in Figure 3.12, the exhaust sample gas is taken by a sampling probe mounted downstream on the exhaust pipe about 2 meters away from the engine exhaust manifold outlet flange (Same configuration as in EEAS-A, but not shown in Figure 3.12). After entering the heated sampling line, the heated sample gas first

enters the first cabinet, passes through a heated coarse filter (DH) and a heated fine filter (BH) to remove soot and particulates, then separates into two tubes. In the downward tube, the heated sample gas goes directly into the heated total hydrocarbon analyzer (RS55). In the upward tube, the heated sample gas passes through a heated pump before a second-time separating into two tubes. In one tube, the heated sample gas goes directly into a $NO_2$ to NO converter to convert all $NO_2$ into NO, then passes through the chiller to condense out water, and finally goes to $NO/CH_4$ analyzer which is located in Cabinet 2 shown in Figure 3.13 (The $NO/CH_4$ analyzer detects the NO and $CH_4$ concentrations at same time). In the other tube, the sample gas flows out of heated closure and into the chiller. After condensing, the dry cool sample gas flows out of Cabinet 1 into Cabinet 2.

In Cabinet 2 as shown in Figure 3.13, the cool sample gas separates into three tubes which lead to $CO_2$, CO and $O_2$ analyzers. The flowmeter is placed in front of each analyzer (except the total hydrocarbon analyzer) to adjust the sample flow rate entering the analyzer. Zero and span gases are used to calibrate the analyzer before a test.

### 3.4.2 Principle of the Analyzers in the EEAS-B System

Total hydrocarbon (THC) analyzer, $NO/CH_4$ analyzer, oxygen ($O_2$) analyzer, carbon monoxide (CO), and carbon dioxide ($CO_2$) analyzers are five analyzers in the EEAS-B. The measurement principle of the CO and the $CO_2$ analyzers was discussed in subsection 3.3.2. The new

THC analyzer has the same detection principle as the old HC analyzer, which operates on the flame ionization detection method described in subsection 3.3.2. The general principle of the NO/CH$_4$ analyzer and the O$_2$ analyzer will be discussed in subsequent subsections.

Measurement Principle of NO/CH$_4$ Analyzer:



| | |
|---|---|
| CO | 1 |
| CO | 2 |
| | 3 |
| | 4 |
| | 5 |
| | 6 |
| | 7 |
| | 8 |
| | 9 |
| | 10 |
| | 11 |

1. Detector cell
2. Secondary detector level
3. Microflow sensor
4. Primary detector level
5. Window
6. Analyzer cell
7. Sample gas inlet
8. Chopper
9. IR source
10. Reflector
11. Chopper motor
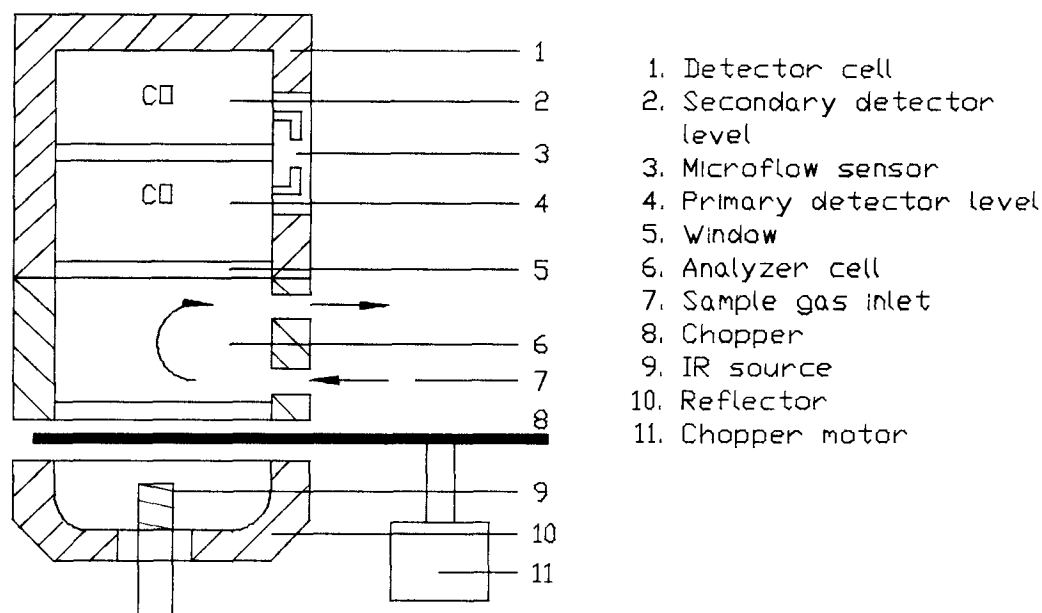
Figure 3.14: Schematic of Non-Dispersive Infrared Detection System with Single-Beam Method.

This instrument operates on the non-dispersive infrared absorption principle using the single-beam method with an opto-pneumatic double-layer detector. Figure 3.14 shows the schematic diagram of the detection system of the analyzer. The radiation spiral (9), heated to approx. 600°C, emits infrared radiation which is modulated by a chopper (8). After passing through the analyzer

cell (6) which contains sample gas, the intensity of the radiation is measured selectively by a specific gas in a double-layer detector cell (1). The gas in the detector cell is capable of absorbing radiant energy and converting it into temperature increment. A gas mass flow caused by the temperature increment between two detector cells is thus produced, and measured by a microflow sensor (3) which converts this flow signal into an electrical output signal.

## Measurement Principle of $O_2$ Analyzer:



1. REFERENCE GAS
2. RESTRICTORS
3. MICROFLOW SENSOR IN
   MEASURING SYSTEM
4. REFERENCE GAS CONDUITS
5. SAMPLE GAS
6. SAMPLE CHAMBER
7. PARAMAGNETIC MEASURING
   EFFECT
8. ELECTROMAGNET WITH
   VARYING FLUX INTENSITY
9. MICROFLOW SENSOR IN
   COMPENSATING SYSTEM
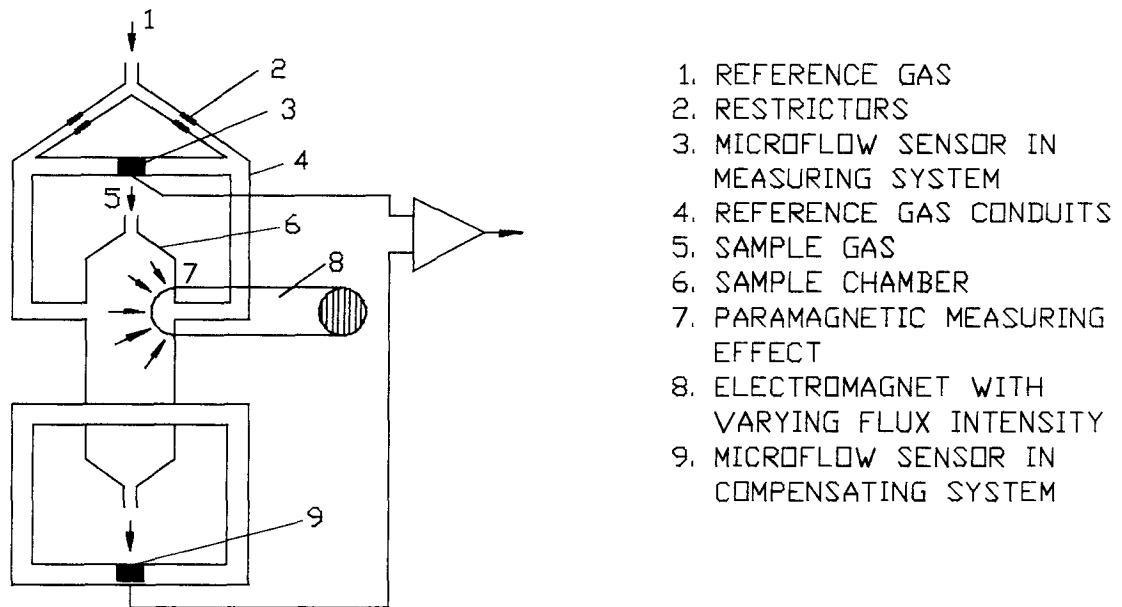
Figure 3.15: Schematic of Oxygen Measurement Principle.

Oxygen molecules in a non-uniform magnetic field are attracted to the strong part of the field because of their paramagnetic property. If two gases having different oxygen contents are brought

together in a magnetic field, a pressure differential will be generated between them. The pressure differential is proportional to the oxygen content of the sample gas. This is the basic measurement principle of the $O_2$ analyzer.

As shown in Figure 3.15, in the analyzer, one of the gases is the sample gas, and the other is a reference gas ($N_2$ of maximum purity, $O_2$ or air). The reference gas is admitted to the sample chamber through two conduits (4). One stream of the reference gas mixes with the sample gas in the area of the magnetic field. Because the two conduits are interconnected, the pressure which is proportional to the oxygen content of the sample gas produces a flow which is measured by a microflow sensor (3) and is converted into an electrical signal.

### 3.4.3 Relationship between the EEAS-A and the EEAS-B Systems

From the operation principles for each analyzer, as well as the overall arrangements of both systems, we can draw some conclusions:

1. CO and $CO_2$ readout from both systems should be consistent because they are using the same analyzers and the readout is the same on the dry basis.

2. Total hydrocarbon (THC) readout from the EEAS-A system is on the dry basis and has non-methane hydrocarbon condensation occurring, whereas the readout from EEAS-B system is on the wet basis.

3. Although the $NO_x$ readout is on the dry basis from both

systems, the one from the EEAS-A system may be slightly lower than the one from the EEAS-B system, caused by some $NO_2$ condensing with water before it enters the $NO_2$ to NO converter and detector in the EEAS-A system. Furthermore, the two analyzers used in the two systems use different detection methods, so that the original readout might also be slightly different.

## 3.5   Smoke Determination (BOSCH Smoke Meter)
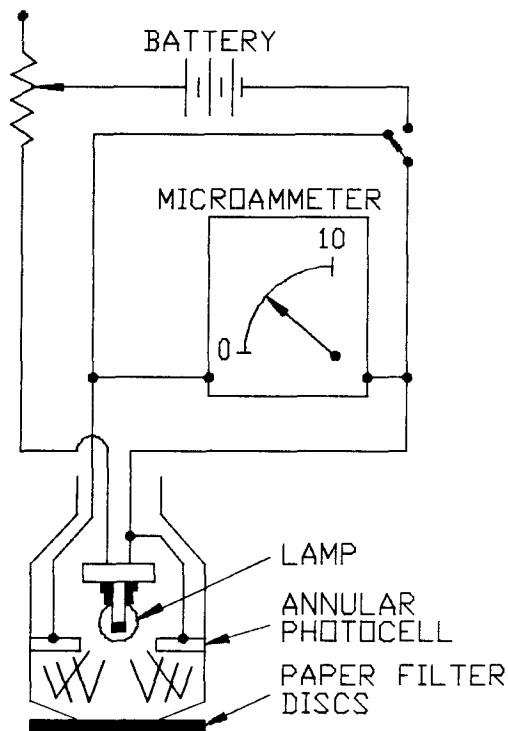
Figure 3.16: Schematic of BOSCH "Spot" Smokemeter.

Independent of the above systems, the concentration of diesel exhaust soot particles is determined by photoelectric evaluation

using a portable Bosch "Spot" Smokemeter [39]. Figure 3.16 shows the measurement principle of this instrument. A spring-operated sampling pump draws a fixed volume of exhaust gas from the exhaust stream through a controlled density paper filter disc (not shown in Figure 3.16). Soot particles from the sample are deposited on the filter disc, causing it to darken in proportion to the soot particle concentration. A separate 110 V AC or battery-powered photoelectric device measures the light reflected from the darkened filter disc. Readout is by a milliammeter calibrated in 0-10 units.

# 4. EXPERIMENTAL PROCEDURES

## 4.1  Introduction

This chapter discusses the three experimental procedures: engine performance and emission test procedure; engine performance calculation procedure; and engine exhaust emission calculation procedure.

The experimental work was divided into two test categories: diesel baseline tests and gas-diesel operation tests. Gas-diesel testing was carried out with different injector geometries and engine operating parameters. The detailed test procedure will be described in a subsequent section.

Nine indices were chosen to represent engine performance and emission characteristics: thermal efficiency, brake mean effective pressure (BMEP), nitrogen oxides emission ($NO_x$), total hydrocarbon emission (THC), non-methane hydrocarbon emission (NMHC), unburned methane emission ($CH_4$), carbon monoxide emission (CO), carbon dioxide emission ($CO_2$), and Bosch smoke index.

The engine performance indices, thermal efficiency, and brake mean effective pressure (BMEP), were not measured directly and require calculations discussed in the section on engine performance calculation procedure (page 62).

The engine exhaust emissions can be expressed as dry-basis, wet-basis or brake specific emissions. The first and second emissions are stated in parts per million (ppm) by volume. The

third is stated in a mass unit as kg/kW-hr. The conversion between the dry-basis and the wet-basis emissions as well as the calculation of brake specific emissions (from the wet-basis emissions) are explained in the section concerning engine exhaust emission calculation procedure (page 64).

## 4.2 The Engine Performance and Emission Test Procedure
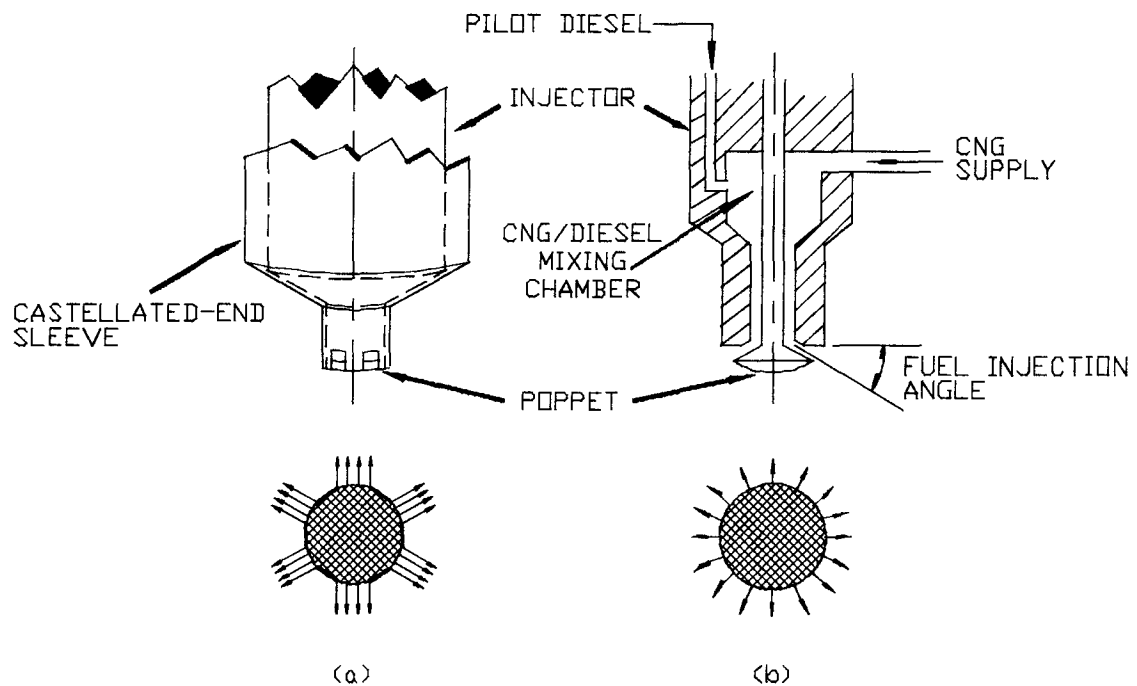


Figure 4.1: Schematic of Injector with Castellated-End Sleeve.

Engine performance and emission tests were conducted with both

diesel and gas-diesel fuel injectors. Baseline testing with pure diesel fuel was conducted for comparison with the results of gas-diesel fuelling. Most tests were done with the gas-diesel injector supplied with compressed natural gas fuel and pilot diesel (ie. ignition liquid). In the original configuration of the gas-diesel injector (see Fig. 3.7 in chapter 3), a poppet nozzle was used so that the fuel jet formed a conical sheet. The injection angle (ie. the poppet seat angle) is defined as the angle between the poppet seat and the cylinder head surface. Figure 4.1 shows the schematic of injector configuration with a castellated-end sleeve to interrupt the conical sheet jet in part of the test. Fuel jet interruption is a method to increase jet penetration, injection speed and tendency of jet stability [42].

The injector geometries and engine operating parameters varied in the engine performance and emission tests are listed in Table 4.1. The fuel jet interruption ratio is defined as the ratio of the shrouded area to the total column area; it is also referred to as shroud %.

In the baseline tests, a production model electronic unit injector (controlled by an electronic module with manufacturer-preprogrammed operating BOI and PW) was used to provide the diesel operation. The engine was operated at constant speed with load setting at increments from 0.5 to 5 bar.

With gas-diesel operation, a modified electronic module was used to control the gas-diesel electronic unit injector. With this module, BOI, PW and diesel/total fuel energy ratio can be easily

adjusted to desired values within the testing range. The pilot diesel used for most cases was cetane number 62 diesel. The engine speed was kept constant at 1200 rpm for most cases by adjusting the PW (ie. the duration of the fuel injection). The injection angles were adjusted by changing the poppet nozzle. The fuel jet interruption ratio was adjusted by modifying the castellated end of the sleeve.

Table 4.1   List of Variable Parameters and Testing Ranges:

------------------------------------------------------------------

Injector Geometrical Parameters

| | |
|---|---|
| Fuel injection angles: | 10°, 20° and 30° |
| Fuel jet interruption ratio: | |
| Conical sheet: | 0% shrouding |
| Conical sheet with six interruptions: | 30 ... 60 % shrouding |

Engine Operating Parameters

| | |
|---|---|
| Speed: | 1000 ... 1400 rpm |
| Load (BMEP): | 0.5 ... 4.5 bar |
| Beginning of injection (BOI): | 16 ... 40°BTDC |
| Pulse width of injection (PW): | 5 ... 25 °CA |
| CNG injection pressure: | 50 ... 90 bar |
| Pilot-diesel/total fuel energy ratio: | 15 ... 25 % |
| Diesel-fuel cetane number: | ~45 or 62 |

------------------------------------------------------------------

The following is the test procedure for obtaining the gas-diesel engine performance and emission data at a given speed.

1.  Modify the nozzle shroud to obtain a specific fuel jet interruption ratio, e.g. 50% shrouding.

2.  Install a poppet nozzle with specific fuel injection angle, e.g. 10° to the cylinder head surface.

3.  Set a specific CNG injection pressure, e.g. 50 bar.

4.  Select a specific pilot-diesel/total fuel energy ratio, e.g. 15%, and keep it constant by adjusting the pilot-diesel metering valve.

5.  Set a specific beginning of injection (BOI), e.g. 24°BTDC.

6.  Increase the load from 0.5 bar to 4.5 bar (or the maximum achievable) and keep speed and pilot-diesel/total fuel energy ratio constant.

7.  Acquire engine performance and emission data for every load point. The operating procedure of the exhaust emission analysis system B is presented in Appendix B.

8.  Repeat for the other BOI, ie. 28, 32, 36 and 40°.

9.  Repeat for the other pilot-diesel/total fuel energy ratios, ie. 20% and 25%.

10. Repeat for the other CNG injection pressures, ie. 60, 70, 80 and 90 bar.

11. Repeat for the other fuel injection angles, ie. 20° to the cylinder-head surface.

12. Repeat for the other fuel jet interruption ratios, ie. 50%, 40%, 30% and 0% shrouding.

Most of the data were acquired at 1200 rpm, but some were collected at 1400 rpm.
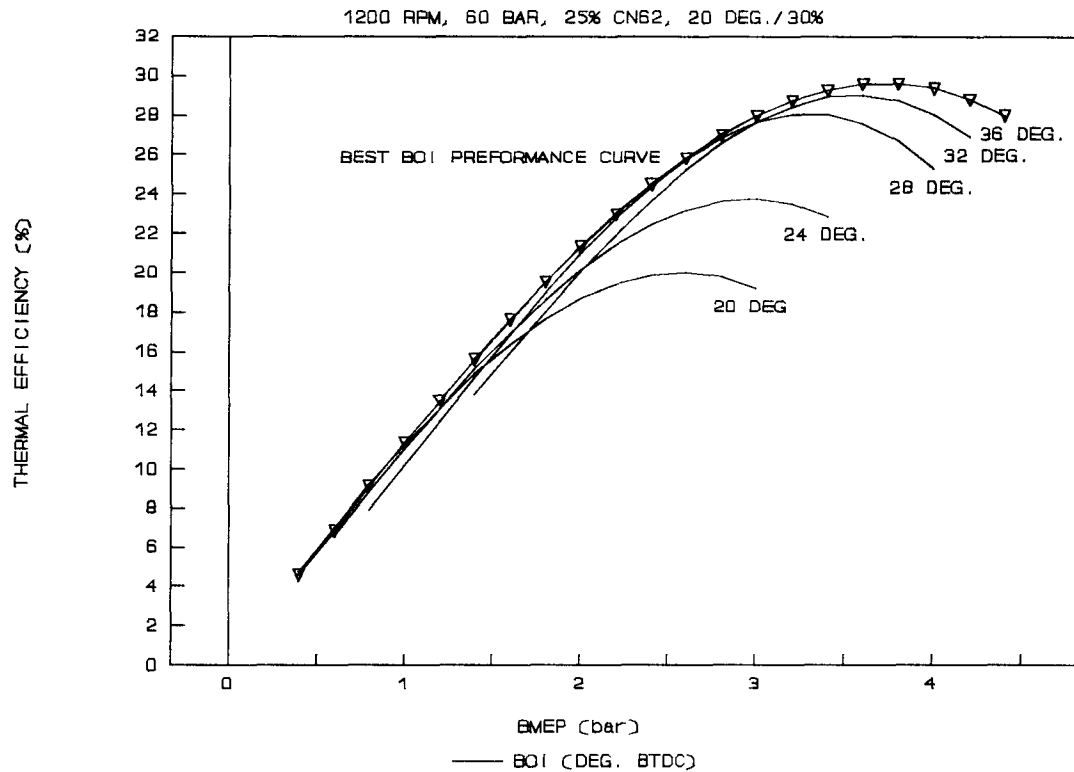


Figure 4.2: Determination of the Best BOI Performance Curve.
(CNG injection pressure 60 bar, diesel-ratio 25%,
CN62, 20° injection angle, 30% shrouding)

Figure 4.2 shows typical results of the above test procedure and how the best BOI performance curve is determined as a envelope of all performance curves for the whole BOI range. This is interesting because:

1.    The best BOI performance curve represents the maximum thermal efficiency that the engine can achieve at any given load.

2.  The engine can be computer-controlled to operate along the best BOI performance curve, as long as the operating parameters are known.

After determining the best BOI performance curve, the operating conditions were selected for acquiring smoke data and cylinder pressure data. These measurements were made at low, medium and high load, and best BOI.

## 4.3  The Engine Performance Calculation Procedure

As mentioned, thermal efficiency, brake mean effective pressure (BMEP) and brake power are the indices that represent the engine performance, and they are not directly measured. The variables that are directly obtained by measurement are engine speed, torque, cylinder displacement, CNG and pilot-diesel mass flow rates. The following is the procedure to calculate the engine performance indices with measured variables.

Brake Power:

Brake power $P_b$ (kW) is the power delivered by the engine and absorbed by the dynamometer (load); it is the product of engine speed N (rev/min or rpm) and torque $T_b$ (N·m) measured with a dynamometer [26].

$$P_b = 2\pi \frac{N}{60} T_b \times 10^{-3}$$  (4.1)

Brake power $P_b$ (kW) can also be expressed as the product of engine shaft work per cycle $W_c$ (kJ) and engine speed N (rpm).

$$P_b = \frac{W_c N}{60 n_R} \tag{4.2}$$

where $n_R$ is the number of crank revolutions for each power stroke per cylinder (two for four-stroke cycle, one for two-stroke cycle).

## Brake Mean Effective Pressure:

Brake mean effective pressure BMEP (bar) of the engine is defined as the engine shaft work per cycle $W_c$ (kJ) divided by the cylinder displacement volume $V_d$ (cm$^3$) [26].

$$BMEP = \frac{W_c}{V_d} \times 10^4 \tag{4.3}$$

BMEP can also be expressed in terms of torque $T_b$ (N·m) by using Eq. (4.2) and (4.1) for a two-stroke engine ($n_R=1$).

$$BMEP = \frac{2\pi T_b \times 10}{V_d} \tag{4.4}$$

Because pressure, humidity and temperature of the ambient air inducted into a engine affect the air mass flow rate and the power output, a correction factor is usually used to adjust brake power and BMEP to the standard atmospheric conditions to provide a common basis for comparisons between engines. The procedure for computing the correction factor is listed in Appendix C.

## Thermal Efficiency:

Thermal efficiency is defined as the ratio of the engine brake power to fuel enthalpy supplied per cycle per second [26].

$$\eta_{th} = \frac{P_b}{\dot{m}_{fuel} \cdot LHV/3600}$$ (4.5)

where $P_b$ (kW) is the brake power, $\dot{m}_{fuel}$ (kg/hr) is mass flow rate of the fuel, and LHV (kJ/kg) is the Lower Heating Value of the fuel. As there are two fuels inducted into the engine, we have

$$\dot{m}_{fuel} \cdot LHV = \sum_{i=1}^{2} (\dot{m}_{fuel})_i \cdot LHV_i$$ (4.6)

where i=1 for CNG fuel, i=2 for pilot diesel fuel.

By substituting Eq. (4.1) and (4.6) into Eq. (4.5), the thermal efficiency of the engine becomes

$$\eta_{th} = \frac{2\pi \frac{N}{60} T_b \times 10^{-3}}{\sum_{i=1}^{2} (\dot{m}_{fuel})_i LHV_i/3600}$$ (4.7)

where N (rpm) is engine speed , $T_b$ (N·m) is torque.

## 4.4  The Engine Exhaust Emission Calculation Procedure

In the engine tail-pipe exhaust, the main components are carbon monoxide, carbon dioxide, nitrogen oxides, total hydrocarbon, oxygen, nitrogen and water vapour. The water vapour in the exhaust comes from hydrocarbon-fuel combustion and the humidity in intake air. The water vapour resulting from hydrocarbon-fuel combustion is the main source.

Depending on the experimental setup, the exhaust emission data

can be measured either on a wet or a dry basis. The wet-basis emission data are measured with exhaust samples which have the same water vapour concentration as the tail-pipe exhaust gas (ie. no water vapour condensed before measurement). The dry-basis emission data are measured with exhaust samples from which the water vapour has been removed before the measurement. Thus the wet-basis emission data are the actual engine exhaust emission data.

The EEAS-A system, for example, has a chiller located on the upstream sample line. Thus all emission data from analyzers are dry-basis emission data. With the EEAS-B system, the heated pipe and enclosure maintain the water vapour in the wet exhaust sample drawn into the total hydrocarbon analyzer so that the unburned THC data are wet-basis emission data. Another part of the exhaust sample flows through a chiller to remove water vapour before entering the other analyzers. Thus the $CH_4$, the $NO_x$, the $CO_2$, the CO and $O_2$ data are measured on the dry basis.

Usually, the emission measurement is based on volume. Thus the unit of measured emission data is ppm, which is the volumetric ratio of 1 volume of measured component to $10^6$ volume of exhaust sample.

### 4.4.1 Conversion between Dry-Basis and Wet-Basis Emissions

The dry-basis emission data can be converted to the wet-basis emission data by using a conversion factor $F_{dw}$, such that

$$ppm(wet\text{-}basis)=F_{dw}\times ppm(dry\text{-}basis) \qquad (4.8)$$

The factor $F_{dw}$ for gas-diesel operation is expressed as the

product of two factors $K_{dw1}$ and $K_{dw2}$.

$$F_{dw} = K_{dw1} \cdot K_{dw2} \qquad (4.9)$$

The correction factor $K_{dw1}$ includes the effect of the water vapour produced by hydrocarbon-fuel combustion. The correction factor $K_{dw2}$ contains the influence of the humidity of the inlet air.

An empirical formula for the correction factor $K_{dw1}$ for pure diesel operation is given in the SAE recommendation [41] and is

$$K_{dw1} = 1 - y_{DSL} (F/A)_{DSL} \qquad (4.10)$$

where $y_{DSL} = 1.8$ [26] is the atomic hydrogen to carbon ratio of the diesel fuel; $(F/A)_{DSL}$ is the diesel fuel-air ratio (dry basis).

The formula for the correction factor $K_{dw1}$ for gas-diesel operation is obtained by modifying Eq. (4.10):

$$K_{dw1} = 1 - [y_{CNG} (F/A)_{CNG} + y_{DSL} (F/A)_{DSL}] = 1 - X_{H2O} \qquad (4.11)$$

where $y_{CNG} = 3.85$ is the atomic hydrogen to carbon ratio of the B.C. CNG fuel; $y_{DSL} = 1.8$ is the atomic hydrogen to carbon ratio of the pilot diesel fuel; $(F/A)_{CNG}$ is the CNG fuel-air ratio (dry basis) and $(F/A)_{DSL}$ is the diesel fuel-air ratio (dry basis). Both $(F/A)_{CNG}$ and $(F/A)_{DSL}$ can be calculated from measured data of CNG mass flow rate, diesel mass flow rate and air mass flow rate. $X_{H2O}$ is the molal fraction of the water vapour in the exhaust.

The relation between dry-basis fuel-air ratio $(F/A)_{dry}$ and wet-basis fuel-air ratio $(F/A)_{wet}$ is:

$$(F/A)_{wet} = (1 - H/1000) (F/A)_{dry} \qquad (4.12)$$

where H is the specific humidity (g of $H_2O$ per kg of dry air),

referring to Appendix D and [40] for calculation of the specific
humidity.

Because the humidity of the inlet air has an effect on the
amount of NO chemically formed in combustion, correction factor $K_{dw2}$
should be applied to NO emission at each test point. According to
the SAE recommendation [41], for NO emission data the following
formula is applied:

$$K_{dw2} = \frac{1}{1 + 7 \cdot B(H - 10.714) + 1.8 \cdot C(T - 29.444)} \qquad (4.13)$$

where B=0.044(F/A)-0.0038 and C=-0.116(F/A)+0.0053; F/A is fuel-air
ratio (dry basis); H is specific humidity (g of $H_2O$ per kg of dry
air) (see Appendix D); T is intake air temperature (°C).

For the other emission data, $K_{dw2} = 1$.

A more exact formula for dry-to-wet basis conversion factor $F_{dw}$
of the gas-diesel operation is presented in Appendix E. The
differences between the above method and the more exact method are:
0.05% at BMEP ~ 0.5 bar, 0.7% at BMEP ~ 2 bar and 0.2% at BMEP ~ 4
bar.

## 4.4.2 Determination of Brake Specific Emissions

The concentrations of gaseous emissions in the engine exhaust
are usually measured in parts per million or percent by volume. But
another more comparable emission indicator, brake specific emission
$bs_e$, is also used. Brake specific emission ($bs_e$) of a component is
defined as the mass flow rate of the component $\dot{m}_e$ per unit of

power output $P_b$.

$$bs_e = \frac{\dot{m}_e}{P_b} \qquad (4.14)$$

The brake specific emissions are calculated based on the following assumptions:

1. The engine exhaust consists of CO, $CO_2$, $NO_x$, $H_2O$, $O_2$, $N_2$ and unburned HC.

2. A combined fuel ($CH_y$) is used to replace CNG ($CH_{3.85}$) and diesel ($CH_{1.8}$) fuels. The hydrogen-to-carbon atom ratio y of the combined fuel is determined by Eq. (E.2) in Appendix E.

3. The unburned HC has the same composition as the combined fuel.

4. All measured emission data have already been converted to a wet basis in ppm (or % by volume).

Exhaust gas mass flow rate $\dot{m}_{exh}$ is determined by summing the intake air mass flow rate $\dot{m}_{air}$ and the total fuel mass flow rate $\sum \dot{m}_{fuel}$.

$$\dot{m}_{exh} = \dot{m}_{air} + \sum \dot{m}_{fuel} = \dot{m}_{air} + \dot{m}_{CNG} + \dot{m}_{DSL} \qquad (4.15)$$

Molal fraction of a component $X_i$ can be evaluated as following:

$$X_i = \frac{[(ppm)_i]_{wet}}{10^4} \qquad (4.16)$$

where $[(ppm)_i]_{wet}$ is concentration of a component "i" on the wet basis. $X_{CO}$, $X_{CO2}$, $X_{HC}$, $X_{NOX}$ and $X_{O2}$ can be determined by Eq. (4.16). $X_{H2O}$ can be evaluated by Eq. (4.11) (or Eq. (E.9) in Appendix E). $X_{N2}$ can be calculated as follows:

$$X_{N2} = 1 - X_{CO} - X_{CO2} - X_{HC} - X_{NOX} - X_{H2O} - X_{O2} \qquad (4.17)$$

Mass flow rate of a component "i" can be determined by

$$\dot{m}_i = \frac{X_i MW_i}{\sum X_i MW_i} \dot{m}_{exh} \qquad (4.18)$$

where $MW_i$ is the molecular weight of a component "i". The molecular weight of CO, $CO_2$, NO, $NO_2$, $H_2O$ and $O_2$ are known.

According to assumptions #2 and #3 of this subsection, the molecular weight of unburned HC can be determined as follows:

$$MW_{HC} = f_{DSL} MW_{DSL} + f_{CNG} MW_{CNG} \qquad (4.19)$$

where $f_{DSL}$ is the molal fraction of pilot diesel ($CH_{1.8}$); $MW_{DSL}$ = 13.825 kg/kmol is the molecular weight of the pilot diesel; $f_{CNG}$ is the molal fraction of the compressed B.C. natural gas; $MW_{CNG}$ = 16.689 kg/kmol is the molecular weight of the compressed B.C. natural gas (see Table 3.4 in Chapter 3).

Based on assumption #2 and #3, it is known that the unburned THC is the combination of 1 mole of B.C. CNG and $(16.689/13.825)r_m$ moles of pilot diesel, so the molal fraction of the pilot diesel is:

$$f_{DSL} = \frac{\dfrac{MW_{CNG}}{MW_{DSL}} r_m}{1 + \dfrac{MW_{CNG}}{MW_{DSL}} r_m} \qquad (4.20)$$

where $r_m$ is the diesel to CNG mass ratio and can be determined by Eq. (E.1) in Appendix E.

The molal fraction of the B.C. compressed natural gas is:

$$f_{CNG} = 1 - f_{DSL} \qquad (4.21)$$

Thereby, the brake specific emissions of the components can be determined by Eq. (4.14).

# 5. EXPERIMENTAL RESULTS

## 5.1 Introduction

The purpose of the chapter is to present and discuss the experimental results. Primarily, diesel baseline and gas-diesel operation tests have been completed and the results are presented and summarized in the following sections. The repeatability of the results is discussed in Appendix F.

The diesel baseline test involves three diesel fuels. The gas-diesel operation test contains the injection geometrical parameters and the engine operating parameters. A comparison of optimum gas-diesel operation against the diesel baseline is presented as the summation.

## 5.2 Diesel Baseline Test results

Commercial grade 1 (DF1), grade 2 (DF2), and cetane number 62 diesel (CN62, an experimental high-cetane fuel) were tested to find the effect of fuel composition on conventional diesel engine performance and emissions. The cetane numbers of DF1 and DF2 are approximately 45 and the other properties of these fuels are listed in Table 3.2 of Subsection 3.2.3. In the computation of thermal efficiency, the lower heating values of the three fuels were taken to be identical. The differences in heating values is estimated to be within 0.3%.

All tests were conducted at 1200 rpm with the same preprogrammed BOI, although the preprogrammed BOI was not optimized for CN62.
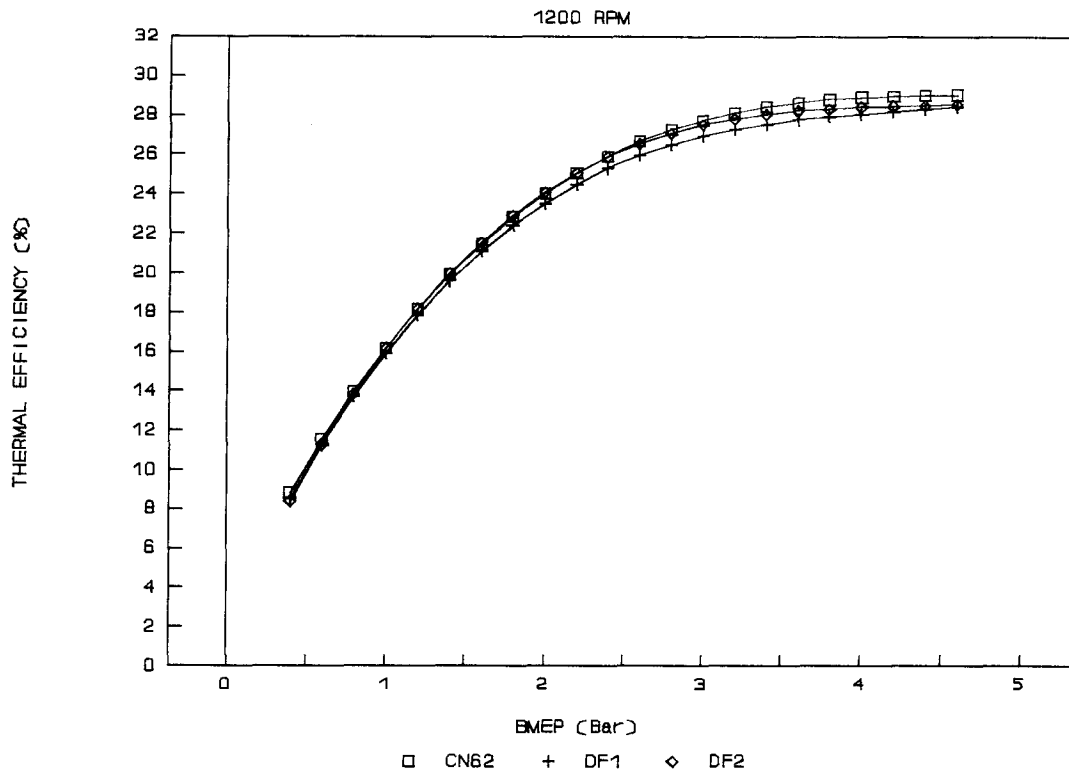


Figure 5.1: Effect of Fuel Composition on Performance.

Figure 5.1 shows the effect of fuel composition on thermal efficiency. As shown, the thermal efficiencies of the three fuels are about the same at low load (BMEP ~ 1 bar). As load increases, the thermal efficiency with CN62 fuel becomes highest, and the thermal efficiency with DF1 fuel is the lowest. The peak thermal

efficiencies for CN62, DF1 and DF2 fuels are 29.0%, 28.4% and 28.6% respectively. The difference in peak thermal efficiency between CN62 and DF1 fuels is about 2%. The maximum achievable load with all three fuels is about 4.5 bar.
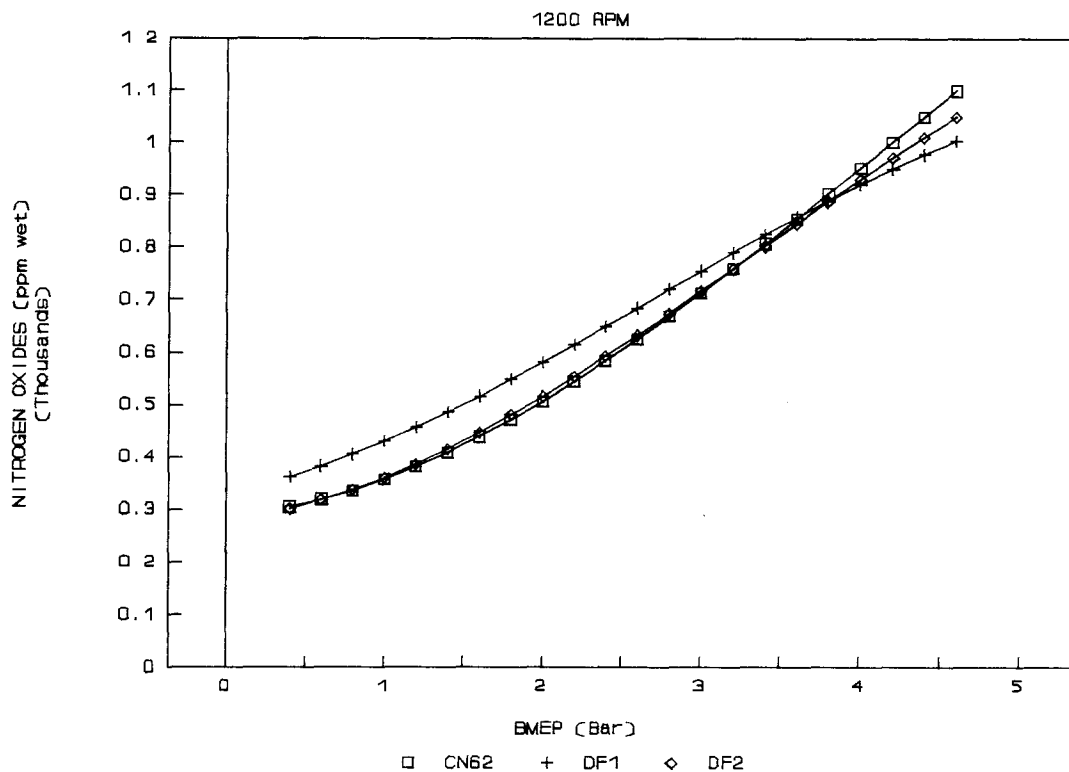


Figure 5.2: Effect of Fuel Composition on Nitrogen Oxides.

Figure 5.2 through Figure 5.5 show the effect of fuel composition on exhaust emissions. Generally, CN62 fuel produces less nitrogen oxides ($NO_x$), total hydrocarbon (THC), non-methane hydrocarbon (NMHC) and carbon monoxide (CO) emissions than DF1 fuel

over most of the load range. The emissions of DF2 fuel are between those of CN62 and DF1 over most of the load range.
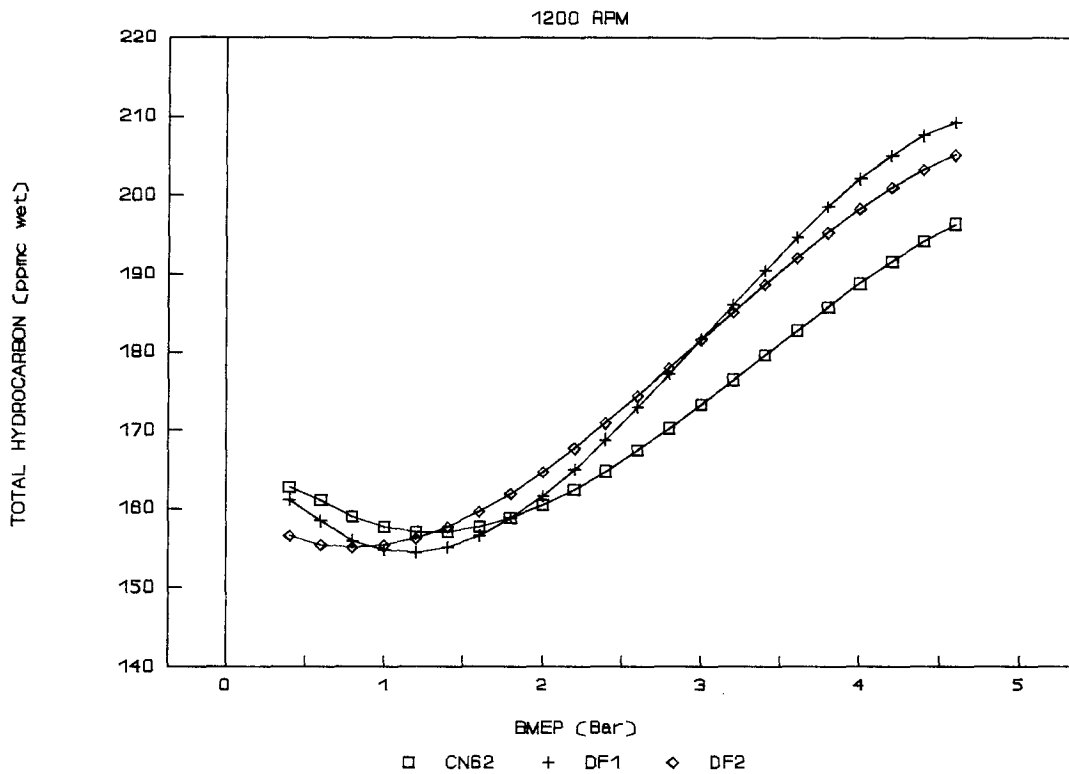


Figure 5.3: Effect of Fuel Composition on Total Hydrocarbon.

The difference between total hydrocarbon and non-methane hydrocarbon is the methane emission in the exhaust. The absolute value of methane emission is very low for diesel operation, being in the range of 10 ~ 35 ppm or 6% ~ 17% of total hydrocarbon emission.
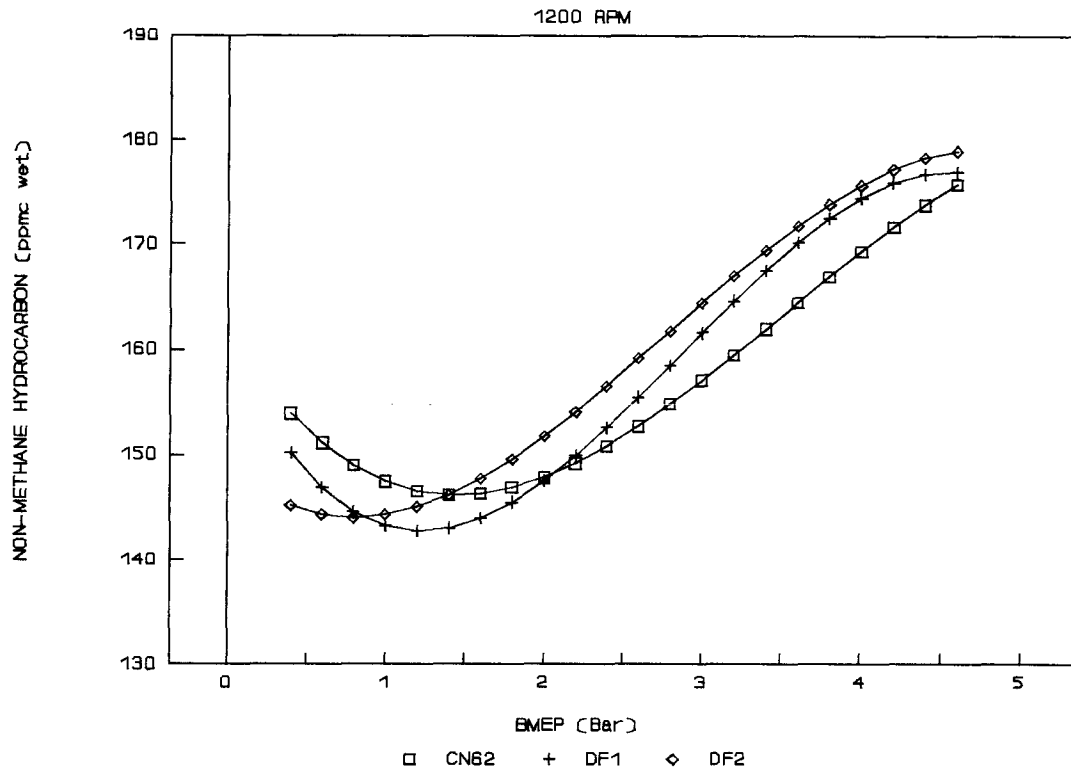
Figure 5.4: Effect of Fuel Composition on Non-Methane
Hydrocarbon.

The performance and emission curves for 100% CN62 fuel were
chosen to represent the engine baseline used in subsequent
comparison with gas-diesel operation in which CN62 is the pilot-
fuel in most tests. The emission curves of engine baseline was on
wet basis.
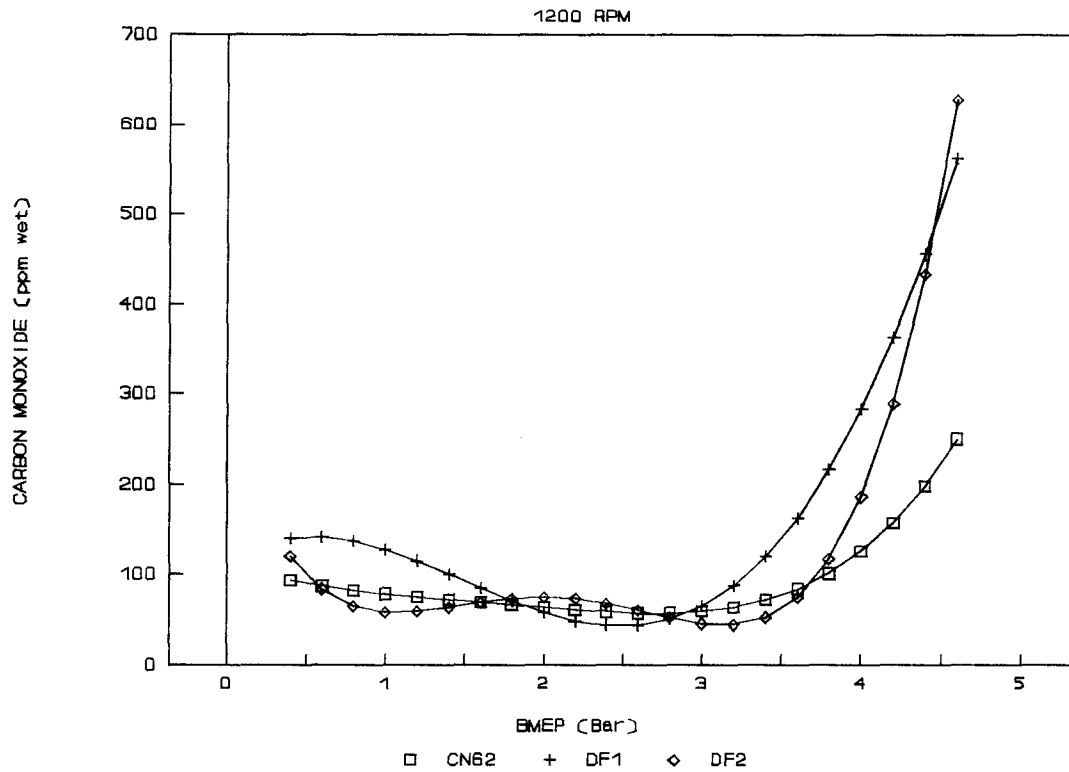
Figure 5.5: Effect of Fuel Composition on Carbon Monoxide.

## 5.3 Effect of Injector Geometrical Parameters

The effects of injector geometrical parameters on gas-diesel engine performance and emissions were investigated and the results are presented in this section. The geometrical parameters that were varied were fuel jet interruption ratio and fuel injection angle. The emission results presented in this section were on dry-basis.

## Fuel Jet Interruption Ratio:

Tests were conducted with different values of fuel jet interruption ratio (ie. percentage shrouding or % SRD) at the following test condition: 1200 rpm speed, 60 bar CNG injection pressure, 25% CN62 pilot-diesel energy ratio, and 20° fuel injection angle.
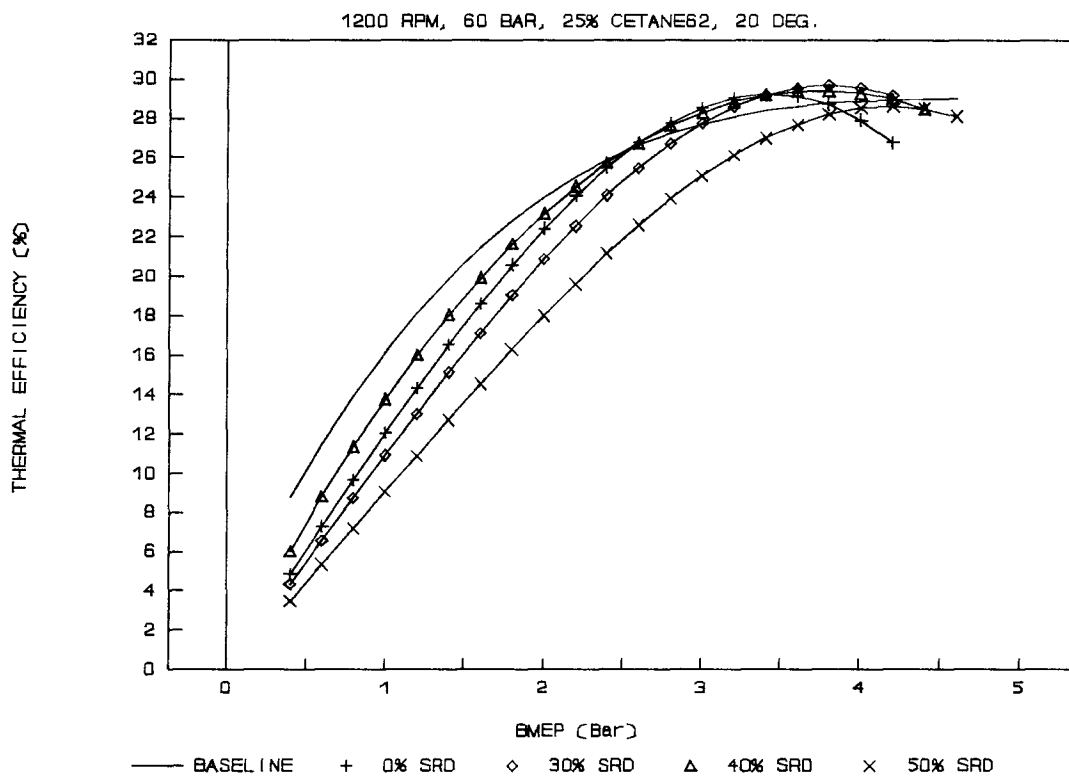


Figure 5.6: Effect of Fuel Jet Interruption Ratio
on Performance.

Figure 5.6 shows the effect of fuel jet interruption ratio (% SRD) on thermal efficiency. As exhibited, there is an optimum fuel

jet interruption ratio (~ 40% SRD for this engine) which provides best thermal efficiency at low and medium load, as well as relatively high thermal efficiency at high load; the maximum load capability increases with the increment of the fuel jet interruption ratio; the thermal efficiency of all cases is lower than that of the baseline at low load, while the peak thermal efficiency of the 40% SRD, 30% SRD and 0% SRD cases exceeds that of the baseline. The reason for this is that fuel jet interruption increases jet penetration, injection speed and jet stability [42] (see Appendix G). The increased jet penetration and higher injection speed of the 50% SRD case may disperse the fuel jet too much at low and medium load, thereby reducing thermal efficiency. At high load, the greater jet penetration and higher injection speed helps the fuel to mix with air, so that it improves thermal efficiency and maximum load capability. The shorter penetration of the 0% SRD case (ie. conical sheet without interruption) helps thermal efficiency at low and medium load, but suffers from reduction of the maximum load capability. The peak thermal efficiency of the 0% SRD case (around BMEP ~ 3.4 bar) also shifts to lower load compared to that of the 50% SRD case (around BMEP ~ 4 bar). This indicates that there should be an optimum jet interruption ratio case between the 50% SRD and the 0% SRD cases.

The effects of fuel jet interruption ratio on total hydrocarbon (THC) and nitrogen oxides ($NO_x$) are shown in Figures 5.7 and 5.8, respectively. Higher THC and lower $NO_x$ are observed for the 50% SRD case at low and medium load because of over
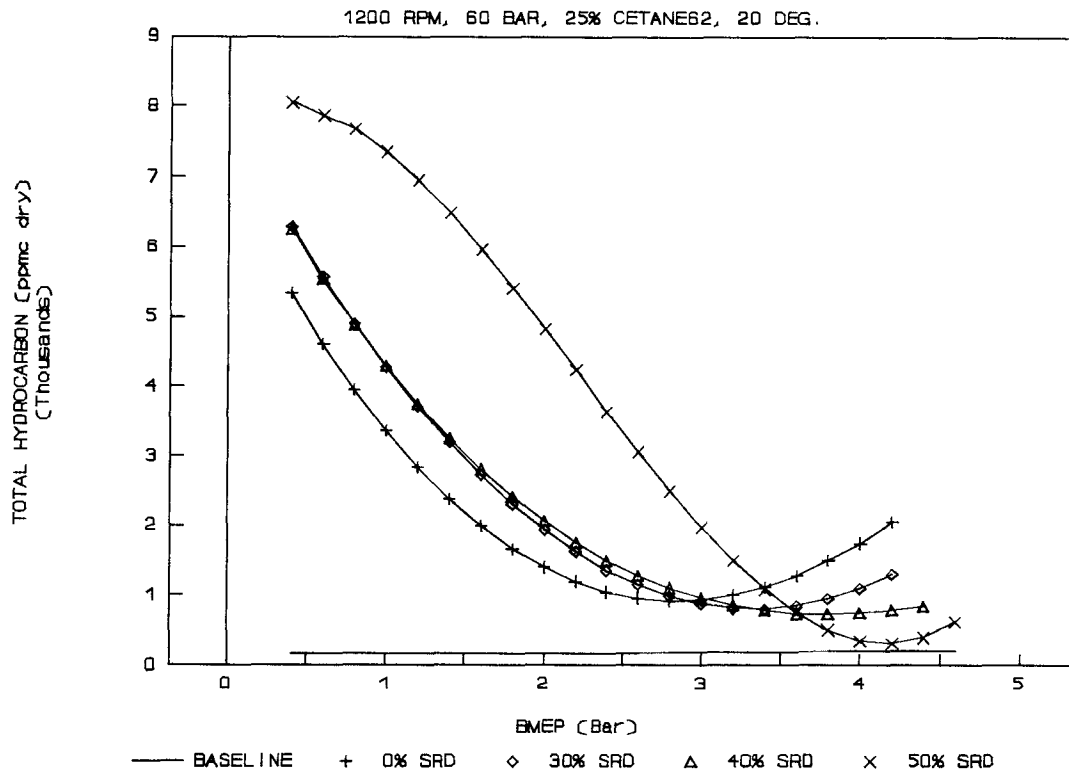
Figure 5.7: Effect of Fuel Jet Interruption Ratio on Total
Hydrocarbon.

dispersion; the THC emission of both the 40% SRD and the 30% SRD cases are very close, but the $NO_x$ emission of the 40% SRD case is lower than that the of the 30% SRD case; the $NO_x$ emissions of all jet interruption cases are lower, however, than that of the diesel baseline except at high load; the THC emission in all cases also surpasses that of the baseline, especially at low loads. All these indicate that the low-load combustion quality needs improvement.

Usually, high thermal efficiency is associated with high combustion temperature, high NO formation rate and high $NO_x$
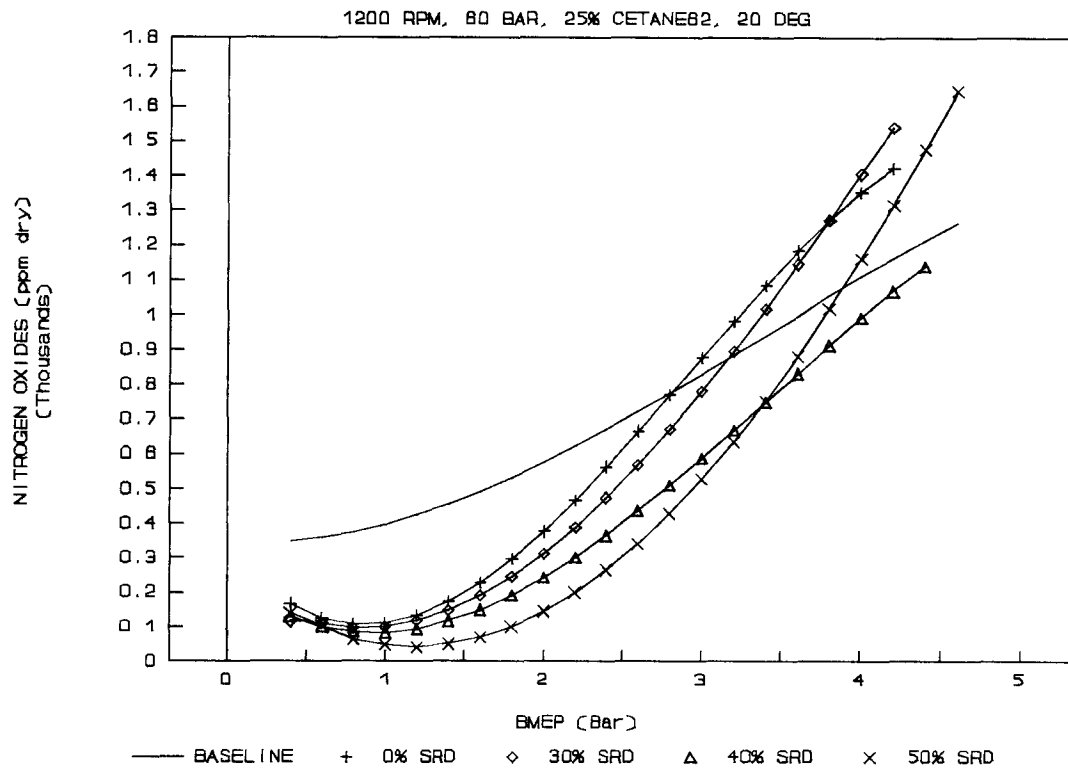
Figure 5.8: Effect of Fuel Jet Interruption Ratio on Nitrogen
Oxides.

emissions. But NO$_x$ emission does not depend on combustion
temperature only, it also depends on combustion duration time and
air concentration in the cylinder. If the air concentration is
constant and the fuel combustion rate could be increased (ie.
reduce combustion duration) in some way, we could still obtain
higher thermal efficiency with lower NO$_x$ emission. The 40% SRD case
might be an example of this condition - for which highest thermal
efficiency in the gas-diesel operation is not associated with
highest NO$_x$.
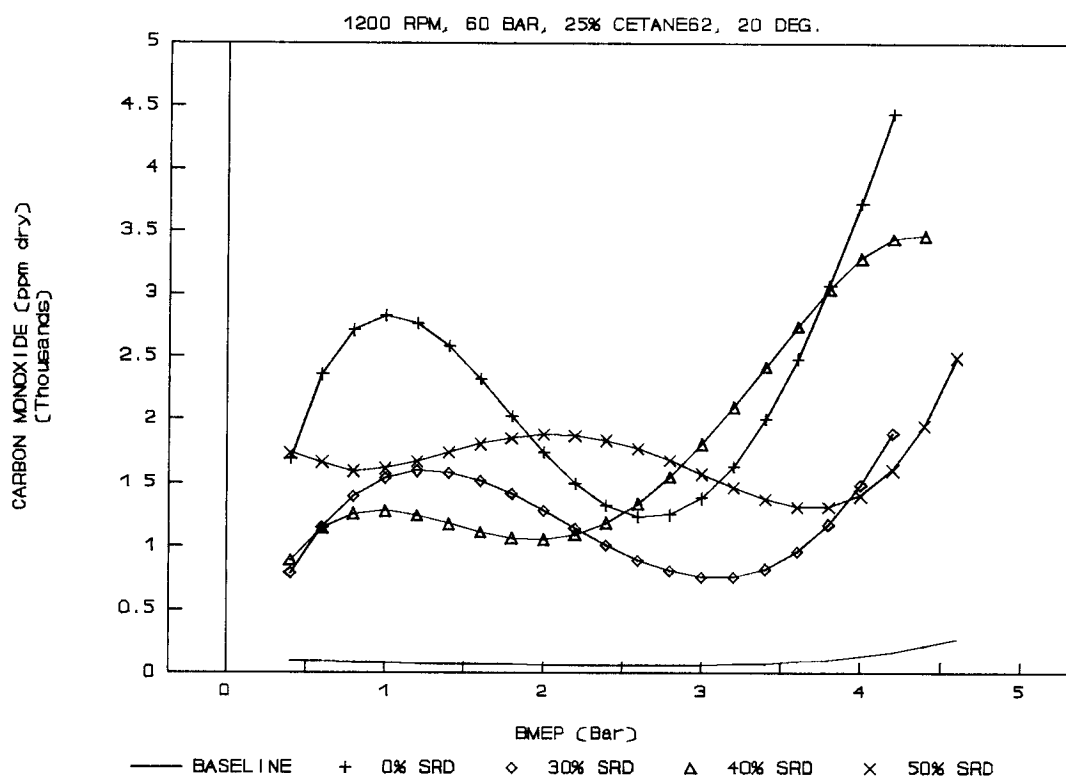
Figure 5.9: Effect of Fuel Jet Interruption Ratio on Carbon Monoxide.

It can also be seen in Figure 5.9 that the carbon monoxide emissions in all cases are much higher than that of the diesel baseline (average about 10 times higher). This suggests that the combustion in all cases took place in locally rich regions.

Fuel Injection Angle:



1200 RPM, 60 BAR, 25% CETANE62, 50% SRD
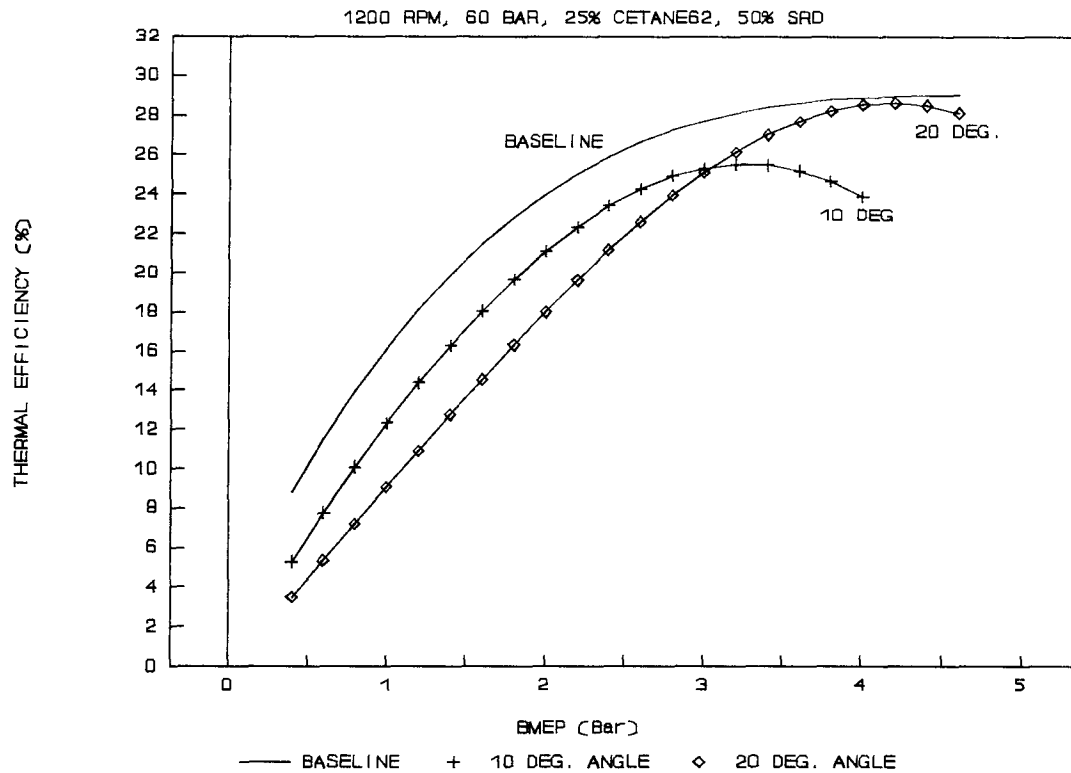
Figure 5.10: Effect of Fuel Injection Angle on Performance
with 50% Shrouding.

Tests were undertaken using two injection angles with four jet
interruption cases. Test condition was 1200 rpm speed, 60 bar CNG
injection pressure, and 25% CN62 pilot-diesel energy ratio. In this
discussion, two typical jet interruption cases (50% SRD and 30%
SRD) were selected as representative of all situations.
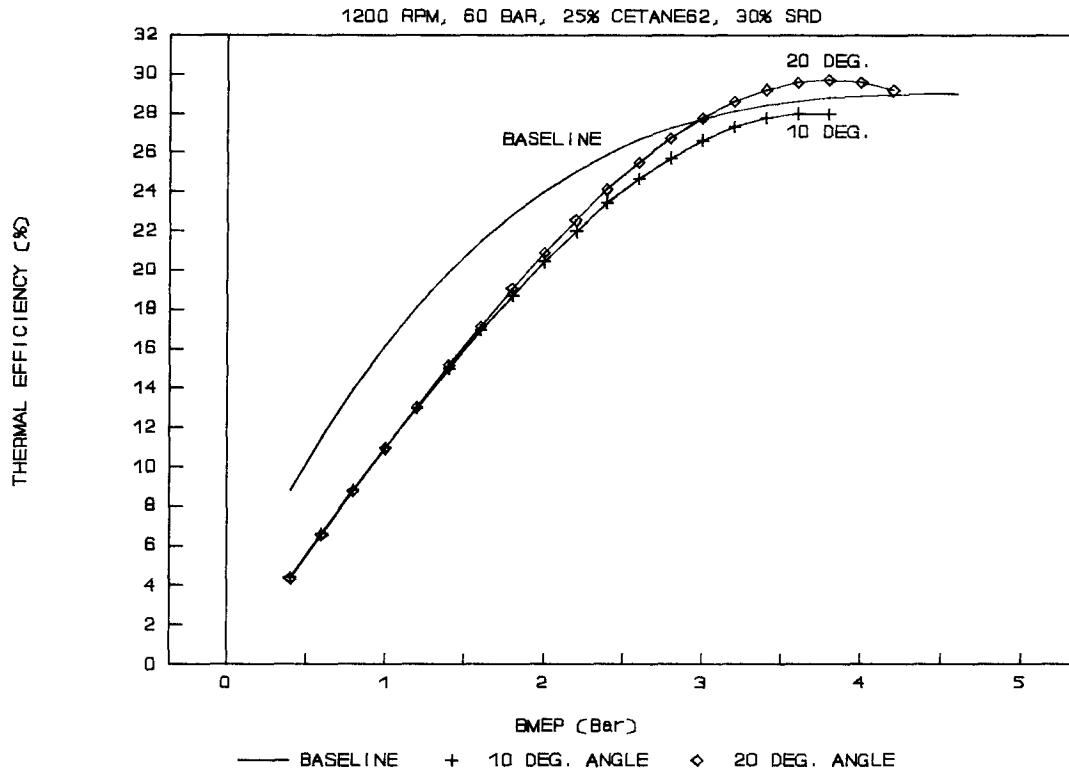
Figure 5.11: Effect of Fuel Injection Angle on Performance with 30% Shrouding.

Figures 5.10 and 5.11 show the effects of fuel injection angle on thermal efficiency with the 50% and the 30% SRD respectively. In the 50% SRD case, operation with the 10° angle provides better thermal efficiency at low and medium load, but much lower peak thermal efficiency and lower maximum load capability than operation with the 20° angle; and vice versa. In the 30% SRD case, the 10° angle loses its advantage at low load, but retains its

disadvantages at high load; the 20° angle becomes dominant over the whole load range.
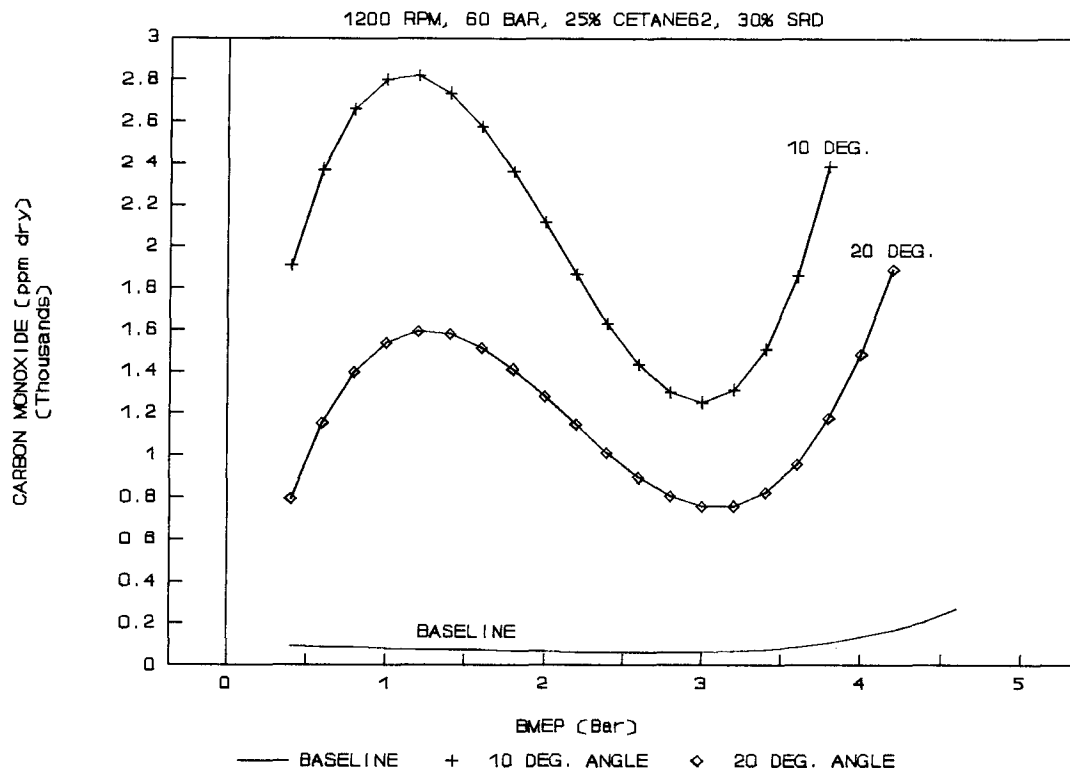


Figure 5.12: Effect of Fuel Injection Angle on Carbon Monoxide.

The reason for that can be explained with the flow visualization results [42] (see Appendix G) and carbon monoxide emission results in Figure 5.12. The fuel jets with the 10° angle tend to cling to the top wall (ie. top wall effect), so that the jet penetration has been reduced, but the 20° angle jets do not.

In the 50% SRD case, large jet interruption increases the penetration of the 20° angle jets more than that of the 10° angle jets, so that the 10° angle jets have less dissipation and burn with locally richer mixtures than the 20° angle jets do. Therefore, operation with the 10° angle provides better thermal efficiency at low and medium load. However, longer penetration of the 20° angle jets still improves peak thermal efficiency and maximum load capability at high load.

The jet penetration is believed to have been reduced when the jet interruption ratio decreased to 30% SRD. Thus the 10° and the 20° angle jets have similar behaviour at low load. But the top wall effect at 10° angle still influences the peak thermal efficiency and maximum load capability at high load. The differences of thermal efficiency and maximum load capability between the 10° and the 20° angle jets, however, have been reduced in the 30% SRD case, which indicates that reducing the top wall effect is associated with decreasing the jet interruption ratio.

The effect of fuel injection angle on carbon monoxide is shown in Figure 5.12. It is observed that operation with the 10° angle produces more carbon monoxide emission than with the 20° angle, which suggests that the top wall effect of the 10° angle may have caused locally rich-mixture burning and top wall quenching.
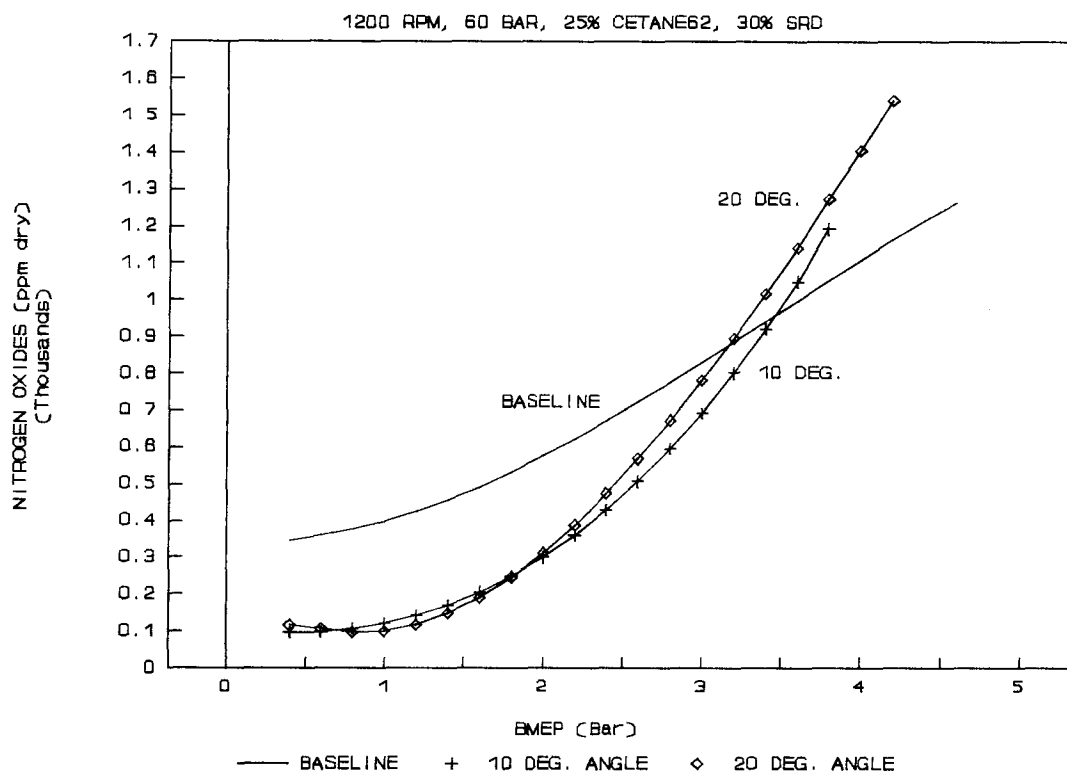
Figure 5.13: Effect of Fuel Injection Angle on Nitrogen Oxides.

It is also seen in Figure 5.13 that operation with the 20°
angle produces almost the same amount of nitrogen oxides emissions
as with the 10° angle at low load, but more at medium and high
load. These trends match the thermal efficiency trends in Figure
5.11.

Figure 5.14 shows the effect of fuel injection angle on
unburned methane emission. Unburned methane emission comes mainly
from CNG fuel, and it is a measurement of the amount of CNG fuel
surviving combustion. It is observed that operation with the 10°
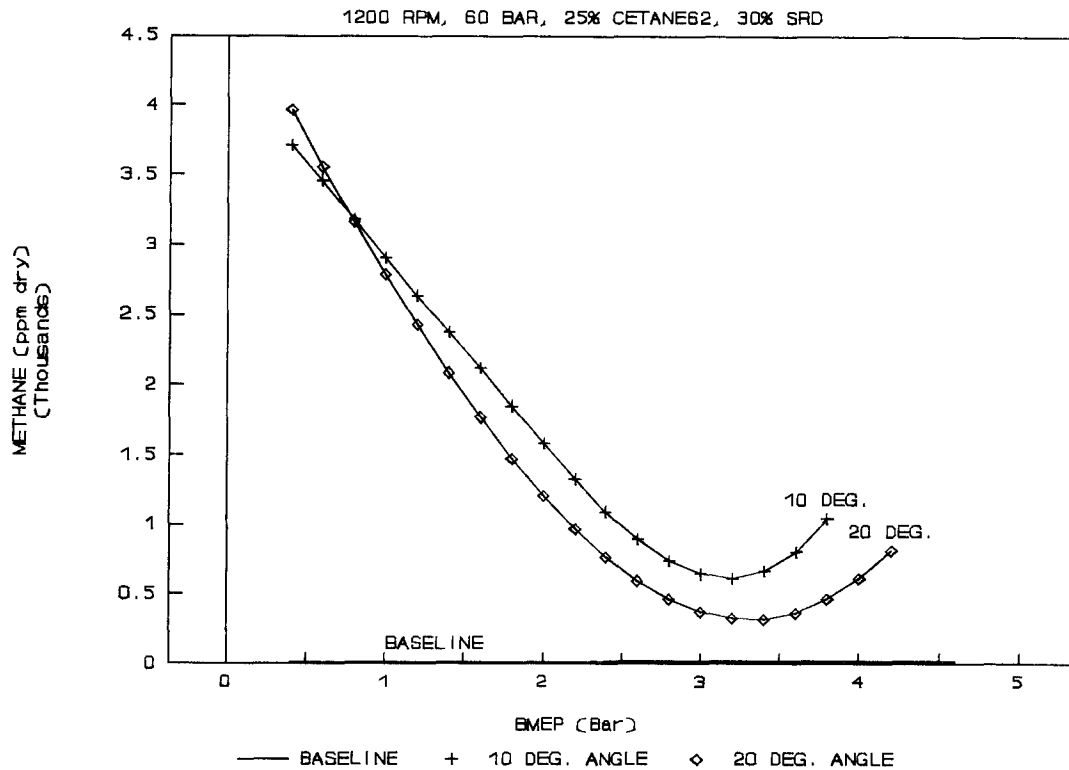
Figure 5.14: Effect of Fuel Injection Angle on Methane.

angle produces almost the same amount of unburned methane emission as with the 20° angle at low load (BMEP ~ 0.8 bar), 50% more unburned methane emission than with the 20° angle at medium load (BMEP ~ 2.5 bar) and 100% more unburned methane emission than with the 20° angle at high load (BMEP ~ 3.5 bar). These trends also match the thermal efficiency trends in Figure 5.11.

The effect of the fuel injection angle on non-methane hydrocarbon emission is shown in Figure 5.15. Non-methane hydrocarbon emission primarily results from incomplete combustion of pilot-diesel fuel and lubrication oil (the latter probably being
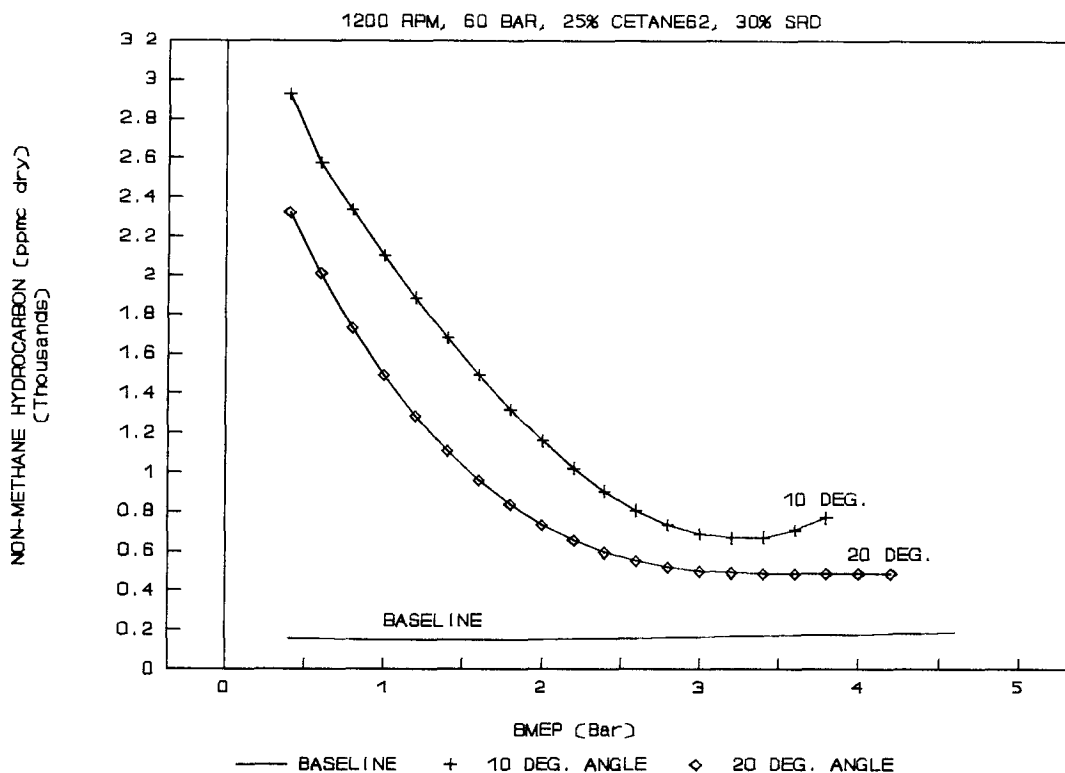
Figure 5.15: Effect of Fuel Injection Angle on Non-Methane Hydrocarbon.

negligible). It is thus a measurement of the amount of pilot-diesel fuel surviving combustion. As shown, operation with the 10° angle produces more non-methane hydrocarbon emission than with the 20° angle over the whole load range, which suggests that the pilot-diesel was not atomized well or did not mix sufficiently with air (ie. burned too rich), or that top wall quenching was significant, or that the gas-air mixture was too lean because of very long ignition delay. This agrees with the carbon monoxide trends in Figure 5.12. The total hydrocarbon emission is the sum of unburned

methane and non-methane hydrocarbon emissions.

## 5.4 Effect of Engine Operating Parameters

In this section, the effects of engine operating parameters on gas-diesel engine performance and emissions are presented. The order of presentation is pilot-diesel cetane number, pilot-diesel/total fuel energy ratio (diesel ratio), CNG injection pressure and engine speed. The emission results presented here are dry-basis.

### Pilot-Diesel Cetane Number:

Two different pilot-diesel fuels with different cetane numbers were tested. They were cetane number 62 diesel (CN62) and commercial grade 2 diesel (DF2). The cetane number of DF2 is approximate 45. Test condition was 1200 rpm speed, 60 bar CNG injection pressure, 25% of pilot-diesel energy ratio, 20° fuel injection angle, and 0% SRD.

Usually, diesel engines perform better (ie. obtain higher thermal efficiency) when the fuel burns evenly. Combustion should begin as soon as possible after injection instead of lagging until pressure, temperature, and the accumulation of fuel build up to a point conducive to detonation. For a given engine at a given speed and load, the ignition delay time depends on the ignition quality of the fuel. Diesel cetane number represents the ignition quality of the fuel. The higher the cetane number of a diesel fuel, the better its ignition quality.

1200 RPM, 60 BAR, 20 DEG. ANGLE, 0% SRD
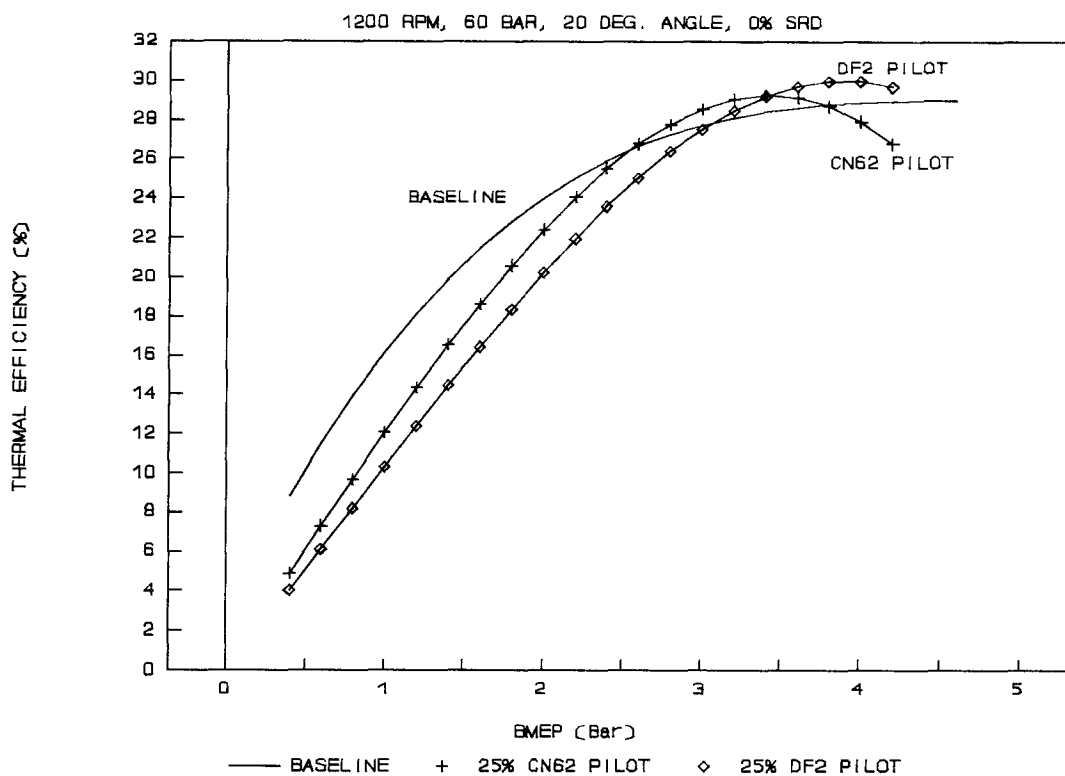
Figure 5.16: Effect of Pilot-Diesel Cetane Number
on Performance.

Figure 5.16 shows the effect of pilot-diesel cetane number on
thermal efficiency. As shown, operation with the CN62 pilot-fuel
provides better thermal efficiency in the load range of BMEP from
0.4 ~ 3.5 bar; the thermal efficiency with the DF2 pilot-fuel
exceeds that with the CN62 pilot-fuel from BMEP equalling 3.5 bar;
there are almost identical maximum load capabilities for operation
with both pilot-fuels.

**1200 RPM, 60 BAR, 20 DEG. ANGLE, 0% SRD**

METHANE (ppm dry) (Thousands)

DF2 PILOT

CN62 PILOT

BASELINE

BMEP (Bar)

———— BASELINE    +  25% CN62 PILOT    ◇  25% DF2 PILOT
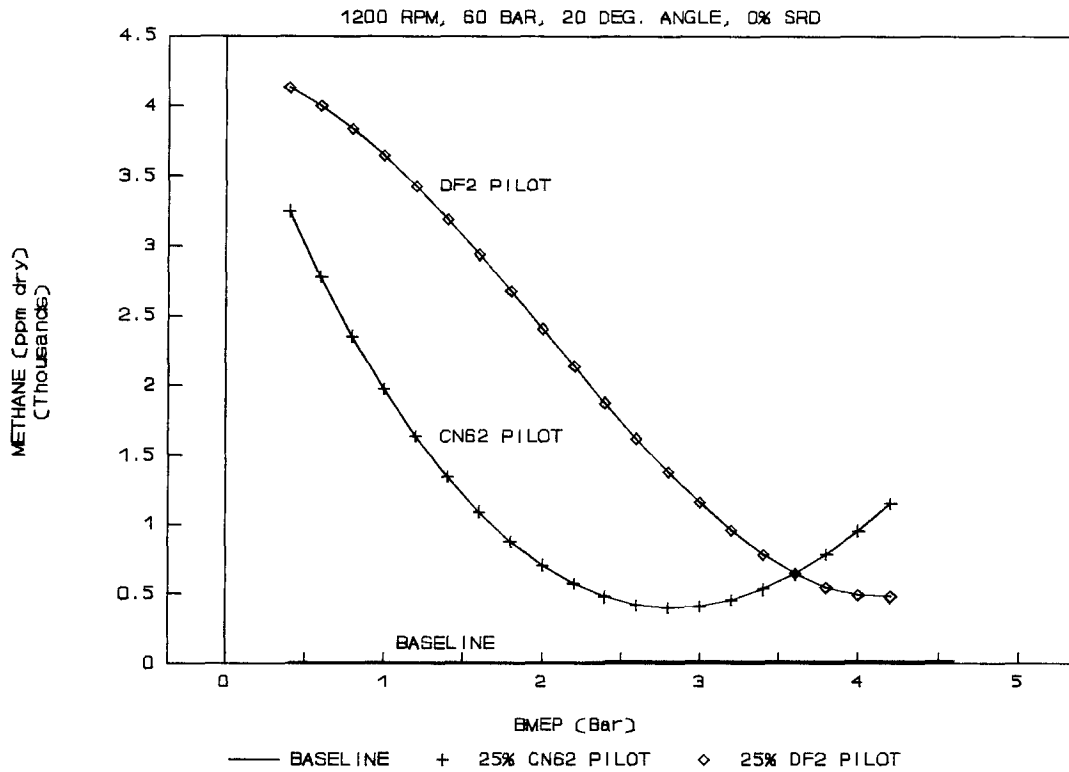
Figure 5.17: Effect of Pilot-Diesel Cetane Number
on Methane.

It is believed that the ignition delay time is relatively long when the engine operates at low and medium load. The good ignition quality of the CN62 pilot-fuel reduces the ignition delay time and the combustion delay time of fuel, thereby the fuel combustion is improved and the thermal efficiency is high. This is consistent with the lower methane and non-methane hydrocarbon emissions shown in Figures 5.17 and 5.18, as well as the higher nitrogen oxides

emissions shown in Figure 5.19 for loads less than 3.5 bar. At loads greater than 3.5 bar, the lower thermal efficiency with the CN62 pilot-fuel may be caused by large amounts of fuel/air mixture burned before TDC.
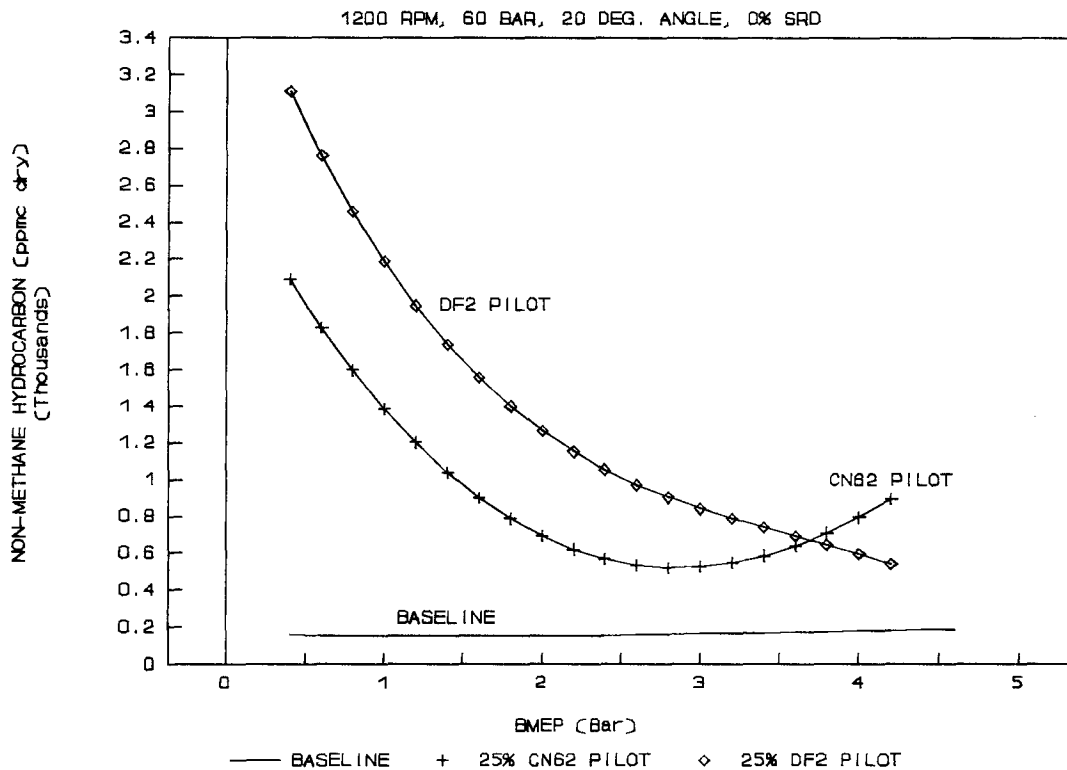


Figure 5.18: Effect of Pilot-Diesel Cetane Number
on Non-Methane Hydrocarbon.
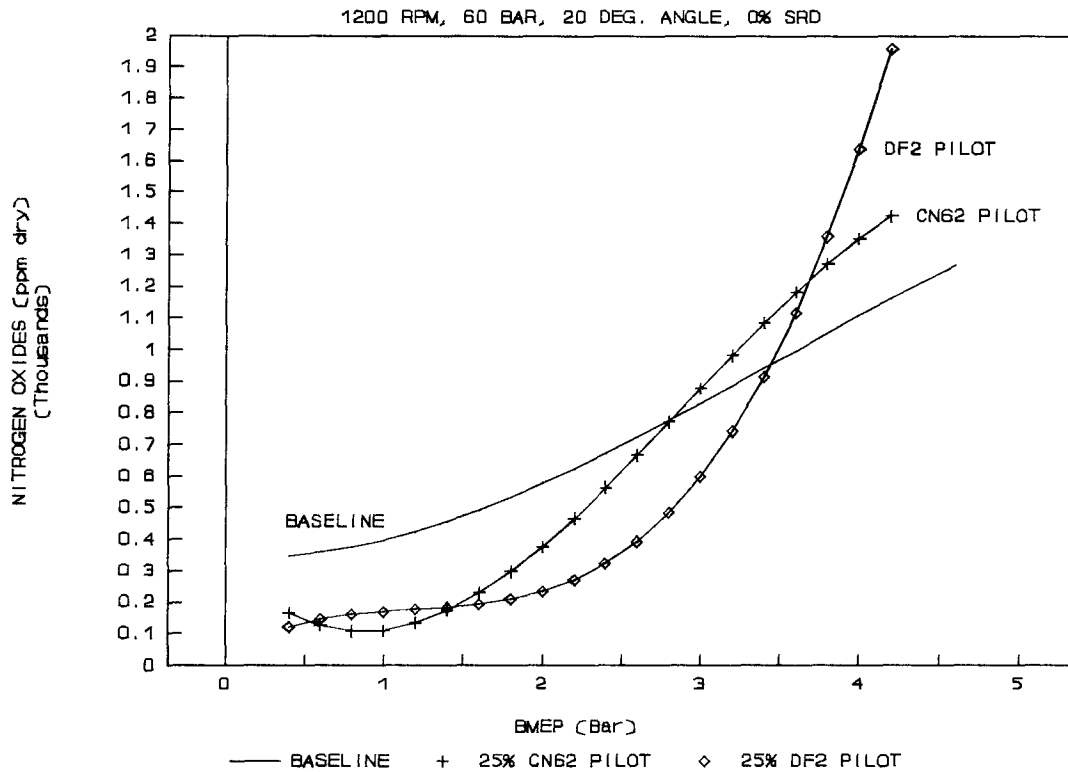
Figure 5.19: Effect of Pilot-Diesel Cetane Number
on Nitrogen Oxides.

## Pilot-Diesel/Total Fuel Energy Ratio (Diesel Ratio):

Tests were performed with three different diesel (DSL) ratios 25%, 20% and 15% in almost all jet interruption cases. Test condition was 1200 rpm speed, 60 bar CNG injection pressure, CN62 pilot-diesel fuel, and 20° fuel injection angle.
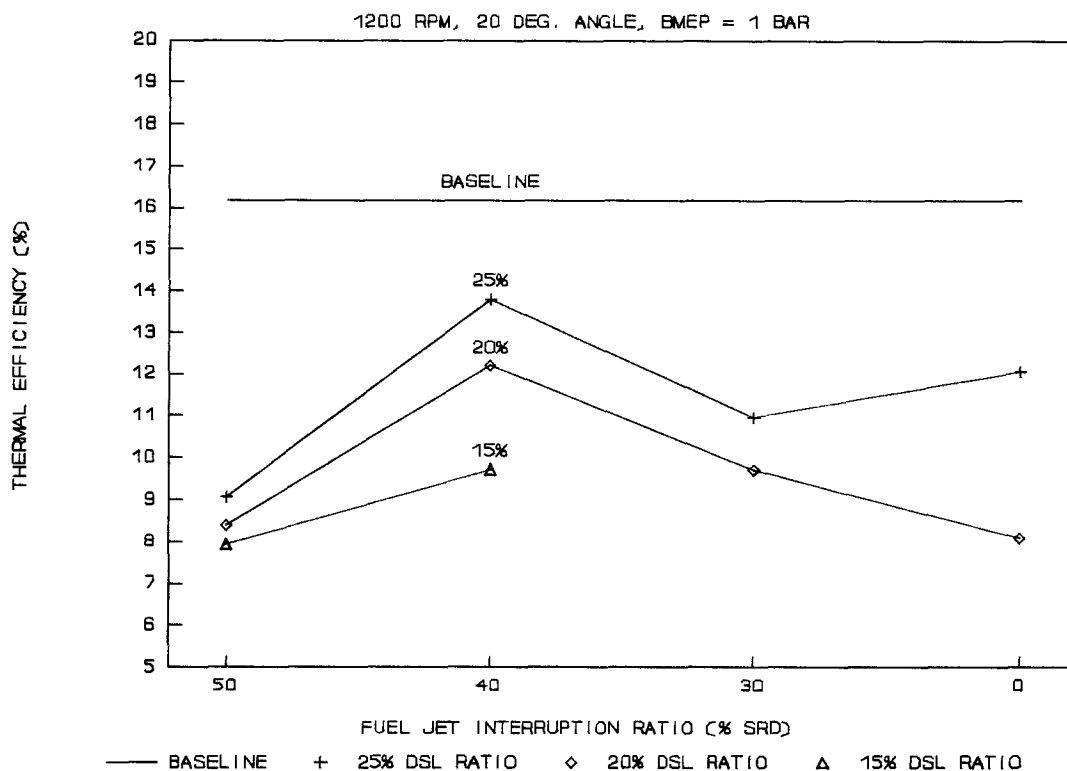
Figure 5.20: Effect of Diesel Ratio on Thermal Efficiency
at Low Load (BMEP = 1 BAR).

Figures 5.20 and 5.21 show the effects of diesel ratio on thermal efficiency and total hydrocarbon at low load (BMEP = 1 bar) respectively. The figures appear to indicate that poor low-load combustion quality was one of the serious problems with this injector configuration for gas-diesel operation in this engine. As illustrated, operation with high diesel ratio (ie. 25% DSL ratio) provides high thermal efficiency and low total hydrocarbon at low load through all jet interruption cases. The tests with the 15% DSL

ratio with 0% SRD and 30% SRD were not done, because of excessive misfiring, especially at low load.
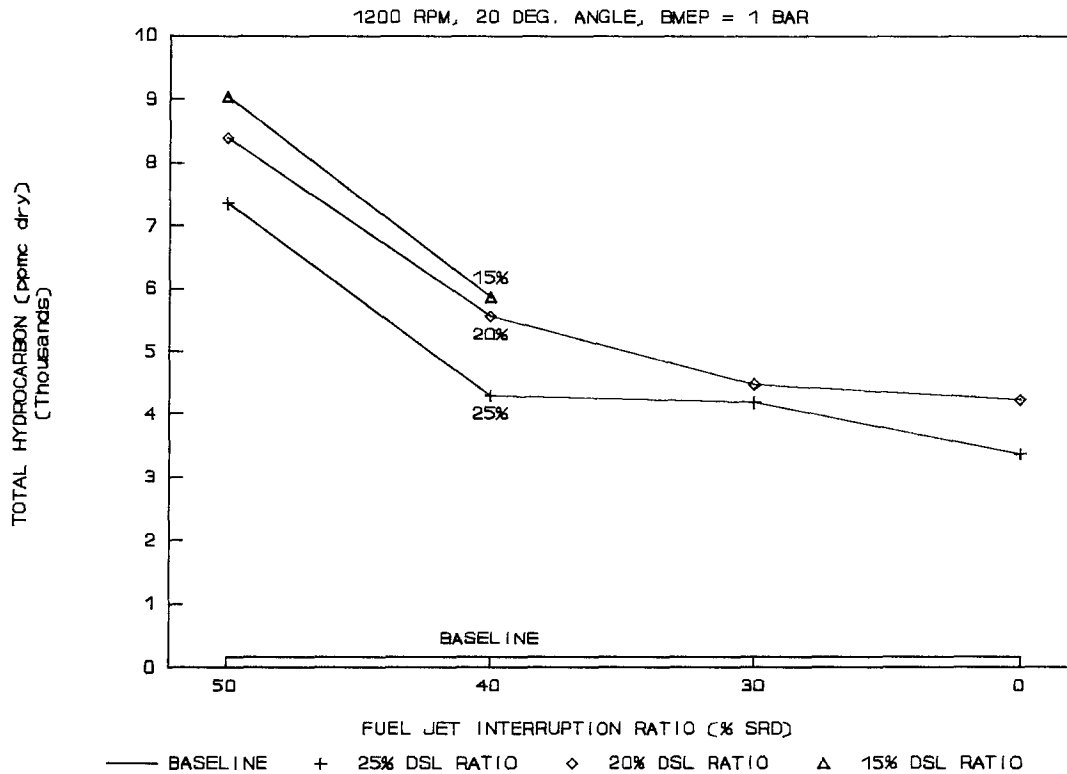


Figure 5.21: Effect of Diesel Ratio on Total Hydrocarbon at Low Load (BMEP = 1 BAR).

As discussed in Section 2.2, CNG fuel will not self-ignite in the typical diesel engine cylinder environment because of the high self-ignition temperature (~ 1200 K [5]) of CNG fuel. A minimum amount of pilot-diesel injected into the cylinder is necessary to heat the CNG fuel to its auto-ignition temperature. The amount of pilot-fuel depends on intake state, compression ratio, distribution
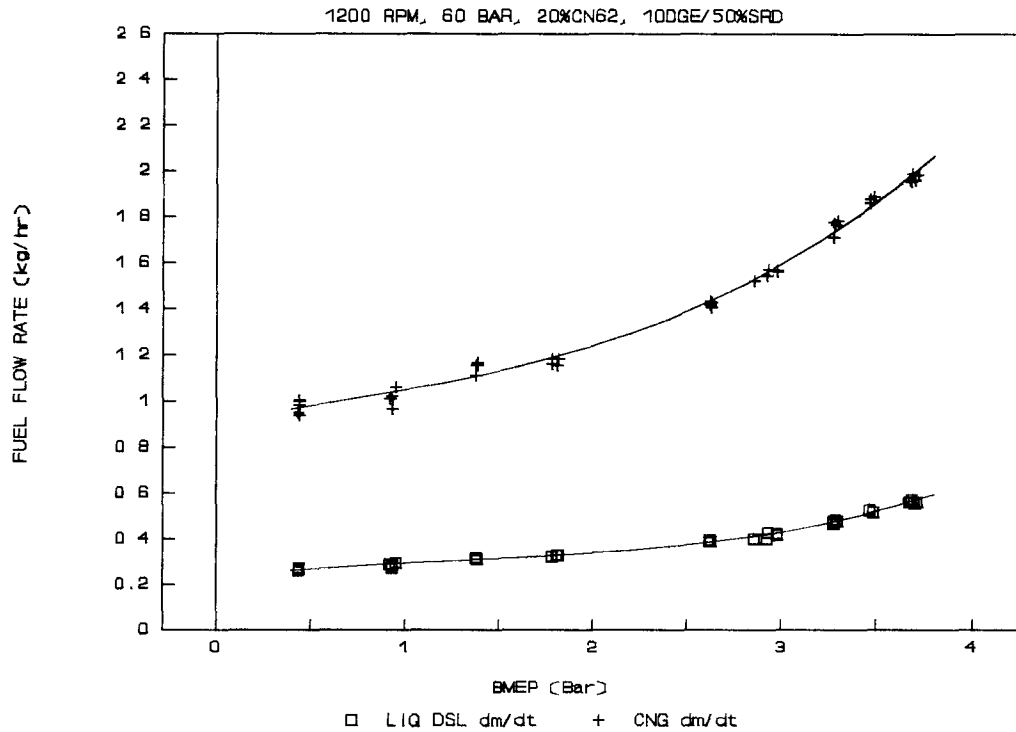
Figure 5.22: Relationship between Mass Flow Rate of the Fuels and Load.

of pilot-diesel and CNG fuels and load of a given engine. Generally speaking, the quantity of pilot-diesel that is necessary to heat the CNG fuel to its auto-ignition temperature could be expected to be approximately constant over the whole load range, thus the diesel ratio would become high at low load and reduced with increased load (when more CNG fuel is injected). Figure 5.22 shows the relationship between mass flow rate of the fuels (CNG and pilot-diesel) and load (BMEP). The test case was 1200 rpm speed, 60 bar CNG injection pressure, 25% CN62 pilot-diesel energy ratio, 20°

fuel injection angle and 50% jet interruption ratio. As shown, diesel mass flow rate remains almost constant at low and medium load, and increases slightly at high load.
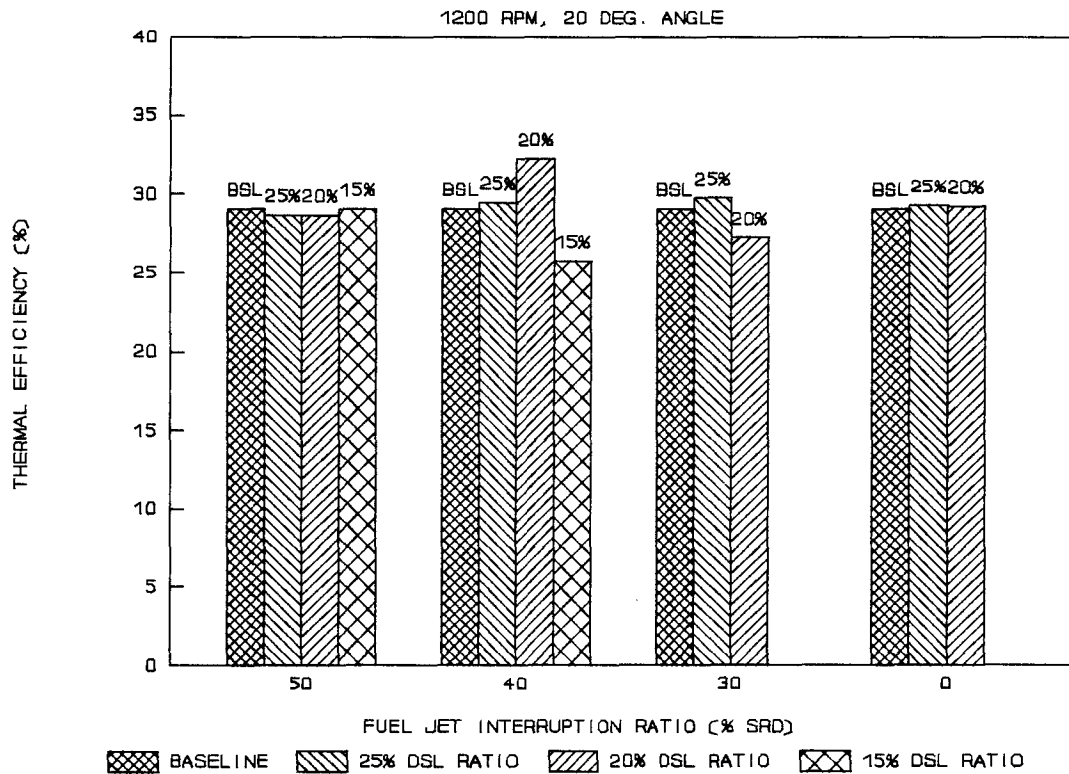


Figure 5.23: Effect of Diesel Ratio on Maximum Thermal Efficiency.

As shown in Figures 5.23 and 5.24 respectively, the effects of diesel ratio on peak thermal efficiency and maximum load capability are associated with the jet interruption ratio (ie. the penetration and distribution of the fuel). For the large jet interruption ratio, low diesel ratio (15% DSL ratio) improves peak thermal efficiency and maximum load capability; High diesel ratio (25% DSL
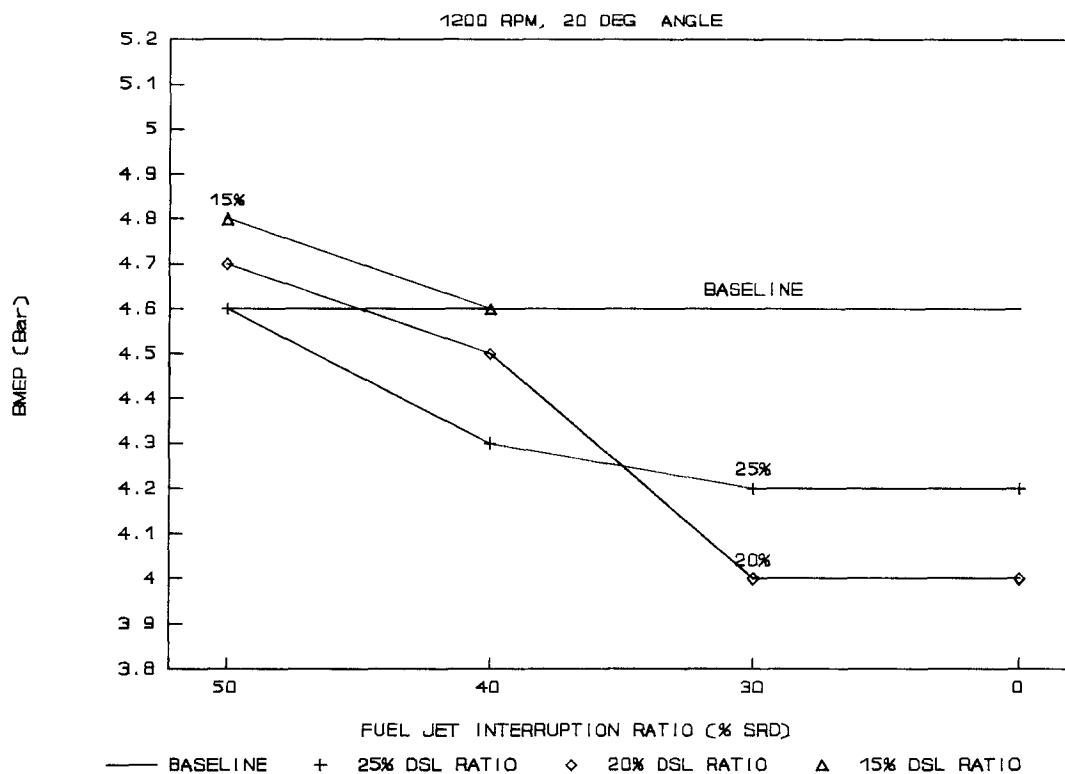
Figure 5.24: Effect of Diesel Ratio on Maximum Load
Capability.

ratio) dominates peak thermal efficiency and maximum load
capability at small jet interruption ratio (from 30% SRD).

one can also see in Figure 5.25 that higher diesel ratio
produces higher nitrogen oxides emissions at high load. From
Figures 5.20 and 5.21, we also see that high diesel ratio produces
high nitrogen oxides emissions at low load.
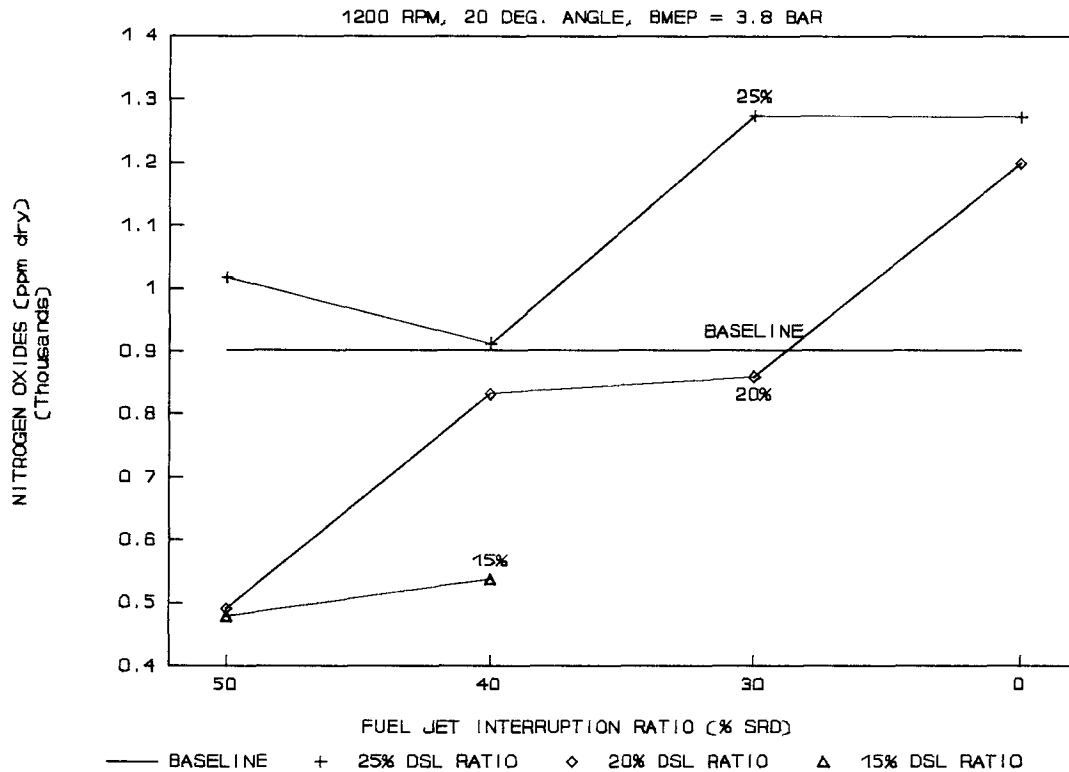
Figure 5.25: Effect of Diesel Ratio on Nitrogen Oxides
at High Load (BMEP = 3.8 BAR).

## CNG Injection Pressure:

Tests were conducted with different CNG injection pressures and different injection angle. Test condition was 1200 rpm speed, 60 bar CNG injection pressure, and 25% CN62 pilot-diesel energy ratio.
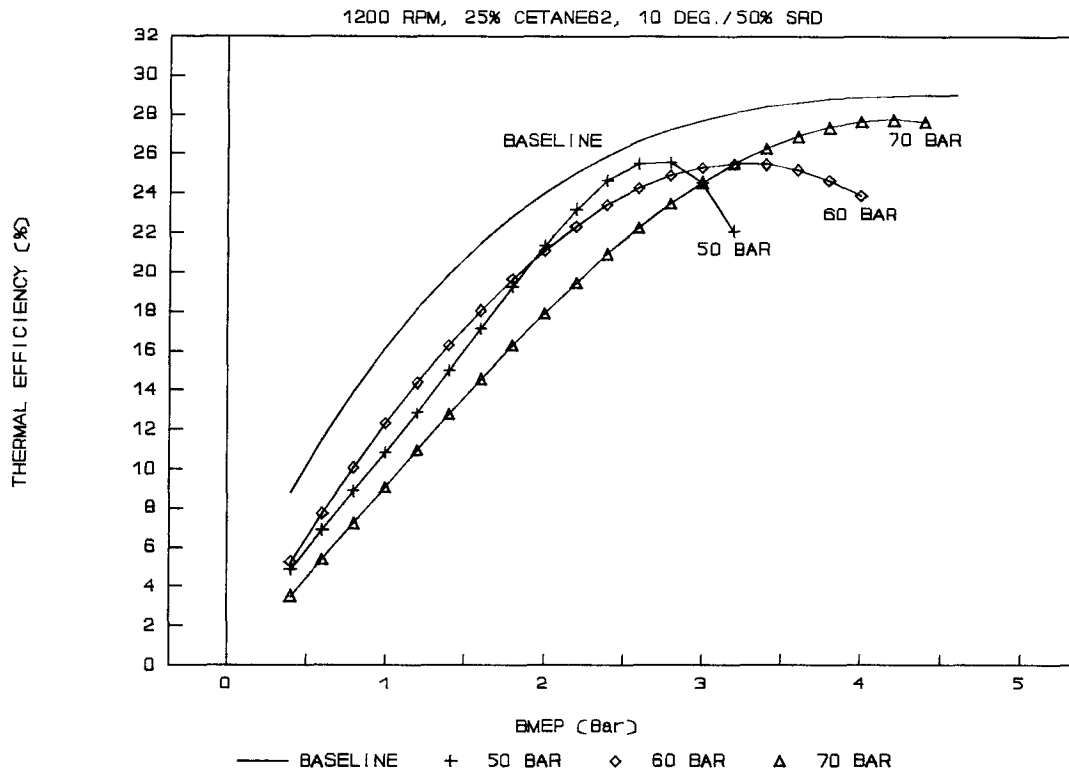
Figure 5.26: Effect of CNG Injection Pressure on Performance with 10 DEG. Injection Angle.

Figure 5.26 and 5.27 show the effects of CNG injection pressures on thermal efficiency with 10° and 20° injection angles respectively. Operation with high CNG injection pressure improves peak thermal efficiency and maximum load capability; The maximum achievable CNG injection pressure with 20° injection angle (80 bar) is higher than that with 10° injection angle (70 bar); Similar to the effect of jet interruption ratio, there is an optimum CNG injection pressure for both injection angles. As shown in Figure 5.26, the optimum pressure for 10° injection angle is 60 bar, which
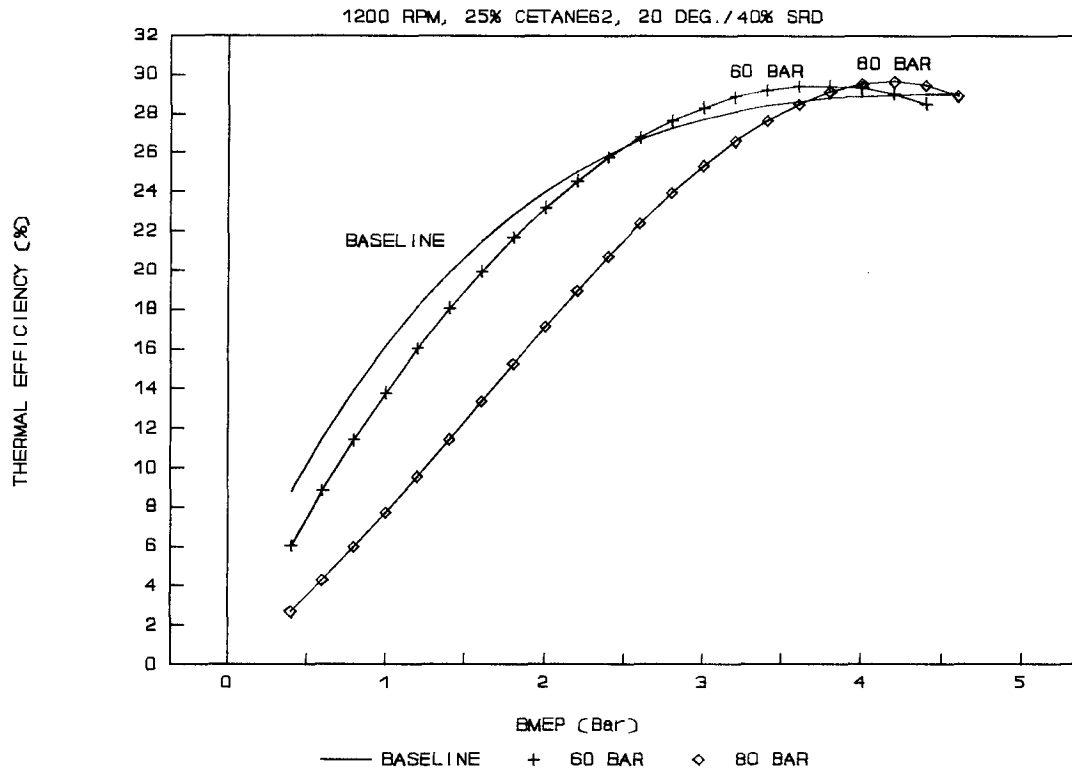
Figure 5.27: Effect of CNG Injection Pressure on Performance with 20 DEG. Injection Angle.

provides good thermal efficiency at the load range of BMEP before 2 bar and relatively good thermal efficiency at medium and high load. In Figure 5.27, 60 bar appears to be the optimum pressure for the 20° injection angle. If there were a curve for 50 bar in Figure 5.27, it could expected to be similar to the 10° injection angle curve in Figure 5.26.

The explanation of the effect of CNG injection pressure on performance is also similar to that of jet interruption ratio. That is, higher CNG injection pressure increases the fuel jet

penetration and injection speed, so that it improves the high-load thermal efficiency and maximum load capability but deteriorates the low-load and medium-load thermal efficiency, and vice versa.
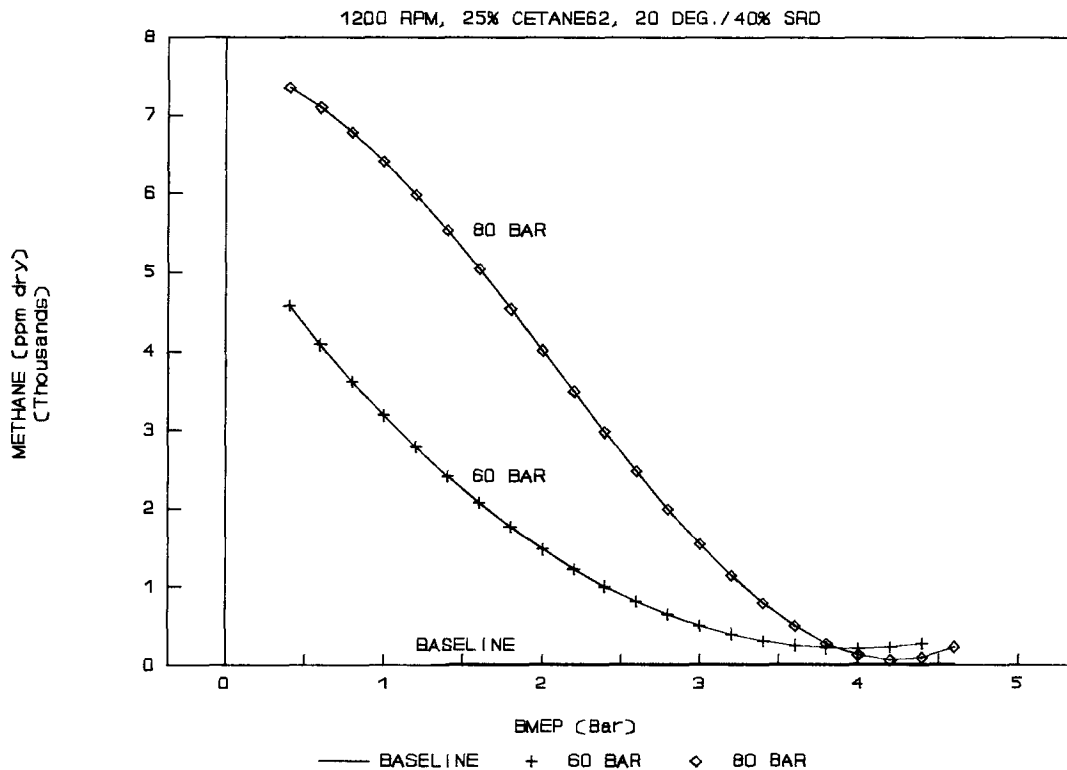


Figure 5.28: Effect of CNG Injection Pressure on Methane.

Considering the requirements of fuel jet penetration, it is reasonable to expect an optimum CNG injection pressure for a given engine which matches the internal cylinder pressure trace (or distribution) and provides appropriate thermal efficiency over the whole load range. The internal cylinder pressure trace (without combustion) for a given engine is fixed, depending only on intake

state (ie. natural aspiration or turbocharging) and compression
ratio of the given engine.

1200 RPM, 25% CETANE62, 20 DEG./40% SRD

NON-METHANE HYDROCARBON (ppmc dry) (Thousands)

BMEP (Bar)

—— BASELINE    + 60 BAR    ◇ 80 BAR
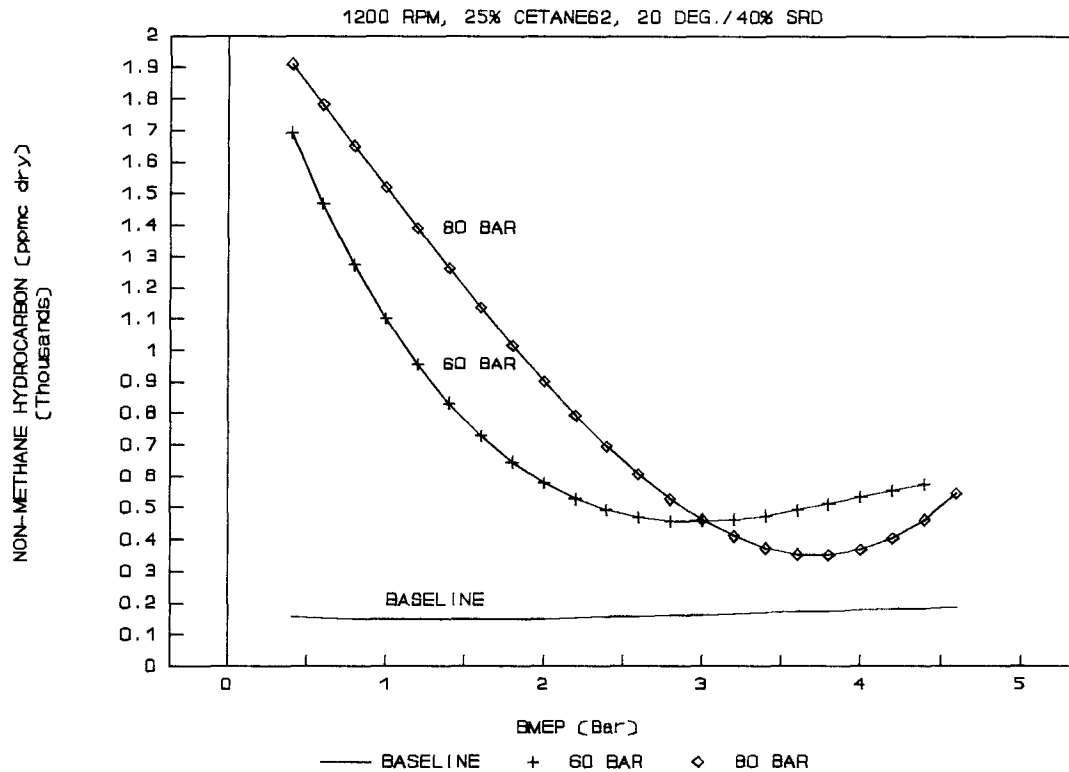
Figure 5.29: Effect of CNG Injection Pressure on Non-Methane
          Hydrocarbon.

The effects of CNG injection pressure on unburned methane and
non-methane hydrocarbon emissions (with 20° injection angle) are
shown in Figures 5.28 and 5.29 respectively. It is observed that 80
bar CNG injection pressure is too high for operating at low and
medium load. High injection pressure disperses the fuel jet and
causes higher methane and non-methane hydrocarbon emissions.
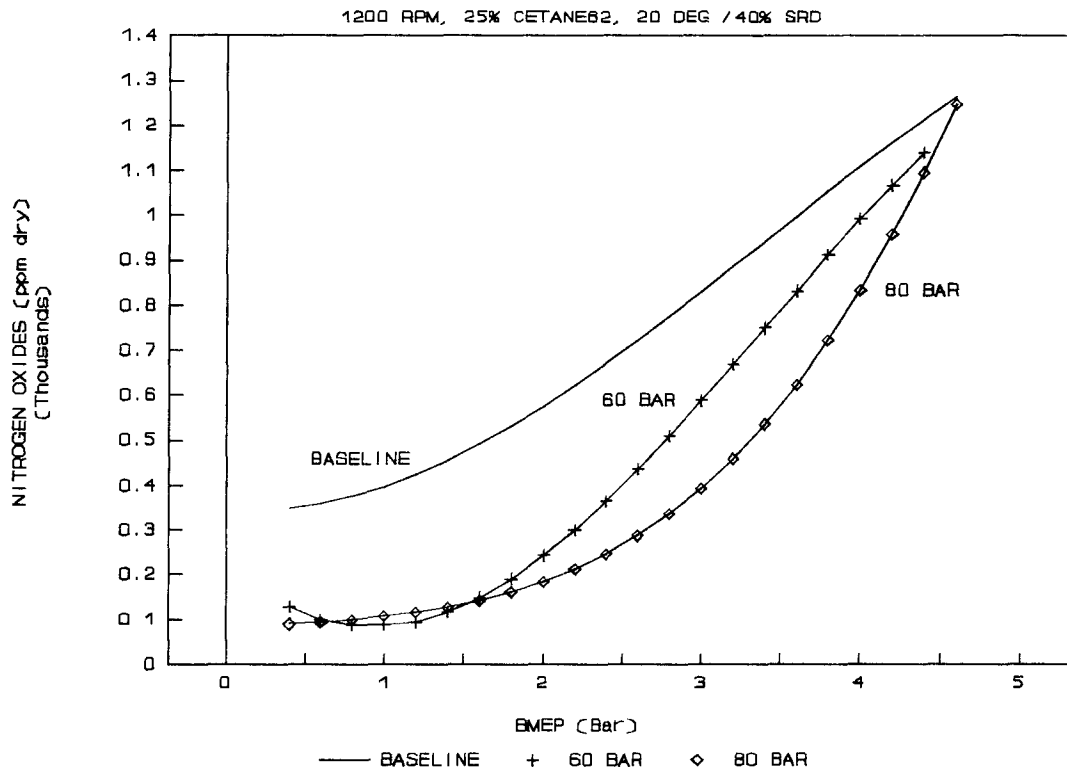
Figure 5.30: Effect of CNG Injection Pressure on Nitrogen Oxides.

Figure 5.30 shows that both pressure cases produce almost the same nitrogen oxides emissions at low load; high CNG pressure produces less nitrogen oxides at medium and high load.

The effect of CNG injection pressure on best operating BOI is shown in Figure 5.31. It is interesting to see that, with higher CNG injection pressure, the engine is able to run with smaller BOI.
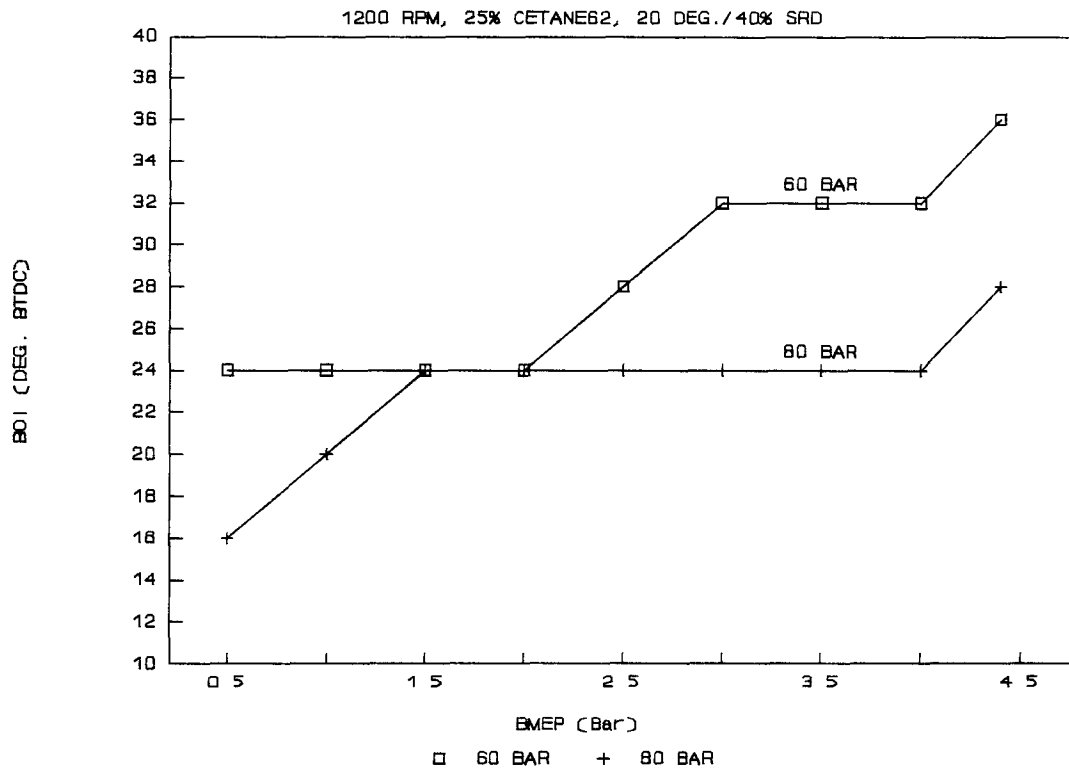
Figure 5.31: Effect of CNG Injection Pressure on BOI.

Engine Speed:

Tests were conducted with engine speeds of 1200 rpm and 1400 rpm. Test condition was 60 bar CNG injection pressure, 25% CN62 pilot-diesel energy ratio, 20° fuel injection angle, and 30% SRD.

Figure 5.32 shows the effect of the engine speed on thermal efficiency. As can be seen, operation with 1400 rpm provides slightly better thermal efficiency than with 1200 rpm at low load; however, much better thermal efficiency is obtained by operating with 1200 rpm at medium and high load.

60 BAR, 25% CETANE62, 20 DEG./30% SRD
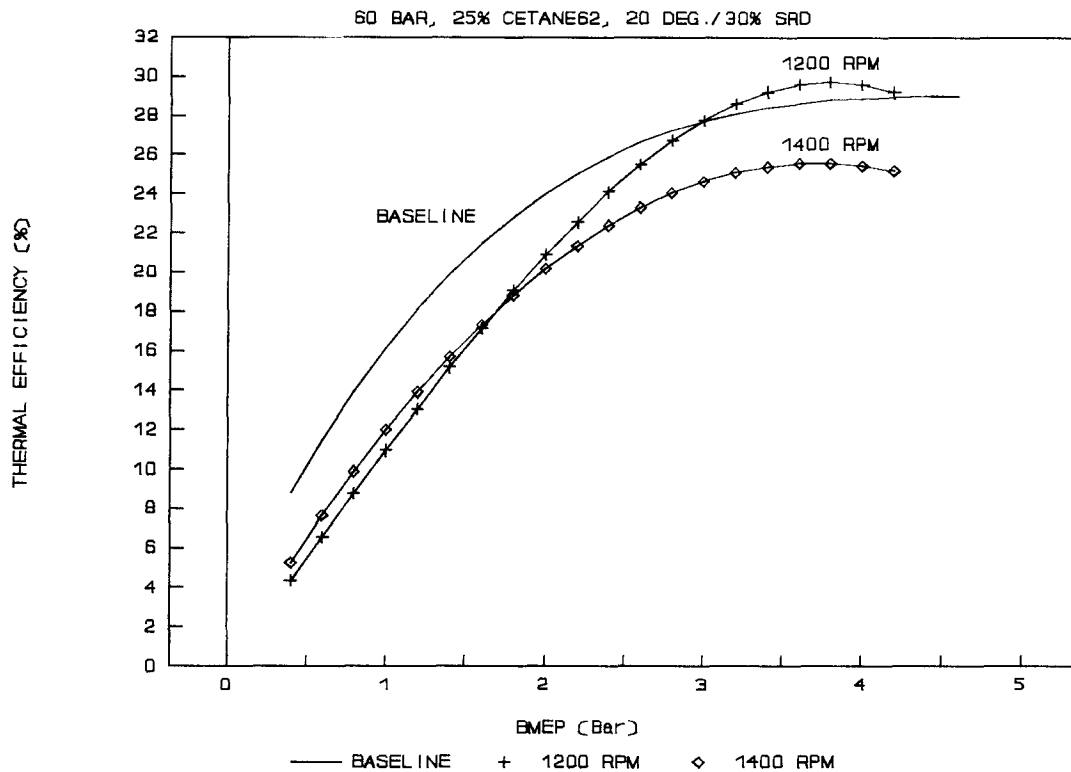


Figure 5.32: Effect of Engine Speed on Performance.

Usually, thermal efficiency is affected by engine speed through load and heat transfer. At low load, operating at 1400 rpm may have less heat loss (per unit time) than at 1200 rpm, thereby increasing thermal efficiency slightly. At medium and high load, operating at 1400 rpm the combustion duration (counted by degree crank angles) is longer than at 1200 rpm. More heat loss (per unit area) and power loss, resulting from longer combustion duration, reduce the thermal efficiency at 1400 rpm.

60 BAR, 25% CETANE62, 20 DEG./30% SRD
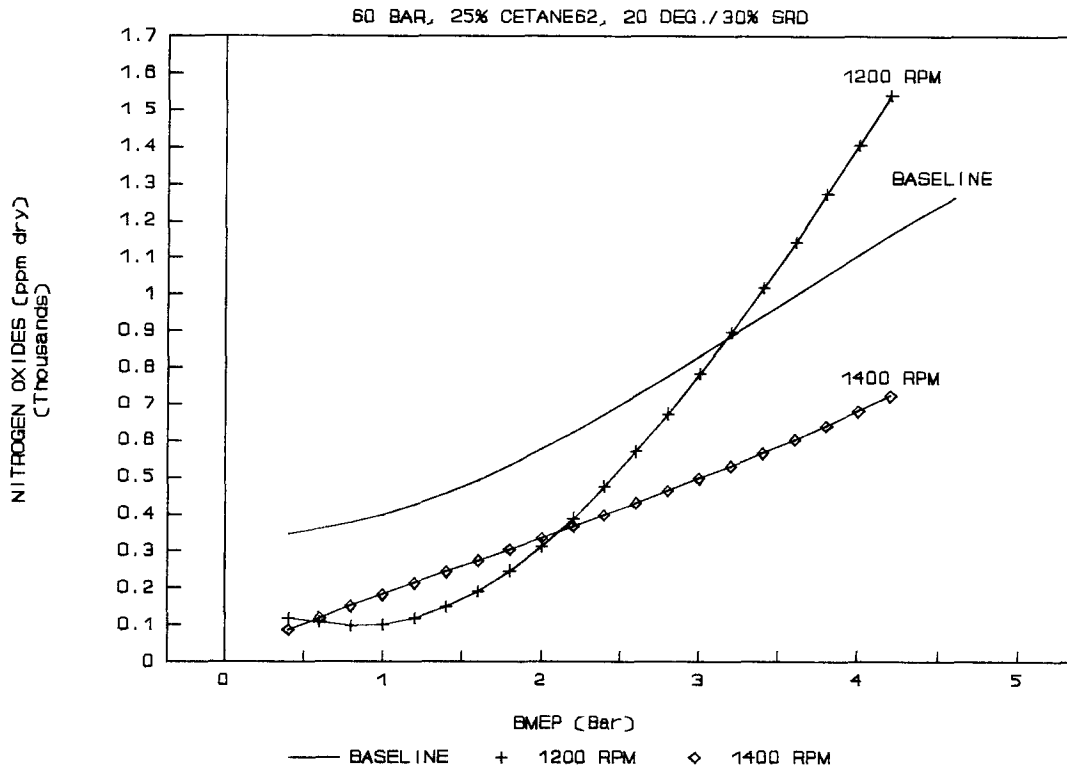
Figure 5.33: Effect of Engine Speed on Nitrogen Oxides.

The effect of engine speed on nitrogen oxides emissions is shown in Figure 5.33. As can be seen from this figure, at 1400 rpm and low load slightly higher nitrogen oxides emissions are associated with slightly higher thermal efficiency. The large difference in nitrogen oxides emissions between 1200 rpm and 1400 rpm at medium and high load is also consistent with the thermal efficiency difference.
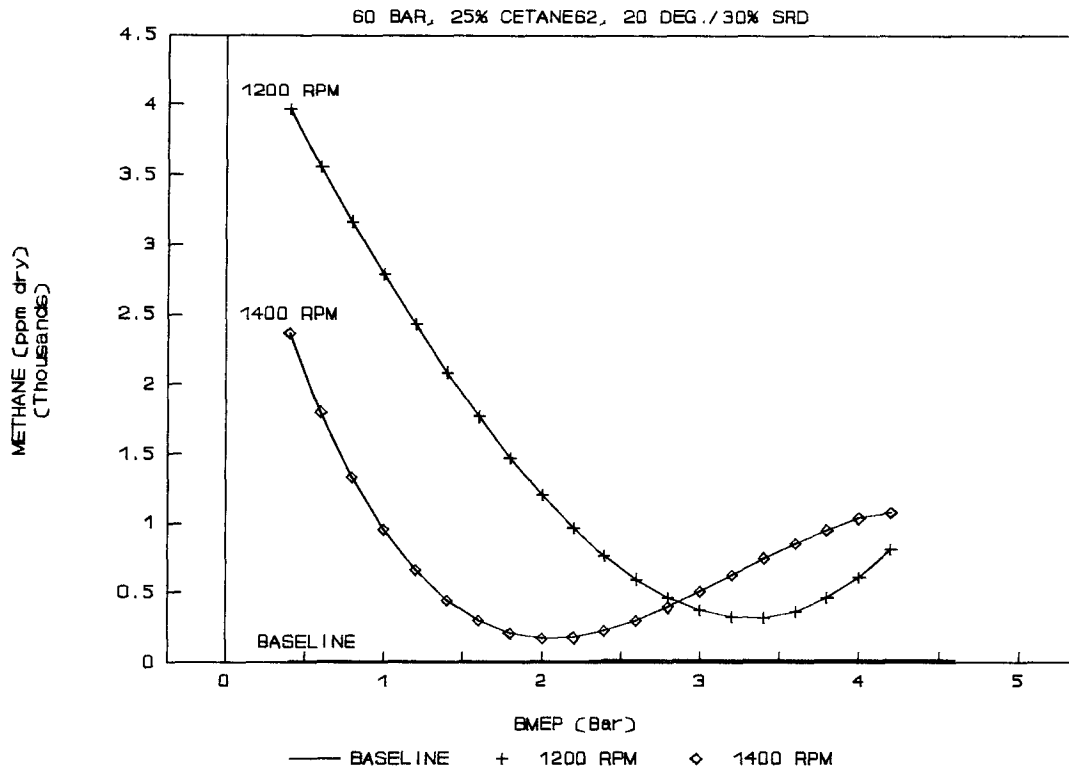
Figure 5.34: Effect of Engine Speed on Methane.

Figure 5.34 shows the effect of engine speed on unburned methane emissions. As shown, operation at 1400 rpm obviously reduces unburned methane emission at low load; with increasing load, the unburned methane emission at 1400 rpm rises at medium load and eventually exceeds that of 1200 rpm at high load; the point at which unburned methane emission of 1400 rpm begins to rise corresponds to the point at where the thermal efficiency at this speed starts to suffer.
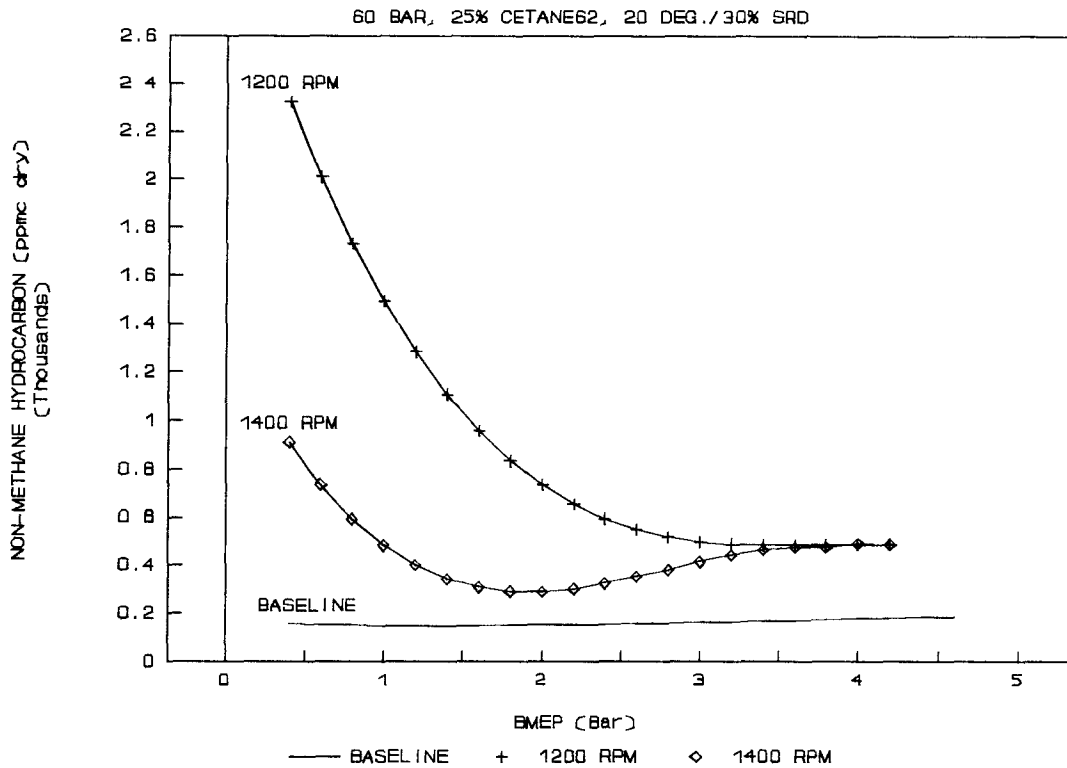
Figure 5.35: Effect of Engine Speed on Non-Methane Hydrocarbon.

Figure 5.35 shows that non-methane hydrocarbon emission at 1400 rpm and low load is much lower than that at 1200 rpm. The non-methane hydrocarbon emission of 1400 rpm ascends at the point corresponding to where the thermal efficiency of 1400 rpm starts to suffer and finally catches up with that of 1200 rpm at high load. These indicate that less heat transfer at higher speed and low load not only improves CNG combustion but also help pilot-diesel burning.

## 5.5  Optimum Gas-Diesel Operation Condition

Summarizing all the effects of the injector geometrical parameters and the engine operating parameters on performance and emissions of the gas-diesel engine, an optimum operation condition can be selected based on the best engine performance (ie. thermal efficiency). The injector geometrical parameters and the engine operating parameters of the optimum operation condition at 1200 rpm engine speed are as follows:
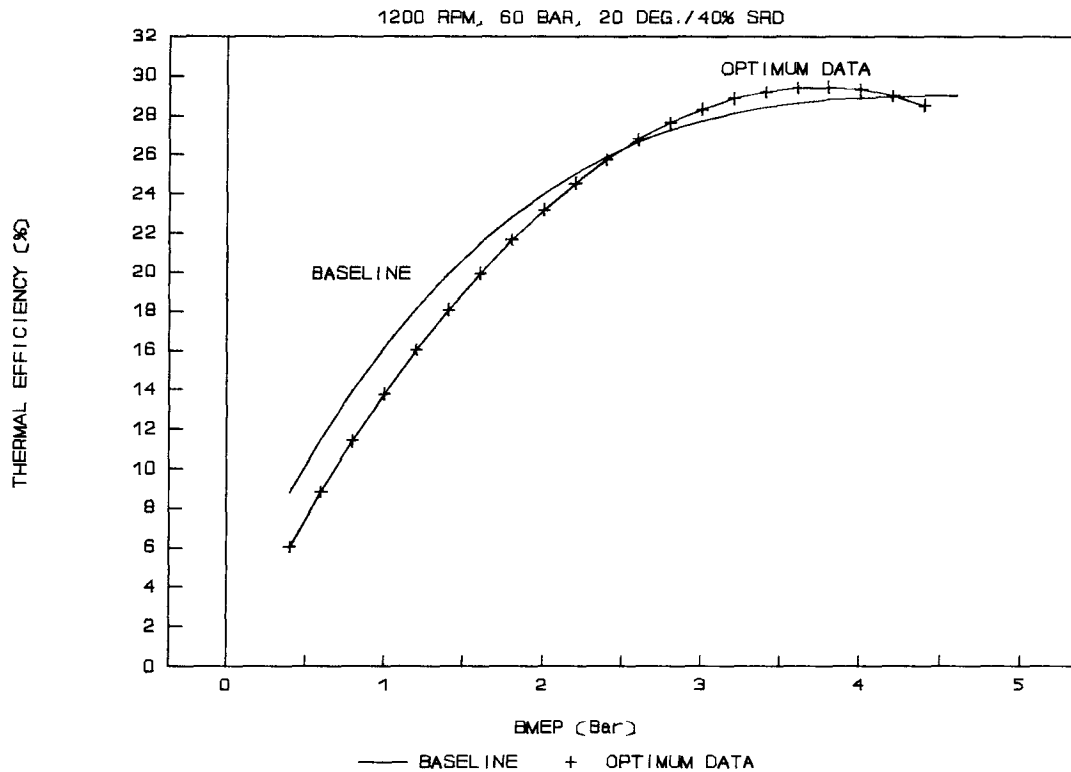
Figure 5.36: Optimum Performance of Gas-Diesel Operation.

1.  40% of jet interruption ratio with 20° injection angle.

2.  60 bar CNG injection pressure.

3.  25% cetane 62 pilot-diesel energy ratio.

The plots presented in this section are performance and emissions of the optimum gas-diesel operation condition against those of CN62 baseline. The dry-basis and wet-basis emissions of the same component are plotted together to give a clear idea. Generally, the dry-basis emission of a given component is higher than the wet-basis emission of this component (The difference between them is due to the water vapour content in exhaust which increases with load).

Figure 5.36 shows the optimum thermal efficiency of the gas-diesel operation. Compared with the baseline, the optimum thermal efficiency of the gas-diesel operation is about 15% lower at BMEP ~ 1 bar, identical at BMEP ~ 2.5 bar and higher 3% at BMEP ~ 3.5 bar.

The nitrogen oxides emissions of the optimum gas-diesel operation are shown in Figure 5.37. As can be seen, the difference between dry-basis and wet-basis nitrogen oxides emissions of the optimum gas-diesel operation is increased with load. This is because the amount of fuel injected into the cylinder is increased with load, so is the water vapour produced in the exhaust. Also, the wet-basis nitrogen oxides emissions of the optimum gas-diesel operation are under the baseline, although the dry-basis data are slightly above baseline at high load.
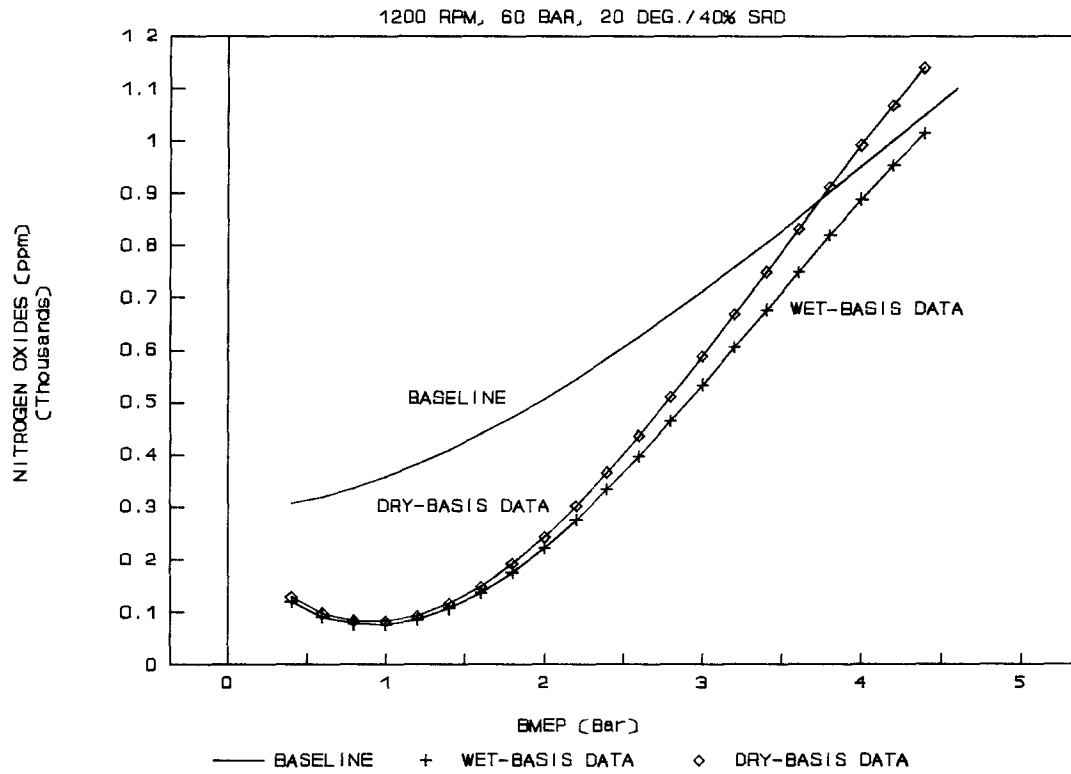
Figure 5.37: Nitrogen Oxides of Optimum Gas-Diesel Operation.

Table 5.1: List of Unburned CNG and Pilot-Diesel Ratio.

| BMEP (bar) | 1.0 | 2.6 | 4.0 |
|---|---|---|---|
| Unburned CNG ratio: | 0.2358 | 0.0555 | 0.0087 |
| Unburned pilot-diesel ratio: | 0.2777 | 0.0610 | 0.0844 |
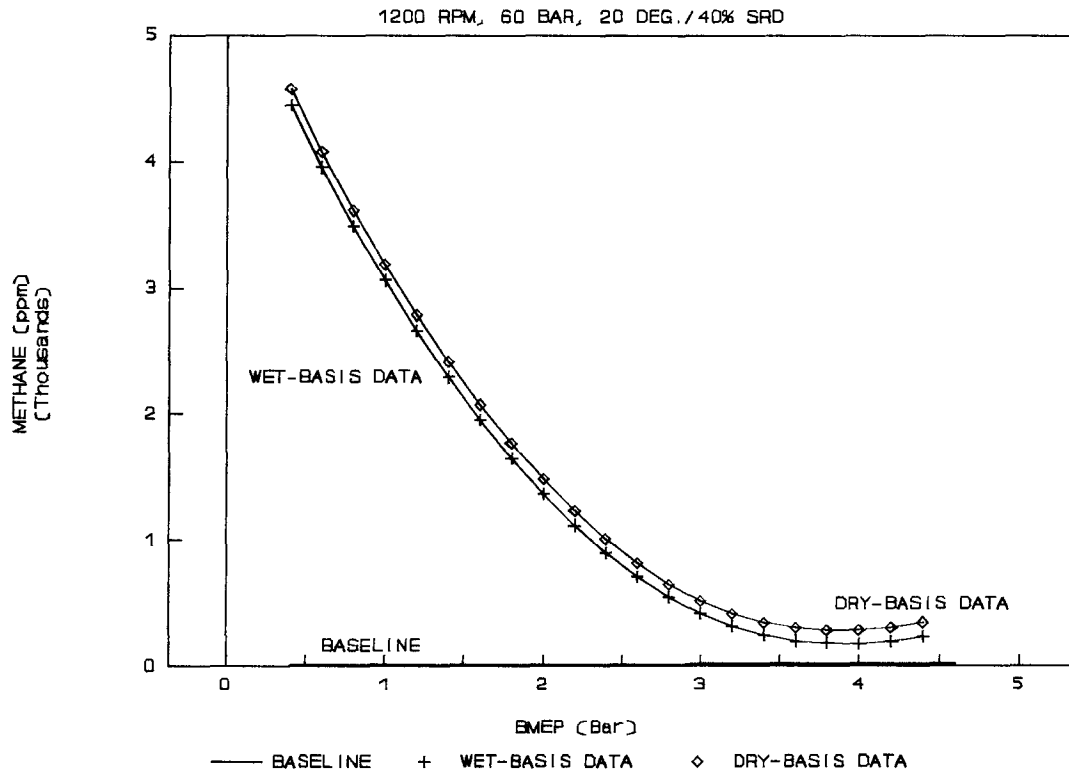
Figure 5.38: Methane of Optimum Gas-Diesel Operation.

The methane and non-methane hydrocarbon emissions of optimum gas-diesel operation are shown in Figure 5.38 and 5.39. Table 5.1 lists the unburned fuel ratio at three specific loads. The unburned fuel (CNG or pilot-diesel) ratio is defined as a mass ratio of the unburned fuel (CNG or pilot-diesel) in the exhaust to the injected fuel (CNG or pilot-diesel). As Table 5.1 shows, A quite large percent of pilot-diesel survives combustion. The ratio of the unburned pilot-diesel is higher than the ratio of the unburned CNG over the whole load range. The worst situation is at low load. This
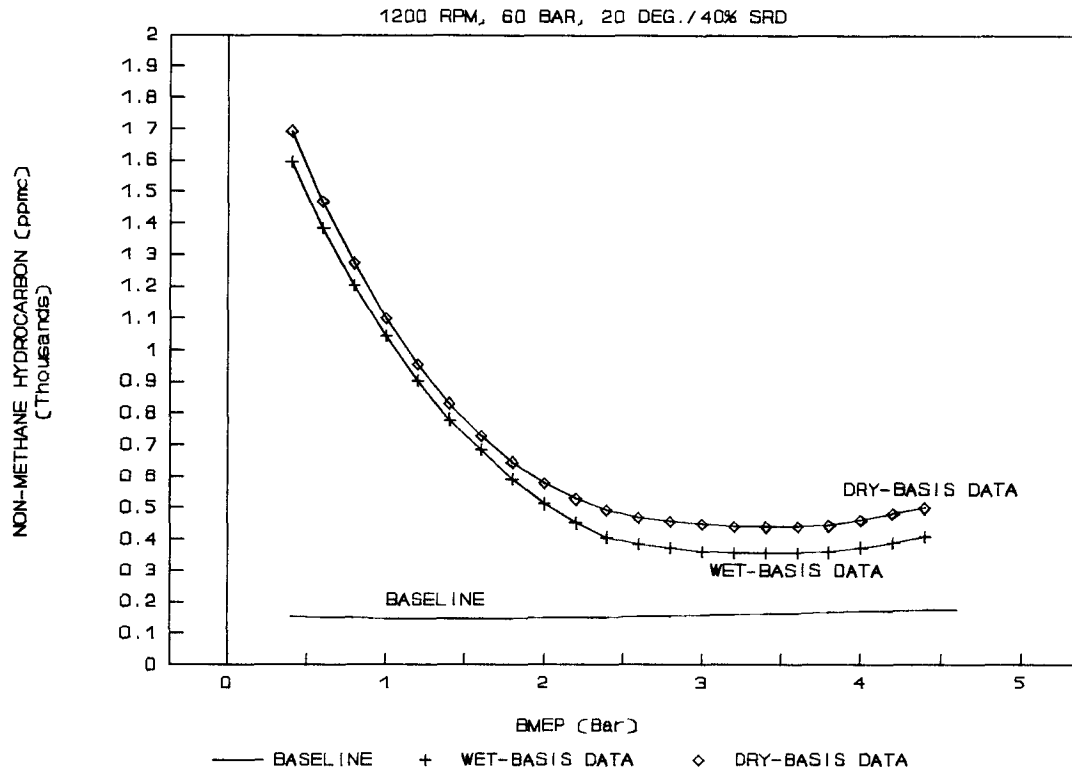
Figure 5.39: Non-Methane Hydrocarbon of Optimum Gas-Diesel
           Operation.

suggests that the pilot-diesel was not atomized well or did not mix

sufficiently with air (ie. burned too rich), or that top wall

quenching was significant, or that the gas-air mixture was too lean

because of very long ignition delay. The low-load thermal

efficiency could be improved if the combustion of pilot-diesel was

improved. The lower diesel ratio operation might be achieved if the

pilot-diesel was burned completely.
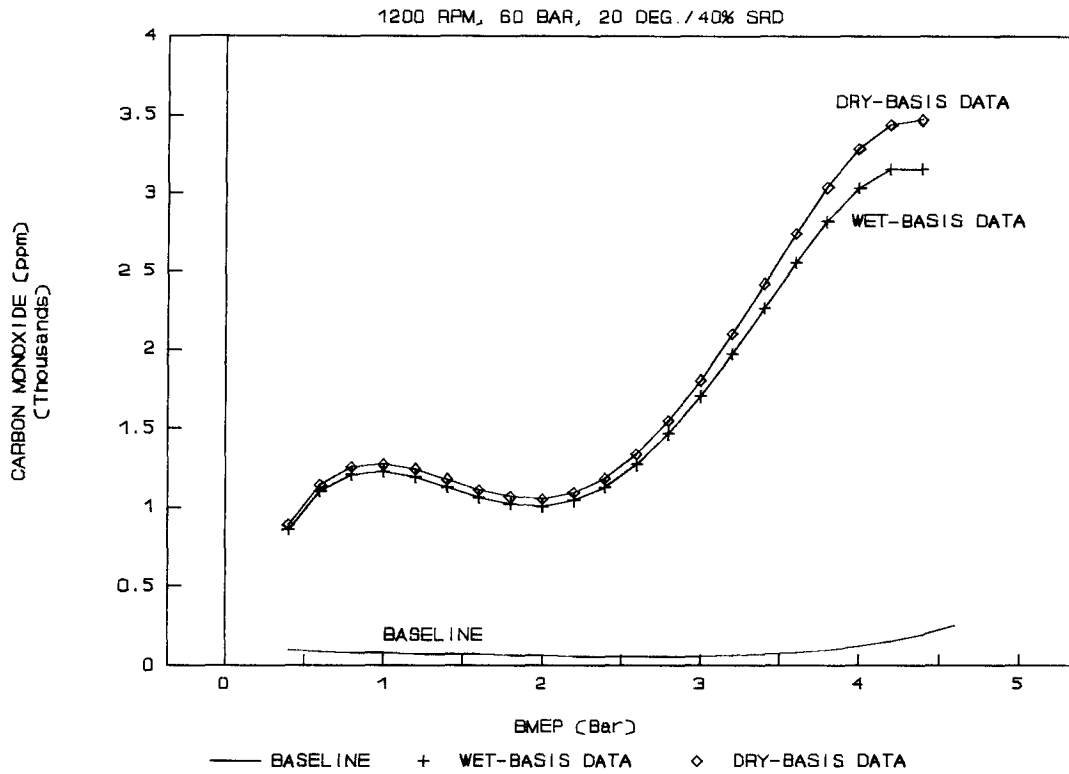
Figure 5.40: Carbon Monoxide of Optimum Gas-Diesel Operation.

The carbon monoxide and the carbon dioxide emissions of the optimum gas-diesel operation are shown in Figures 5.40 and 5.41. High carbon monoxide and low carbon dioxide emissions indicate that the burned fuel/air mixture is still locally rich, although some unburned mixture is already too lean to burn. Wall quenching can be another reason.
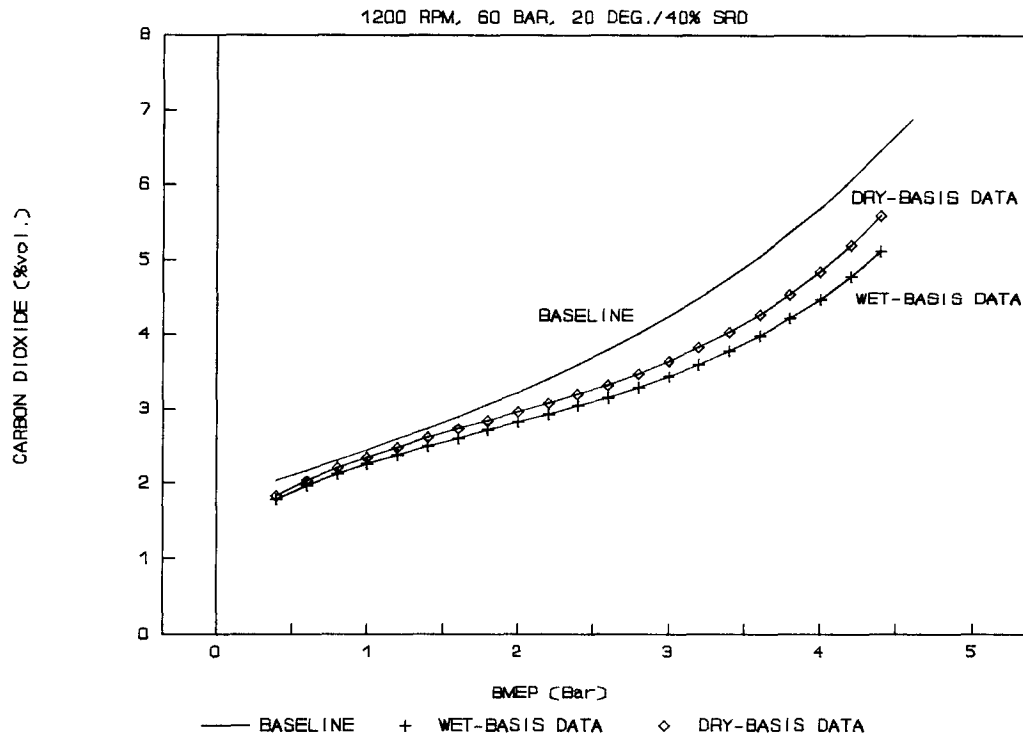
Figure 5.41: Carbon Dioxide of Optimum Gas-Diesel Operation.

Figure 5.42 shows that gas-diesel operation produces slightly higher smoke emission at low and medium load, but much higher smoke emission at high load than that baseline. It is believed that the higher smoke emission resulted from incomplete burning of the locally rich pilot-diesel fuel. The high smoke emission at BMEP ~ 4 bar indicates that the smoke limit of gas-diesel operation is about 4 bar. The smoke limit is related to the maximum achievable load. The diesel baseline has slightly higher smoke limit because of the better penetration and atomization which allows better air entrainment.
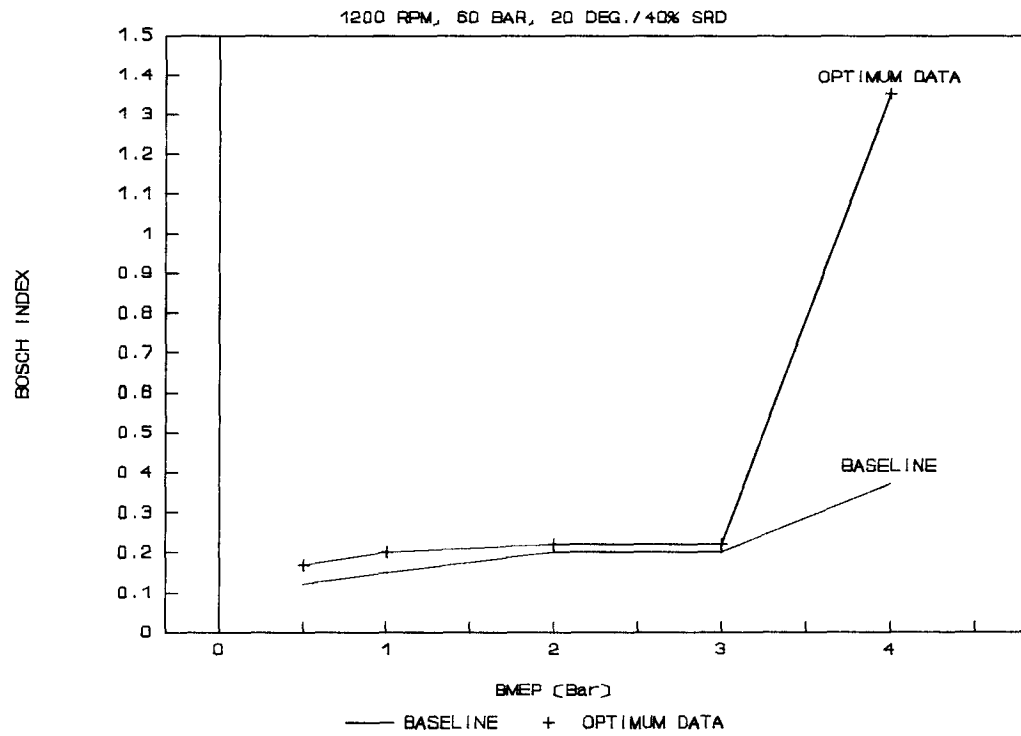
Figure 5.42: Bosch Smoke Index of Optimum Gas-Diesel Operation.

# 6. NUMERICAL SIMULATION CALCULATION

# OF COMBUSTION -- ONE ZONE MODEL

## 6.1 Introduction

In order to simulate the diesel engine working process and calculate the exhaust emission compositions, a one-zone exhaust emission analysis (EEA) model was created. In this model, fresh air, fuel (either natural gas or diesel) and residual gas from previous cycle underwent a Modified Air-Standard Diesel (MASD) Cycle. The constant-pressure heat transfer to the working fluid in the Air-Standard Diesel Cycle was replaced by the constant-pressure combustion process of air, fuel and residual gas mixture (ie. unburned gas mixture). The STANJAN program (ie. STANJAN Chemical Equilibrium Solver version 3.60 written by Stanford University) was used in place of constant-pressure combustion process to calculate the equilibrium compositions of the combustion products [43].

Primarily, two subjects were investigated theoretically with the EEA model, the effect of different fuels (diesel fuel and natural gas fuel) on exhaust emissions of the diesel engine and the effect of exhaust gas recycling (EGR) on NO emission of the diesel engine.

This chapter contains seven sections: the introduction; a detailed description about the formulation of EEA model; the calculation of mixture compositions of the unburned gas; the determination of initial condition; the thermodynamic properties

the computation results; the summary.

## 6.2  Formulation of the Exhaust Emission Analysis Model
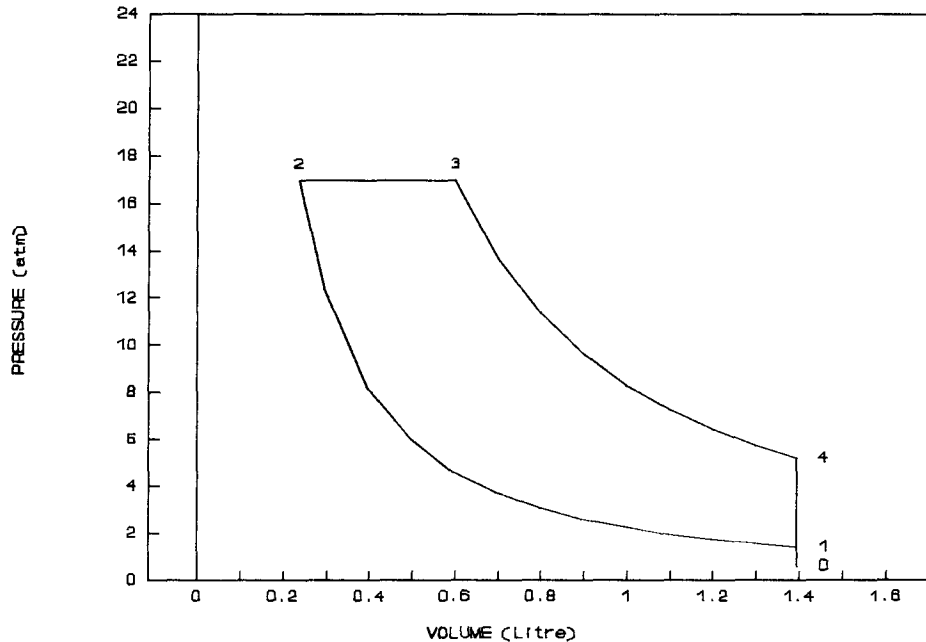


Figure 6.1: The Modified Air-Standard Diesel Cycle (MASD).

Usually, there are four processes for an actual diesel cycle: exhaust and aspiration; compression; combustion; expansion. In order to simulate the actual diesel cycle, a Modified Air-Standard Diesel (MASD) Cycle is applied to the EEA model. As shown in Figure 6.1, the MASD cycle is a closed cycle which consists of five processes: 1. Process 1-2 is an isentropic compression (ie. reversible adiabatic compression). 2. Process 2-3 is a constant-pressure and adiabatic combustion. 3. Process 3-4 is an isentropic expansion. 4. Process 4-0 is a constant-volume exhaust. 5. Process 0-1 is a constant-volume inlet. In some cases, in order to account

for the influence of heat transfer, the isentropic processes can be replaced with the reversible polytropic processes.

For the isentropic compression process (ie. process 1-2 in Fig. 6.1), the relationships in term of the initial and final states can be expressed as follows: [40]

$$\frac{P_2}{P_1} = (\frac{v_1}{v_2})^k$$
(6.1)

and

$$\frac{T_2}{T_1} = (\frac{P_2}{P_1})^{(k-1)/k}$$
(6.2)

where P is the fresh-charge pressure inside the cylinder, T is the fresh-charge temperature inside the cylinder, v is the specific volume of the fresh-charge inside the cylinder and k is the ratio of constant-pressure and constant-volume specific heats at zero pressure. The subscripts "1" and "2" denote the initial and final states of the isentropic compression process respectively.

If we replace the specific heat ratio "k" with the polytropic constant "n" in Eqs. (6.1) and (6.2), then the two equations which are suitable for the reversible polytropic process can be written as follows:

$$\frac{P_2}{P_1} = (\frac{v_1}{v_2})^n$$
(6.3)

and

$$\frac{T_2}{T_1} = (\frac{P_2}{P_1})^{(n-1)/n}$$

(6.4)

The total energy of the system is assumed to remain the same between the combustion in the constant pressure and adiabatic combustion process (ie. process 2-3 in Fig. 6.1). By neglecting changes in kinetic and potential energies, the first law of thermodynamics applied to this constant-pressure process is [40]

$$\delta Q = dU + \delta W = dU + PdV = dH = 0$$

(6.5)

where Q is the heat transfer to the system, U is the internal energy of the system, W is the work done to the piston, H is enthalpy of the system. By integrating Eq. (6.5) from state 2 to state 3, we can get the important relation

$$H_2 = H_3$$

(6.6)

where subscript "2" and "3" present the initial and final states of the combustion process.

An interactive program, STANJAN, has been used for the constant pressure and adiabatic combustion process to perform the chemical equilibrium analysis by the method of element potentials [44].

By using the same Eqs. (6.1), (6.2) or (6.3), (6.4) , and resetting the initial and final states "1" and "2" with "3" and "4" respectively, four corresponding equations can be established for the isentropic or reversible polytropic expansion process (ie, process 3-4 in Fig. 6.1). These relationships can be used to calculate the exhaust temperature which can be used to correlate

test engine exhaust temperature.

Although the exhaust process (ie. process 4-0 in Fig. 6.1) in the MASD cycle (close cycle) differs from that in the actual diesel cycle (open cycle), this process has less effect on pollutant formation, so the Air Standard Cycle representation still remains.

The inlet process (ie. process 0-1 in Fig. 6.1) is specially designed to simulate the inlet condition of the 1-71 test engine. This is another instance that differs from the Air Standard Cycle. Details of which are discussed in Section 6.4.

To simplify the computation process, the following assumptions are applied:

1. The thermodynamic state inside the cylinder is considered to be homogeneous and uniform.

2. The fresh charge trapped in the cylinder after the inlet valve closure (corresponding to the state "1" in Fig. 6.1) includes only residual gas from the previous cycle and fresh air, and behaves as an ideal gas.

3. Fuel (either natural gas or diesel) is directly injected into cylinder at top-dead-centre (TDC) which correspond to state "2" in Fig. 6.1, and mixes with fresh charge immediately, uniformly and homogeneously (ie. the whole mixture has the same air-fuel ratio, temperature and pressure immediately).

4. Natural gas is considered to be methane ($CH_4$), and the diesel fuel can be approximated by $CH_{1.8}$. Vaporization of the injected diesel fuel is assumed to take place very quickly, so that the injected diesel fuel can be treated as a gaseous

diesel fuel with allowance made for heat of vaporization. All the fuel vaporizes immediately after injection in the cylinder.

5.  The combustion products are in thermodynamic equilibrium.

## 6.3  Mixture Compositions of the Unburned Gas
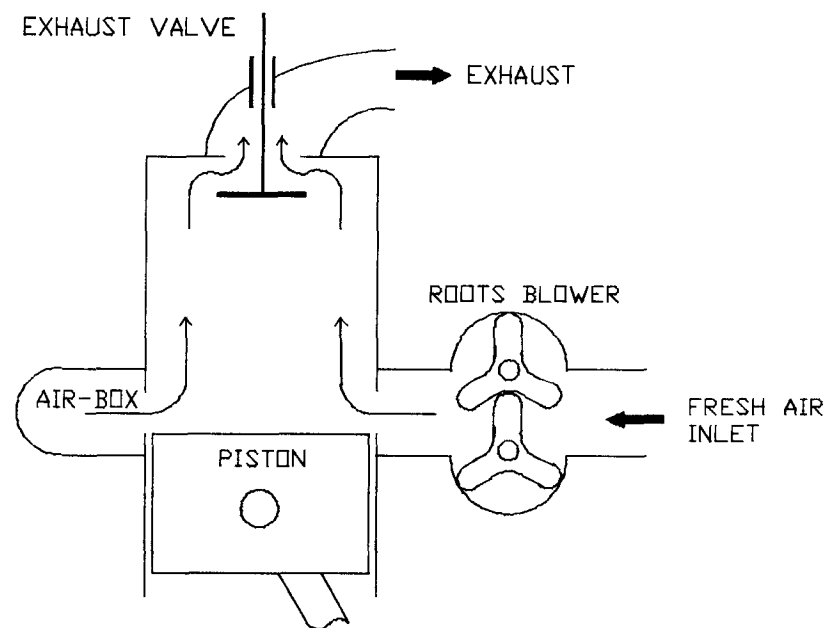


Figure 6.2: Schematic of Uniflow-Scavenged Configuration.

As shown in Figure 6.2, the original test engine is a uniflow-scavenged two-stroke cycle diesel engine. A separate Roots blower is used to displace the burned gases from the previous cycle as well as to supply fresh air to the engine cylinder. With this configuration, however, some of the incoming fresh air escapes with the burned gas and part of the burned gas still remains in the cylinder after exhaust port closure. That portion of burned gas

remaining from the previous cycle is defined as the residual gas of this cycle. To find the effect of the residual gas on the equilibrium compositions of the combustion products, the compositions of unburned gas inside the cylinder have to be determined [26].

## 6.3.1 Terminology

The following terms are defined for use in the subsequent sections of this chapter.

● Fresh air:

The portion of inducted air trapped in the cylinder.

● Fresh charge:

The whole contents of a cylinder at the inlet port closure (IPC). It consists of fresh air and residual gas from the previous cycle.

● Unburned gas:

The whole contents of a cylinder after fuel injection but before combustion. It consists of fresh air, residual gas and fuel.

● Basic cycle:

The last non-combustion cycle in engine starting state.

● Consequent cycles:

The combustion cycles after the basic cycle in the engine operating state.

● Transient operating state:

The non-combustion cycles at the starting and first few

burning cycles in which the mixture compositions of the
unburned gas differ from cycle to cycle.

●Steady operating state:

The operating state that the cyclic variations of the
unburned-gas mixture composition are very small.

●Moles of trapped fresh air, $M_{air}$:

The portion of inducted air moles per cycle trapped in the
cylinder at IPC.

●Residual moles, $M_{res}$:

The moles of the combustion products remaining in the cylinder
from the previous cycle.

●Moles of trapped fresh charge, $M_{charge}$:

The cylinder content at IPC, which is the summation of the
moles of air trapped and the residual moles.

$$M_{charge} = M_{air} + M_{res}$$

(6.7)

●Residual molal fraction, $F_{res}$:

The ratio of the residual moles to the moles of fresh charge
trapped in the cylinder at IPC.

$$F_{res} = \frac{M_{res}}{M_{charge}} = \frac{M_{res}}{(M_{air} + M_{res})}$$

(6.8)

●Residual-air molal ratio, r:

The ratio of the residual moles to the moles of air trapped.

$$r = \frac{M_{res}}{M_{air}} = \frac{F_{res}}{(1 - F_{res})} \qquad (6.9)$$

## 6.3.2 Compositions of Residual Gas and Unburned Gas

For the two-stroke test engine because of residual gas from the previous cycle, the working condition can be divided into two stages, the transient operating stage and the steady operating stage. The transient operating stage includes the non-combustion cycles in the starting and first few transient burning cycles that the mixture compositions of the unburned gas are different from cycle to cycle. After a few transient burning cycles, the engine will run into a steady operating stage in which the cyclic variations of the unburned-gas mixture composition are negligible.

PROGRAM#2 is the computation program that is designed to simulate the transient operating stage and calculate the mixture compositions of the unburned gas at the steady operating stage. It is designed to have the final results with the cycling variation less than 0.01%. This program is documented in Appendix I and the assumptions applied to it is as follows:

1.  The diesel cycle concept is used, so the cylinder contents being compressed is only fresh air and residual gas from previous cycle.

2.  The residual gas is only the fresh air in the basic cycle, which contains 21% Oxygen and 79% Nitrogen.

3.  The combustion products or the residual gas consist of only $CO_2$, $H_2O$, $O_2$ and $N_2$ in the consequent cycles. The dissociation reactions can be neglected because the burning temperature is

low in the transient operating state.

4. The volumetric percentage of the residual gas is constant for every cycle (ie. the residual molal fraction is constant for every cycle), and the mixture compositions of the unburned gas are different from cycle to cycle in the transient operating stage.

5. The relative air-fuel ratio is constant for every cycle. Only fresh air and fuel are considered to be involved in combustion, but residual gas is not.

The combustion reaction equation used in the PROGRAM#2 for the general fuel ($CH_y$) is

$$CH_y + 2\lambda (O_2 + 3.76N_2)$$

$$+ \beta [ (X^i_{CO2}) CO_2 + (X^i_{H2O}) H_2O + (X^i_{O2}) O_2 + (X^i_{N2}) N_2]$$

$$\rightarrow (1 + \beta X^i_{CO2}) CO_2 + (\frac{y}{2} + \beta X^i_{H2O}) H_2O \qquad (6.10)$$

$$+ (2\lambda - 1 - \frac{y}{4} + \beta X^i_{O2}) O_2 + (7.52\lambda + \beta X^i_{N2}) N_2$$
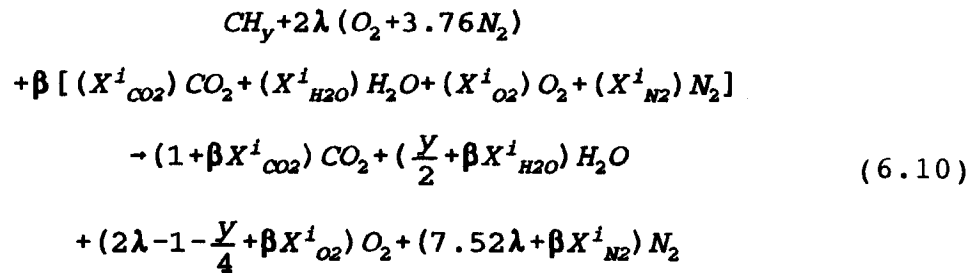
in which

$$\beta = 9.52 r\lambda \qquad (6.11)$$

where $\lambda$ is the relative air-fuel ratio, r is the residual-air molal ratio which was defined in Subsection 6.3.1. y is the atomic hydrogen-to-carbon ratio of the fuel, for methane ($CH_4$) y=4. $X^i_{CO2}$, $X^i_{H2O}$, $X^i_{O2}$ and $X^i_{N2}$ are the molal fractions of cycle "i" for $CO_2$, $H_2O$, $O_2$ and $N_2$ respectively which are

$$X^{i}{}_{CO2} = \frac{1 + \beta X^{i-1}{}_{CO2}}{n_T}$$
(6.12)

$$X^{i}{}_{H2O} = \frac{\frac{Y}{2} + \beta X^{i-1}{}_{H2O}}{n_T}$$
(6.13)

$$X^{i}{}_{O2} = \frac{2\lambda - 1 - \frac{Y}{4} + \beta X^{i-1}{}_{O2}}{n_T}$$
(6.14)

$$X^{i}{}_{N2} = \frac{7.52\lambda + \beta X^{i-1}{}_{N2}}{n_T}$$
(6.15)

and

$$n_T = \frac{Y}{4} + 9.52\lambda(1 + r)$$
(6.16)

where $n_T$ is the total moles of the combustion products.

## 6.4  Determination of Initial Condition

As mentioned in Section 6.3 and shown in Fig. 6.2, a scavenged-blower on the 1-71 test engine is used to displace burned gases from the previous cycle as well as to supply enough fresh air to the engine cylinder.

To simulate the operation of the actual two-stroke engine more closely, the measured experimental data from 1-71 test engine is used to determine the initial state "1" of the MASD cycle. They are the inlet temperature $T_0 = 30$ °C (ie. 303 K), inlet pressure $P_0 = 103$ kPa (ie. 1.03 atm) and air-box pressure $P_1 = 140$ kPa (ie. 1.4 atm). The inlet state "0" is very close to the ambient state. The air-box

state is the scavenged-blower exit which is the same as the intake
state "1" of the MASD cycle in Fig. 6.1. The air-box temperature,
$T_1$, can be calculated by the following equation [45].

$$T_1 = T_0 \{ 1 + \frac{1}{\eta_b} [ (\frac{P_1}{P_0})^{\frac{k-1}{k}} - 1 ] \}$$  (6.17)

where $\eta_b$ is the scavenged-blower efficiency, here assume $\eta_b = 0.75$.
k is the specific heat ratio of air, for isentropic process k=1.4.
Thus, $T_1$ and $P_1$ are known.

## 6.5    Thermodynamic Properties of the Unburned Gas

In computing the combustion product compositions and their
thermodynamic properties in the constant pressure and adiabatic
combustion process (ie. process 2-3 in Fig. 6.1), it is important
to prepare the thermodynamic properties of the unburned gas at
state "2" as the input parameters for the STANJAN program. Because
of the constant pressure and adiabatic combustion process, $P_2 = P_3$
and $H_2 = H_3$ are two important relations, thus $P_2$ and $H_2$ are the input
parameters required for running the combustion function of the
STANJAN program. The combustion function is one of the functions in
STANJAN, which deal with the combustion equilibrium analysis.

STANJAN has the non-combustion function to compute the
thermodynamic properties of the unburned gas. It can, for example,
calculate internal energy U, enthalpy H, entropy S, specific volume
v, temperature T and pressure P for unburned gas. This function can
be used to prepare the $H_2$ required for running the combustion

function.

PROGRAM#1 is the program to compute the unburned-gas pressure $P_2$ and temperature $T_2$ which are the two input parameters for running the non-combustion function of the STANJAN. It involves Eq. (6.1), (6.2), (6.3), (6.4) and (6.17) (see Appendix H).

The detailed procedures for calculating the thermodynamic properties of the unburned gas are presented in Appendix J.

## 6.6 Computation Results and Discussion

In the diesel engine combustion process, the combustion is carried on only when the air-fuel ratio and temperature are appropriate for burning. Much unburned gas still remained in the exhaust with over-lean (or over-rich) mixtures. Thus the exhaust gas concentrations of the diesel engine (ie. experimental results) are averaged concentrations of the burned and the unburned gases.

The equilibrium calculation results of the combustion product composition can be considered as the burned-gas composition. The calculation procedure is presented in Appendix K.

### 6.6.1  Effect of Different Fuels on Burned-Gas Composition

A computation was conducted to investigate the effect of two different fuels on the combustion-product NO concentrations. The fuels involved in this computation are the diesel and the natural gas fuels. To simplify the computation, the residual-gas influence is omitted (ie. set the residual molal fraction to zero). The results of equilibrium calculation are shown in Figures 6.3

through 6.6.
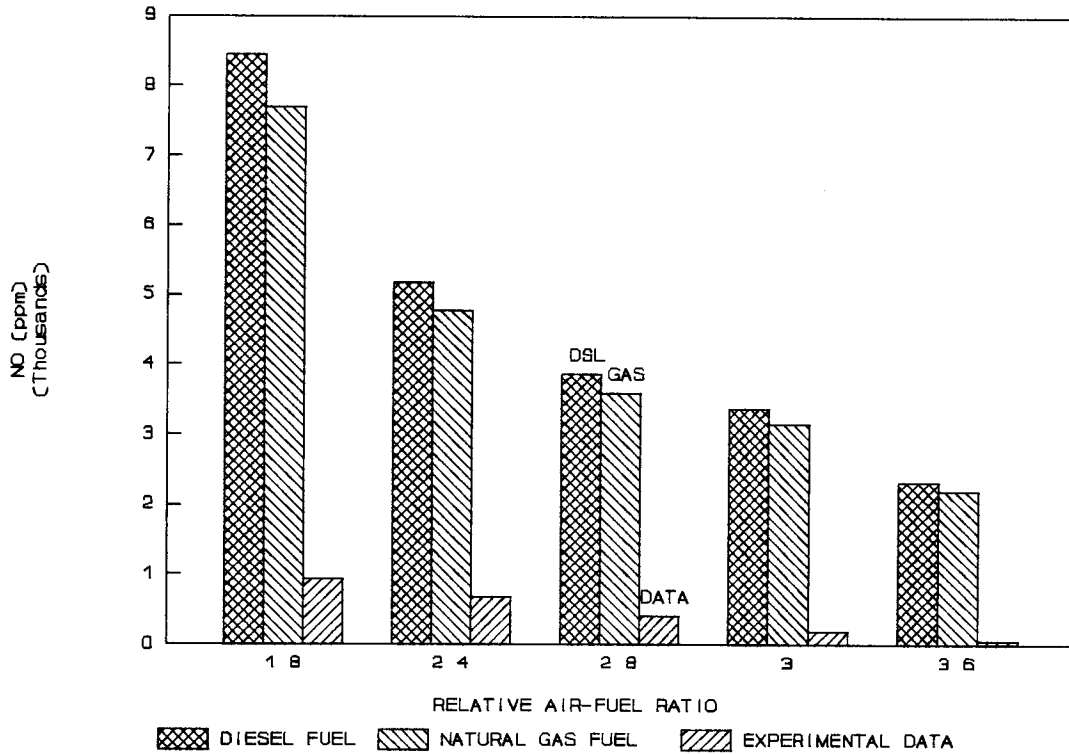


Figure 6.3: Effect of Different Fuels on NO Concentration.
(MASD cycle, compression ratio = 16:1, specific
heat ratio = 1.4, inlet temperature = 303 K and
inlet pressure = 1.03 atm)

Figure 6.3 shows the effect of two different fuels on NO
concentration of burned gas. The computation was conducted in the
range of relative air-fuel ratio from 1.8 to 3.6, which corresponds
to the break mean effective pressure (BMEP) 4.5 bar to 1 bar of the
test engine operating range. It can be seen from Figure 6.3 that
burning natural gas fuel reduces NO emission from 8.9% to 6%

compared to diesel fuel in the computation range of relative air-fuel ratio 1.8 to 3.6. This is because the adiabatic flame temperature of the natural gas fuel is lower, about 1.08% averaged over the computation range, than that of the diesel fuel, as shown in Figure 6.4.
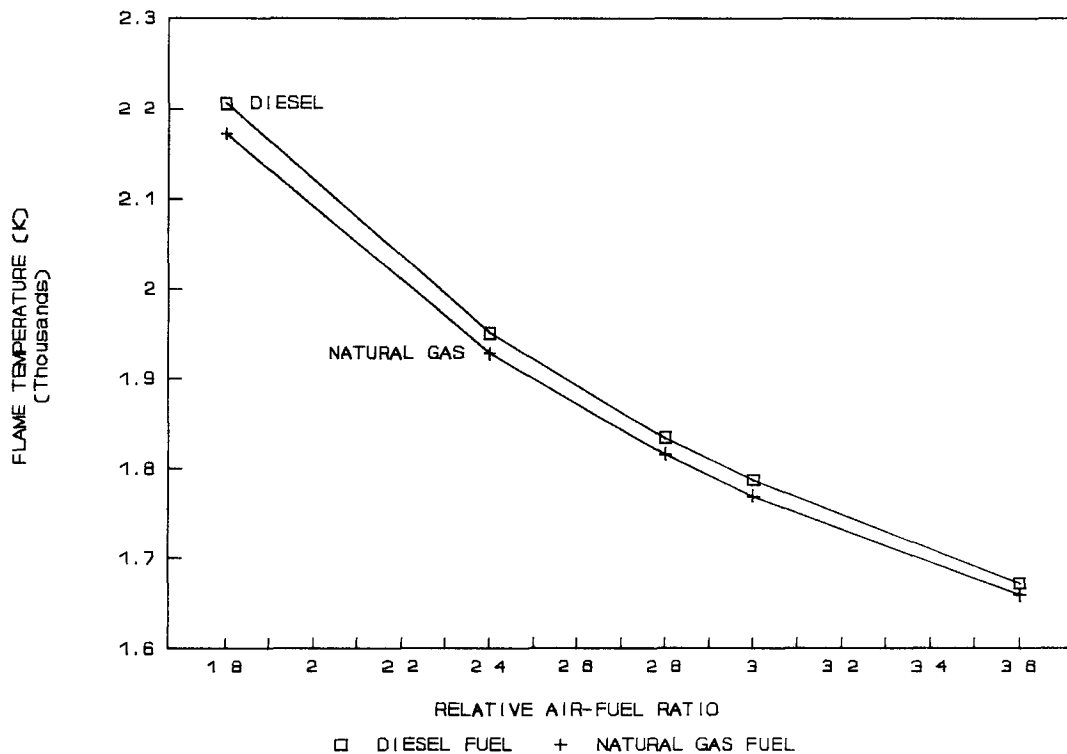


Figure 6.4: Effect of Different Fuels on Adiabatic Flame Temperature.

Figure 6.3 also shows that the equilibrium calculation results of NO concentration for both fuels are considerably higher than the experimental result of NO concentration from the test engine. There
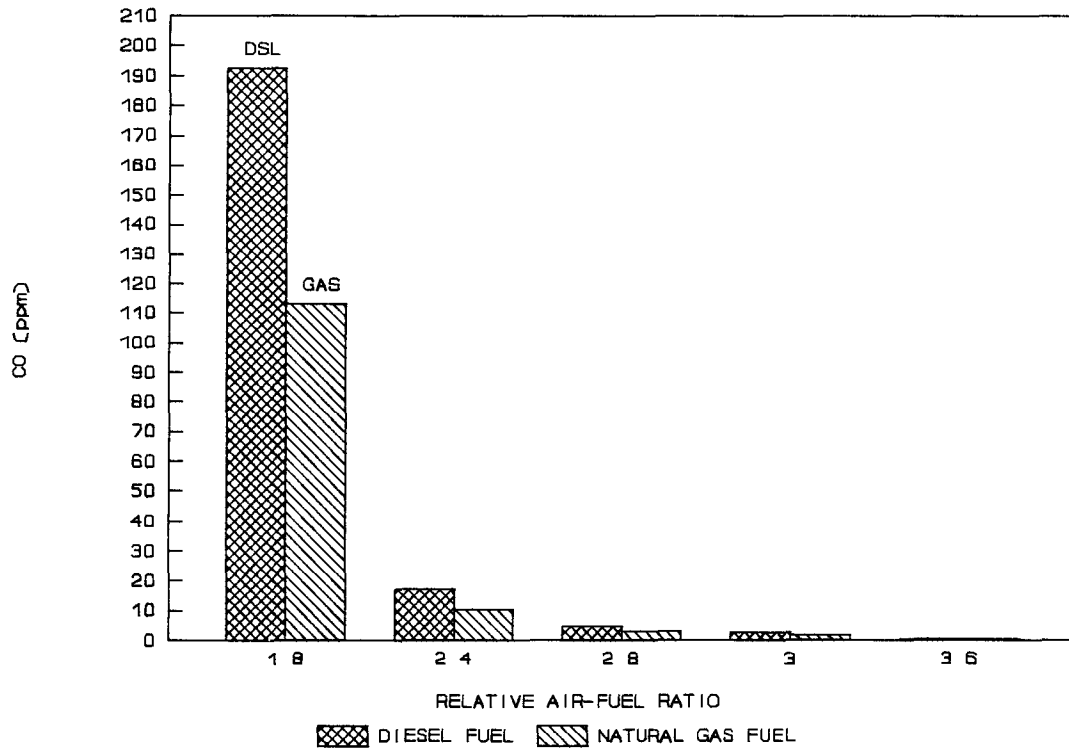
Figure 6.5: Effect of Different Fuels on Equilibrium CO
Concentration in the Cylinder.

are three possible reasons for this. First, the time period of NO

formation reaction is very short in the test engine, thus the

reaction may not have reached the equilibrium state. This means

that the burned-gas NO concentration of the test engine is lower

than the equilibrium reaction NO concentration. Secondly, the

measured NO concentration of the test engine is the averaged result

over the cylinder contents, and it is lower than the burned-gas NO

concentration. Thirdly, the existence of the residual gas in the

test engine cylinder will reduce the NO concentration, though this

possibility has not been considered in this calculation. The NO calculation result, however, is the only one that can correlate with the experimental result because of the freezing behaviour of the NO reactions.
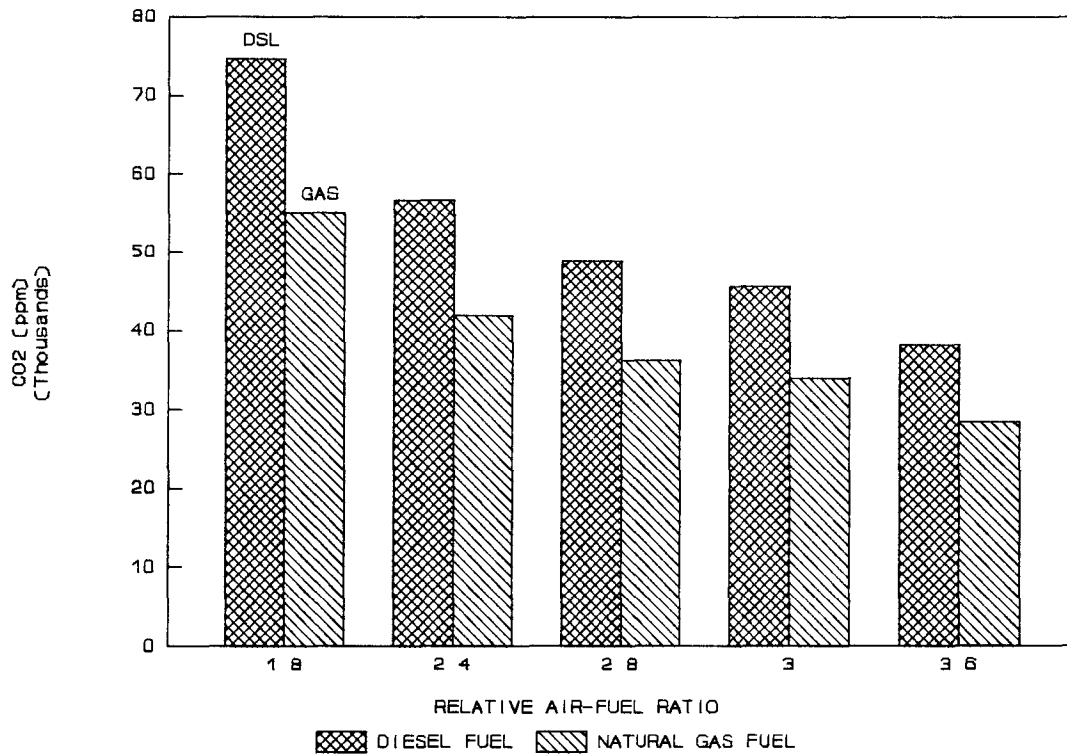


Figure 6.6: Effect of Different Fuels on Equilibrium $CO_2$ Concentration in the Cylinder.

Figures 6.5 and 6.6 show the effects of burning diesel and natural gas fuels on CO and $CO_2$ concentrations of burned gas respectively. Burning natural gas fuel reduces average 25.94% CO and 46.4% $CO_2$ respectively, compared to burning diesel fuel.

Because CO will still be oxidized into $CO_2$ after the combustion and the oxidization rate are unable to determine, the equilibrium calculation results of CO and CO2 concentrations can not be correlated with the experimental results.

## 6.6.2 Effect of the Residual Gas on Burned-Gas Compositions
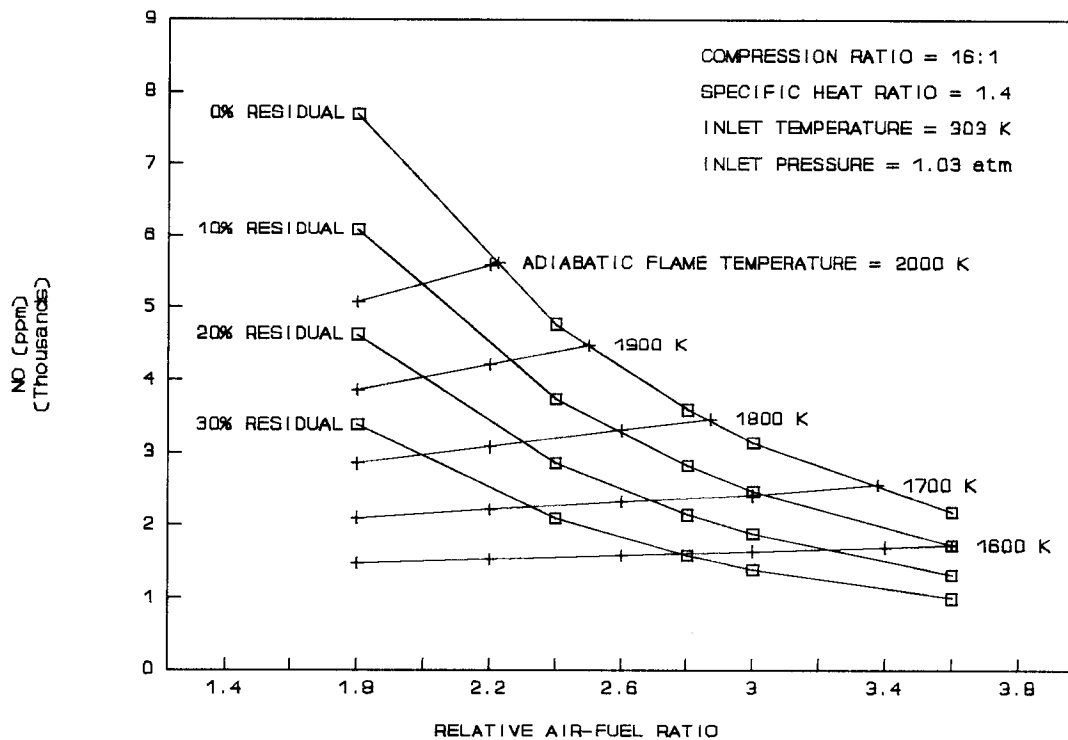


Figure 6.7: Effect of Residual Gas on NO Concentration.

The effect of the cold residual gas on burned-gas composition was calculated. The results for natural gas fuel are presented as a map in Figure 6.7. The residual-gas influence is presented as the

residual molal fraction in the range from 0% to 30%. The adiabatic flame temperature is presented from 1600 K to 2000 K. The computation range of relative air-fuel ratio is from 1.8 to 3.6. With this map, if one knows the residual molal fraction and relative air-fuel ratio, the equilibrium NO concentration which is the maximum critical NO concentration value from the test engine can easily be found. The measured experimental results will be lower than the critical value because the NO formation reaction in the diesel engine has not reached the equilibrium state. The farther the NO formation reaction is from equilibrium, the less NO will be formed. Thus one approach to reduce NO concentration might be to match the injection parameters with cylinder pressure and temperature as well as possibly to shorten the combustion time.

## 6.7 Summary

The Exhaust Emission Analysis (EEA) model (one-zone) with a Modified Air-Standard Diesel (MASD) cycle for diesel engine is well established. Based on equilibrium calculation results, the following conclusions can be drawn:

1. Burning natural gas instead of diesel fuel in a compression-ignition engine reduces burned-gas NO concentration within the whole engine operation range.

2. Recycling exhaust gas in diesel engines can reduce burned-gas NO concentration within the whole engine operation range.

3. A new method is established, which can be used to calculate the burned-gas equilibrium NO concentration values for the

specific diesel engine.

4.  A possible approach to reduce NO concentration is to match the injection parameters of injector with cylinder environment (ie. pressure and temperature) as well as possibly to shorten combustion time (ie. to shorten the NO formation time) so that the actual NO formation reaction is far from equilibrium.

5.  Limitations of this model are: constant pressure and adiabatic combustion; equilibrium dissociation at single-zone adiabatic temperature.

# 7. NUMERICAL SIMULATION CALCULATION

# OF COMBUSTION -- THREE ZONE MODEL

## 7.1 Introduction

In order to reveal combustion quality and predict NO emission of the gas-diesel engine more exactly, a three-zone combustion and exhaust emission analysis model XPRESSD was established. With measured cylinder pressure distribution, it was used to compute the flame temperature and the mass-burned fraction of fuel with stoichiometric (or diffusion) combustion in the gas-diesel engine.

With pressure and temperature distribution, as well as reactant C:H:O:N ratio of stoichiometric complete combustion, STANJAN [43] was used to calculate the equilibrium composition of the combustion products. The calculated equilibrium NO concentration after dilution by unburned-gas was used to correlate the measured test engine tail-pipe NO concentration.

The principle of the correlation of the calculated equilibrium NO concentration to the measured engine tail-pipe NO concentration was based on the sudden-freezing theory of the NO formation reaction [26]. This theory indicates: the NO formation rate increases exponentially with the burned-gas temperature inside the cylinder until reaching the peak temperature; as the burned gas cools during the expansion stroke, the NO reaction suddenly freezes. According to this theory, the engine tail-pipe NO concentration should close to the equilibrium NO concentration

corresponding to the peak burned-gas temperature.

In the following text of this chapter, a detailed description of this model will be given before the discussion of the calculated results, followed by a summary.

## 7.2 Formulation of the Three-Zone Combustion Model

In the gas-diesel engine, natural gas and diesel fuel are injected together and proportionally, beginning at the crank angle denoted by BOI. The injection duration is called the pulse width (PW). Combustion is initiated by the pilot diesel when the temperature of the cylinder contents is above the self-ignition temperature of the diesel. Natural gas is then ignited by locally high temperature. Mainly, the fuels undergo a diffusion combustion (ie. nearly stoichiometric combustion).
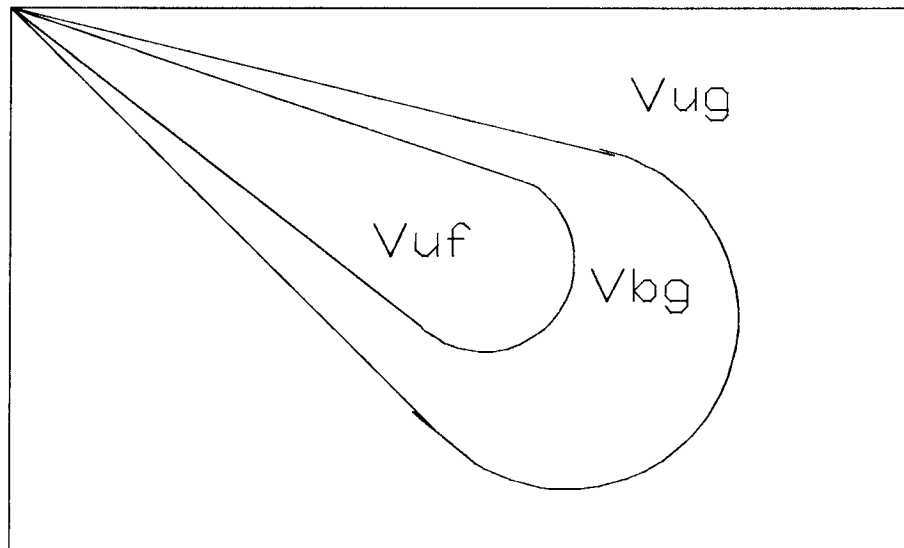
Figure 7.1: Schematic of the Three-Zone Combustion Model.

A three-zone combustion model designed for representing the combustion in the gas-diesel engine is shown in Figure 7.1. "Three zone" indicates unburned-gas, unburned-fuel and burned-gas zones. They are denoted by subscripts "ug", "uf" and "bg" respectively. The following assumptions are applied to this model:

1. The pressure inside the cylinder is uniform.

2. The cylinder constituents (both unburned and burned) behave as ideal gases.

3. The thermodynamic state of each zone is considered to be homogeneous and uniform.

4. The molecular formulae, $CH_4$ and $CH_2$, are used to represent natural gas and diesel fuel respectively.

5. The fuels (natural gas and diesel fuel) are injected into the cylinder at a uniform rate over the crank angle interval PW from BOI with the room temperature (298 K). Diesel fuel remains liquid in the unburned-fuel zone until it burns. Vaporization of the diesel fuel takes place quickly.

6. A combined fuel ($CH_y$) is used to replace natural gas ($CH_4$) and diesel ($CH_2$) fuels. The hydrogen-to-carbon atom ratio y of the combined fuel is determined by:

$$y = \frac{H}{C} = \frac{4 + \frac{16.043}{14.026} r_m \cdot (2)}{1 + \frac{16.043}{14.026} r_m} \qquad (7.1)$$

in which $r_m$ is the diesel to natural gas mass ratio and can be determined by Eq. (E.1) in Appendix E.

7. Stoichiometric combustion reaction is taken to represent the diffusion combustion in the cylinder.

8. Natural gas and diesel fuels are burned with the same mass-burned fraction at any instant during combustion (proportional burning).

9. The content of the unburned-gas zone is the mixture of the intake air and the residual gas from the previous cycle which is considered to consist of $O_2$, $N_2$, $CO_2$ and $H_2O$.

10. The content of the unburned-fuel zone is the uniform mixture of the natural gas and the diesel fuel. The natural gas and the diesel have the same temperature as the temperature of the unburned-fuel zone.

11. The content of the burned-gas zone is the combustion products which are in thermodynamic equilibrium.

## Properties of the Unburned-Gas Zone:

The specific internal energy of the unburned gas $u_{ug}$ (kJ/kg) is a function of the temperature of the unburned-gas zone $T_{ug}$ (K).

$$u_{ug} = u_{ug}(T_{ug}) = u^0_{ug} + C_{vug}(T_{ug} - T_0)$$

where $u^0_{ug}$ (kJ/kg) is the specific internal energy of the unburned gas at 298 K, $T_0$ (298 K) is the standard temperature, and $C_{vug}$ (kJ/kg·K) is the constant-volume specific heat of the unburned gas.

The specific volume of the unburned gas $v_{ug}$ ($m^3$/kg) is a function of the temperature of the unburned-gas zone $T_{ug}$ (K) and the cylinder pressure P (kPa).

$$V_{ug} = \frac{R_{ug} T_{ug}}{P} \qquad (7.2)$$

where $R_{ug}$ (kN·m/kg·K) is the unburned-gas constant.

$T_{ug}$ can be evaluated by applying the first law of thermodynamics to the unburned gas.

$$dq = dh_{ug} - v_{ug} dP = C_{pug} dT_{ug} - v_{ug} dP \qquad (7.3)$$

where dq is the heat transfer with the cylinder wall which is,

$$dq = \frac{c_1 \Delta Q}{m_{ug}} \qquad (7.4)$$

where let $c_1 = c_2 (m_{ug}/m_{tot})$ be a constant, $c_2$ is another constant. $\Delta Q_{WALL}$ (kW/CA) is the instantaneous heat transfer with the cylinder wall, $m_{ug}$ (kg) is the instantaneous mass of the unburned gas, and $m_{tot}$ (kg) is the instantaneous total mass in the cylinder.

Substituting Eq. (7.2), (7.4) and constant $c_1$ into Eq. (7.3), we have

$$\frac{dT_{ug}}{T_{ug}} = \frac{\gamma - 1}{\gamma} \frac{dP}{P} + \frac{c_2 \Delta Q_{WALL}}{m_{tot} C_{pug} T_{ug}} \qquad (7.5)$$

where $\gamma = C_{pug}/C_{vug}$ is the specific heat ratio of the unburned gas, $C_{pug}$ and $C_{vug}$ (kJ/kg·K) are the constant-pressure and constant-volume specific heats of the unburned gas.

By applying Eq. (7.5) to two states which are one crank angle degree apart, we have,

$$(T_{ug})_2 = (T_{ug})_1 + (T_{ug})_1 \left( \frac{\gamma - 1}{\gamma} \right) \left( \frac{P_2 - P_1}{P_1} \right) + \frac{c_2 \Delta Q_{WALL}}{m_{tot} C_{pug}} \qquad (7.6)$$

where subscripts "1" and "2" denote starting and ending states. $c_2$ is a constant which can be adjusted in the program to satisfy the mixture and unburned-gas temperatures at the state of exhaust-port opening. The range is found in 0.3~0.5 for gas-diesel operation.

## Properties of the Unburned-fuel Zone:

The specific internal energy of the unburned CNG $u_{CNG}$ (kJ/kg) is a function of the temperature of the unburned-fuel zone $T_{uf}$ (K).

$$u_{CNG} = u_{CNG}(T_{uf}) = u^0{}_{CNG} + C_{vCNG}(T_{uf} - T_0)$$

where $u^0{}_{CNG}$ (-4821 kJ/kg) is the specific internal energy of the unburned CNG at 298 K, $T_0$ (298 K) is the standard temperature, and $C_{vCNG}$ (kJ/kg·K) is the constant-volume specific heat of the CNG fuel.

The specific volume of the unburned CNG $v_{CNG}$ (m$^3$/kg) is a function of the temperature of the unburned-fuel zone $T_{uf}$ (K) and the cylinder pressure P (kPa).

$$V_{CNG} = \frac{R_{CNG} T_{uf}}{P} \qquad (7.7)$$

where $R_{CNG}$ (kN·m/kg·K) is the unburned-CNG constant.

The specific internal energy of the unburned diesel $u_{DSL}$ (kJ/kg) is a function of the temperature of the unburned-fuel zone $T_{uf}$ (K).

$$u_{DSL} = u_{DSL}(T_{uf}) = u^0{}_{DSL} + C_{vDSL}(T_{uf} - T_0)$$

where $u^0{}_{DSL}$ (-3216 kJ/kg) is the specific internal energy of the unburned diesel at 298 K, and $C_{vDSL}$ (kJ/kg·K) is the constant-volume specific heat of the diesel fuel.

The specific volume of the unburned diesel $v_{DSL}$ ($m^3$/kg) can be neglected because $v_{DSL} \ll v_{CNG}$.

Assuming that the unburned fuel inside the cylinder undergoes a two-stage process.

1.  Adiabatic constant-pressure mixing with newly injected fuel.

2.  Isentropic compression (or expansion).

Within the crank angle interval of fuel injection, the existing unburned fuel in the cylinder has a adiabatic constant-pressure mixing with newly injected fuel. By applying the first law of thermodynamics to this process with instantaneous unburned fuel, we have

$$dH = m_g C_{pCNG} dT_{uf} + \delta m_g C_{pCNG} (T_{uf} - T_0) + m_d C_{pDSL} dT_{uf} + \delta m_d C_{pDSL} (T_{uf} - T_0) = 0 \quad (7.8)$$

where $m_g$ and $\delta m_g$ (kg) are the existing and newly injected masses of CNG fuel; $m_d$ and $\delta m_d$ (kg) are the existing and newly injected masses of diesel fuel; $C_{pCNG}$ and $C_{pDSL}$ (kJ/kg·K) are the constant-pressure specific heats of the CNG and diesel fuel.

By rearranging Eq. (7.8), we can determine the temperature change caused by mixing $(dT_{uf})_{mix}$.

$$(dT_{uf})_{mix} = - \frac{(\delta m_g C_{pCNG} + \delta m_d C_{pDSL}) \, ((T_{uf})_1 - T_0)}{m_g C_{pCNG} + m_d C_{pDSL}} \quad (7.9)$$

where subscript "1" denotes the state of the fuel injection.

By applying the first law of thermodynamics to isentropic compression (or expansion) process with instantaneous unburned fuel, we have

$$dH-VdP=m_g C_{pCNG} dT_{uf}+m_d C_{pDSL} dT_{uf}-m_g V_{CNG}dP-m_d V_{DSL}dP=0 \qquad (7.10)$$

Substituting Eq. (7.7) and $v_{DSL}=0$ in to Eq. (7.10), we can determine the temperature change caused by compression.

$$(dT_{uf})_{comp}=\frac{m_g R_{CNG}T_{uf}}{m_g C_{pCNG}+m_d C_{pDSL}}\frac{dP}{P}$$

or

$$(dT_{uf})_{comp}=\frac{m_g R_{CNG}(T_{uf})_1}{m_g C_{pCNG}+m_d C_{pDSL}}\frac{(P_2-P_1)}{P_1} \qquad (7.11)$$

where subscripts "1" and "2" denote starting and ending states.

Thus, the temperature of the unburned fuel at state "2" can be evaluated from the previous state "1".

$$(T_{uf})_2=(T_{uf})_1+(dT_{uf})_{mix}+(dT_{uf})_{comp} \qquad (7.12)$$

## Properties of the Burned-Gas Zone:

Both the specific internal energy of the burned gas $u_{bg}$ (kJ/kg) and the specific volume of the burned gas $v_{bg}$ ($m^3$/kg) are a function of the temperature of the burned-gas zone $T_{bg}$ (K) and the cylinder pressure P (kPa).

$$u_{bg}=u_{bg}(T_{bg},P)$$
$$v_{bg}=v_{bg}(T_{bg},P)$$

The relation among instantaneous volumes of cylinder V, unburned-fuel zone $V_{uf}$, burned-gas zone $V_{bg}$ and unburned-gas zone $V_{ug}$ is

$$V = V_{uf} + V_{bg} + V_{ug} = m_g v_g + m_d v_d + m_{bg} v_{bg} + (m_{tot} - m_g - m_d - m_{bg}) v_{ug} \qquad (7.13)$$

where v ($m^3/kg$) is the specific volume, and m (kg) is the instantaneous mass. Subscripts "g", "d", "bg", "ug", "uf" and "tot" denote CNG, diesel, burned-gas, unburned-gas, unburned-fuel and total cylinder contents respectively.

Dividing $m_{tot}$ on both sides of the Eq. (7.13) and rearranging it, we can get the mass conservation equation.

$$\frac{V - m_g (v_g - v_{ug}) - m_d (v_d - v_{ug})}{m_{tot}} = \frac{m_{bg}}{m_{tot}} v_{bg} + (1 - \frac{m_{bg}}{m_{tot}}) v_{ug} \qquad (7.14)$$

$x_1 = m_{bg}/m_{tot}$ is defined as the burned-gas mass fraction. Because the left side of Eq. (7.14) is the known quantity, let $v_m = [V - m_g (v_g - v_{ug}) - m_d (v_d - v_{ug})]/m_{tot}$. The mass conservation equation can now be simplified to

$$v_m = x_1 v_{bg} (T_{bg}, P) + (1 - x_1) v_{ug} \qquad (7.15)$$

The instantaneous relation of internal energy for the whole cylinder contents is

$$E_{tot} = U_{uf} + U_{bg} + U_{ug} = m_g u_g + m_d u_d + m_{bg} u_{bg} + (m_{tot} - m_g - m_d - m_{bg}) u_{ug} \qquad (7.16)$$

where $E_{tot}$ is the total internal energy of the cylinder contents, U (kJ) and u (kJ/kg) are the internal energy and the specific internal energy respectively, and m (kg) is the instantaneous mass. Subscripts "g", "d", "bg", "ug", "uf" and "tot" denote CNG, diesel, burned-gas, unburned-gas, unburned-fuel and total cylinder contents

respectively.

Dividing $m_{tot}$ on both sides of the Eq. (7.16) and rearranging it, we can get the energy conservation equation.

$$\frac{E_{tot}-m_g(u_g-u_{ug})-m_d(u_d-u_{ug})}{m_{tot}} = \frac{m_{bg}}{m_{tot}}u_{bg}+(1-\frac{m_{bg}}{m_{tot}})u_{ug} \qquad (7.17)$$

Because the left side of Eq. (7.17) is the known quantity, let $u_m=[E_{tot}-m_g(u_g-u_{ug})-m_d(u_d-u_{ug})]/m_{tot}$ and $x_1=m_{bg}/m_{tot}$. The energy conservation equation can now be simplified to

$$u_m=x_1 u_{bg}(T_{bg},P)+(1-x_1)u_{ug} \qquad (7.18)$$

By given $P$, $v_m$, $u_m$, $v_{ug}$ and $u_{ug}$, two equations, Eq. (7.15) and (7.18), can be used to solve $T_{bg}$ and $x_1$ iteratively [47].

$x$ is defined as the mass-burned fraction of the fuel which can be computed as follows:

$$X=\frac{m_{bf}}{m_{fuel}} = \frac{x_1(m_{trap}+m_{CNG}+m_{DSL})}{(m_{CNG}+m_{DSL})(1+\frac{1}{RFASTOIC})} \qquad (7.19)$$

where $m_{bf}$ and $m_{fuel}$ (kg/cycle) are masses of burned fuel and total mass of the fuel per cycle, $m_{trap}$ (kg/cycle) is the mass of the cylinder contents at IPC, which is the sum of the mass of air trapped in the cylinder and the residual mass from the previous cycle. $m_{CNG}$ (kg/cycle) and $m_{DSL}$ (kg/cycle) are the total masses of the CNG and the diesel fuels per cycle. RFASTOIC is the equivalent stoichiometric fuel-air ratio.

Total Internal Energy of the System:

   If one considers the whole cylinder contents as a system, the first law of thermodynamics that applies to the system for a small time change $\Delta t$ is

$$dE_{tot} = \delta Q - \delta W + \delta m_g h_{CNGin} + \delta m_d h_{DSLin}$$

where Q is the heat transfer with the cylinder wall, W is the work done to the piston, and $E_{tot}$ is the total internal energy of the system. $\delta m_g$ and $\delta m_d$ are injected masses of CNG and diesel fuel. Assume both fuels enter the cylinder at 298 K. Thus, $h_{CNGin}$ (-4667 kJ/kg) is the enthalpy of CNG at 298 K, and $h_{DSLin}$ (-3216 kJ/kg) is the enthalpy of diesel at 298 K. Thus the total internal energy at state "2" can be evaluated from previous state "1" over a given time step $\Delta t$ corresponding to 1 degree crank angle in this model.

$$(E_{tot})_2 = (E_{tot})_1 + \Delta Q_{1-2} - \Delta W_{1-2} + \delta m_g h_{CNGin} + \delta m_d h_{DSLin} \qquad (7.20)$$

Work Done to the Piston:

   The average pressure of the system from state "1" to "2" for a time step $\Delta t$ can be defined as

$$\overline{P} = \frac{P_1 + P_2}{2}$$

Thus the work done on the piston from system can be written as

$$\Delta W_{1-2} = \frac{P_1 + P_2}{2}(V_2 - V_1) \qquad (7.21)$$

where P is the pressure of the cylinder, and V is the volume of the cylinder.

Heat Transfer with Cylinder Wall:

Usually, heat transfer in engine consists of convective and radiative heat transfers with cylinder wall (including piston top wall and cylinder head flame wall). In order to simplify the computation, in this model assume that only the unburned gas contacts the cylinder wall and has convective and radiative heat transfer with the cylinder wall. The total heat transfer to the cylinder wall $Q_{WALL}$ is the sum of the convective $Q_{CONV}$ and the radiative $Q_{RAD}$ heat transfer to the cylinder wall.

$$Q_{WALL} = Q_{CONV} + Q_{RAD}$$

The heat transfer between state "1" and "2" for a given time step $\Delta t$ can be evaluated as

$$\Delta Q_{1\rightarrow 2} = \frac{Q_{WALL}}{(360)(\frac{N}{60})}$$

where $Q_{WALL}$ is in kW and $\Delta Q_{1\rightarrow 2}$ is in kJ/CA, and N (rpm) is the engine speed.

The general formula of convective heat transfer $Q_{CONV}$ is

$$Q_{CONV} = -h \times A_{surf} \times (T_{bulk} - T_{wall}) \qquad (7.22)$$

where h is the convection heat transfer coefficient (kW/m$^2\cdot$K), $A_{SURF}$ (m$^2$) is the wall surface area which the unburned gas contacted, $T_{wall}$ is the averaged cylinder wall temperature (assume $T_{wall}$=450 K in this model), and $T_{bulk}$ is the bulk temperature of the cylinder content [48] which is determined by

$$T_{bulk} = \frac{m_{ug}T_{ug} + m_{bg}T_{bg}}{m_{ug} + m_{bg}} = (1 - x_1) T_{ug} + x_1 T_{bg} \qquad (7.23)$$

where $m_{ug}$ and $T_{ug}$ are the instantaneous mass and the temperature of the unburned-gas zone. $m_{bg}$ and $T_{bg}$ are instantaneous mass and temperature of the burned-gas zone. $x_1$ is the burned-gas mass fraction.

As recommended by Woschni [48], the Nusselt number (Nu) in the engine can be expressed as

$$Nu = \frac{hB}{k} = c_3 (Re)^{c_4} \qquad (7.24)$$

The instantaneous heat transfer coefficient in the engine can be expressed as

$$h = \frac{c_3 k (Re)^{c_4}}{B} \qquad (7.25)$$

where $c_3$ is a coefficient and in the range of 0.35~0.8, $c_4$ is another coefficient and in the range of 0.75~0.87 for the gas-diesel operation, and B is the diameter of the cylinder bore (m). $k = C_{pug} \cdot \mu / Pr$ (kW/m·K) is the thermal conductivity of the unburned gas, in which $C_{pug}$ (kJ/kg·K) is the specific heat of unburned gas, $\mu$ (kg/m·s) is the dynamic viscosity of unburned gas, and Pr is the Prandtl number, Pr=0.7 in this model.

Re=$\rho \cdot V_{pis} \cdot B / \mu$ is the Reynolds number, in which $\rho$ (kg/m$^3$) is the density of unburned gas, $V_{pis}$ (m/s) is the piston velocity.

Radiative heat transfer $Q_{RAD}$ can be computed with the following equation.

$$Q_{RAD} = -F \times A_{surf} \times (T_{ug} - T_{wall}) \qquad (7.26)$$

where $F = F_\varepsilon \times F_G \times \sigma = 1.6 \times 10^{-12}$ is the multiply of three factors, $F_\varepsilon$ is the emissivity function, $F_G$ is the geometric function, and $\sigma$ is the Stefan-Boltzmann constant with a valve of $5.669 \times 10^{-8}$ $W/m^2 \cdot K^4$.

## 7.3 Mass of Air Trapped in the Cylinder and Residual Mass Fraction

In the uniflow-scavenged, two-stroke test engine, the unburned gas is the mixture of the fresh air trapped in the cylinder and the residual gas from the previous cycle. To estimate the amount of air trapped in the cylinder at the end of the scavenging process, the following definitions are used.

●Delivered air mass, $m_{air}$:

The mass of air delivered to the engine per cycle as measured at the intake line.

●Mass of air trapped, $m_{atrap}$:

The portion of the delivered air mass per cycle trapped in the cylinder at the inlet port closure (IPC).

●Residual mass, $m_{res}$:

The mass of the combustion products remaining from the previous cycle.

●Trapped mass, $m_{trap}$:

The mass of the cylinder contents at IPC, which is the sum of

the mass of air trapped and the residual mass.

$$m_{trap} = m_{atrap} + m_{res}$$

●Delivery ratio, $\Lambda$:

The ratio of the delivered air mass to the trapped mass.

$$\Lambda = \frac{m_{air}}{m_{trap}}$$

●Degree of purity of the charge, DP:

The ratio of the mass of air trapped to the trapped mass.

$$DP = \frac{m_{atrap}}{m_{trap}} = \frac{m_{atrap}}{m_{atrap} + m_{res}}$$

●Residual mass fraction, $f_{res}$:

The ratio of the residual mass to the trapped mass.

$$f_{res} = \frac{m_{res}}{m_{trap}} = \frac{m_{res}}{m_{res} + m_{atrap}}$$

If one assumes that the residual gas has the same molecular weight as air, the residual mass fraction is equal to the residual mol fraction.

An iteration process is used for the computation of $m_{atrap}$ and $f_{res}$. For given exhaust temperature $T_{exh}$, air box temperature $T_{abox}$, and estimated DP and $m_{trap}$, the initial temperature of the residual, $T_{res}$ (K), can be determined from

$$T_{res} = \frac{T_{exh} C_{pexh} (m_{air} + m_{CNG} + m_{DSL}) - T_{abox} C_{pair} (m_{air} - DP \times m_{trap})}{C_{pres} (DP \times m_{trap} + m_{CNG} + m_{DSL})} \qquad (7.27)$$

where $m_{air}$, $m_{CNG}$ and $m_{DSL}$ (kg/cycle) are the delivered air mass, total

injected mass of CNG per cycle and total injected mass of diesel per cycle respectively. Cpexh, Cpair and Cpres (kJ/kg·K) are the constant-pressure specific heats of exhaust gas, air and residual respectively. Detailed derivation of this equation is given in Appendix L.

The temperature of the cylinder contents at IPC $T_{ipc}$ (K) is

$$T_{ipc} = T_{abox}DP + T_{res}(1 - DP)$$

For given temperature, pressure and volume at IPC, the trapped mass in the cylinder at IPC and the delivery ratio can be determined with the formulae:

$$m_{trap} = \frac{P_{ipc}V_{ipc}}{R_{ug}T_{ipc}}$$

$$\Lambda = \frac{m_{air}}{m_{trap}}$$

where $R_{ug}$ (kN·m/kg·K) is the gas constant of the unburned gas (ie. the cylinder contents at IPC has the same composition as the unburned gas).

An empirical equation of the degree of purity as a function of the delivery ratio for the uniflow scavenging [47] is used in this model, which is

$$DP = 0.173611\Lambda^3 - 0.95982\Lambda^2 + 1.774305\Lambda - 0.19642 \qquad (7.28)$$

Figure 7.2 shows a typical uniflow-scavenging data range for the two-stroke diesel engine [26] and the position of the above
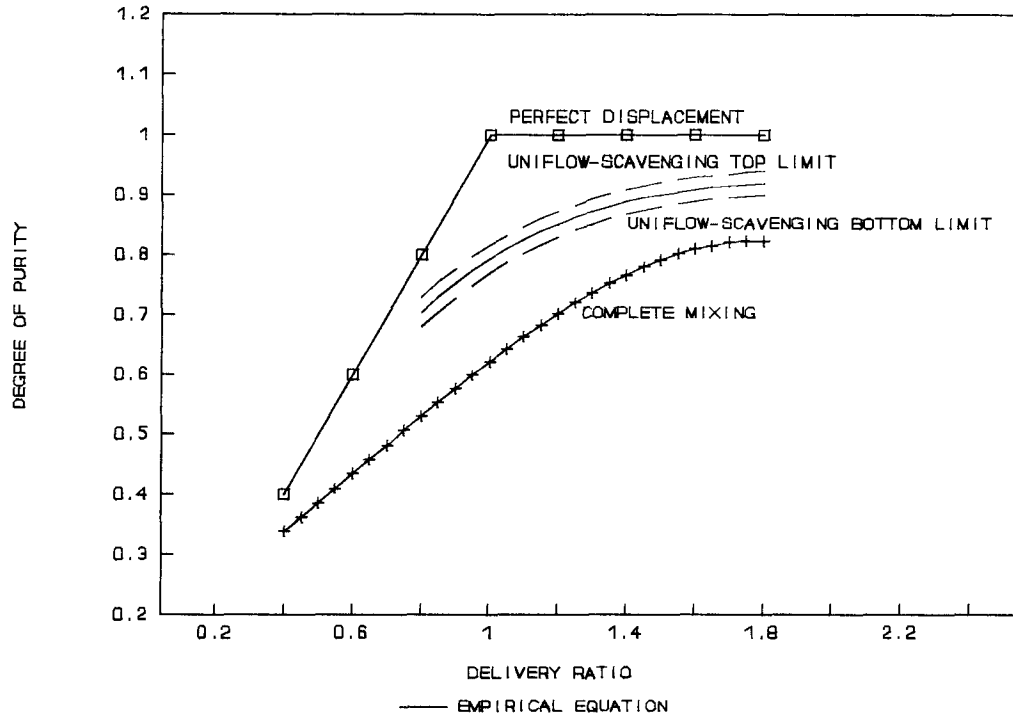
Figure 7.2: Typical Scavenging Data Range of Two-Stroke Diesel.

empirical equation curve.

After entering the new DP and $m_{trap}$ into the Eq. (7.27) and doing the iteration until the new DP equals the previous DP, then $m_{atrap}$ (kg/cycle) and $f_{res}$ are evaluated from

$$m_{atrap} = DP \times m_{trap} \qquad (7.29)$$

and

$$f_{res} = 1 - DP \qquad (7.30)$$

## 7.4 Unburned-Gas Composition

Because of the residual gas, the composition of the unburned gas varies during the first few cycles after firing. PROGRAM#2 and Eqs. (6.10) through (6.16) in Subsection 6.3.2 are adopted into this model to simulate the initial transient variation of the composition and calculate the composition of residual gas at steady state. The following assumptions are made for simplifying the calculation.

1.  Residual gas consists of only $CO_2$, $H_2O$, $O_2$ and $N_2$. The molal fractions of these components (ie. $X^i_{CO2}$, $X^i_{H2O}$, $X^i_{O2}$ and $X^i_{N2}$) and the molecular weight of the residuals (ie. $MW_{res}$) have already been calculated in the previous cycle. Residual mass fraction (ie. $f_{res}$) is known.

2.  Fresh intake air consists of only $O_2$ and $N_2$. Mass of air trapped in the cylinder (ie. $m_{atrap}$) is known.

The number of moles of the residuals $N_{res}$ is determined in the formula:

$$N_{res} = \frac{f_{res}}{1-f_{res}} \frac{m_{atrap}}{MW_{res}}$$

The total number of moles of the unburned-gas before combustion taking place $N_{totug}$ is determined in the formula:

$$N_{totug} = \frac{m_{atrap}}{MW_{air}} + N_{res}$$

The molal fractions of the unburned-gas components, $X_{O2}$, $X_{N2}$, $X_{CO2}$ and $X_{H2O}$, are evaluated in the formulae:

$$X_{O2} = \frac{N_{O2}}{N_{totug}} = \frac{0.21\left(\frac{m_{atrap}}{MW_{air}}\right) + N_{res} X^i_{O2}}{N_{totug}}$$

$$X_{N2} = \frac{N_{N2}}{N_{totug}} = \frac{0.79\left(\frac{m_{atrap}}{MW_{air}}\right) + N_{res} X^i_{N2}}{N_{totug}}$$

(7.31)

$$X_{CO2} = \frac{N_{CO2}}{N_{totug}} = \frac{N_{res} X^i_{CO2}}{N_{totug}}$$

$$X_{H2O} = \frac{N_{H2O}}{N_{totug}} = \frac{N_{res} X^i_{H2O}}{N_{totug}}$$

where $N_{O2}$, $N_{N2}$, $N_{CO2}$ and $N_{H2O}$ are the number of moles of $O_2$, $N_2$, $CO_2$ and $H_2O$ in the unburned-gas. $MW_{air}$ (28.97 kg/kmol) is the molecular weight of the intake air.

## 7.5 Unburned-Fuel Mass Ratio in Exhaust

Unburned-fuel mass ratio in the exhaust, UFRAT, is defined as a mass ratio of unburned fuel in the exhaust to the total injected fuels (including CNG and diesel fuel). It is used to normalize the fuel mass-burned fraction. It can be computed directly from measured engine exhaust emission data, air mass flow rate and fuel mass flow rate. Unburned fuel in the exhaust is measured as the total hydrocarbon emission HC. The following assumptions are applied in the computation process.

1.  The engine exhaust consists of CO, $CO_2$, $NO_x$, $H_2O$, $O_2$, $N_2$ and unburned HC.

2. The unburned HC has the same composition as the combined fuel.

3. All measured emission data have already been converted to wet basis in ppm (or % by volume).

Unburned-fuel mass ratio in the exhaust, UFRAT, can be calculated from the following equation.

$$UFRAT = \frac{\dot{m}_{HC}}{\dot{m}_{DSL} + \dot{m}_{CNG}}$$  (7.32)

where $\dot{m}_{HC}$, $\dot{m}_{DSL}$ and $\dot{m}_{CNG}$ (kg/hr) are mass flow rate of unburned

HC, diesel and CNG respectively.

The mass flow rate of unburned HC, then, can be calculated by using Eqs. (4.15) through (4.21) in Subsection 4.4.2. In consistent to the molecular formulae of CNG and diesel, 16.043 kg/kmol and 14.026 kg/kmol are used as the molecular weights of CNG and diesel fuels in Equ. (4.20). The mass flow rate of the diesel and the CNG are measured.

## 7.6 Averaged Equilibrium NO Concentration

To simulate the diffusion combustion in the test engine, a stoichiometric complete combustion pattern was applied in this model. The combustion equation for the fuel ($CH_y$) and the unburned gas at the maximum burned-gas temperature $T_{bgmax}$ and corresponding pressure $P_{T_{bgmax}}$ is

$$CH_y + (1+\frac{y}{4}) \ (O_2 + \frac{X_{N2}}{X_{O2}} N_2 + \frac{X_{H2O}}{X_{O2}} H_2O + \frac{X_{CO2}}{X_{O2}} CO_2)$$

$$\Rightarrow [1+(1+\frac{y}{4}) \frac{X_{CO2}}{X_{O2}}] \ CO_2 + [\frac{y}{2}+(1+\frac{y}{4})] \frac{X_{H2O}}{X_{O2}} H_2O + (1+\frac{y}{4}) \frac{X_{N2}}{X_{O2}} N_2$$

$$(7.33)$$

where y is the hydrogen-to-carbon atom ratio of the combined fuel as determined by Equ. (7.1). $X_{O2}$, $X_{N2}$, $X_{H2O}$ and $X_{CO2}$ are the molal fraction of oxygen, nitrogen, water and carbon dioxide in the unburned gas which are determined by Equ. (7.31) in Section 7.4.

The C:H:O:N ratio at stoichiometric complete combustion can be determined as

$$\frac{H}{C} = \frac{n[1+\frac{2}{n}(1+\frac{n}{4}) \frac{X_{H2O}}{X_{O2}}]}{1+(1+\frac{n}{4}) \frac{X_{CO2}}{X_{O2}}} \qquad (7.34)$$

$$\frac{O}{C} = \frac{(1+\frac{n}{4}) \ (2+\frac{X_{H2O}}{X_{O2}}+2\frac{X_{CO2}}{X_{O2}})}{1+(1+\frac{n}{4}) \frac{X_{CO2}}{X_{O2}}} \qquad (7.35)$$

$$\frac{N}{C} = \frac{2(1+\frac{n}{4}) \frac{X_{N2}}{X_{O2}}}{1+(1+\frac{n}{4}) \frac{X_{CO2}}{X_{O2}}} \qquad (7.36)$$

STANJAN is the program that is used to calculate the equilibrium burned-gas composition with dissociation combustion. Thus, the equilibrium NO concentration in the burned-gas zone $[NO]_{EQUIL}$ can be obtained by entering C:H:O:N ratio, $T_{bgmax}$ and $P_{Tbgmax}$ into Stanjan. A correction factor, CFK, is used to average

equilibrium NO concentration over whole cylinder contents.

$$[NO]_{AVG-EQUIL}=CFK\times [NO]_{EQUIL} \qquad (7.37)$$

where $[NO]_{AVG-EQUIL}$ is the averaged equilibrium NO concentration over whole cylinder contents.

Determination of the CFK starts at maximum burned-gas temperature (ie. $T_{bg} = T_{bgmax}$).

Mass of fuel per cycle $m_{fuel}$ (kg/cycle) is determined in the formula:

$$m_{fuel}=m_{DSL}+m_{CNG} \qquad (7.38)$$

where $m_{DSL}$ and $m_{CNG}$ (kg/cycle) are the mass of diesel and CNG per cycle respectively, which can be calculated from the measured mass flow rates of diesel and CNG.

Mass of the fuel burned $m_{fbmax}$ (kg/cycle) and number of moles of fuel burned $N_{fbmax}$ at maximum temperature $T_{bgmax}$ are determined in the formulae:

$$m_{fbmax}=X_{Tbgmax}\times m_{fuel}$$

$$N_{fbmax}=\frac{m_{fbmax}}{MW_{HC}}$$

where $x_{Tbgmax}$ is the fuel mass-burned fraction at $T_{bgmax}$, and $MW_{HC}$ is the molecular weight of the fuel ($CH_y$).

Considering that the fuel ($CH_y$) undergoes a stoichiometric complete combustion with unburned gas at $T_{bgmax}$ and $P_{Tbgmax}$, Eq. (7.33) is used to determine the number of moles of burned gas $N_{bgmax}$ at $T_{bgmax}$, $P_{Tbgmax}$.

$$N_{bgmax} = N_{fbmax} \times [1 + \frac{y}{2} + (1 + \frac{y}{4}) (\frac{X_{CO2} + X_{H2O} + X_{N2}}{X_{O2}})]$$

Total mass and total number of moles of the engine exhaust, $m_{exh}$ and $N_{exh}$, are

$$m_{exh} = m_{air} + m_{fuel}$$

$$N_{exh} = \frac{m_{exh}}{MW_{exh}}$$

where $m_{air}$ (kg/cycle) is delivered air mass determined from measured air mass flow rate, $m_{fuel}$ (kg/cycle) is mass of the fuel determined from Equ. (7.38), and $MW_{exh}$ is the molecular weight of the exhaust. Then the average equilibrium NO concentration, $[NO]_{AVG-EQUIL}$, can be calculated by

$$[NO]_{AVG-EQUIL} = \frac{N_{bgmax}}{N_{exh}} [NO]_{EQUIL}$$

where CFK is defined as:

$$CFK = \frac{N_{bgmax}}{N_{exh}} \qquad (7.39)$$

# 7.7 Computation Results
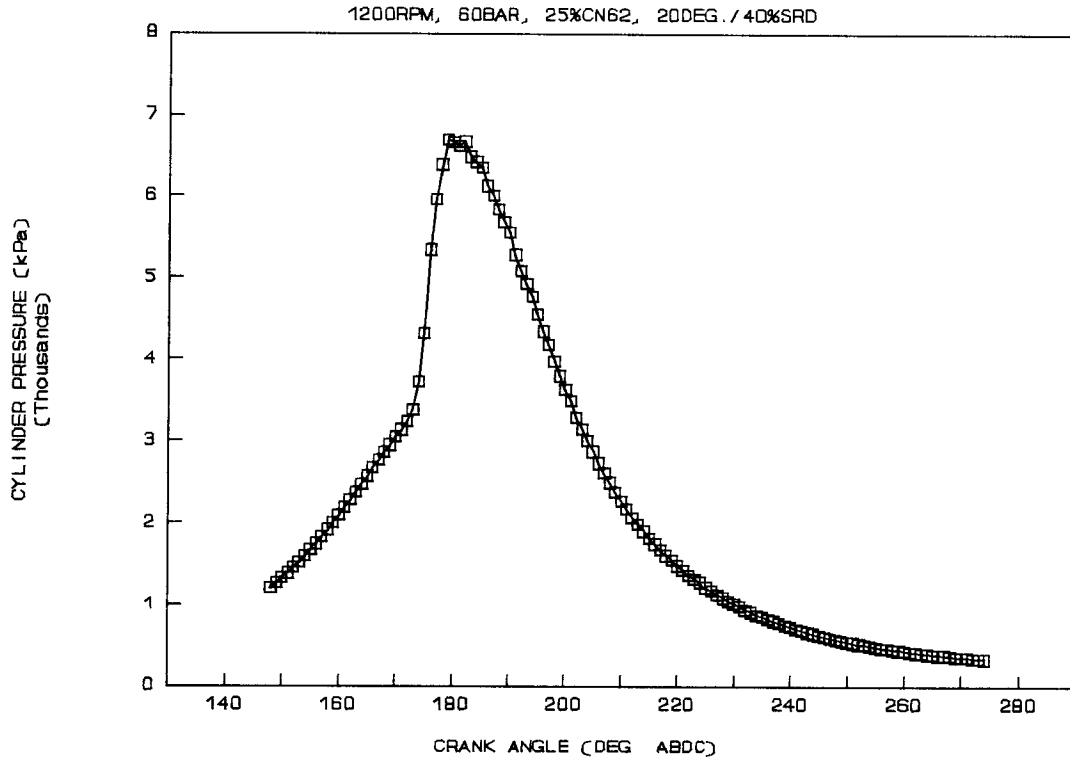


Figure 7.3: Cylinder Pressure Distribution (BMEP = 4 bar).

Computations were conducted to investigate the fuel combustion pattern, the effect of various operation parameters on the ignition delay, the relationship of calculated NO to measured NO, and the effect of EGR on NO concentration. The calculation procedure in terms of work sheet is presented in Appendix M and the program XPRESSD is documented in Appendix N.

The cylinder pressure distributions were the source data for the calculation. Figure 7.3 shows a example of these data.
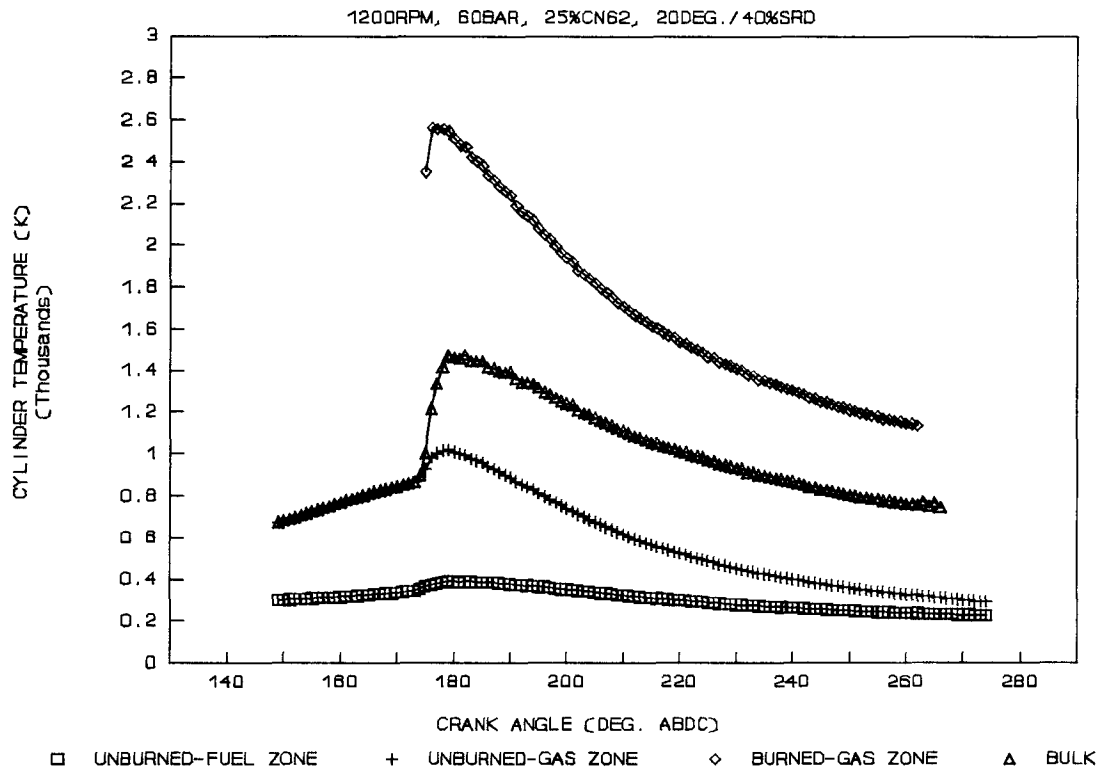
Figure 7.4: Temperature Distributions (BMEP = 4 bar).

The typical temperature distributions of the three-zone model are shown in Figure 7.4. They were directly calculated from the cylinder pressure distribution shown in Figure 7.3. The bulk temperature was used to evaluate heat transfer to the cylinder wall.

## Combustion Pattern in the Gas-Diesel Engine:

The three test conditions investigated were:

1)  Straight diesel operation at 1200 rpm speed, 4 bar load, and 12°BTDC BOI (ie. diesel baseline).

2)  Gas-diesel operation at 1200 rpm speed, 4 bar load, 60 bar gas
    pressure, 25% diesel ratio, 40% fuel jet interruption ratio
    (% SRD), 20° injection angle, and 32°BTDC BOI.

3)  Gas-diesel operation at 1200 rpm speed, 4 bar load, 60 bar gas
    pressure, 25% diesel ratio, 0% fuel jet interruption ratio
    (% SRD), 20° injection angle, and 32°BTDC BOI.
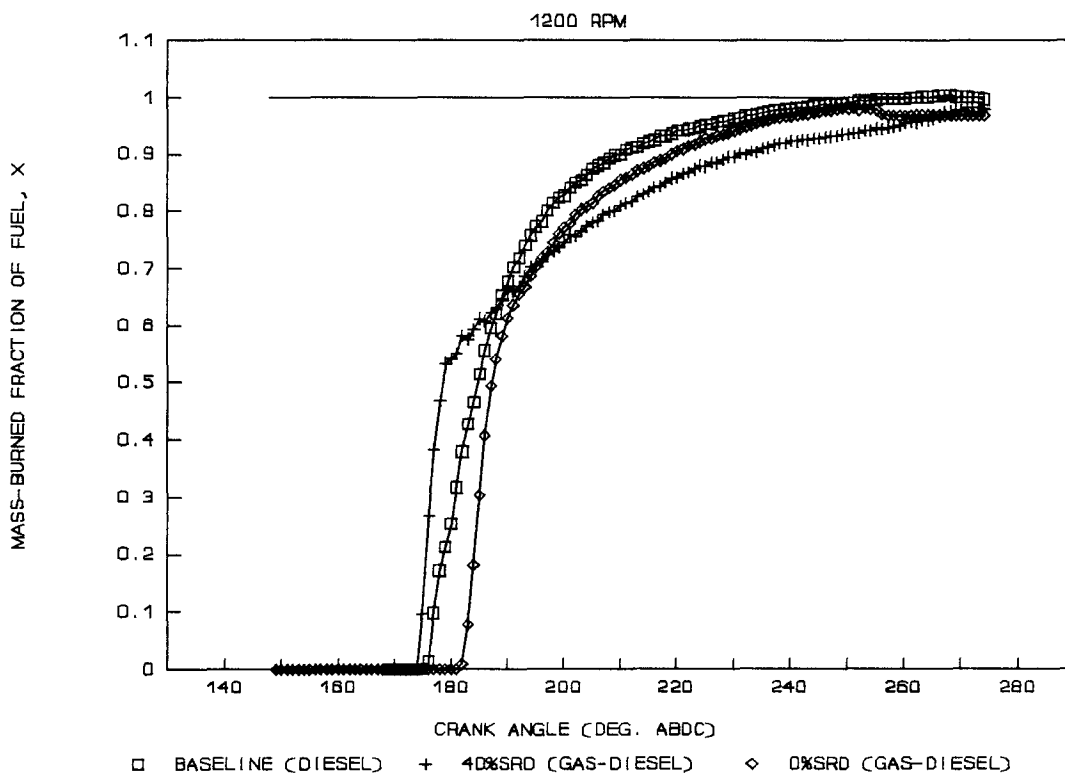


Figure 7.5: Fuel Mass-Burned Fraction (BMEP = 4 bar).

The combustion rates of three test cases are shown in Figure
7.5. As shown, operation with straight diesel has shorter ignition
delay than that with gas-diesel. Ignition delay is defined as a
crank angle interval (or time period) from BOI to the point with 1%

of fuel burned. From two gas-diesel operation cases, it is seen that pilot-diesel fuel burns first with a fast burning rate and natural gas burns later with a slow burning rate. This may suggest that considerable amount of pilot diesel is well mixed with air after a long ignition delay, thereby suddenly burning with a premixture burning rate when the temperature is ready.

Ignition Delay:
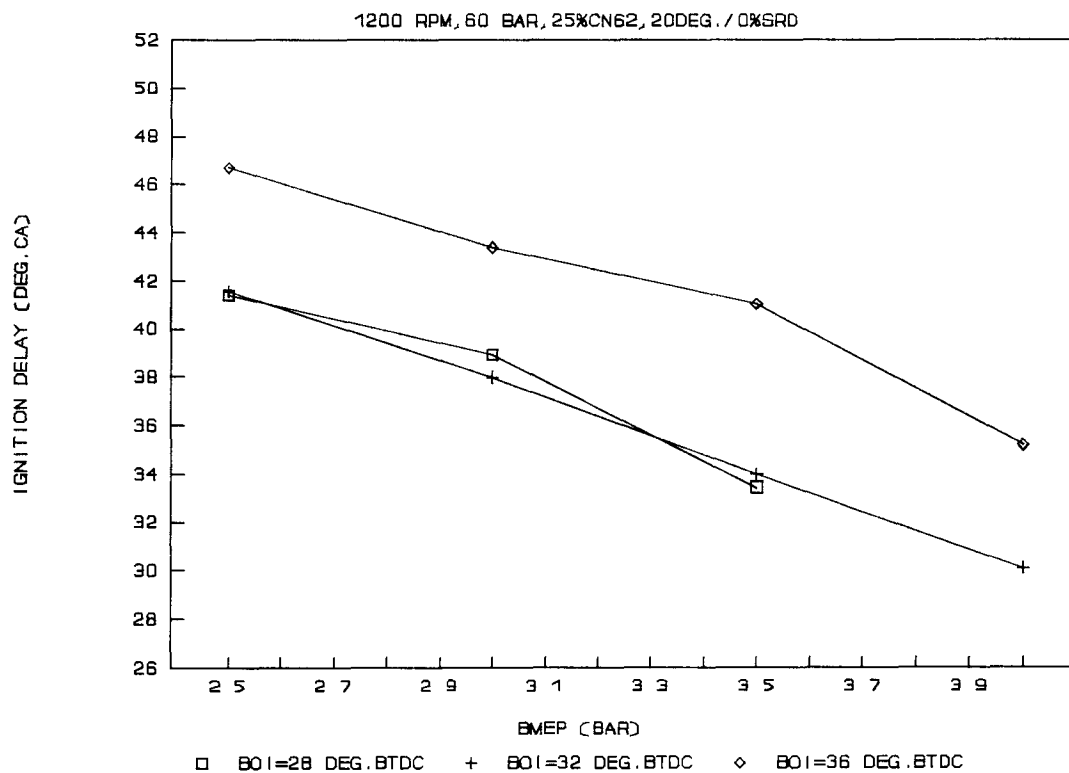


Figure 7.6: Effects of BOI on Ignition Delay.

The ignition delay was calculated according to above definition in the model within 5% error range at 1200 rpm.

The effect of BOI on ignition delay is shown in Figure 7.6. Test condition was gas-diesel operation at 1200 rpm speed, 60 bar gas pressure, 25% diesel ratio, 0% fuel jet interruption ratio (% SRD), and 20° injection angle. It is interesting to see that there is almost no difference in ignition delay with BOI at 28°BTDC and at 32°BTDC; but a big difference results from increasing BOI to 36°BTDC.
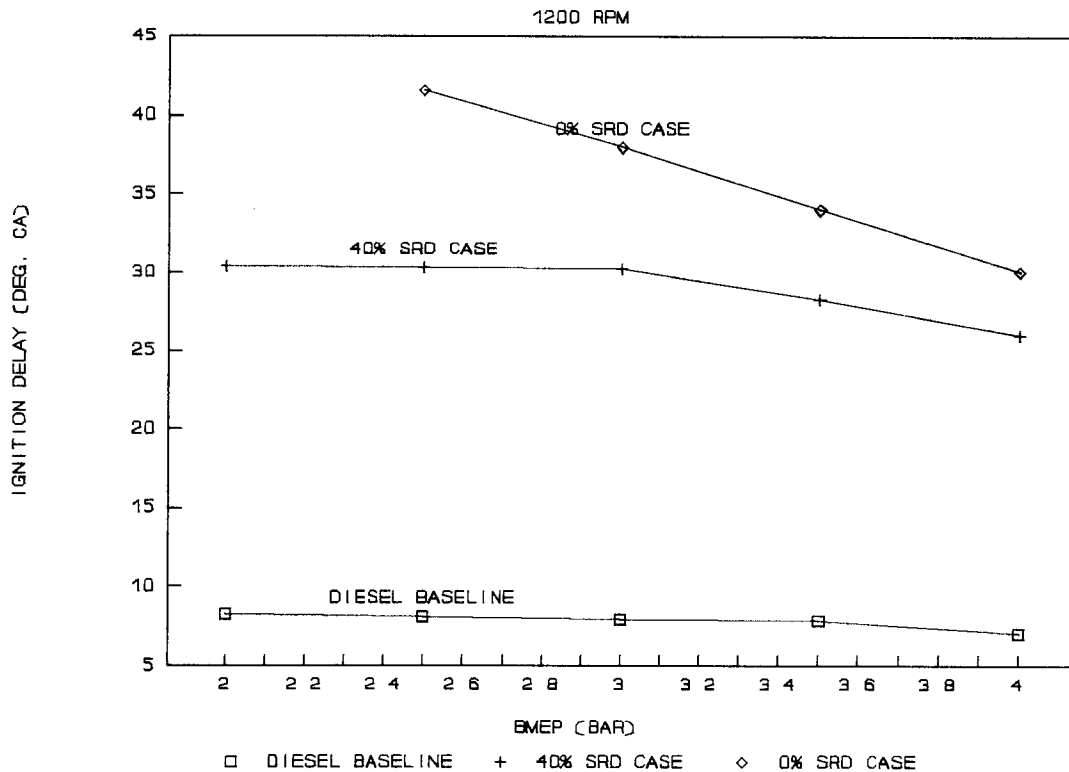


Figure 7.7: Effect of Fuel Jet Interruption Ratio on Ignition Delay.

Figure 7.7 shows the effect of fuel jet interruption on the ignition delay. It can be seen that operating with gas-diesel has

much longer ignition delay than with straight diesel. The typical ignition delay for diesel operation is in the range of 7 ~ 9 °CA (or 0.97 ~ 1.25 ms) at 1200 rpm, and for gas-diesel operation is in the range of 26 ~ 46 °CA (or 3.6 ~ 6.4 ms) at 1200 rpm. It is also found that ignition delay is shorter with 40% SRD than with 0% SRD (ie. no interruption), which indicates that fuel jet interruption helps fuel ignition.
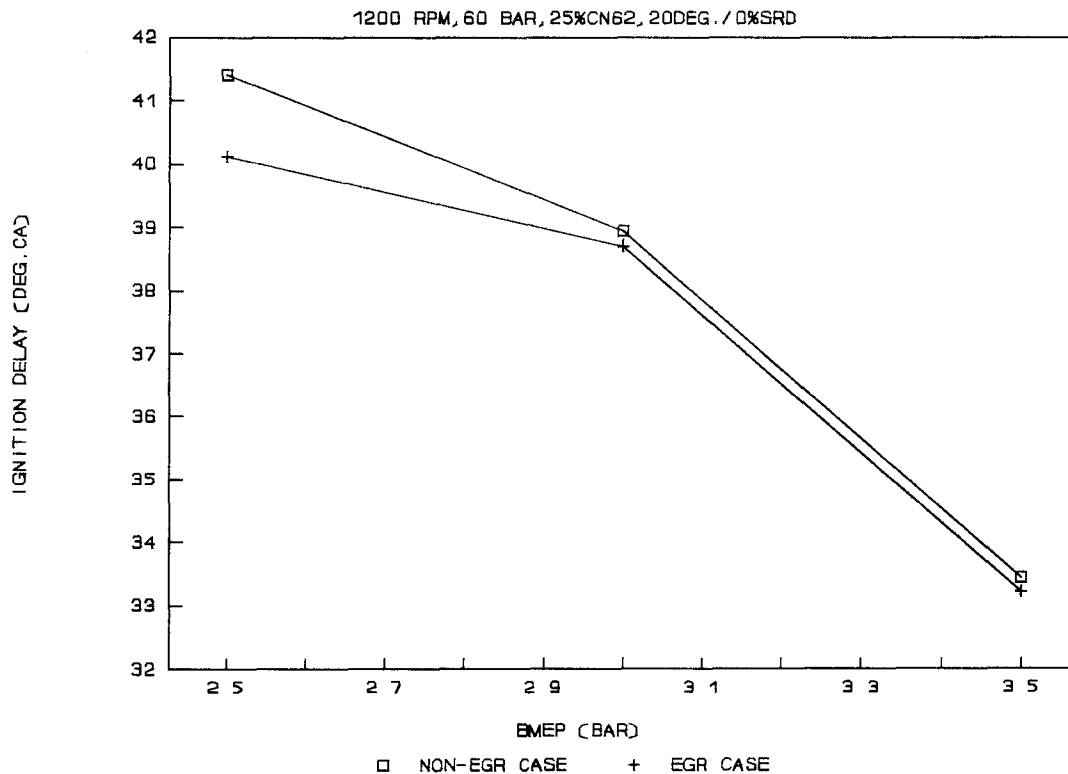


Figure 7.8: Effect of EGR on Ignition Delay
(with BOI = 28 °BTDC).

The effect of EGR on ignition delay is shown in Figure 7.8. In this case, about 20% of exhaust gas was recycled into the cylinder

and the residual fraction in the cylinder increased about 35%. It is found that EGR slightly reduces ignition delay and is more effective at low load than at high load.

## Relationship between Calculated NO and Measured NO:
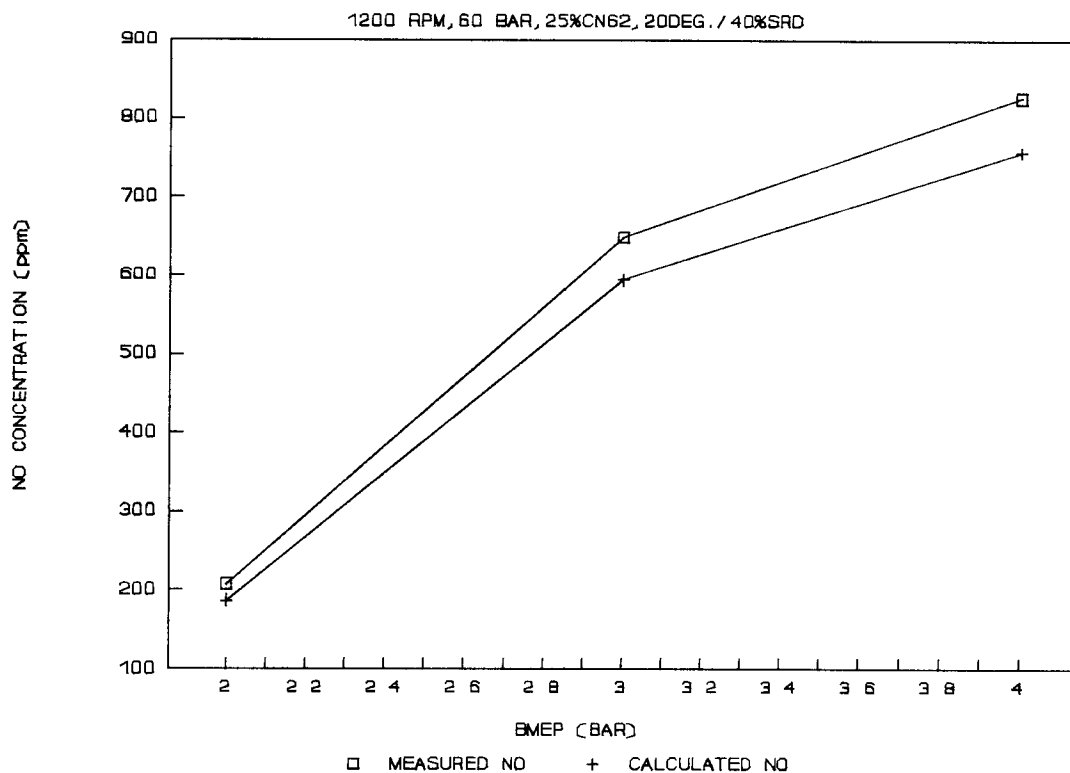


Figure 7.9: Correlation of Measured NO and Calculated NO.

The equilibrium NO concentration of the combustion products was calculated in the model. An example of the correlation of the calculated NO concentration to the measured NO concentration (or tail-pipe NO concentration) is shown in Figure 7.9. The difference between calculated and measured NO was within 20% for the whole

gas-diesel operation cases and up to 40% difference for the diesel
baseline.

Reduction of Tail-Pipe NO with EGR:



1200 RPM, 60 BAR, 25%CN62, 20DEG./0%SRD

□ NON-EGR (MEASURED)    + EGR (MEASURED)
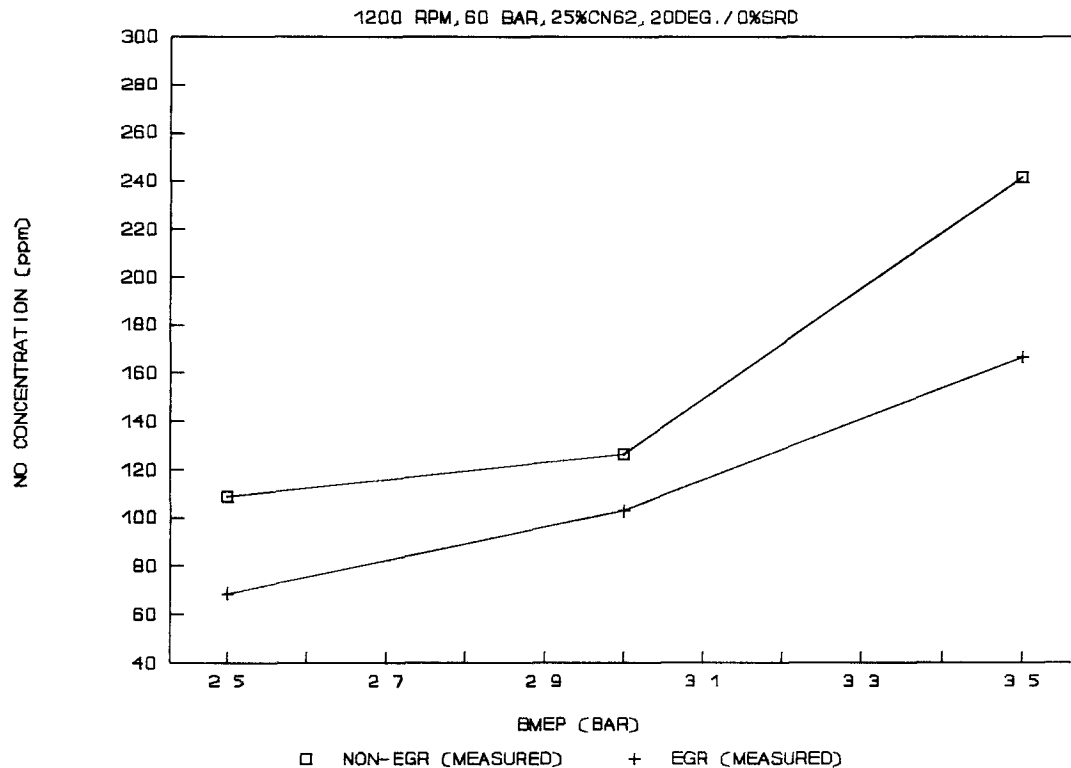
Figure 7.10: Effect of EGR on Measured NO Concentration
(with BOI = 28 °BTDC).

The effects of EGR on both measured and calculated NO
concentration shown in Figures 7.10 and 7.11. In this case, about
20% of exhaust gas was recycled into the cylinder and the residual
fraction in the cylinder increased about 35%. It is found that EGR
reduces NO emission significantly (about 50% reduction at low load

and 25% reduction at high load for measured data). The NO reduction with measured data is larger than with calculated data.
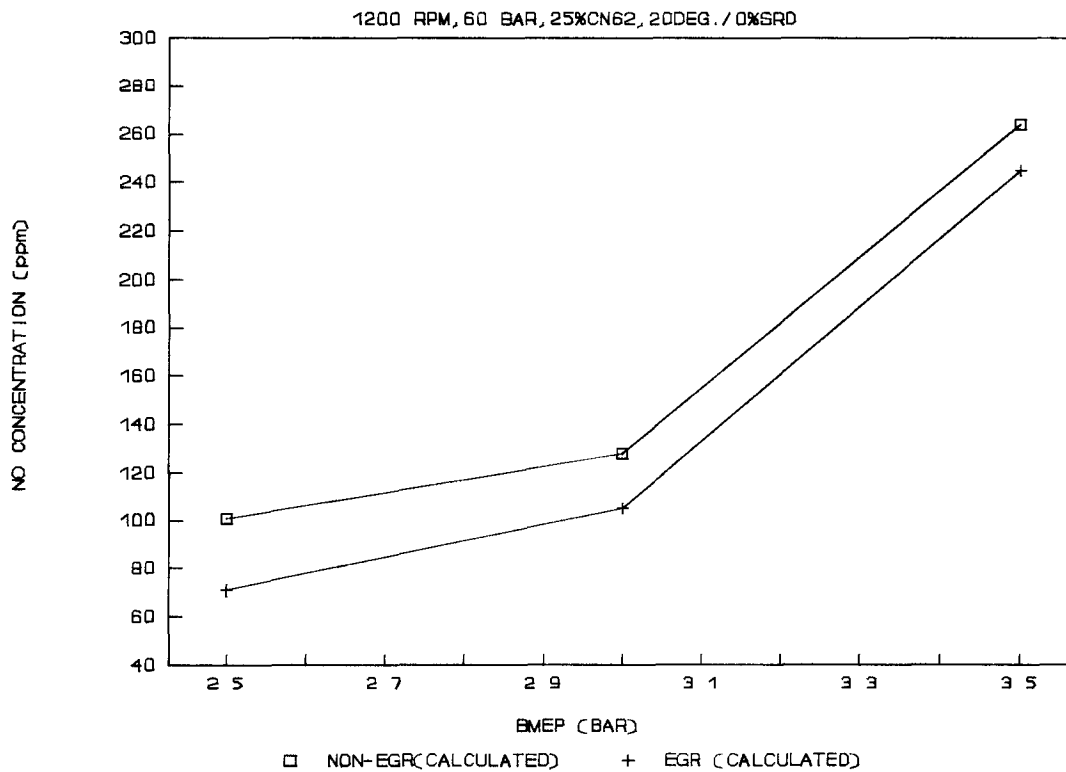


Figure 7.11: Effect of EGR on Calculated NO Concentration (with BOI = 28 °BTDC).

## 7.8 Summary

1. The three-zone combustion and exhaust emission analysis model XPRESSD was established on the mass and the energy conservation equations.

2. The estimation of the amount of fresh air trapped in the cylinder and residual fraction followed the procedure recommended

by Heywood [26] has been employed.

3. A method for simulating the initial transient variation of the composition and calculating the composition of the residual gas at steady state was adopted into this model. The evaluation of the unburned-gas compositions was based on the result of this method.

4. The stoichiometric complete combustion was applied in this model to simulate the diffusion combustion. The burned-gas temperature was calculated with a error range of ±25 K.

5. The equilibrium NO concentration was evaluated with STANJAN [43] and correlated with the measured tail-pipe NO concentration.

6. The unburned-fuel mass ratio in the exhaust determined by the unburned hydrocarbon in the exhaust was used to normalize the fuel mass-burned fraction curve.

7. The heat transfer with the cylinder wall was applied in the model. The heat transfer coefficients were used to adjust the fuel mass-burned fraction curve to a normalized value.

8. The ignition delay was defined and evaluated within 5% error at 1200 rpm. The ignition delay of the gas-diesel operation was found to be 3 ~ 5 times longer than the straight diesel operation.

9. Fuel jet interruption was a method of reducing ignition delay.

10. EGR was an efficient method to reduce NO emission.

# 8. CONCLUSIONS AND RECOMMENDATIONS

## 8.1 Conclusions

The influences of variable parameters on performance and emissions of a gas-diesel engine were investigated both experimentally and theoretically. The conclusions drawn are as follows:

1. Replacing diesel fuel by natural gas in a diesel engine can reduce $NO_x$ and $CO_2$ emissions while meeting or exceeding diesel engine efficiency.

2. With a poppet-valve gas injector and entrained diesel pilot ignition fluid, a minimum diesel energy ratio of about 25% was found to be necessary to provide stable operation over the whole load range.

3. The optimum natural gas injection pressure was 60 bar, which means an injection pressure ratio varying over the injection period in the range 2.8 to 1.5; engine performance and exhaust emissions depended strongly on injection pressure.

4. With a poppet-valve gas injector and entrained diesel pilot ignition fluid, combustion was typically incomplete at low load, as shown by excessive emissions of CO and unburned hydrocarbon (THC).

5. Engine performance and exhaust emissions were sensitive to injection angle and jet sheet geometry (ie. jet interruption); improvements made in the light of flow visualization studies

lead to small improvements in the engine efficiency and exhaust emissions.

6. Diesel pilot fluid with high cetane number can improve engine efficiency and reduce unburned hydrocarbon (THC) emission at low and medium load.

7. Replacing diesel fuel with natural gas in a diesel engine can significantly reduce NO formation, as shown by both measurements and equilibrium estimates of NO concentration.

8. Ignition delay of the gas-diesel operation was found to be much longer than that of the straight diesel operation; proper fuel jet sheet geometry (ie. jet interruption) can reduce ignition delay.

9. BOI retardation can significantly reduce $NO_x$ with only slight reduction of thermal efficiency.

10. Reduction of NO concentration by EGR (exhaust gas recycling) was been shown to be significant over the whole engine operation range, but this also resulted in a slight increase in carbon monoxide (CO) and unburned hydrocarbon (THC) emissions.

11. Correlation between NO concentration measured in the exhaust pipe and NO estimated from equilibrium concentration (at peak temperature in the cylinder and averaged over the whole cylinder contents) was close at low and medium load.

## 8.2 Recommendations

From the above conclusions, to improve engine performance and emissions, especially at low load, the present injection pattern and injector configuration ought to be modified. The following change are suggested:

1. Separate the diesel-pilot-fluid passage in the injector from the CNG passage completely to control the quantity and BOI of the pilot diesel precisely.

2. Inject the diesel pilot fluid first; inject the CNG into the high temperature zone close to the combustion zone of the diesel pilot fluid to ignite the in coming CNG/air mixture.

3. Improve spray quality of the diesel pilot fluid and atomize diesel droplets for more rapid vaporization and mixing.

4. In order to achieve above purpose, a multi-orifice injector with separate fuel passages is suggested. The size of CNG orifices, which should be larger than pilot-diesel orifices, can be determined experimentally. A injection angle of about $20°$ is recommended. CNG injection pressure should be adjusted for each engine.

# REFERENCES

[1]   Journal of Air Pollution Control Association, v24, January
      1974.

[2]   Wark, K. and Warner, C.F., Air Pollution -- Its origin and
      Control, First Edition, 1976.

[3]   Karim, G.A. and Wierzba, I., Comparative Studies of Methane
      and Propane as Fuels for Spark Ignition and Compression
      Ignition Engines, Society of Automotive Engineer, SAE Paper
      831196, 1983.

[4]   Karim, G.A., The Dual Fuel Engine of the Compression Ignition
      Type - Prospects, Problem and Solution - A Review, Society of
      Automotive Engineer, SAE Paper 831073, SAE Trans. v92, pp.
      569-577, 1983.

[5]   Fraser, R.A., Siebers, D.L. and Edwards, C.F., Autoignition of
      Methane and Natural Gas in a Simulated Diesel Environment,
      Society of Automotive Engineer, SAE Paper 910227, 1991.

[6]   Karim, G.A., On the Emission of Carbon Monoxide and Smoke from
      Compression Ignition Engines; Including Natural Gas Fuelled
      Engines, Proceedings of 2nd Int. Clean Air Congress, Academic
      Press, p. 617, 1970.

[7]   McJones, R.W. and Corbeil, R.J., Natural Gas Fuelled
      Vehicles; Exhaust Emissions and Operational Characteristics,
      Society of Automotive Engineer, SAE Paper 700078, 1970.

[8]   Fleming, R.D. and Allsup, J.R., Emission Characteristics of
      Natural Gas as an Automotive Fuel, Society of Automotive
      Engineer, SAE Paper 710833, 1970.

[9]   Nicholls, J.A., Sichel, M., Gabrijel, A., Oza, R.D., and
      Vandermolen, R., Detonability of Unconfined Natural
      Gas-Air Clouds, Seventeenth Symposium (International) on
      Combustion, The Combustion Institute, Pittsburgh, p. 1223,
      1978.

[10]  Bull, D.C., Elsworth, J.E., and Hooper, G., Susceptibility of
      Methane-Ethane Mixtures to Gaseous Detonation in Air,
      Combustion and Flame, v34, p.327, 1979.

[11]  Vandermolen, R. and Nicholls, J.A., Blast Wave Initiation
      Energy for the Detonation of Methane-Ethane Mixtures,
      Combustion Science and Technology, v21, p.75, 1979.

[12] Eubnk, C.S., Rabinowitz, M.J., Gardener, W.C., Jr., and Zellner, R.E., Shock-Initiated Ignition of Natural Gas-Air Mixtures, Eighteenth Symposium (International) on Combustion, The Combustion Institute, Pittsburgh, p. 1767, 1980.

[13] Westbrook, C.K. and Pitz, W.J., High Pressure Autoignition of Natural Gas/Air Mixtures and the Problem of Engine Knock, Gas Research Institute Technical Report No. GRI-87/0264, Sept. 1987.

[14] Siebers, D.L. and Edwards, C.F., Autoignition of Methanol and Ethanol Sprays under Diesel Engine Conditions, Society of Automotive Engineer, SAE Trans. v96, pp. 5.140-5.152, 1987.

[15] Glassman, I., Combustion, Second Edition, ACADEMIC PRESS INC., 1987.

[16] Beck, N.J., Johnson, W.P., George, A.F., Petersen, P.W., van der Lee, B., and Klopp, G., Electronic Fuel Injection for Dual Fuel Diesel Methane, Society of Automotive Engineer, SAE Paper 891652, 1989.

[17] Simonson, J.R., Some Combustion Problems of the Duel-Fuel Engine, Engineering v178, p. 363, 1954.

[18] Moor, N.P.W. and Mitchell, R.W.S., Combustion in Duel-Fuel Engine, Joint Conference on Combustion, ASME/Institute of Mechanical Engineering, p. 300, 1955.

[19] Wong, J.K.S., Messenger, G.S., Moyes, B.W., and Chippiior, W. Conversion of a Two-Stroke Detroit Diesel Allison Model 12V-149T Diesel Engine to Burn Natural Gas with Pilot Injection of Diesel Fuel for Ignition, Society of Automotive Engineer, SAE Paper 841001, 1984.

[20] Ding, X. and Hill, P.G., Emissions and Fuel Economy of a Prechamber Diesel Engine with Natural Gas Dual Fuelling, Society of Automotive Engineer, SAE Paper 860096, 1986, SAE Trans. v95, pp. 612-625, 1986.

[21] Johnson, W.P., Beck, N.J., Lovkov, O., van der Lee, A., Koshkin, V.K. and Piatov, I.S., All Electronic Dual Fuel Injection System for the Belarus D-144 Diesel Engine, Society of Automotive Engineer, SAE Paper 901502, 1990.

[22] Miyake, M. and Ass., The Development of High Output, Highly Efficient Gas Burning Diesel Engines, CIMAC 15 Paper D112, Conference Proceeding, Paris-France, Jun. 1983.

[23] Miyake, M., Endo, Y., Biwa, T., Mizuhara, S., Grone, O. and Pedersen, P.S., Resent Development of Gas Injection Diesel Engine, CIMAC 17 Paper.

[24] Wakenell, J.F., O'Neal, G.B. and Baker, Q.A., High Pressure Late Cycle Direct Injection of Natural Gas in a Rail Medium Speed Diesel Engine, Society of Automotive Engineer, SAE Paper 872041, 1987.

[25] Lom, E.J. and Ly, K.H., High Pressure Injection of Natural Gas in a Two Stroke Diesel Engine, Society of Automotive Engineer, SAE Paper 902230, 1990.

[26] Heywood, J.B., Internal Combustion Engine Fundamentals, McGraw-hill Publishing Company, 1988.

[27] Komiyama, K. and Heywood, J.B., Predicting $NO_x$ Emissions and Effects of Exhaust Gas Recirculation in Spark-Ignition Engines, Society of Automotive Engineer, SAE Paper 730475, SAE Trans. v82, pp. 1458-1476, 1973.

[28] Haynes, B.S. and Wagner, H.G., Soot Formation, Prog. Energy Combust. Sci., v7, pp. 229-273, 1981.

[29] Whitehouse, N.D., Clough, E. and Uhunmwangho, S.O., The Development of Some Gaseous Products during Diesel Engine Combustion, Society of Automotive Engineer, SAE Paper 800028, 1980.

[30] Aoyagi, Y., Kamimoto, T., Matsui, Y. and Matsuoka, S., A Gas Sampling Study on the Formation Processes of Soot and NO in a DI Diesel Engine, Society of Automotive Engineer, SAE Paper 800254, SAE Trans. v89, 1980.

[31] Duggal, V.K., Priede, T. and Khan, I. M., A Study of Pollutant Formation within the Combustion Space of a Diesel Engine, Society of Automotive Engineer, SAE Paper 780227, SAE Trans. v87, 1978.

[32] Torpey, P.M., Whitehead, M.J., Wright, M., Experiments in the Control of Diesel Emissions, Paper C124/71, "Air Pollution Control In Transport Engines", A Symposium arranged by the Automobile Division and the Combustion Engines Group of the Institution of Mechanical Engineers, 9th-11th November, 1971.

[33] Khan, I.M., Wang, C.H.T., Factors Affecting Emissions of Smoke and Gaseous Pollutants from Direct Injection Diesel Engines, Paper C151/71, "Air Pollution Control In Transport Engines", A Symposium arranged by the Automobile Division and the Combustion Engines Group of the Institution of Mechanical Engineers, 9th-11th November, 1971.

[34] Herzog, P.L., Burgler, L. and Winklhofer, E., NOx Reduction Strategies for DI Diesel Engines, Society of Automotive Engineer, SAE Technical Paper Series 920470, 1992.

[35] Hames, R.J., Straub, R.D., and Amann, R.W., DDEC --Detroit Diesel Electronic Control, Society of Automotive Engineer, SAE Paper 850542, 1985.

[36] Hames, R.J., Hart, D.L., Gillham, G.V., Weisman, S.M., Peitsch, B.E., DDEC II -- Advanced Electronic Diesel Control, Society of Automotive Engineer, SAE Paper 861049, 1986.

[37] Yuen, D. and Hodgins, K.B., Data Acquisition System for Alternate Fuels Engine Testing, Unpublished Report, Mech. Eng. Dept. - The University of British Columbia, May 1991.

[38] Rohling, N.R., Operation and Performance of Emissions Console, Unpublished Report, Mech. Eng. Dept.- The University of British Columbia, August, 1990.

[39] Diesel Engine Smoke Measurement, Society of Automotive Engineer, SAE Recommended Practice, 1991 Handbook, v3, SAE J255a.

[40] Van Wylen, G.J. and Sonntag, R.E., Fundamentals of Classical Thermodynamics, Third Edition, Jone Wiey & Sons, Inc., New York, 1985.

[41] Measurement of Carbon Dioxide, Carbon Monoxide, and Oxides of Nitrogen in Diesel Exhaust, Society of Automotive Engineer, SAE Recommended Practice, 1991 Handbook, v3, SAE J177 APR82.

[42] Ouellette, P. and Hill, P.G., Visualization of Natural Gas Injection for a Compression Ignition Engine, Society of Automotive Engineer, SAE Paper 921555, 1992.

[43] Reynold, Wm.C., Chemical Equilibrium Solver Ver.3.60 - An Application Software, Mech. Eng. Dept, Stanford University, 1987.

[44] Van Zeggeren and Storey, The Computation of Chemical Equilibria, Cambridge University, Press, 1970.

[45] Hill, P.G. and Peterson, C.R., Mechanics and Thermodynamics of Propulsion, Second Edition, Addison-Wesley Publishing Company, Inc., 1992.

[46] Song, S. and Hill, P.G., Dual Fuelling of a Pre-Chamber Diesel Engine, with Natural Gas, J.Eng for Turbines and Power, Trans. ASME, Vol.107 pp914-921, October 1985.

[47] Gunawan, H., Performance and Combustion Characteristics of a Diesel-Pilot Gas Injection Engine, Unpublished Master Thesis, Department of Mechanical Engineering, UBC. 1992.

[48] Woschni, G., <u>A Universally Applicable Equation for the Instantaneous Heat Transfer Coefficient in the Internal Combustion Engine</u>, Society of Automotive Engineer, SAE Paper 670931, 1967.

# APPENDICES

APPENDIX A             NO FORMATION RATE

The mechanism of NO formation from atmospheric nitrogen are generally understood [26] [27]. It is generally accepted that in combustion of near stoichiometric fuel-air mixtures the principal reactions governing the formation of NO from molecular nitrogen are

$$O_2 + N_2 = NO + N \tag{A.1}$$

$$N + O_2 = NO + O \tag{A.2}$$

$$N + OH = NO + H \tag{A.3}$$

The forward $(k_i)$ and reverse $(k_{ir})$ rate constants for these reactions are as follows:

$$k_1 = (7.6E+13)\exp(-38,000/T)$$

$$k_{1r} = 1.6E+13$$

$$k_2 = (6.4E+9)T \cdot \exp(-3150/T)$$

$$k_{2r} = (1.5E+9)T \cdot \exp(-19,500/T)$$

$$k_3 = 4.1E+13$$

$$k_{3r} = (2E+14)\exp(-23,650/T)$$

where the units are $cm^3/mol\text{-}s$.

The rate of formation of NO via reactions (A.1) to (A.3) is

$$\frac{d[NO]}{dt} = k_1 [O] [N_2] - k_{1r}[NO] [N] + k_2 [N] [O_2]$$
$$- k_{2r}[NO] [O] + k_3 [N] [OH] - k_{3r}[NO] [H]$$

(A.4)

where the brackets denote concentrations in units of moles/cm$^3$.

A similar relation to (A.4) can be written for d[N]/dt:

$$\frac{d[N]}{dt} = k_1 [O] [N_2] - k_{1r}[NO] [N] - k_2 [N] [O_2]$$
$$+ k_{2r}[NO] [O] - k_3 [N] [H] + k_{3r}[NO] [H]$$

(A.5)

In order to apply Eq. (A.4), two approximations are introduced:

1) N atoms change concentration by a quasi-steady process.

2) The combustion and NO formation processes are decoupled, and the concentrations of O, $O_2$, OH, H and $N_2$ can be calculated by their equilibrium values at the local pressure and equilibrium temperature.

The first approximation means that d[N]/dt can be set to zero and Eq. (A.5) can be used to solve [N]. Substitute [N] expression into Eq. (A.4). The NO formation rate then becomes

$$\frac{d[NO]}{dt} = 2k_1 [O] [N_2] \frac{1 - [NO]^2 / K [O_2] [N_2]}{1 + k_{1r}[NO] / (k_2 [O_2] + k_3 [OH])}$$

(A.6)

where K = $(k_1/k_{1r})(k_2/k_{2r})$.

The second approximation means that one can simply use the equilibrium composition (ie. $[O]_e$, $[O_2]_e$, $[H]_e$, $[HO]_e$ and $[N_2]_e$) to

determine the concentrations of O, $O_2$, H, HO and $N_2$. It is convenient to use the following notations for the one-way equilibrium rates

$$R_1 = k_1[O]_e[N_2]_e = k_{1r}[NO]_e[N]_e \qquad \text{for Eq. (A.1)}$$

$$R_2 = k_2[N]_e[O_2]_e = k_{2r}[NO]_e[O]_e \qquad \text{for Eq. (A.2)}$$

$$R_3 = k_3[N]_e[OH]_e = k_{3r}[NO]_e[H]_e \qquad \text{for Eq. (A.3)}$$

where [ ]$_e$ denotes equilibrium concentration.

Substituting $[O]_e$, $[O_2]_e$, $[OH]_e$, $[H]_e$ and $[N_2]_e$ for [O], $[O_2]$, [OH], [H] and $[N_2]$ in Eq. (A.6). The NO formation rate then becomes

$$\frac{d[NO]}{dt} = \frac{2R_1\{1 - ([NO]/[NO]_e)^2\}}{1 + ([NO]/[NO]_e)R_1/(R_2+R_3)} \qquad (A.7)$$

Typical values of $R_1$, $R_1/R_2$ and $R_1/(R_2+R_3)$ are given in Table A.1. The difference between $R_1/R_2$ and $R_1/(R_2+R_3)$ indicates the relative importance of adding reaction (A.3) to the mechanism.

Table A.1  Typical Values of $R_1$, $R_1/R_2$ and $R_1/(R_2+R_3)$:

| Equivalence ratio | $R_1$ | $R_1/R_2$ | $R_1/(R_2+R_3)$ |
|---|---|---|---|
| 0.8 | 5.8E-05 | 1.2 | 0.33 |
| 1.0 | 2.8E-05 | 2.5 | 0.26 |
| 1.2 | 7.6E-06 | 9.1 | 0.14 |

The strong temperature dependence of the NO formation rate can be determined by considering the initial term of d[NO]/dt, when

$[NO]/[NO]_e \ll 1$. Then from Eq. (A.7),

$$\frac{d[NO]}{dt} = 2R_1 = 2k_1 [O]_e [N_2]_e \tag{A.8}$$

The equilibrium oxygen atom concentration is given by

$$[O]_e = \frac{K_p [O_2]_e^{1/2}}{(RT)^{1/2}} \tag{A.9}$$

where $K_p$ is the equilibrium constant for the reaction

$$(1/2)O_2 = O$$
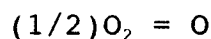
and is given by

$$K_p = (3.6E+13)\exp(-31,090/T) \quad atm^{1/2} \tag{A.10}$$

Combining Eqs. (A.8), (A.9) and (A.10) with

$k1 = (7.6E+13)\exp(-38,000/T)$, the initial NO formation rate may then be written as

$$\frac{d[NO]}{dt} = \frac{6 \times 10^{16}}{T^{1/2}} \exp\left(\frac{-69,090}{T}\right) [O_2]_e^{1/2} [N_2]_e \tag{A.11}$$

where the unit of d[NO]/dt is mol/cm$^3$-s. The strong dependence of d[NO]/dt on temperature in the exponential term is evident. High temperature and high oxygen concentrations result in high NO formation rates.

APPENDIX B

EXHAUST EMISSION ANALYSIS SYSTEM B

OPERATING PROCEDURE

As mentioned in Section 3.4, the exhaust emission analysis system B (EEAS-B) mainly includes the heated sampling system and six emission analyzers. The $CH_4$, NO, CO and $CO_2$ analyzers use the NDIR method; the THC analyzer uses the FID method. The EEAS-B operating procedure includes starting procedure, analyzer calibration and emission measurement.

1. The Starting Procedure

   1) Turn on the power switches for the sample line heater (1B) and the heated enclosure (5A). Set the temperatures of the sample line and heated enclosure both to 190°C for diesel engine (130°C for gasoline engine). The main power switch box is located in the right side of the first cabinet from back. The temperature control switch box for the sample line is near the main power switch box. The temperature controller of the heated enclosure is located on the front panel of the first cabinet.

   2) Switch on the power to the sampling pump (5B), chiller (7A), $NO_2$ to NO converter (8A) and the six emission analyzers. Allow a minimum 2 hours warmup if the system has been turned off.

3) Check the sample gas pressure inside system. A pressure meter is located on the front panel of the second cabinet. A pressure less than 6 psig indicates a large restriction. Therefore, the filter cores of the sample gas must be changed.

4) Open all the zero and span gas cylinders, the air and fuel (hydrogen) cylinders used by the THC analyzer.

5) Set the flow rate for each analyzer (except THC analyzer) from the flow rate meters on the front panel of the second cabinet. A typical setting is 4.5 SCFH for $CH_4$ and $NO_x$ analyzer, 1.5 SCFH for $CO_2$ and CO analyzers, and 3 SCFH for $O_2$ analyzer. Set the same sample flow rate for zero, span and exhaust sample gases by adjusting the regulators of the zero and the span gases to match exhaust sample gas.

6) For the THC analyzer only. Turn on the analyzer power, pump and heater oven. Set the inlet pressure consistent for zero, span and sample gas at 200 mbar by adjusting the regulators of the zero and span gas as well as the regulator on the analyzer. Set the air pressure to 0.8 bar. Do not try to ignite the detection burner until the temperature of the heater oven reaches 90°C. Push "$H_2^-$" button to adjust fuel (ie. hydrogen) pressure to about 0.5 bar. Try to ignite the detection burner by holding down and the "$H_2^-$" button, and pushing the "ignition" button. The fuel pressure can be adjusted slightly higher to produce a richer fuel mixture to provide better ignition. After the

burner has ignited, set the fuel pressure back to 0.4 bar. Let it warm up.

2. The Analyzer Calibration

After the temperatures of the sample line and heated enclosure reach 190°C and the emission analyzers have been warmed, start calibrating the analyzers. Table B.1 shows the typical operating ranges and corresponding signal-output voltage ranges of six analyzers.

Table B.1:  Typical Operating Ranges of Emission Analyzers.

----------------------------------------------------------------

| Name of the analyzers | Operating range $A_i$ (ppm) | Output range $B_i$ (volts) |
|---|---|---|
| Methane ($CH_4$): | 0 ... 5,000 | 0 ... 5 |
| Nitric oxide (NO): | 0 ... 3,000 | 0 ... 5 |
| Carbon dioxide ($CO_2$): | 0 ... 20 % | 0 ... 5 |
| Carbon monoxide (CO): | 0 ... 10,000 | 0 ... 5 |
| | (0 ... 2500 for diesel baseline) | |
| Oxygen ($O_2$): | 0 ... 21 % | 0 ... 5 |
| Total hydrocarbon (THC): | 0 ... 10,000 | 0 ... 10 |
| | (0 ... 1,000 for diesel baseline) | |

----------------------------------------------------------------

Table B.2 shows the typical zero and span gases for the analyzers and the typical concentrations for the span gases.

Table B.2: Typical Zero and Span Gases.

---

| Name of analyzer | Zero gas | Span gas and concentration | Output voltage of the span |
|---|---|---|---|
| | | $Z_i$ | $Y_i$ |
| Methane ($CH_4$): | $N_2$ | $CH_4$, 3470 ppm | 3.47 volts |
| Nitric oxide (NO): | $N_2$ | NO, 2113 ppm | 3.522 volts |
| Carbon dioxide ($CO_2$): | $N_2$ | $CO_2$, 19.3% | 4.825 volts |
| Carbon monoxide (CO): | $N_2$ | CO, 510 ppm | 0.255 volts |
| Oxygen ($O_2$): | $N_2$ | Air, 20.9% $O_2$ | 4.976 volts |
| Total hydrocarbon (THC): | $N_2$ | $CH_4$, 3940 ppm | 3.94 volts |

---

The following equation is used to calculate the signal-output voltage of the span for a specific analyzer, $Y_i$, which is shown in Table B.2.

$$Y_i = \frac{B_i}{A_i} Z_i \qquad \text{(B.1)}$$

where $A_i$ is the maximum scale of the operating range (ppm) for the specific analyzer; $B_i$ is the maximum signal-output voltage (volts) for the specific analyzer; $Z_i$ is the concentration of the span gas (ppm or %) for the specific analyzer.

1)   $CH_4$ and $NO_x$ analyzer:

(1) Turn on the pump.

(2) Switch on the zero gas valve; wait for one minute before

pushing the zero calibration button. The analyzer has an
inside microprocessor to do the zero calibration. If the
analyzer does not zero, repeat this step again. The signal
output for the zero gas should be zero volts or very
close to zero. Switch off the zero gas valve.

(3) Switch on the span gas valve and wait until the signal-
output voltage becomes steady. Adjust the potential meter
until the output voltage matches the signal-output voltage
of the span for $CH_4$, $Y_{CH4}$, (or for NO, $Y_{NO}$, refer to Table
B.2 and Eq. (B.1)). Switch off the span gas valve.


2)   $CO_2$ analyzer:

(1) Switch on the zero gas valve and wait for one minute
before undertaking zero calibration. Push the "ZERO" key
and the "ENTER" key to start zero calibration. Use the "↑"
or the "↓" key to adjust the potential meter to chose a
value which is zero or very close to zero, then press the
"ENTER" again to accept this value. If the analyzer does
not zero, repeat this step again. The signal output for
the zero gas should be zero volts or very close to zero.
Switch off the zero gas valve.

(2) Switch on the span gas valve and wait until the readout
becomes steady. Push the "SPAN" and the "ENTER" keys to
start span calibration. Use the "↑" or the "↓" key to
adjust the potential meter to chose a value which is less
but very close to the $CO_2$ span gas concentration, then

push "ENTER" again to accept this value. The analyzer has
a microprocessor inside to calculate the span. You can
repeat this step again and chose a smaller value if the
analyzer displays an "ERROR" message. Switch off the span
gas valve.

3)   CO analyzer:

(1) This analyzer is the oldest one in this system. In order
to do the calibration easily and precisely, the span
calibration must be done first, following the zero
calibration. Repeat those two steps. Using this procedure,
one will find that it is easier to achieve the desired
calibration results.

(2) Switch on the span gas valve and wait until the signal-
output voltage becomes steady. Adjust the span knob to set
the output to the signal-output voltage of the span for
CO, $Y_{CO}$ (refer to Table B.2). Switch off the span gas
valve.

(3) Switch on the zero gas valve and wait until the signal-
output voltage becomes steady. Adjust the zero knob to set
the output voltage to zero. Switch off the zero gas valve.

4)   $O_2$ analyzer:

(1) Push ".111" and " MEAS./CAL." into calibration mode from
measurement mode.

(2) Switch on the zero gas valve and wait until the signal-

output voltage becomes steady. Push "5" and "ENTER" and wait for the microprocessor of the analyzer to do the zero calibration. If the analyzer does not zero, repeat this step. The signal output for the zero gas should be zero volts or very close to zero. Switch off the zero gas valve.

(3) Switch on the span gas valve and wait until the signal-output voltage becomes steady. Push "8" and "ENTER" and wait for the analyzer to do the span calibration. If the analyzer does not span well, repeat this step again. The span gas concentration should always be 20.9% oxygen. Switch off the span gas valve.

(4) Push "MEAS./CAL." back to the measurement mode.


5)  Total HC analyzer:

(1) Place the three-way valve in the zero gas position and wait until the signal-output voltage becomes steady. Adjust the zero knob to set the output voltage to zero. Switch the valve to sample position.

(2) Switch the three-way valve to span gas position and wait until the signal-output voltage becomes steady. Adjust fuel (ie. hydrogen) pressure to about 0.4 bar and look at the values on the indicator. Set a fuel pressure which corresponds with the peak value on the indicator. Adjust the span knob to set the output to the signal-output voltage of the span for THC, $Y_{THC}$ (refer to Table B.2).

Switch the valve to sample position.


3. The emission measurement

All the emission measurements for this study are based on steady-state operating conditions, which are different from EPA Highway Driving Cycle or Transit Cycle. The reason for using steady-state operating condition is that proceeding EPA Transit Cycle needs very sophistical equipments that we do not have. The following is the measurement procedure.

1)  Start the engine and warm it up under load until the temperatures of the lubricate oil and the cooling water both reach 80°C.

2)  Calibrate every analyzer and make the system ready to work.

3)  Operate for at least 10 min in each test mode, record the emission data until the engine runs steady and the monitor shows steady emission data.

4)  Check and record the zero and span offset after each test. Turn off all the gas cylinders and some analyzers.

APPENDIX C

## POWER CORRECTION FACTOR CALCULATION METHOD

### (in accordance with SAE J1349)

1.  The correction is made against the standard inlet air

    conditions, i.e.,

    | | | |
    |---|---|---|
    | Inlet Air Pressure (Absolute) | : | 100kPa |
    | Inlet Air Temperature | : | 25 C(298K) |
    | Dry Inlet Air Pressure (Absolute) | : | 99kPa |

2.  The correction factor $f_{corr}$ applied to the observed brake power

    depends on the atmospheric factor $f_a$ and engine factor $f_m$ which

    is calculated using the empirical relationship:

    $$f_{corr} = (f_a)^{fm}$$

    The atmospheric factor is calculated based on dry inlet air

    pressure $B_{do}$ and inlet air temperature t,

    $$f_a = [99/B_{do}] [(t+273)/298]^{0.7}$$

    The engine factor depends on the fuel flow F(g/s), the engine

    displacement $D(dm^3)$, the engine speed N(RPM), and the pressure

    ratio r of inlet manifold pressure $P_o$ to inlet air pressure $B_o$.

    It has the following value:

    | | |
    |---|---|
    | $f_m = (0.036 q/r) - 1.14$ | if $40 < (q/r) < 65$ |
    | $f_m = 0.3$ | if $(q/r) < 40$ |
    | $f_m = 1.2$ | if $(q/r) > 65$ |

    where q = (60,000 F)/(D N), for a two-stroke cycle engine.

3.  The correction factor used in the calculation is within the

    range of 0.90 to 1.10.

# APPENDIX D

## DETERMINATION OF SPECIFIC HUMIDITY

Specific humidity H (g of $H_2O$ per kg of dry air) of an air-water vapour mixture is defined as the ratio of the mass of water vapor $m_w$ (kg) to the mass of dry air $m_a$ (kg) [40].

$$H=1000\frac{m_w}{m_a} \qquad (D.1)$$

The equations of state both for water vapor and for dry air can be expressed in terms of partial pressure, volume, mass of substance and temperature.

$$P_wV=m_wR_wT \qquad (D.2)$$

$$P_aV=m_aR_aT \qquad (D.3)$$

where subscripts "w" and "a" denote water vapor and dry air respectively. $R_w$ = 461.52 (J/kg-K) is the gas constant of water vapor. $R_a$ = 287.0 (J/kg-K) is the gas constant of dry air.

Eq. (D.2) divided by Eq. (D.3), then

$$\frac{m_w}{m_a}=\left(\frac{R_a}{R_w}\right)\left(\frac{P_w}{P_a}\right) \qquad (D.4)$$

where $R_a/R_w$ = 0.6219.

Substitute Eq. (D.4) into Eq. (D.1):

$$H = 621.9 \frac{P_w}{P_a}$$ (D.5)

Relative humidity $\phi$ is defined as a ratio of the partial pressure of water vapor $P_w$ to the saturated pressure of water vapor at dry bulb temperature $P_s$.

$$\phi = \frac{P_w}{P_s}$$ (D.6)

Wet-air pressure (ie. ambient pressure or barometric pressure) $P_b$ is defined as the sum of the partial pressure of dry air $P_a$ and the partial pressure of water vapor $P_w$.

$$P_b = P_a + P_w$$ (D.7)

Substitute Eqs.(D.6) and (D.7) into Eq. (D.5):

$$H = 621.9 \frac{\phi P_s}{P_b - \phi P_s}$$ (D.8)

Barometric pressure $P_b$ (inHg), relative humidity $\phi$ (%) and dry bulb temperature $T_d$ (°F) are measured directly from the gauges. $P_s$ (inhg) can be expressed in terms of $T_d$ (°F) in following equation, which is the fitting curve equation of the Saturated Steam Temperature Table [40] from 40 to 140 °F.

$$P_s = -0.461920 + 0.029439 T_d - 0.000450 T_d^2 + 0.000004 T_d^3$$ (D.9)

APPENDIX E

## A MORE EXACT FORMULA

## FOR DRY-WET BASIS CONVERSION FACTOR

The definitions that are used in the formula of the dry-wet basis conversion factor ($F_{dw}$) are the following:

Pilot-diesel fuel to CNG fuel mass ratio, $r_m$:

The ratio of pilot-diesel mass flow rate $\dot{m}_{DSL}$ to CNG mass flow rate $\dot{m}_{CNG}$. Both of them are measured data.

$$r_m = \frac{\dot{m}_{DSL}}{\dot{m}_{CNG}} \tag{E.1}$$

Atomic hydrogen-to-carbon ratio of the combined fuel, y:

The ratio of hydrogen to carbon atoms of a combined fuel ($CH_y$) which is used to replace CNG ($CH_{3.85}$) and diesel ($CH_{1.8}$) fuels.

$$y = \frac{H}{C} = \frac{3.85 + \frac{16.689}{13.825} r_m \cdot (1.8)}{1 + \frac{16.689}{13.825} r_m} \tag{E.2}$$

The more exact formula of the dry-wet basis conversion factor ($F_{dw}$) is based on the following assumptions:

1.  Considering the effect of the humidity of the intake air on
    the reaction of fuel combustion, the reactants of the
    combustion are combined fuel, air and water vapour in the
    intake air.

2.  Consider a real situation that the combined fuel is not 100%
    burned. The unburned fuel in the exhaust (which has the same
    composition as combined fuel) will affect the water vapour in
    the exhaust. Thus the products of the combustion are carbon
    dioxide, water vapour, oxygen, nitrogen and unburned fuel.

A general equation of the combined-fuel combustion can be defined
based on above assumptions.

$$CH_y + n(O_2 + 3.76N_2) + mH_2O$$

$$==> (1-x) CO_2 + [\frac{y(1-x)}{2} + m] H_2O \qquad (E.3)$$

$$+ [n - (1 + \frac{y}{4}) (1-x)] O_2 + 3.76nN_2 + xCH_y$$
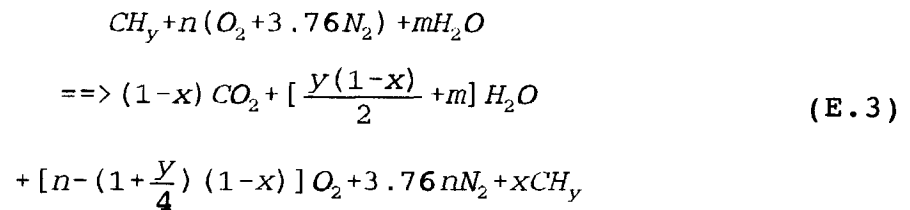
where y is the atomic hydrogen-to-carbon ratio of the combined
fuel; n is the number of moles of oxygen in intake air; m is the
moles of water vapour in 4.76n moles of dry air; x is the number of
moles of unburned fuel in the exhaust. The following is the
calculation procedure for the variables n, m and x.

1). Evaluation of n and m:

From Eq. (E.3), the mass flow rate of combined fuel and intake air
can be determined.

Mass of combined fuel per unit time, $F = 12.011 + 1.008y$

Mass of intake air per unit time, A=31.998n+105.330n+18.015m =137.328n+18.015m. Then,

$$F/A = \frac{12.011 + 1.008y}{137.328n + 18.015m}$$  (E.4)

where F and A can be measured; y can be determined from Eq. (E.2).

Referring to the general Eq. (E.3), the molal ratio of water vapour to dry air in the intake air can be expressed in terms of the specific humidity H (g $H_2O$ / kg of dry air) which can be determined by Eq. (D.8) in Appendix D.

$$\frac{m}{4.76n} = 1.608 \times 10^{-3} H$$  (E.5)

Solve for Eq. (E.4) and Eq. (E.5), n and m are determined,

$$n = (\frac{A}{B})(\frac{12.011 + 1.008y}{137.328 + 0.1379H})$$  (E.6)

and

$$m = 7.654 \times 10^{-3} Hn$$  (E.7)

2). Evaluation of x:

Referring to Eq. (E.3), the total moles of the combustion products is $n_T = x(1-y/4) + y/4 + m + 4.76n$. The molal ratio of the unburned fuel to the combustion products can be expressed in terms of a measured value of total hydrocarbon z (ppm) in the wet-basis.

$$\frac{x}{x(1-\frac{y}{4})+\frac{y}{4}+m+4.76n}=z\times10^{-6}$$

Thus, x can be determined by

$$x=\frac{(\frac{y}{4}+m+4.76n)\,z}{10^6-(1-\frac{y}{4})} \qquad (E.8)$$

The volumetric fraction (or molal fraction) of the water vapour in the exhaust can be expressed in terms of the variables n, m and x.

$$X_{H2O}=\frac{\frac{y(1-x)}{2}+m}{x(1-\frac{y}{4})+\frac{y}{4}+m+4.76n} \qquad (E.9)$$

The more exact formula of the dry-wet basis conversion factor $F_{dw}$ is,

$$F_{dw}=1-X_{H2O} \qquad (E.10)$$

APPENDIX F REPEATABILITY OF THE TEST RESULTS
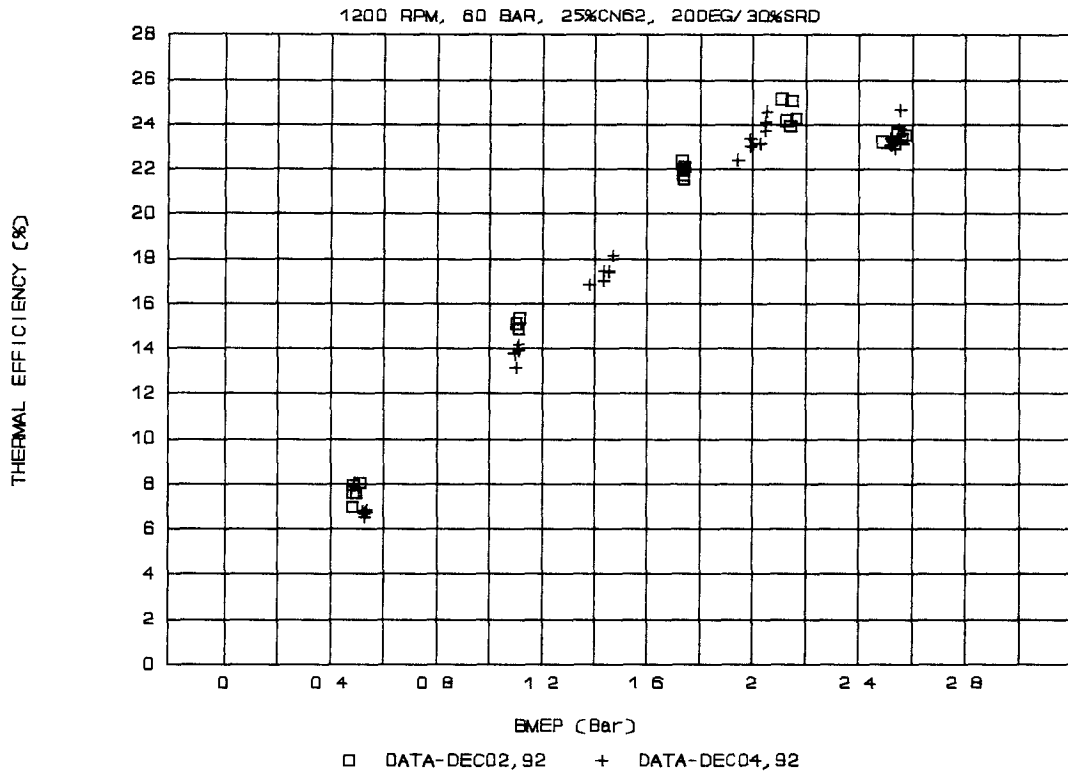


Figure F.1: Repeatability of Thermal Efficiency.
(at BOI=24°BTDC)

Repeatability of engine performance and exhaust emissions at a given test condition are shown in Figure F.1 through Figure F.6. Tests were conducted in two different days. The exhaust emission data presented are on the wet-basis. The test condition is: 1200 rpm speed, 60 bar CNG injection pressure, 25% cetane 62 pilot-diesel, 20° injection angle, 30% SRD and 24° BTDC of BOI.

The following factors are consider to affect the repeatability of different-day data: gas-diesel fuel injector reliability, calibration off-set and detection error of analyzers (or instrumentations) and manual error in the process of data taking.
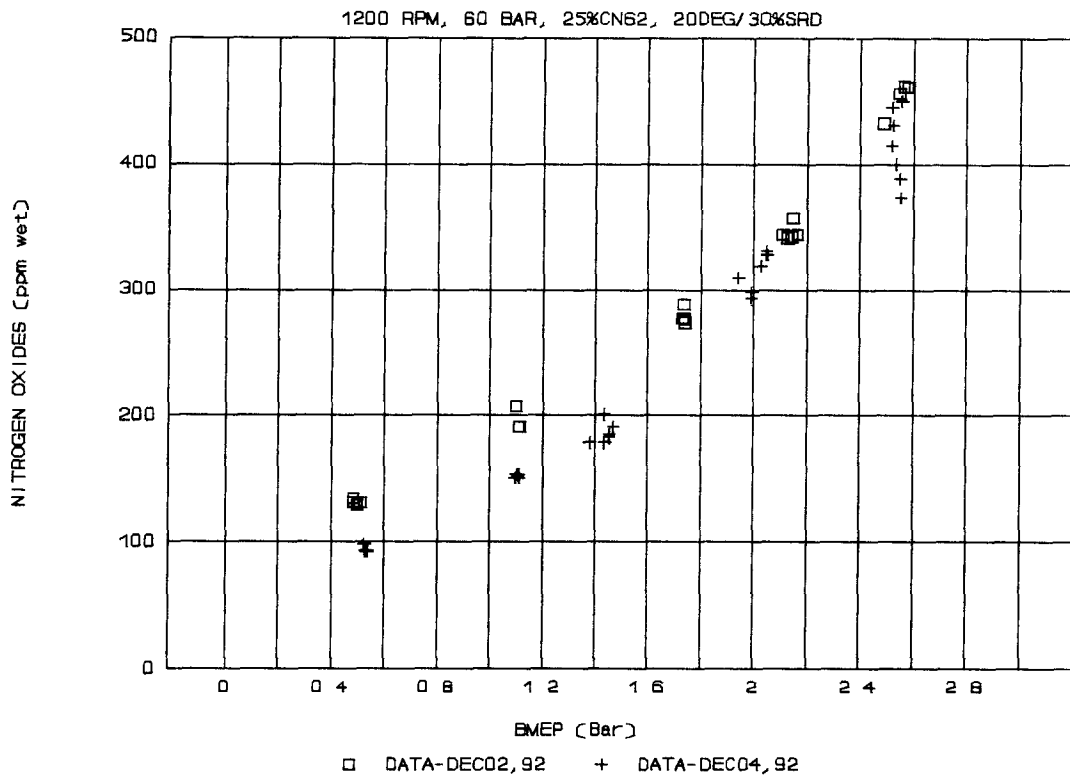


Figure F.2: Repeatability of Nitrogen Oxides Emissions.
(at BOI=24°BTDC)

Figure F.1 shows the repeatability of thermal efficiency data. it appears that the thermal efficiency data of Dec.04 are slightly lower than that of Dec.02 over whole load range. The maximum difference is about 13% at BMEP ~ 0.5 bar.
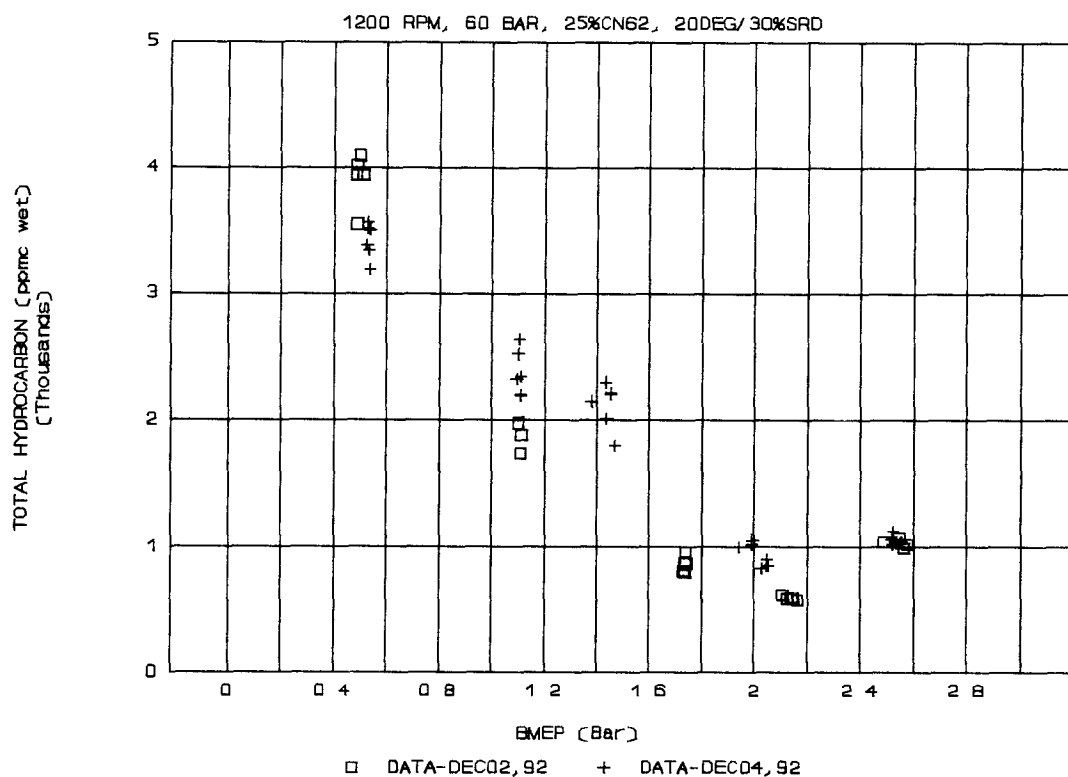
Figure F.3: Repeatability of Total Hydrocarbon Emissions.
(at BOI=24°BTDC)

The repeatability of nitrogen oxides emissions is shows in Figure F.2. There are quite big differences between two-day data at low and high load. They are quite close to each other at medium load. The maximum difference is about 30% at BMEP ~ 0.5 bar. For 24° BTDC of BOI, the operating load range is BMEP from 0 to 2.5 bar, so that BMEP ~ 2.5 bar is the high load. Figure F.3 shows the repeatability of total hydrocarbon emissions. The maximum difference is about 19% at BMEP ~ 0.5 bar.
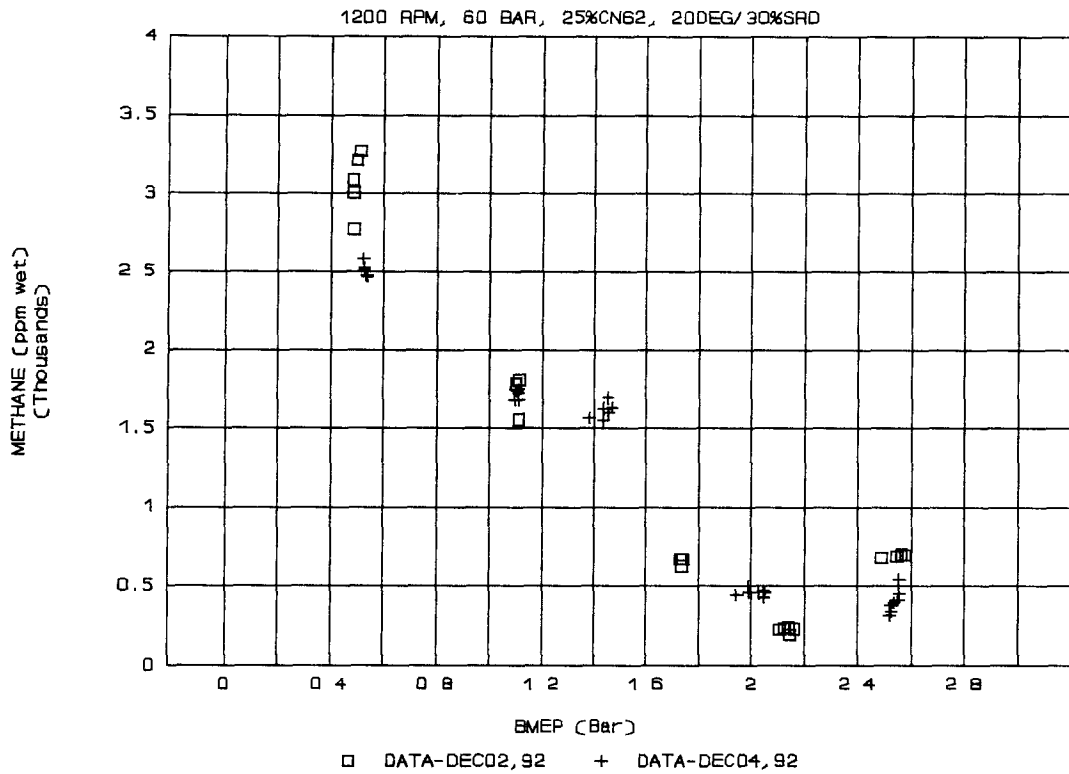
Figure F.4: Repeatability of Unburned Methane Emission.
(at BOI=24°BTDC)

It can be seen in Figure F.4 that the quite big differences between two-day unburned methane data are at low and high load. The differences are 21 % and 50% at BMEP ~ 0.5 bar and BMEP ~ 2.5 bar respectively.

Figure F.5 shows the repeatability of carbon monoxide emission. The maximum difference is at BMEP ~ 2.5 bar, which is about 17%. Carbon dioxide emission has the best repeatability in whole data. As shown
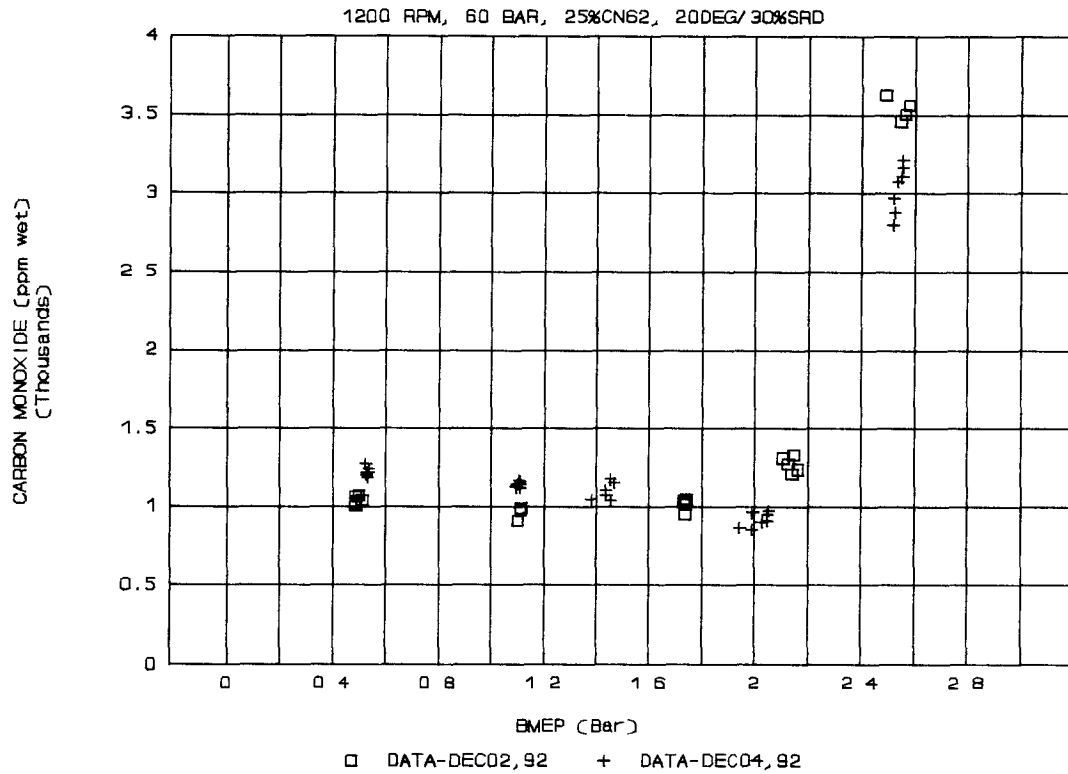
Figure F.5: Repeatability of Carbon Monoxide Emission.
(at BOI=24°BTDC)

in Figure F.6, the maximum difference is 9% at BMEP ~ 0.5 bar.

Summarizing from above, we know that the low (BMEP ~ 0.5 bar) and the high load (BMEP ~ 2.5 bar) are two regions where create more errors. The cycling variations of the low-load data resulted by unsteady operation produce more error in the process of data taking at low load. The unsteady operation caused by load limitation is the reason of creating error at high load.
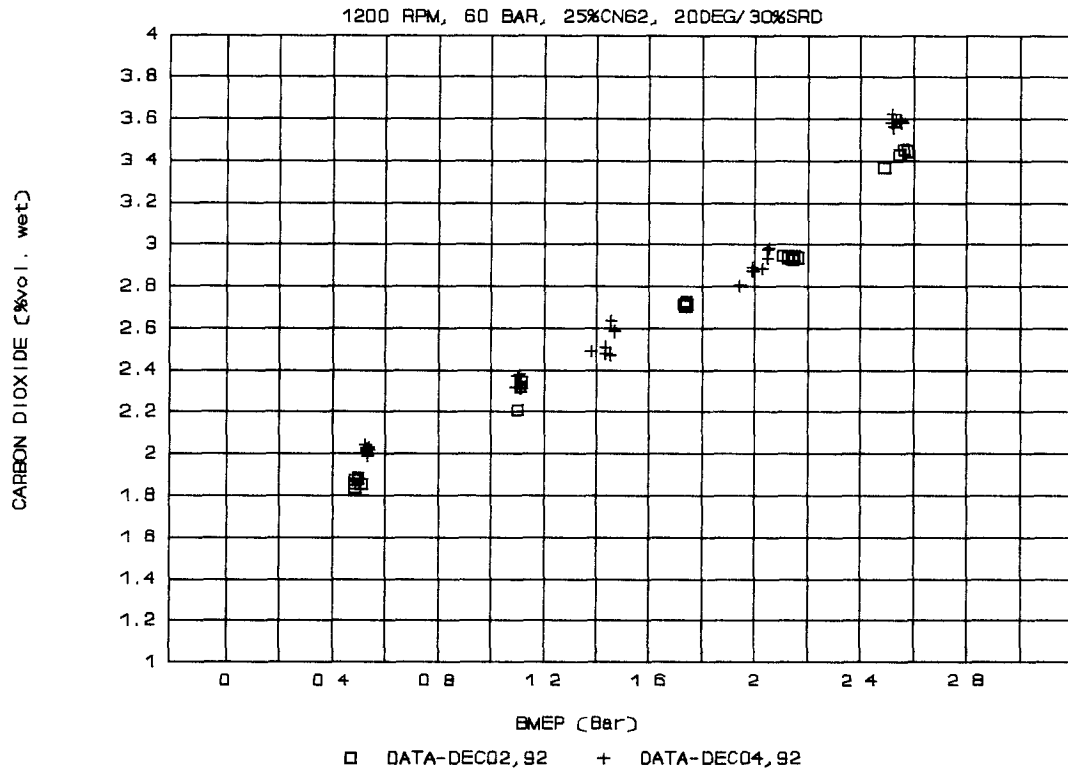
Figure F.6: Repeatability of Carbon Dioxide Emission.
(at BOI=24°BTDC)

In the determination of the best BOI performance curve, two places may include more errors, which are very low-load region (BMEP ~ 0.5 bar) and very high-load region (BMEP ~ 4.4 bar). The good repeatability can be obtained over the rest of the load range.

APPENDIX G

## PHOTOGRAPHS OF THE VISUALIZATION RESULTS

## OF NATURAL GAS INJECTION

The four photographs presented in the following is from the flow visualization results of natural gas injection [42] and courtesy of Patric Ouelette. The configuration of the gas injector used in Ouelette's flow visualization work is similar to the gas-diesel fuel injector used in engine test.
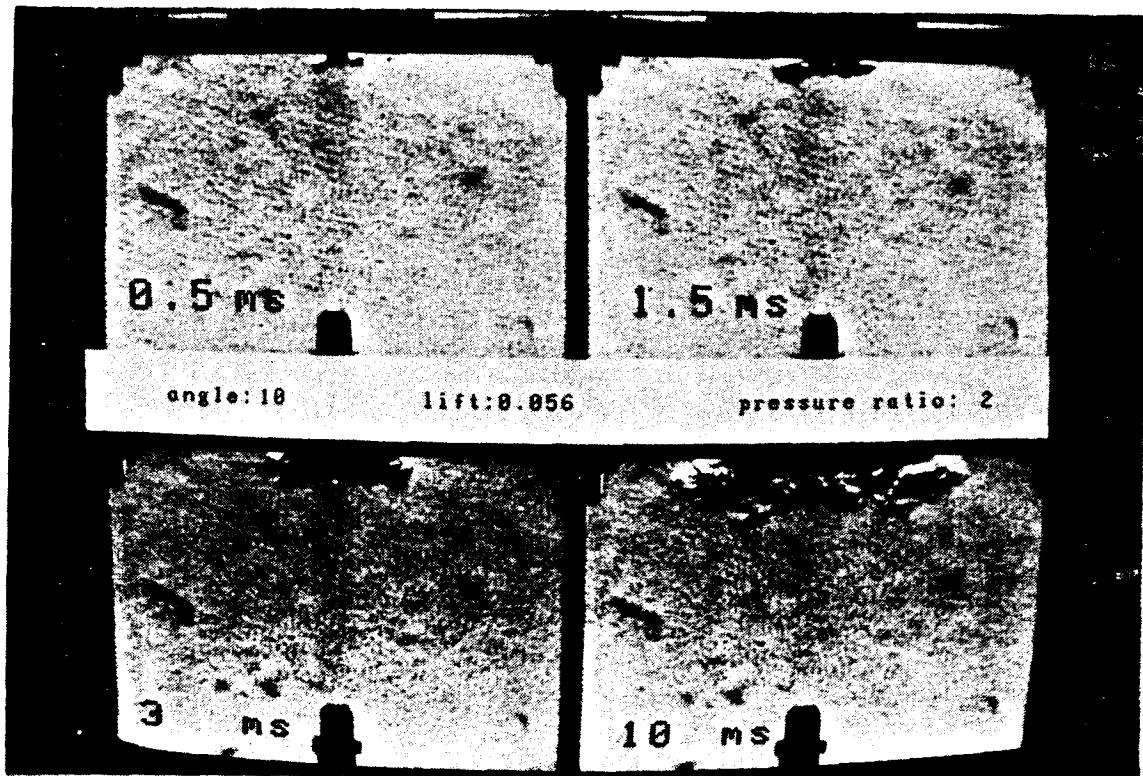


Figure G.1: Free Conical Sheet Jet with 10° Injection Angle.
(Pressure Ratio of 2; Lift of 0.056 mm)
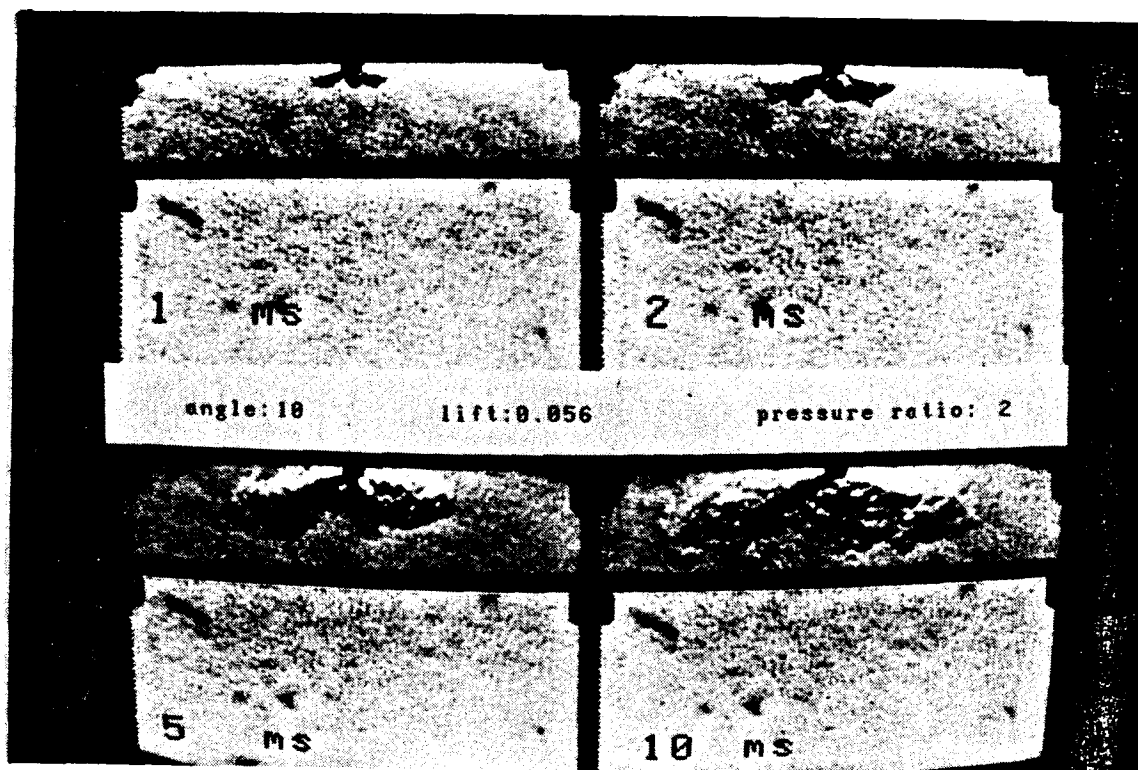
Figure G.2: Interrupted Conical Jet with 10° Injection Angle.
(Pressure Ratio of 2; Lift of 0.056 mm)

Figure G.1 shows the free conical sheet jet with 10° injection angle. The free conical sheet jet has the same condition as the gas-diesel fuel jet with 0% interruption ratio (or 0% SRD). It appears that the free conical sheet jet with 10° injection angle has very strong tendency of the top wall clinging, which is so called top wall effect.

Figure G.2 shows the interrupted conical jet with 10° injection angle. The interrupted conical jet has the same situation as the gas-diesel fuel jet with interruption. Compared with Figure G.1,

Figure G.2 shows that the interruption of the conical sheet jet reduces the top wall effect and increases the jet penetration.
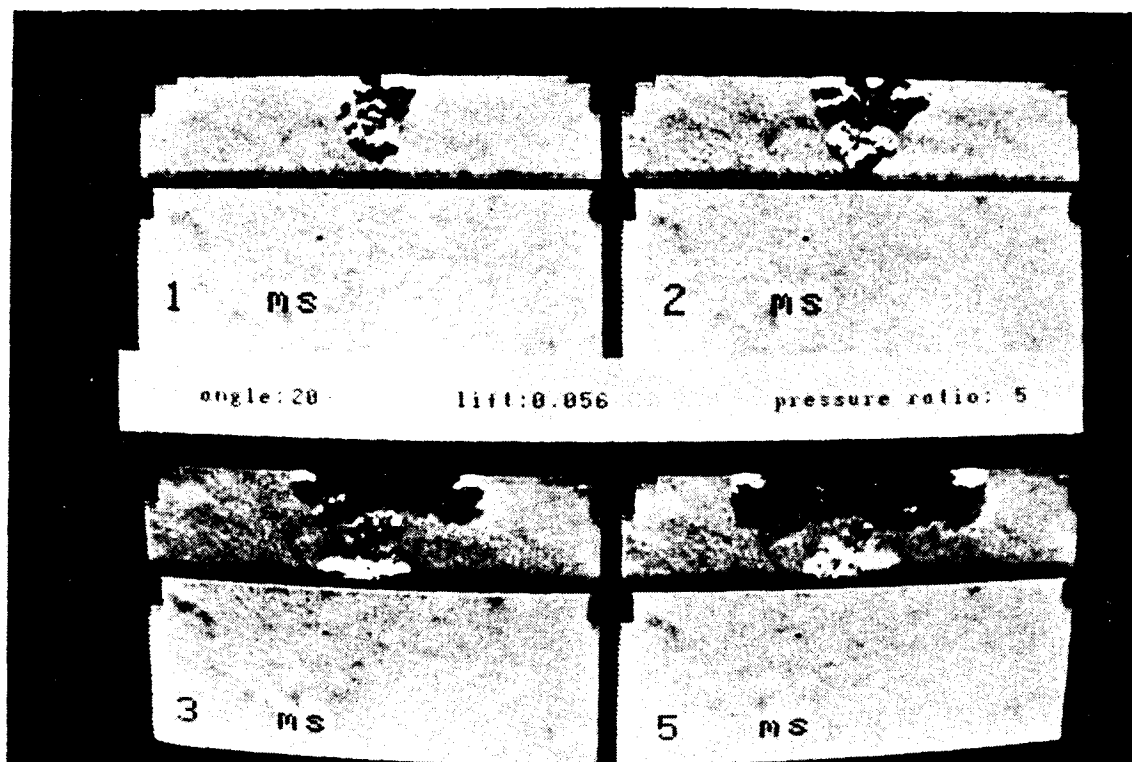


Figure G.3: Free Conical Sheet Jet with 20° Injection Angle. (Pressure Ratio of 5; Lift of 0.056 mm)

Figure G.3 and G.4 show the free conical sheet jet and the interrupted conical jet with 20° injection angle respectively. The free conical sheet jet with 20° injection angle has the tendency of collapsing and the interrupted conical jet with 20° injection angle do not.

The conclusion from above four photographs is that the interruption of the conical sheet jet can increase the stability and penetration
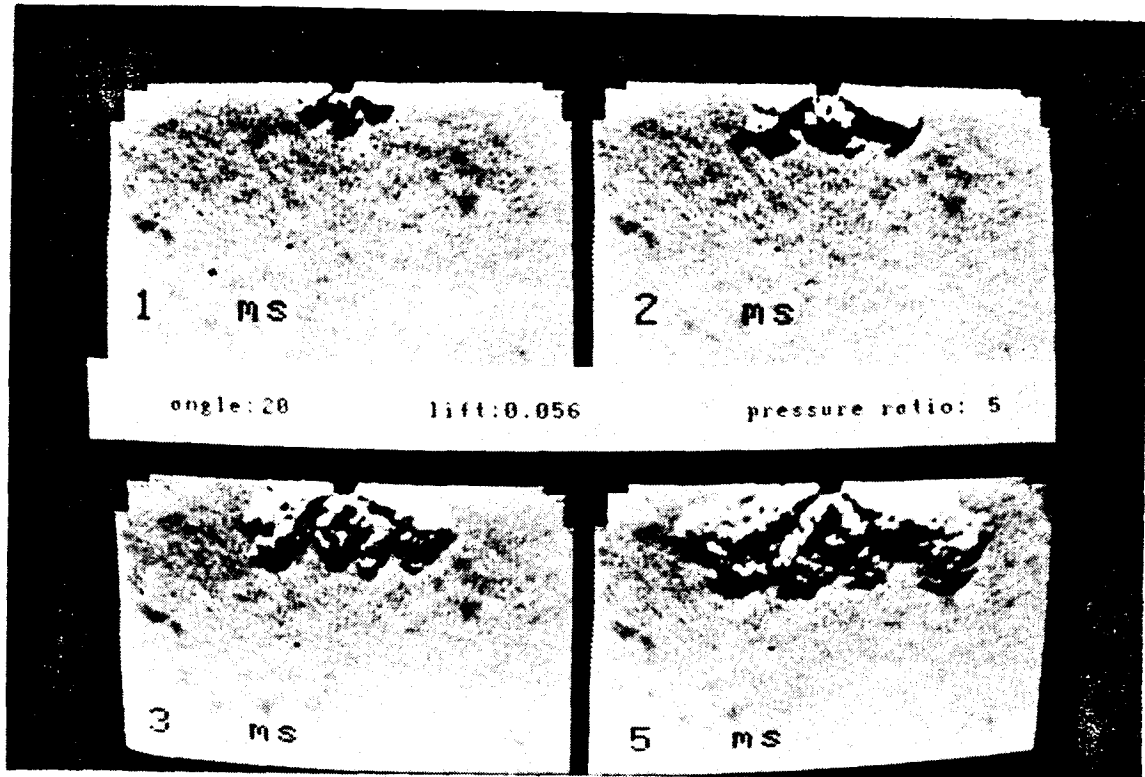
Figure G.4: Interrupted Conical Jet with 20° Injection Angle.
(Pressure Ratio of 5; Lift of 0.056 mm)

of fuel jet.

APPENDIX H           PROGRAM #1

1. Input Parameters

   *Engine inlet temperature, T0.

   *Engine inlet pressure, P0.

   *Engine air-box pressure, P1.

   *Engine compression ratio, E.

   *Specific heat ratio (or polytropic constant), N.

2. List of the PROGRAM #1

```
-----------------------------------------------------------------
C        THIS PROGRAM IS MADE TO FIND THE UNBURNED GAS TEMPERATURE
C        AND PRESSURE (UNBURNED GAS INCLUDES FUEL, FRESH AIR AND
C        RESIDUAL GAS FROM PREVIOUS CYCLE).
-----------------------------------------------------------------
         IMPLICIT REAL(N)
         OPEN (UNIT=3,FILE='B:\PROJ01\PROJ01.DAT',STATUS='UNKNOWN')
1        PRINT 2
2        FORMAT (1X,'PLEASE MAKE YOUR CHOICE:')
         PRINT 3
3        FORMAT(1X,'0==>QUIT THE PROGRAM'
     1          /1X,'1==>CONTINUE THE PROGRAM')
         READ *, J
         IF (J.EQ.0) THEN
         GOTO 140
         ELSE IF (J.EQ.1) THEN
         GOTO 4
         ELSE
         GOTO 1
         END IF
4        PRINT 5
5        FORMAT (1X,'PLEASE INPUT ENGINE INLET TEMPERATURE (K)')
         READ *, T0
         PRINT 6
6        FORMAT (1X,'PLEASE INPUT ENGINE INLET PRESSURE (atm)')
         READ *, P0
7        PRINT 8
8        FORMAT (1X,'PLEASE INPUT ENGINE AIR-BOX PRESSURE (atm)')
         READ *, P1
         IF (P1.LT.P0) THEN
         GOTO 7
         END IF
```

```
                PRINT 9
9               FORMAT (1X,'PLEASE INPUT ENGINE COMPRESSION RATIO')
                READ *, E
                PRINT 10
10              FORMAT (1X,'PLEASE INPUT SPECIFIC HEAT RATIO',
     1                 1X,'(OR POLYTROPIC CONSTANT)')
                READ *, N
                WRITE (3,15) T0
                PRINT 15, T0
15              FORMAT (1X,'ENGINE INLET TEMPERATURE IS',1X,F7.2,1X,'(K)')
                WRITE (3,16) P0
                PRINT 16, P0
16              FORMAT (1X,'ENGINE INLET PRESSURE IS',1X,F5.2,1X,'(atm)')
                WRITE (3,17) P1
                PRINT 17, P1
17              FORMAT(1X,'ENGINE AIR-BOX PRESSURE IS',1X,F5.2,1X,'(atm)')
                WRITE (3,18) E
                PRINT 18, E
18              FORMAT (1X,'ENGINE COMPRESSION RATIO IS',1X,F5.2)
                WRITE (3,19) N
                PRINT 19, N
19              FORMAT(1X,'SPECIFIC HEAT RATIO',
     1                 '(OR POLYTROPIC CONSTANT) IS',1X,F4.2)


C--------------------------------------------------------------------
C       MAIN PROGRAM:
C       CALCULATE THE UNBURNED GAS TEMPERATURE AND PRESSURE
C--------------------------------------------------------------------
                A=(N-1)/N
                B=(P1/P0)**A
                T1=T0*(1+(B-1)/0.75)
                WRITE (3,100) T1
                PRINT 100, T1
100             FORMAT (1X,'ENGINE AIR-BOX TEMPERATURE IS',
     1                 1X,F7.2,1X,'(K)')
                T2=T1*(E**(N-1))
                P2=P1*(E**N)
                WRITE (3,110) P2
                PRINT 110, P2
110             FORMAT(1X,'UNBURNED GAS PRESSURE IS',1X,F5.2,1X,'(atm)')
                WRITE (3,120) T2
                PRINT 120, T2
120             FORMAT (1X,'UNBURNED GAS TEMPERATURE IS',1X,F7.2,1X,'(K)')
                WRITE (3,130)
                PRINT 130
130             FORMAT (1X,'      ')
                GOTO 1
140             CLOSE (UNIT=3)
                END
```

APPENDIX I                PROGRAM #2


1.  Input Parameters

    *Relative air-fuel ratio, Lambda.

    *Residual molal fraction, FRES.

    *Atomic hydrogen-to-carbon ratio of fuel, RHC.


2.  List of the PROGRAM #2

```
----------------------------------------------------------------
C       THIS PROGRAM IS MADE TO FIND THE FINAL UNBURNED GAS
C       COMPOSITIONS (INCLUDING FUEL, FRESH AIR AND RESIDUAL GAS
C       FROM PREVIOUS CYCLE) INSIDE THE ENGINE CYLINDER AFTER
C       CERTAIN CYCLES OF RUN. ASSUME BOTH THE RESIDUAL MOLAL
C       FRACTION AND THE RELATIVE AIR-FUEL RATIO REMAIN CONSTANT
C       FOR EACH CYCLE.
----------------------------------------------------------------
        IMPLICIT REAL(M)
        OPEN (UNIT=3,FILE='B:PROJ03.DAT',STATUS='UNKNOWN')
1       PRINT 2
2       FORMAT (1X,'PLEASE MAKE YOUR CHOISE:')
        PRINT 3
3       FORMAT(1X,'0==>QUIT THE PROGRAM'
     1          /1X,'1==>CONTINUE THE PROGRAM')
        READ *, J
        IF (J.EQ.0) THEN
        GOTO 340
        ELSE IF (J.EQ.1) THEN
        GOTO 4
        ELSE
        GOTO 1
        END IF
4       PRINT 5
5       FORMAT (1X,'PLEASE INPUT RELATIVE AIR-FUEL RATIO')
                   R E A D   * ,     Y
----------------------------------------------------------------
C       Y = LAMBDA, IS RELATIVE AIR-FUEL RATIO
----------------------------------------------------------------
10      PRINT 15
15      FORMAT (1X,'PLEASE INPUT RESIDUAL MOLAL FRACTION')
        READ *, FRES
        WRITE (3,25) Y
        PRINT 25, Y
25      FORMAT (1X,'RELATIVE AIR-FUEL IS',1X,F4.2)
        WRITE (3,35) FRES
```

```
          PRINT 35, FRES
35        FORMAT (1X,'RESIDUAL MOLAL FRACTION IS',1X,F4.2)
          WRITE (3,40) RHC
          PRINT 40, RHC
40        FORMAT (1X,'H TO C ATOMIC RATIO OF THE FUEL',1X,F6.3)
          WRITE (3,45)
          PRINT 45
45        FORMAT(1X,'CHn+2Y(O2+3.76N2)
     1              +(9.52YR)(A*CO2+B*H2O+C*O2+D*N2)')
          WRITE (3,55)
          PRINT 55
55                FORMAT(10X,'==>E*CO2+F*H2O+G*O2+H*N2')
-------------------------------------------------------------------
C         CALCULATION OF THE RESIDUAL-AIR MOLAL RATIO, R:
-------------------------------------------------------------------
100       R=FRES/(1-FRES)
-------------------------------------------------------------------
C         THE BASIC CYCLE (WITH RESIDUAL GAS OF 21% O2 AND 79% N2):
C         THE REACTION EQUATION IS:
C             CHn+2Y(O2+3.76N2)+(9.52YR)(A*CO2+B*H2O+C*O2+D*N2)
C                     =>E*CO2+F*H2O+G*O2+H*N2      (n=RHC)
-------------------------------------------------------------------
200       MRES=9.52*Y*R
          AA=0
          BB=0
          CC=0.21
          DD=0.79
          EE=1+MRES*AA
          FF=RHC/2+MRES*BB
          GG=2*Y-1-RHC/4+MRES*CC
          HH=7.52*Y+MRES*DD
          MTOTAL=RHC/4+9.52*Y*(1+R)
          WRITE (3,210)
          PRINT 210
210       FORMAT(4X,'A',8X,'B',8X,'C',8X,'D',8X,'E',8X,'F',
     1          8X,'G',8X,'H')
          WRITE (3,215)
          PRINT 215
215       FORMAT(1X,'THIS IS BASIC CYCLE')
          WRITE (3,220) AA,BB,CC,DD,EE,FF,GG,HH
          PRINT 220, AA,BB,CC,DD,EE,FF,GG,HH
220       FORMAT(8(1X,F8.5))
-------------------------------------------------------------------
C         MAIN PROGRAM:
C         CALCULATE COMPOSITIONS OF COMBUSTION REACTANTS AND PRODUCTS
-------------------------------------------------------------------
300       I=1
305       A=EE/MTOTAL
          B=FF/MTOTAL
          C=GG/MTOTAL
          D=HH/MTOTAL
          E=1+MRES*A
```

```
          F=RHC/2+MRES*B
          G=2*Y-1-RHC/4+MRES*C
          H=7.52*Y+MRES*D
          WRITE (3,315) I
          PRINT 315, I
315       FORMAT (1X,'THIS IS CYCLE',1X,I4)
          WRITE (3,325) A,B,C,D,E,F,G,H
          PRINT 325, A,B,C,D,E,F,G,H
325       FORMAT(8(1X,F8.5))
          A1=ABS(AA-A)/A
          IF (A1.GT.0.001) THEN
          AA=A
          BB=B
          CC=C
          DD=D
          EE=E
          FF=F
          GG=G
          HH=H
          I=I+1
          GOTO 305
          END IF
          MCO2=E
          MH2O=F
          MO2=G
          MN2=H
          WRITE (3,330) MCO2,MH2O,MO2,MN2
          PRINT 330, MCO2,MH2O,MO2,MN2
330       FORMAT (1X,'MCO2=',F8.5,1X,'MH2O=',F8.5,1X,'MO2=',F8.5,
     1           1X,'MN2=',F8.5)
          WRITE (3,335)
          PRINT 335
335       FORMAT (1X,'      ')
          GOTO 1
340       CLOSE (UNIT=3)
          END
```

APPENDIX J

PROCEDURES FOR CALCULATING THERMODYNAMIC PROPERTIES

The following are the preparing procedures of the thermodynamic properties of the unburned gas in three different cases:

Case 1, the unburned gas only involves fresh air and natural gas fuel:

1.  Input the experimental data (inlet pressure $P_0$, inlet temperature $T_0$ and air-box pressure $P_1$) into PROGRAM#1 to compute the unburned-gas pressure $P_2$ and temperature $T_2$.

2.  Input the unburned-gas compositions, $P_2$ and $T_2$ into the non-combustion function of the STANJAN to compute the unburned-gas thermodynamic properties which are $U_2$, $H_2$, $S_2$ etc. Therefore, $P_2$ and $H_2$ are known.

Case 2, the unburned gas contains fresh air, residual gas and natural gas fuel:

1.  Use same procedure as the step 1 of case 1 to find $T_2$ and $P_2$.

2.  It is known that the unburned gas contains fuel, $O_2$, $N_2$, $CO_2$ and $H_2O$. Then, divide fuel (ex. $CH_4$), $O_2$ and $N_2$ into Group A and $CO_2$, $H_2O$ into Group B.

3.  Use same procedure twice as the step 2 of case 1 to calculate the enthalpy of unburned gas, as $H_{2A}$ for Group A and as $H_{2B}$ for Group B.

4.  Calculate the mass, $m_A$ and $m_B$, for Group A and Group B

respectively.

5.  Use the following equation to calculate the total enthalpy of the unburned gas, $H_2$

$$H_2 = \frac{H_{2A} m_A + H_{2B} m_B}{m_A + m_B}$$     (J.1)

Therefore, $P_2$ and $H_2$ are known.

Case 3, the unburned gas contains fresh air and diesel fuel:

1.  Use same procedure as the step 1 of case 1 to find $T_2$ and $P_2$.

2.  Put diesel fuel ($CH_{1.8}$) in Group A and air in Group B.

3.  Calculate $H_{2A}$, the enthalpy of gaseous diesel at state "2" in Fig. 6.1 in chapter 6, with the following equations

$$H_{2A} = H_{T_2} = H^0{}_{298K} + \Delta H_{T_2}$$     (J.2)

where

$$\Delta H_{T_2} = [2327.6 \, (T_2)^2 + 10418 \, (T_2) - 51714.3] / 12$$     (J.3)

and

$$H^0{}_{298K} = -1852.4 \, (kJ/kg)$$

where $H^0{}_{298K}$ is the enthalpy of formation of the diesel ($CH_{1.8}$) which is evaluated from HHV$=-45220$ kJ/kg for liquid diesel. vaporization of the diesel has already counted in. Then calculate the mass of diesel, $m_A$.

4.  Use same procedure as the step 2 of case 1 to calculate the enthalpy of Group B (ie. air), $H_{2B}$. Then the mass of Group B,

$m_B$.

5.     Determine the total enthalpy of the unburned gas, $H_2$, by Eq. (J.1). Therefore, $P_2$ and $H_2$ are known.

APPENDIX K

PROCEDURE FOR COMPUTATION OF EQUILIBRIUM COMPOSITION

The calculation procedure of the equilibrium compositions of the combustion produces is as follows:

1. Obtain the test engine specification data and experiment data. The following is the data needed for later calculations:

   *Engine inlet temperature, $T_0$.

   *Engine inlet pressure, $P_0$.

   *Engine air-box pressure, $P_1$.

   *Engine compression ratio, E.

   *The actual range of the relative air-fuel ratio which correspond to actual load range of the engine.

   *Engine residual molal fraction, $F_{res}$.

   *Specific heat ratio, k (or polytropic constant, n ).

   *Engine exhaust temperature.

   *Atomic hydrogen-to-carbon ratio of the fuel.

2. Calculate the unburned-gas temperature, $T_2$ and pressure, $P_2$ with the PROGRAM#1 (as explained in Section 6.4, 6.5 and Appendix H).

3. Determine the unburned-gas compositions with the PROGRAM#2 (as mentioned in Subsection 6.3.2 and Appendix I).

4. Evaluate the thermodynamic properties of the unburned gas with the non-combustion function of the STANJAN. Only $H_2$ and $P_2$ are needed for later calculation.

5. Compute the burned-gas equilibrium compositions of the

constant pressure and adiabatic combustion process with the combustion function of the STANJAN by inputting the unburned-gas compositions, $P_2$ and $H_2$.

6. Determine the exhaust temperature of MASD cycle only when it is necessary.

APPENDIX L

# EVALUATION OF THE RESIDUAL TEMPERATURE
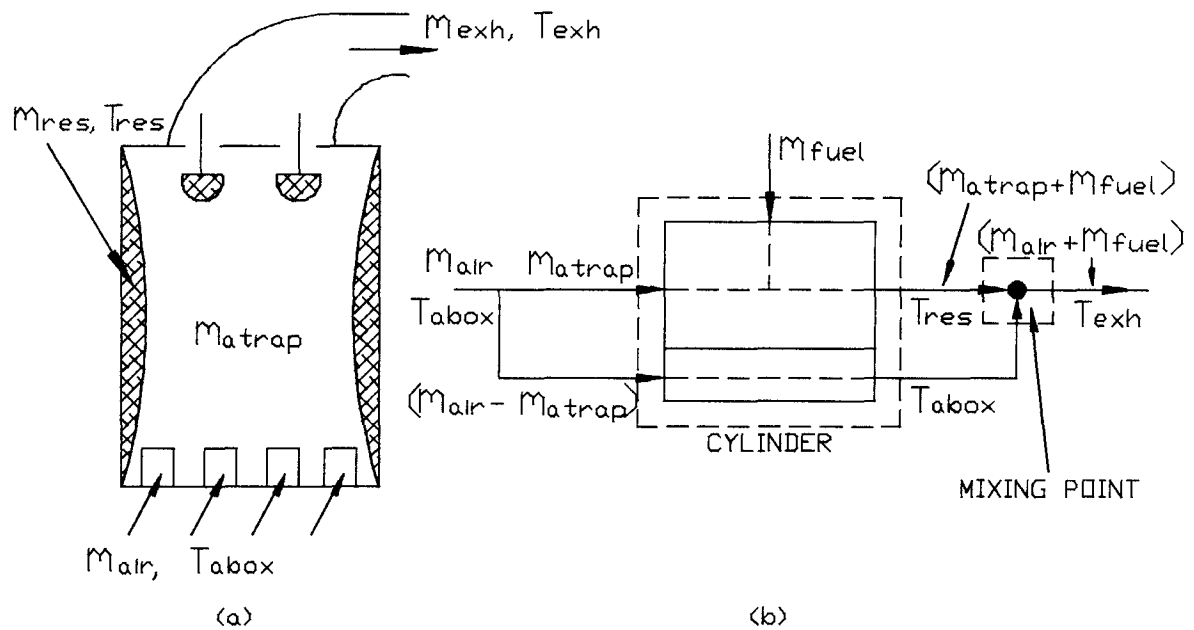


Figure L.1: Schematic of Residual Temperature Evaluation Model.

Figure L.1 shows a schematic of the residual temperature evaluation model. After inlet port opening, most combustion products are pushed out from the cylinder by intake air. Part of the intake air passes the cylinder with combustion products, which is defined as passed air. We assumes that there is a mixing point in the exhaust pipe and there is no mixing and heat exchange before

this point; combustion products and passed air mix adiabatically with constant pressure into exhaust gas at the mixing point. That is, before mixing, the combustion products remain at the same temperature as the residual gas in the cylinder and the passed air keeps the air-box temperature; after mixing, all the mixture has exhaust temperature which can be measured.

For the mixing point, we can write the mass conservation and energy conservation equations as following:

$$(m_{atrap}+m_{fuel}) + (m_{air}-m_{atrap}) = (m_{air}+m_{fuel}) \qquad (L.1)$$

and

$$(m_{atrap}+m_{fuel}) \, C_{pres}T_{res}+ (m_{air}-m_{atrap}) \, C_{pair}T_{abox}$$
$$= (m_{air}+m_{fuel}) \, C_{pexh}T_{exh} \qquad (L.2)$$

where $m_{air}$, $m_{atrap}$ and $m_{fuel}$ are the delivered air mass, mass of the air trapped and total mass of the fuel per cycle respectively. Cpair, Cpres and Cpexh are the constant-pressure specific heat of the air, the residual gas and the exhaust gas respectively. $T_{abox}$, $T_{res}$ and $T_{exh}$ are the temperature of the air box, the residual gas and exhaust gas respectively.

From the energy conservation Eq. (L.2), we can determine the residual temperature by

$$T_{res}=\frac{(m_{air}+m_{fuel}) \, C_{pexh}T_{exh}- (m_{air}-m_{atrap}) \, C_{pair}T_{abox}}{(m_{atrap}+m_{fuel}) \, C_{pres}} \qquad (L.3)$$

Substituting $m_{atrap}$ = DP × $m_{trap}$ and mfuel = m_CNG + m_DSL into Eq. (L.3), we can have

$$T_{res} = \frac{(m_{air}+m_{CNG}+m_{DSL})\, C_{pexh} T_{exh} - (m_{air}-DP\times m_{trap})\, C_{pair} T_{abox}}{(DP\times m_{trap}+m_{CNG}+m_{DSL})\, C_{pres}} \qquad (L.4)$$

where DP is the degree of purity of the charge. $m_{trap}$ is the trapped mass. $m_{CNG}$ and $m_{DSL}$ are the mass of the CNG and the diesel fuels.

APPENDIX M WORK SHEET OF THE PROGRAM XPRESSD

XPRESSD.WK1/JULY 05, 93.
Vipc/VTDC: 12.96558
TEST CONDITION:
1) 1200 RPM, 60 BAR, 20DEG. ANGLE (FOR GAS-DIESEL OPERATION).
2) 1200 RPM DIESEL BASELINE.

BLOCK 1: Intake and exhaust parameters.

| ## | Speed (RPM) | Ambient Pressure (kPa) | Gage Pressure (kPaG) | Ambient Temp. (K) | Air Box Pressure (kPa) | Air Box Temp. (K) | Exhaust Temp. (K) |
|----|------|--------|---------|----------|----------|----------|-----|
| 1) 40% SRD, 25% CN62 (Humidity Ratio: 9.0 gH2O/kgAIR): | | | | | | | |
| 1 | 1212 | 102.32 | 24.4254 | 305.2485 | 126.7454 | 346.2125 | 527 |
| 2 | 1215 | 102.32 | 23.90182 | 307.0763 | 126.2218 | 347.4647 | 560 |
| 3 | 1193 | 102.32 | 25.65576 | 307.1113 | 127.9757 | 350.2453 | 593 |
| 2) NON-EGR, 0% SRD, 25% #2 (Humidity Ratio: 11.37 gH2O/kgAIR): | | | | | | | |
| 1 | 1234 | 101.65 | 24.16911 | 314.4150 | 125.8191 | 354.1821 | 686 |
| 2 | 1219 | 101.65 | 24.99256 | 314.9412 | 126.6425 | 355.6633 | 688 |
| 3 | 1236 | 101.65 | 23.82741 | 315.4908 | 125.4774 | 356.2527 | 665 |
| 4 | 1218 | 101.65 | 23.52503 | 316.3694 | 125.1750 | 356.2569 | 618 |
| 5 | 1214 | 101.65 | 23.4193 | 316.7745 | 125.0693 | 355.6569 | 634 |
| 6 | 1220 | 101.65 | 23.48546 | 316.8956 | 125.1354 | 356.2425 | 633 |
| 7 | 1236 | 101.65 | 24.16105 | 317.0172 | 125.8110 | 357.7293 | 678 |
| 8 | 1197 | 101.65 | 23.94655 | 317.2572 | 125.5965 | 357.7263 | 624 |
| 9 | 1217 | 101.65 | 23.22568 | 317.3026 | 124.8756 | 356.2331 | 641 |
| 10 | 1230 | 101.65 | 23.03895 | 317.3101 | 124.6889 | 356.6492 | 622 |
| 11 | 1206 | 101.65 | 24.31713 | 317.3135 | 125.9671 | 357.4188 | 657 |
| 3) EGR, 0% SRD, 25% #2 (Humidity Ratio: 13.26 gH2O/kgAIR): | | | | | | | |
| 1 | 1216 | 101.64 | 24.25391 | 317.3723 | 125.8939 | 371.1421 | 720 |
| 2 | 1227 | 101.64 | 24.0868 | 317.3965 | 125.7268 | 374.2451 | 710 |
| 3 | 1196 | 101.64 | 25.2216 | 317.4268 | 126.8616 | 377.4058 | 694 |
| 4 | 1205 | 101.64 | 23.96791 | 317.4516 | 125.6079 | 380.2706 | 693 |
| 5 | 1223 | 101.64 | 23.23388 | 317.4763 | 124.8738 | 380.4395 | 685 |
| 6 | 1193 | 101.64 | 24.41961 | 317.4793 | 126.0596 | 381.2838 | 673 |
| 7 | 1214 | 101.64 | 23.97048 | 317.4903 | 125.6104 | 383.302 | 707 |
| 8 | 1222 | 101.64 | 24.31868 | 317.515 | 125.9586 | 385.6313 | 706 |
| 9 | 1228 | 101.64 | 23.80001 | 317.5391 | 125.4400 | 385.885 | 665 |
| 4) Baseline (Humidty Ratio: 4.52 gH2O/kgAIR): | | | | | | | |
| 1 | 1205 | 100.6 | 25 | 315 | 125.6 | 358.8775 | 550 |
| 2 | 1222 | 100.6 | 23.3 | 316 | 124 | 357.3976 | 580 |
| 3 | 1188 | 100.6 | 25 | 316 | 125.6 | 360.0168 | 600 |

BLOCK 2: Input and exput parameters.

| Air Massflow (kg/hr) | Liq.fuel dm/dt (kg/hr) | CNG dm/dt (kg/hr) | Inject. PW | Inject. BOI (°BTDC) | Corr. Power (kW) | Corr. MEP (kPa) | Thermal Effic. (%) |
|---|---|---|---|---|---|---|---|
| **1) 40% SRD, 25% CN62 (Humidity Ratio: 9.0 gH2O/kgAIR):** | | | | | | | |
| 113 | 0.372602 | 1.033945 | 8 | 24 | 4.590035 | 1.965267 | 24.4186 |
| 116 | 0.485392 | 1.329538 | 10 | 32 | 7.185184 | 3.050826 | 29.53114 |
| 113 | 0.63034 | 1.766822 | 13 | 32 | 9.479388 | 4.117704 | 29.48404 |
| **2) NON-EGR, 0% SRD, 25% #2 (Humidity Ratio: 11.37 gH2O/kgAIR):** | | | | | | | |
| 109 | 0.648701 | 1.848526 | 11 | 28 | 5.798951 | 2.425195 | 17.38516 |
| 107 | 0.667318 | 1.970625 | 11 | 28 | 7.210735 | 3.053528 | 20.46398 |
| 109 | 0.765553 | 1.981506 | 12 | 28 | 8.330941 | 3.479745 | 22.72406 |
| 106 | 0.552986 | 1.59209 | 10 | 32 | 5.946683 | 2.520408 | 20.72375 |
| 105 | 0.571115 | 1.575998 | 10 | 32 | 7.25618 | 3.0863 | 25.28698 |
| 106 | 0.660883 | 1.6943 | 11 | 32 | 8.427998 | 3.56694 | 26.80346 |
| 107 | 1.010106 | 2.328081 | 5 | 32 | 9.494095 | 3.965298 | 21.33126 |
| 102 | 0.495288 | 1.513703 | 12 | 36 | 5.703078 | 2.459298 | 21.19061 |
| 108 | 0.54983 | 1.672513 | 12 | 36 | 7.11388 | 3.01803 | 23.91148 |
| 109 | 0.589926 | 1.664481 | 12 | 36 | 8.37678 | 3.516791 | 27.77336 |
| 105 | 0.79208 | 1.99166 | 14 | 36 | 9.324703 | 3.992163 | 25.08096 |
| **3) EGR, 0% SRD, 25% #2 (Humidity Ratio: 13.26 gH2O/kgAIR):** | | | | | | | |
| 87.7 | 0.735073 | 1.862798 | 11 | 28 | 6.157891 | 2.614098 | 17.5845 |
| 88.8 | 0.782023 | 2.016833 | 12 | 28 | 7.215641 | 3.034691 | 19.11895 |
| 83.4 | 0.749656 | 2.057158 | 12 | 28 | 8.208283 | 3.542856 | 22.01056 |
| 87.9 | 0.569808 | 1.6342 | 11 | 32 | 6.00669 | 2.573048 | 20.17173 |
| 89.6 | 0.69326 | 1.727946 | 12 | 32 | 7.341525 | 3.099348 | 22.49895 |
| 84.7 | 0.73886 | 1.827525 | 12 | 36 | 8.129796 | 3.518398 | 23.55241 |
| 88.1 | 0.560663 | 1.633711 | 12 | 36 | 5.974646 | 2.540025 | 20.15241 |
| 92.4 | 0.587615 | 1.812251 | 12 | 36 | 7.15562 | 3.023678 | 22.05023 |
| 90.9 | 0.60977 | 1.833738 | 13 | 36 | 8.623358 | 3.625296 | 26.08955 |
| **4) Baseline: (Humidty Ratio: 4.52 gH2O/kgAIR):** | | | | | | | |
| 101.1 | 1.9231 | | 0 | 9 | 12 | 4.63 | 1.98 | 19.1 |
| 101.9 | 2.3399 | | 0 | 12 | 12 | 8.22 | 3.48 | 27.8 |
| 94.9 | 2.9997 | | 0 | 13 | 12 | 9.25 | 4.02 | 24.4 |

```
BLOCK 3: Exhaust emissions.
CO          CO2         NOx        O2          THC        H2O(wet)   N2
[wet]       [wet]       [wet]      [wet]       [wet]      [wet]      [wet]
(ppm)       (%vol)      (ppm)      (%vol)      (ppm)      (%vol)     (ppm wet)
-------------------------------------------------------------------------
1) 40% SRD, 25% CN62 (Humidity Ratio: 0.0090):
981.4663 2.775269 207.5841 15.19777 1345.601 4.674310 77.09918
516.4374 3.465667 648.5362 13.82398 820.4102 5.746264 76.76554
2530.389 4.703483 825.9376 11.16361 850.3722 8.033601 75.67862

2) NON-EGR, 0% SRD, 25% #2 (Humidity Ratio: 11.37 gH2O/kgAIR):
 5136.23 4.828243 108.9531 9.840656 3267.516 8.630271 75.84955
5437.075 4.871955  126.206 9.636355 2646.596 8.776316 75.89438
5846.996 4.775346 241.8171   9.6462  2366.01 8.510363 76.22260
1928.955 4.012528 135.6853 12.28996  3171.17 6.916358 76.25756
2051.331 4.462478 248.7756 11.47011 1934.925 7.636873 76.00702
2939.885 4.750616 435.6068 10.80065 1204.173 8.134726 75.85604
6746.935 4.886815 376.0823 8.735898 3446.818 8.647666 76.67263
 1356.98  3.79284 162.0435 12.72445 3666.546 6.532228 76.43192
 1655.15 4.511855  194.582 11.38461 2575.331  7.77086 75.89016
1614.746 4.560831 319.5783 11.32321 1105.928  7.77232 76.03960
 3609.03 5.209126 534.3126 9.900576  1625.96  8.93886 75.37450

3) EGR, 0% SRD, 25% #2 (Humidity Ratio: 13.26 gH2O/kgAIR):
5457.311 4.768828 68.85998 9.949586 3236.405 8.430988 75.97433
6142.453 4.630793 102.7665 9.778838 3097.733 8.300078 76.35599
6048.575 4.351735 166.7753 10.35601  2533.54 7.895495 76.52186
3261.598 4.218713 81.30516 11.69213 2871.175  7.40756 76.06018
4081.285 4.505443 106.5993 11.05431 1838.235 7.828541 76.00908
4841.933 4.543085  214.455 10.73595 1680.361 7.962108 76.08518
2884.738  4.42245 89.21936 11.39918 3221.893 7.720701 75.83807
 3312.81 4.840675  103.829  10.4961 2027.468 8.529641 75.58917
3338.115 4.807608 332.9111 10.58241 1244.821 8.451136 75.66725

4) Baseline (Humidty Ratio: 4.52 gH2O/kgAIR):
      64.2      3.2   483.15     15.5      158      2.9 78.32946
     79.75     4.97   735.23     13.7      178      4.5 76.73070
     143.5     6.13   1042.1     11.3      192      5.6 76.83224
```

```
BLOCK 4: Heat transfer adjustment parameters (June 30, 93).
  C2        C3        C4        Ignition Delay
            A         B         (CA)      (sec)
----------------------------------------------------------

1) 40% SRD, 25% CN62 (Humidity Ratio: 0.0090):
0.45    0.35/0.8    0.7/0.774      30.4    0.00418
0.45    0.35/0.8    0.7/0.786      30.2    0.004142
0.45    0.35/0.8    0.7/0.79      26.04    0.003637

2) NON-EGR, 0% SRD, 25% #2 (Humidity Ratio: 11.37 gH2O/kgAIR):
0.4    0.6/0.8    0.7/0.853      41.42    0.005594
0.4    0.6/0.8    0.7/0.843      39.1     0.005346
0.4    0.6/0.8    0.7/0.831      33.44    0.004513
0.4    0.6/0.8    0.7/0.821      41.59    0.005691
0.4    0.6/0.8    0.7/0.816        38     0.005221
0.4    0.6/0.8    0.7/0.813      34.01    0.004647
0.4    0.6/0.8    0.7/0.843      30.01    0.004047
0.4    0.6/0.8    0.7/0.834      46.72    0.006505
0.4    0.6/0.8    0.7/0.812      43.39    0.005942
0.4    0.6/0.8    0.7/0.806      41.06    0.005564
0.4    0.6/0.8    0.7/0.826      35.19    0.004863

3) EGR, 0% SRD, 25% #2 (Humidity Ratio: 13.26 gH2O/kgAIR):
0.35    0.8/0.8    0.7/0.867      40.12    0.005499
0.35    0.8/0.8    0.7/0.86       38.71    0.005258
0.35    0.8/0.8    0.7/0.84       33.22    0.00463
0.35    0.8/0.8    0.7/0.844      43.27    0.005985
0.35    0.8/0.8    0.7/0.83       39.8     0.005424
0.35    0.8/0.8    0.7/0.832      35.57    0.004969
0.35    0.8/0.8    0.7/0.804      48.37    0.006641
0.35    0.8/0.8    0.7/0.825      46.7     0.006503
0.35    0.8/0.8    0.7/0.813      39.56    0.005369

4) Baseline (Humidty Ratio: 4.52 gH2O/kgAIR):
0.45      0.8        0.775        8.27    0.001144
0.45      0.8        0.762        7.81    0.001066
0.45      0.8        0.789        7.01    0.000985
```

BLOCK 5: Stoichiometric combustion results (June 30, 93).

| STORHC | STOROC | STORNC | Tbmax (K) | Pmax (atm) | EQUI.NO (ppm) | CFK | AVG.NO (ppm) |
|---|---|---|---|---|---|---|---|
| **1) 40% SRD, 25% CN62 (Humidity Ratio: 0.0090):** | | | | | | | |
| 3.419 | 3.709 | 13.948 | 2380 | 35.5 | 2015 | 0.093 | 187 |
| 3.389 | 3.695 | 13.892 | 2558 | 58.1 | 3416 | 0.174 | 594 |
| 3.397 | 3.699 | 13.906 | 2590 | 64.1 | 3711 | 0.204 | 757 |
| **2) NON-EGR, 0% SRD, 25% #2 (Humidity Ratio: 11.37 gH2O/kgAIR):** | | | | | | | |
| 3.428 | 3.714 | 13.965 | 2160 | 24 | 873 | 0.116 | 101 |
| 3.442 | 3.721 | 13.991 | 2209 | 31.1 | 1037 | 0.128 | 133 |
| 3.387 | 3.694 | 13.888 | 2344 | 42.6 | 1715 | 0.15 | 257 |
| 3.432 | 3.716 | 13.972 | 2169 | 29.4 | 877 | 0.12 | 105 |
| 3.414 | 3.707 | 13.939 | 2300 | 38.6 | 1462 | 0.17 | 249 |
| 3.383 | 3.692 | 13.881 | 2455 | 53.7 | 2467 | 0.189 | 466 |
| 3.337 | 3.669 | 13.794 | 2449 | 53.3 | 2409 | 0.158 | 380 |
| 3.456 | 3.728 | 14.017 | 2091 | 26 | 620 | 0.121 | 75 |
| 3.454 | 3.727 | 14.013 | 2249 | 35.2 | 1204 | 0.148 | 178 |
| 3.423 | 3.712 | 13.956 | 2381 | 45.8 | 1943 | 0.19 | 369 |
| 3.375 | 3.687 | 13.865 | 2479 | 59 | 2622 | 0.221 | 527 |
| **3) EGR, 0% SRD, 25% #2 (Humidity Ratio: 13.26 gH2O/kgAIR):** | | | | | | | |
| 3.378 | 3.689 | 13.871 | 2003 | 21.3 | 410 | 0.173 | 71 |
| 3.386 | 3.693 | 13.885 | 2072 | 28.9 | 555 | 0.194 | 108 |
| 3.412 | 3.706 | 13.934 | 2230 | 42.8 | 1074 | 0.228 | 245 |
| 3.431 | 3.715 | 13.969 | 2001 | 23.5 | 398 | 0.17 | 68 |
| 3.371 | 3.686 | 13.858 | 2156 | 33 | 816 | 0.2 | 163 |
| 3.368 | 3.684 | 13.852 | 2289 | 47.4 | 1351 | 0.224 | 303 |
| 3.437 | 3.718 | 13.981 | 2074 | 23.6 | 578 | 0.179 | 103 |
| 3.456 | 3.728 | 14.017 | 2079 | 26 | 584 | 0.222 | 130 |
| 3.449 | 3.725 | 14.005 | 2348 | 48.1 | 1670 | 0.246 | 411 |
| **4) Baseline (Humidty Ratio: 4.52 gH2O/kgAIR):** | | | | | | | |
| 2.017 | 3.009 | 11.313 | 2440 | 56.3 | 2124 | 0.148 | 314 |
| 2.017 | 3.009 | 11.313 | 2458 | 50.6 | 2689 | 0.153 | 411 |
| 2.017 | 3.009 | 11.313 | 2431 | 65 | 2340 | 0.265 | 620 |

APPENDIX N          PROGRAM XPRESSD

1.   Input Parameters

     *Engine speed, rpm.

     *Ambient temperature and engine exhaust temperature, K.

     *Ambient pressure and engine air-box pressure, kPa.

     *Delivered air mass, total mass of CNG and diesel, kg/cycle.

     *Crank angle of the first pressure record, CA.

     *Crank angle of the BOI.

     *Crank angle of the interval size, CA.

     *Crank angle interval of the PW, CA.

     *Number of lines of pressure records per cycle.

     *Number of CA intervals per cycle to be analyzed after BOI.

     *Number of engine cycles to be analyzed.

     *Engine wet-basis emission data, ppm for CO, $NO_x$, THC,

      %vol for $CO_2$, $O_2$, $H_2O$.

     *Engine pressure data.


2.   List of the program XPRESSD.FOR

```
C   XPRESSD.FOR
C   This program takes engine pressure data at regular crank angle
C   increments DCA and determines mass-burned fraction.
C   The source program was XPRESSE.FOR, originated by Dr. P.G. Hill.
C   Modified for gas-diesel engine by H.Gunawan (May14,1992).
C   Modified for three-zone combustion and exhaust emission analysis
C   model of gas-diesel engine by Yinchu Tao and Dr. P.G. Hill
C   (June 30, 1993).

C   THIS VERSION IS ONLY FOR STOICHIOMETRIC (OR DIFFUSION)
C   COMBUSTION (WITH SUBROUTINE QWALL CONNECTED).

        IMPLICIT REAL*8(A-H,O-Z)
        REAL*8 MAIR,MDSL,MGAS,MG,MD
```

```
      REAL*8  MTRAP,MATRAP,MTOT
      REAL*8  MWO2,MWN2,MWCH4,MWCH2,MWH2O,MWCO2
      REAL*8  MWCO,MWNOX,MWTHC,MWEXH
      REAL*8  CA(360),P(360),XMB(360),T(360),X(360)
      REAL*8  PAVG(360),XAVG(360),TAVG(360)
      REAL*8  WRK(360),WAVG(360)
      REAL*8  QAVG(360),QWL(360)
      REAL*8  TU(360),TUAVG(360)
      REAL*8  TBRN(360),TBAVG(360)
      COMMON/PROPS/RDG,RHC,FRES,EQVR,RU
      COMMON/STATS/CABOI,RPM,N,NCYC,NCA
      COMMON/GEOM/BORE,STROKE,ROD,CLRH
      COMMON/MASS/MTOT,MAIR,MDSL,MGAS
      COMMON/PORT/PABOX,CAIPC,PIPC,TIPC,TEXH,TABOX
      COMMON/AMBNT/PAMB,TAMB
      COMMON/BURN/UB
      COMMON/EMIS/YCO,YCO2,YNOX,YO2,YTHC,YH2O,UFRAT
      COMMON/PREP/STORHC,STOROC,STORNC,RFASTO
      COMMON/MW1/MWCO2,MWO2,MWH2O,MWN2,MWCH4,MWCH2
      COMMON/MW2/MWCO,MWNOX,MWTHC,MWEXH
      COMMON/AVGNO/XTBMAXAVG
      COMMON/MOLFRAC/XO2,XN2,XCO2,XH2O,WTMOLU

C  Specify the cylinder geometry of 1-71 engine:
C  BORE   is cylinder bore(m), STROKE(m),
C  ROD    is conn rod length(m),
C  CR     is compression ratio,
C  CLRH   is clearance height(m).
C  CAIPC  is a crank angle (ABDC) after all ports are closed.
C  CAEXH  is a crank angle (BBDC) that exhaust ports open.

      STROKE = 0.1270D0
      BORE = 0.10795D0
      ROD = 0.2540D0
      CR = 16.0D0
      CLRH = STROKE/(CR-1.0D0)
      CAIPC = 50.0D0
      CAEXH = 86.0D0

C  Specify the molecular weights of the components:
      MWCO = 28.011D0
      MWCO2 = 44.011D0
      MWNOX = 30.006D0
      MWO2 = 31.999D0
      MWH2O = 18.015D0
      MWN2 = 28.013D0
      MWCH4 = 16.043D0
      MWCH2 = 14.026D0

C*******************Initialize*********************
C  RDG    is the mass ratio of diesel to natural gas.
C  RHC    is the atomic ratio of H to C in combined fuel.
```

```
C  FRES   is the residual mole fraction.
C  EQVR   is the fuel-air equivalence ratio.
C  RU     is the gas constant for the unburned gas per kg and
C  CVU    is the specific heat for unburned gas.
C  TIPC   is the cylinder contents temp at ipc after mixing
C         with residual gas. The residual gas mass fraction
C         is determined using a scavenging data typical of
C         two-stroke diesels.
C  ROC    is the atomic ratio of O2 to C in unburned mixture.
C  RNC    is the atomic ratio of N2 to C in unburned mixture.
C  UFRAT  is the mass ratio of the unburned fuel to the
C         total fuel per unit time.
C  CA     is crank angle.
C  PR1    subscript which refers to the first pressure record.
C  IPC    subscript which refers to intake port closing.
C  BOI    subscript which refers to beginning of injection.

       OPEN(UNIT=2,FILE='BSLPD-3.DAT',STATUS='OLD')
       OPEN(UNIT=9,FILE='Y.OUT',STATUS='UNKNOWN')
       OPEN(UNIT=10,FILE='BSL-3.OUT',STATUS='UNKNOWN')
       OPEN(UNIT=16,FILE='CH4EQ1.DAT',STATUS='OLD')
       OPEN(UNIT=26,FILE='CH2EQ1.DAT',STATUS='OLD')

C  Read the input data:
C  PABOX  is the pressure of air box (kPa).
C  TABOX  is the temperature of air box (K).
C  TEXH   is the exhaust temperature (K).
C  MAIR   is the air mass flow (kg/cycle/cylinder).
C  MDSL   is the diesel mass flow (kg/cycle/cylinder).
C  MGAS   is the natural gas mass flow (kg/cycle/cylinder).
C  CAPR1  is the crank angle of the first pressure record.
C  CABOI  is the crank angle of the beginning of injection.
C  DCA    is the crank angle interval size.
C  CAPW   is the crank angle interval of the PW.
C  NPR    is the number of lines of pressure records per cycle.
C  NCA    is the number of CA intervals per cycle to be analyzed
C         after BOI.
C  NCYC   is the number of engine cycles to be analyzed.

       READ(2,*)RPM,PABOX,TABOX,TEXH,PAMB,TAMB
       READ(2,*)MAIR,MDSL,MGAS
       READ(2,*)CAPR1,CABOI,DCA,CAPW
       READ(2,*)NPR,NCA,NCYC
       READ(2,*)YCO,YCO2,YNOX,YO2,YTHC,YH2O
C     UNITS: ppm FOR CO,NOX,THC; % FOR CO2,O2,H20
       UFRAT = 0.D0

C Read pressure data:
       PRINT*,'reading pressure data'
       DO 1000 N = 1,NCYC
       DO 41 I = 1,NPR
41        READ(2,*)CA(I),P(I)
```

```
C  For PCB pressure transducer (PABOX not equal to PIPC) only:
      DDP = P(CAIPC) - PABOX
      DO 42 I = 1,NPR
 42   P(I) = P(I) - DDP

C  Estimate the mass of air trapped in cylinder MATRAP
C  and the equivalence ratio EQVR:
      PIPC = P(CAIPC)
      CALL INTAKE(MATRAP)
      MTRAP = MATRAP/(1.D0-FRES)
      MTOT = MTRAP
C  Note: MTOT is a instantaneous total mass which is changed during
C      the injection.
      IF (N .NE. 1) GO TO 100

C  Calculate the unburned fuel ratio UFRAT:
      CALL UNBFUEL
      PRINT*,'UFRAT = ',UFRAT
      PRINT*,'MWTHC = ,MWEXH = ,',MWTHC,MWEXH

      WRITE(10,50)NCYC
      WRITE(10,51)RPM,EQVR,CABOI
      WRITE(10,52)MAIR,TIPC,TABOX
      WRITE(10,53)FRES,MATRAP,MTOT
      WRITE(10,54)RDG,UFRAT,RFASTO
      WRITE(10,55)STORHC,STOROC,STORNC
 50          FORMAT(/,1X,I4,'cycles   of   press.data   reduced   by
XPGDSL.FOR')
 51       FORMAT(/,1X,'RPM',F7.1,'  Equiv Ratio ',F6.3,'
     1          CAboi',F8.3)
 52       FORMAT(1X,'Mair kg ',D10.4,'   Tipc K',F6.1,'
     1          Tabox',F9.3)
 53       FORMAT(1X,'Fres',F8.3,' Matrap kg ',E10.4,' Mtot kg
     1          ',E10.4)
 54       FORMAT(1X,'Mdsl/Mgas= ',F7.4,' UFRAT= ',F8.6,' RFASTO=
     1          ',F8.6)
 55       FORMAT(1X,'Carbon = 1',2X,'STORHC = ',F7.3,'   STOROC =
     1             ',F7.3, '  STORNC = ',F7.3)

C  Initialize subroutines:
      PRINT*,'initializing subroutines'
      CALL BURNED(Q1,Q2,Q3,Q4,Q5,Q6,Q7,Q8,1)
      PBOIAV = 0.D0
      DO 90 I = 1,NCA
      PAVG(I) = 0.D0
      TAVG(I) = 0.D0
      TUAVG(I) = 0.D0
      TBAVG(I) = 0.D0
      QAVG(I) = 0.D0
      WAVG(I) = 0.D0
      XAVG(I) = 0.D0
      STBMAX = 0.D0
```

```
              SPTBMAX = 0.D0
    90        SXTBMAX = 0.D0
   100        CONTINUE

C   Calculate the temperature at BOI:
C   Assume fuel injection start in between BOI and BOI+1, thus there
C   is no fuel in cylinder at BOI.

              KBOI = DINT((CABOI - CAPR1)/DCA) + 1
              VBOI = VCYL(CABOI)
              PBOI = P(KBOI)
              TUBOI = PBOI*VBOI/MTOT/RU
              CALL UNBURNED(TUBOI,UU,CVU,VISC,1)
              ETOT = MTOT*UU
              CA(1) = CABOI + DCA
              DO 125 I = 1,NPR-KBOI
                IF(I .GT. 1)CA(I) = CA(I-1) + DCA
   125        P(I) = P(I+KBOI)
              PRINT*,'UU=',UU
              V1 = VBOI
              P1 = PBOI
              TU1 = TUBOI
              T1 = TU1
              XMB1 = 0.D0
              XMB(I) = 0.D0
              TFU = 298.D0
              MG = 0.D0
              MD = 0.D0
              WRITE(10,103)
C             WRITE(10,104)CABOI,PBOI,TUBOI
   103        FORMAT(7X,'CA',10X,'P kPa',9X,'Tu K',8X,'Tb K',8X,
       1             'Tfu K',11X,'X')
   104        FORMAT(1X,6(2X,E11.5))

C   Calculate conditions at end of each crank angle interval:
C   Assume: 1) Injection of fuel at constant rate over crank angle
C              interval CAPW.
C           2) Partial injected fuel begine burning in BOI+1.

              XMAXP = 0.D0
              XMAX = 0.D0
              CAXMAX = CABOI
              WRK1 = 0.D0
              QWL1 = 0.D0
              NCA = NPR-CABOI-CAEXH
              DO 200 I = 1,NCA
                IF (I .GT. CAPW) GO TO 107
                MTOT = MTRAP+(DCA*I/CAPW)*(MDSL+MGAS)
                ETOT = ETOT +(DCA/CAPW)*(MDSL*(-3216)+MGAS*(-4667))
   107        CONTINUE
              CALL UNBURNED(TU1,UU,CVU,VISC,2)
              G = 1.D0/(1.D0+CVU/RU)
```

```
             GAMMA = 1.D0 + RU/CVU
             V2 = VCYL(CA(I))
             AA = 0.8
             BB = 0.789
             IF (XMB1 .LT. 0.1) GO TO 112
             AA=0.8
             BB=0.789
   112       ASURF = ACYL(CA(I))
             CALL QWALL(T1,V2,ASURF,AA,BB,DQWL)
             TU2 = TU1+TU1*G*(P(I)-P1)/P1+0.45D0*DQWL/(MTOT*(CVU+RU))
             CALL UNBURNED(TU2,UU,CVU,VISC,1)
             VU = RU*TU2/P(I)
             DWRK = (P1+P(I))/2.D0*(V2-V1)
             ETOT = ETOT - DWRK + DQWL
C            WRITE(10,105)ASURF,DQWL,DWRK,ETOT
C 105        FORMAT(1X,'ASURF=,DQWL=,DWRK=,ETOT=,',4(E9.3,1X))
C  Determine the temperature of unbrned fuel, TFU.
             IF (I .GT. CAPW) GO TO 109
             DMG = (DCA/CAPW)*MGAS
             DMD = (DCA/CAPW)*MDSL
             MG = I*DMG - XMB1*MGAS
             MD = I*DMD - XMB1*MDSL
             CALL UNBURNED(TFU,UU,CVG,VISC,3)
             CPG = CVG + 8.3143D0/MWCH4
             CALL UNBURNED(TFU,UU,CVD,VISC,4)
             CPD = CVD
C  TFU changes due to adiabatic constant-pressure mixing with
C       injected fuels.
             DTMIX = -(DMG*CPG+DMD*CPD)*(TFU-298.D0)/(MG*CPG+MD*CPD)
   109       IF (I .LE. CAPW) GO TO 110
             MG = (1-XMB1)*MGAS
             MD = (1-XMB1)*MDSL
             CALL UNBURNED(TFU,UU,CVG,VISC,3)
             CPG = CVG + 8.3143D0/MWCH4
             CALL UNBURNED(TFU,UU,CVD,VISC,4)
             CPD = CVD
             DTMIX = 0.D0
   110       CONTINUE
C  TFU changes due to isentropic compression of fuel.
             DTCOMP =
     1       MG*TFU*(8.3143D0/MWCH4)*(P(I)-P1)/P1/(MG*CPG+MD*CPD)
             TFU = TFU + DTMIX + DTCOMP
             UG = (-4821) + CVG*(TFU-298.D0)
             UD = (-3216) + CVD*(TFU-298.D0)
             VG = (8.3143D0/MWCH4)*TFU/P(I)
             VD = 0.D0
             VM = (V2 - MG*(VG-VU) - MD*(VD-VU))/MTOT
             UM = (ETOT - MG*(UG-UU) - MD*(UD-UU))/MTOT
             CALL BURNED(P(I),TB,VU,VM,UU,UM,VB,XMB(I),2)
C  CORRECTION OF X BECAUSE OF THE STOICHIOMETRIC BURNING.
             IF (XMB(I) .LT. 0.D0) XMB(I)=0.D0
             X(I) = XMB(I)
```

```
                    XMB(I) = XMB(I)*MTOT/(MGAS+MDSL)/(1+1/RFASTO)
                    IF (N .NE. 1) GO TO 1111
                    WRITE(10,104)CA(I),P(I),TU2,TB,TFU,XMB(I)
C                   WRITE(10,1999)V2,VM,VU,VB,UM,UU,UB
C 1999              FORMAT(1X,'V2,VM,VU,VB,UM,UU,UB=',7(1X,D9.3))
   1111             CONTINUE
                    IF(XMB(I) .LT. XMAXP) GO TO 170
                    XMAXP = XMB(I)
                    CAXMAX = CA(I)
    170             CONTINUE
                    TBRN(I) = TB
                    TU(I) = TU2
                    WRK(I) = WRK1 + DWRK
                    QWL(I) = QWL1 + DQWL

C*************prepare for next step
                    V1 = V2
                    P1 = P(I)
                    TU1 = TU2
                    QWL1 = QWL(I)
                    WRK1 = WRK(I)
                    T(I) = TB*X(I) + TU2*(1 - X(I))
                    T1 = T(I)
                    XMB1 = XMB(I)
    200             CONTINUE

C*********do statistics for each cycle
                    XMAX = 1.D0 - UFRAT
                    DO 280 I = 1,NCA
                    IF (CA(I) .LT. CAXMAX) GO TO 280
                    XMB(I) = XMAX
    280             CONTINUE
                    DO 300 I = 1,NCA
                    XAVG(I) = XAVG(I) + XMB(I)
                    WAVG(I) = WAVG(I) + WRK(I)
                    QAVG(I) = QAVG(I) + QWL(I)
                    TAVG(I) = TAVG(I) + T(I)
                    TBAVG(I) = TBAVG(I) + TBRN(I)
                    TUAVG(I) = TUAVG(I) + TU(I)
    300             PAVG(I) = PAVG(I) + P(I)
                    PBOIAV = PBOIAV + PBOI
C                   CALL CYCSTATS(CA,P,XMB,2)

C****Find the Max. burned temp. 'TBMAX' and the corresponding
C       mass-burned fraction 'XTBMAX':
                    TBMAX = 1600.D0
                    DO 301 I=1,70
                    IF (XMB(I) .LT. 0.05) GO TO 301
                    IF (TBRN(I) .LT. TBMAX) GO TO 301
                    TBMAX = TBRN(I)
                    XTBMAX = XMB(I)
                    PTBMAX = P(I)
```

```
301       CONTINUE
          PRINT*,'TBMAX =, PTBMAX =, XTBMAX =,',TBMAX,PTBMAX,XTBMAX
          STBMAX = STBMAX + TBMAX
          SPTBMAX = SPTBMAX + PTBMAX
          SXTBMAX = SXTBMAX + XTBMAX
1000      CONTINUE

C****Calaulate the conversion factor for converting equilibrium
C        NO (ppm) to tail-piper NO (ppm):
          TBMAXAVG = STBMAX/NCYC
          PTBMAXAVG = SPTBMAX/NCYC
          XTBMAXAVG = SXTBMAX/NCYC
          WRITE(10,302)TBMAXAVG,PTBMAXAVG,XTBMAXAVG
302       FORMAT(1X,'TBMAXAVG =, PTBMAXAVG =, XTBMAXAVG
     1           =,',3(E11.5,1X))
          PRINT*,'TBMAXAVG =, PTBMAXAVG =, XTBMAXAVG =,',
     1           TBMAXAVG,PTBMAXAVG,XTBMAXAVG
          CALL CONVF(CFK)
          WRITE(10,303)CFK
303       FORMAT(1X,'CFK = ',E11.5,/,
     1      '(NOTE: AVG NO (ppm) = CFK*(NO)bmax, (NO)bmax is from
     2      STANJAN)')

C****do statistical analysis for all cycles
          WRITE(10,102)
102       FORMAT(1X,'ensemble-avgd pressures and mass-burned
     1           fractions')
          WRITE(10,101)
101       FORMAT(6X,'CA',7X,'PAVG kPa',6X,'XAVG',7X,'TAVG K',
     1           6X,'TUAVG K',5X,'TBAVG K')
          PBOIAV = PBOIAV/FLOAT(NCYC)
          WRITE(10,1105)CABOI,PBOIAV
          DO 1500 I = 1,NCA
          TIME = (CA(I) - CABOI)/6.D0/RPM
          XAVG(I) = XAVG(I)/FLOAT(NCYC)
          QAVG(I) = QAVG(I)/FLOAT(NCYC)
          WAVG(I) = WAVG(I)/FLOAT(NCYC)
          TAVG(I) = TAVG(I)/FLOAT(NCYC)
          TUAVG(I) = TUAVG(I)/FLOAT(NCYC)
          TBAVG(I) = TBAVG(I)/FLOAT(NCYC)
          PAVG(I) = PAVG(I)/FLOAT(NCYC)
          WRITE(10,1105)CA(I),PAVG(I),XAVG(I),TAVG(I),TUAVG(I),
     1           TBAVG(I)
1105      FORMAT(1X,6(E11.5,1X))
C         WRITE(6,104)CA(I),PAVG(I),XAVG(I),TIME
1500      CONTINUE
          DO 1600 I=1,NCA
          IF (XAVG(I) .GT. 0.01) GO TO 1610
          PP1=CA(I)
          QQ1=XAVG(I)
1600      CONTINUE
1610      PP2=CA(I)
```

```
          QQ2=XAVG(I)
          CAIGND =(0.01-QQ1)*(PP2-PP1)/(QQ2-QQ1) + PP1 - CABOI
          TIGND=60*CAIGND/360/RPM
          PRINT*,'PP1,QQ1,PP2,QQ2,CAIGND,TIGND,',PP1,QQ1,PP2,
     1          QQ2,CAIGND,TIGND
          WRITE(10,1620)CAIGND,TIGND
 1620     FORMAT(1X,'IGNITION DELAY',F8.2,1X,'(CA)',1X,F10.6,
     1          1X,'(SEC)')
          STOP
          END
C********************************************************************
          DOUBLE PRECISION FUNCTION VCYL(CA)
          IMPLICIT REAL*8 (A-H,O-Z)
          COMMON/GEOM/BORE,STROKE,ROD,CLRH
C   CA is crank angle degrees ABDC.
          PI = 3.14159D0
          APSTON = PI/4.D0*BORE**2
          CAR = CA*PI/180.D0
          Z = (1.D0 + 2.D0*ROD/STROKE + DCOS(CAR)
     1          - DSQRT((2.D0*ROD/STROKE)**2 - (DSIN(CAR))**2))
     2          * STROKE/2.D0 + CLRH
          VCYL = Z*APSTON
          RETURN
          END


C*******************************************************************
          SUBROUTINE INTAKE(MATRAP)
C*******************************************************************
          IMPLICIT REAL*8(A-H,O-Z)
          REAL*8 NRESOUT,NO2,NN2,NH2O,NCO2,NEXH
          REAL*8 MAIR,MDSL,MGAS
          REAL*8 MTRAP,MATRAP,MTOT
          REAL*8 MWCO2,MWO2,MWH2O,MWN2,MWCH4,MWCH2
          REAL*8 D(3)
          COMMON/AMBNT/PAMB,TAMB
          COMMON/PORT/PABOX,CAIPC,PIPC,TIPC,TEXH,TABOX
          COMMON/MASS/MTOT,MAIR,MDSL,MGAS
          COMMON/PROPS/RDG,RHC,FRES,EQVR,RU
          COMMON/MW1/MWCO2,MWO2,MWH2O,MWN2,MWCH4,MWCH2
          COMMON/MOLFRAC/XO2,XN2,XCO2,XH2O,WTMOLU

C****Calculate the blower-exit air temperature, TXBLO:
C         EFFBLO = 0.47D0
C         GSTAR = 0.2857D0
C         TABOX = TAMB*(1.D0+((PABOX/PAMB)**GSTAR-1.D0)/EFFBLO)

C****Estimate the residual gas mass fraction,
C     Fres=Mres/(Mres+Matrap)
C     and the mass of air in trapped cylinder charge, MATRAP:
          RA = 0.287D0
          VTRAP = VCYL(CAIPC)
C         Start iteration to find Degree of Purity:
```

```
              MTRAP = 0.5*MAIR
              CPAIR = 1.0035
              CPEXH1 = CPAIR
              CPRES1 = CPAIR
     20       DEGP = 0.60
     30       D(1) = 0.D0
              D(2) = 0.D0
              D(3) = 0.D0
              I = 1
              M = 1
     40       DEGP = DEGP + 0.05D0
C     Correct the residual temperature TRES.
     50       TRES = (TEXH*CPEXH1*(MAIR + MGAS + MDSL) - TABOX*CPAIR*
          1       MAIR - DEGP*MTRAP))/CPRES1/(DEGP*MTRAP + MGAS + MDSL)
              TIPC = TABOX*DEGP + TRES*(1.D0-DEGP)
              MTRAP = PIPC*VTRAP/RA/TIPC
              RDELIV = MAIR/MTRAP
              DEGPUR = 0.173611D0*RDELIV**3.D0-0.95982D0*RDELIV**2.D0
          1          +1.774305*RDELIV - 0.19642D0
              Y = TIPC - (TABOX*DEGPUR+TRES*(1.D0-DEGPUR))
              IF (Y .GT. 0.D0) GO TO 52
              D(1) = DEGP
              GO TO 53
     52       D(2) = DEGP
     53       D(3) = D(1)*D(2)
              IF (D(3) .EQ. 0.D0) GO TO 40
              M=M+1
              DEGP = 0.5D0*(D(1)+D(2))
              IF (DABS(Y) .LE. 0.5D0) GO TO 55
              IF (M .LT. 50) GO TO 50
     55       CONTINUE
              FRES = 1.D0 - DEGPUR
              TIPC = (1.D0-FRES)*TABOX + FRES*TRES
              MATRAP = (1.D0-FRES) * MTRAP

C    ****Calculate CPEXH AND CPRES, (kJ/kgK):
              CALL COMPOS(MATRAP,XXO2,XXN2,XXCO2,XXH2O)
              XTOTAL=RHC/4+9.52*(1+FRES/(1-FRES))/EQVR
              XCO2 = XXCO2/XTOTAL
              XH2O = XXH2O/XTOTAL
              XO2 = XXO2/XTOTAL
              XN2 = XXN2/XTOTAL
              WTMOLU = XO2*MWO2 + XN2*MWN2 + XCO2*MWCO2 + XH2O*MWH2O
              RU = 8.3143D0/WTMOLU
              CALL UNBURNED(TIPC,UU,CVRES,VISC,2)
              CPRES = CVRES + RU
C    No. of moles of escaped air.
              NO2 = ((MAIR-MATRAP)/28.97D0)*0.21
              NN2 = 3.76*NO2
C    No. of moles of residual out.
              NRESOUT= (MTRAP+MGAS+MDSL)/WTMOLU - FRES*MTRAP/WTMOLU
C    Total moles of exhaust.
```

```
            NEXH = NO2 + NN2 + NRESOUT
C    Add escaped air and residual out together.
            NO2 = NO2 + NRESOUT*(XXO2/XTOTAL)
            NN2 = NN2 + NRESOUT*(XXN2/XTOTAL)
            NCO2 = NRESOUT*(XXCO2/XTOTAL)
            NH2O = NRESOUT*(XXH2O/XTOTAL)
            XO2 = NO2/NEXH
            XN2 = NN2/NEXH
            XCO2 = NCO2/NEXH
            XH2O = NH2O/NEXH
            WTMOLU = XO2*MWO2 + XN2*MWN2 + XCO2*MWCO2 + XH2O*MWH2O
            RU = 8.3143D0/WTMOLU
            CALL UNBURNED(TIPC,UU,CVEXH,VISC,2)
            CPEXH = CVEXH + RU
            YY = DABS(CPRES-CPRES1)
            IF (YY .LT. 0.001) GO TO 57
            CPRES1 = CPRES
            CPEXH1 = CPEXH
            I = I+1
            IF (I .LT. 50) GO TO 50
   57       CONTINUE
            CALL COMPOS(MATRAP,XXO2,XXN2,XXCO2,XXH2O)
            WRITE(10,58) XO2,XN2,XCO2,XH2O,WTMOLU,RU
   58       FORMAT(1X,'X O2, N2, CO2, H2O, WTMOLU, RU=',6(F7.4))
            WRITE(10,60)RDELIV,MTRAP,TEXH,TRES
   60       FORMAT(1X,'RDELIV,MTRAP,TEXH,TRES',4(1X,E10.4))
            RETURN
            END


C*******************************************************************
        SUBROUTINE COMPOS(MATRAP,XXO2,XXN2,XXCO2,XXH2O)
C*******************************************************************
            IMPLICIT REAL*8(A-H,O-Z)
            REAL*8 NTOTU,NRES,NO2,NN2,NH2O,NCO2
            REAL*8 MATRAP,MTOT,MAIR,MDSL,MGAS
            REAL*8 MWCO2,MWO2,MWH2O,MWN2,MWCH4,MWCH2,MWRES
            COMMON/PROPS/RDG,RHC,FRES,EQVR,RU
            COMMON/MASS/MTOT,MAIR,MDSL,MGAS
            COMMON/PREP/STORHC,STOROC,STORNC,RFASTO
            COMMON/MW1/MWCO2,MWO2,MWH2O,MWN2,MWCH4,MWCH2
            COMMON/MOLFRAC/XO2,XN2,XCO2,XH2O,WTMOLU


C    ****CALCULATE FUEL-AIR EQUIVALENT RATIO, EQVR:
C    Stoichiometric complete combustion of a combined fuel (CHn):
C        RDG is mass ratio of diesel-fuel(CH2) to gas(CH4)
C            Replace  CH4 + (16/14)*RDG CH2   by   CHn
C        where
C        RHC = n = (4+16/14*RDG*2)/(1+16/14/*RDG), which is
C            combined-fuel hydrogen (H) to carbon (C) atomic ratio.
C        CHn + (1+n/4)(O2 + 3.76 N2) ===> (n/2)H2O + CO2 +
C            (3.76)(1+n/4)N2
```

```
C          RFASTO is the stoichiometric fuel-air ratio
C          RFA is the fuel-air ratio

           J = 1
           RDG = MDSL/MGAS
           RHC = (28.D0+16.D0*RDG)/(7.D0+8.D0*RDG)
           RFASTO1 =
      1        (12.D0+RHC)/((1.D0+RHC/4.D0)*(32.D0+3.76D0*28.D0))
           RFA = (MDSL+MGAS)/MATRAP
   55      EQVR = RFA/RFASTO1
C   ****CALCULATE THE RESIDUAL COMPOSITIONS:
C    Assume:
C      1) Both residual molal fraction and equivalent fuel-air ratio
C         remain constant for each cycle in cycling iterations.
C      2) Residual molal fraction equals residual mass fraction.
C      3) Basic cycle residual is pure air (with 21% O2 and 79% N2).
C      4) The equation used is:
C    CHn + 2/EQVR*(O2+3.76N2) + 9.52*RR/EQVR*(A*CO2+B*H2O+C*O2+D*N2)
C       ----> E*CO2 + F*H2O + G*O2 + H*N2      (RR=FRES/(1-FRES))

           RR=FRES/(1-FRES)
           BATA=9.52*RR/EQVR
           AA=0
           BB=0
           CC=0.21
           DD=0.79
           EE=1+BATA*AA
           FF=RHC/2+BATA*BB
           GG=2/EQVR-1-RHC/4+BATA*CC
           HH=7.52/EQVR+BATA*DD
           XTOTAL=RHC/4+9.52*(1+RR)/EQVR
           I=1
   62      AAA=EE/XTOTAL
           BBB=FF/XTOTAL
           CCC=GG/XTOTAL
           DDD=HH/XTOTAL
           EEE=1+BATA*AAA
           FFF=RHC/2+BATA*BBB
           GGG=2/EQVR-1-RHC/4+BATA*CCC
           HHH=7.52/EQVR+BATA*DDD
           A1=DABS(AA-AAA)/AAA
           IF(A1 .LT. 0.001) GO TO 64
           AA=AAA
           BB=BBB
           CC=CCC
           DD=DDD
           EE=EEE
           FF=FFF
           GG=GGG
           HH=HHH
           I=I+1
           IF(I .LT. 100) GO TO 62
```

```
 64      CONTINUE
         XXCO2=EEE
         XXH2O=FFF
         XXO2=GGG
         XXN2=HHH
C****CALCULATE THE COMPOSITIONS OF THE CYLINDER CONTENTS BETWEEN
C      IPC AND BOI:
C      Assume:
C      1) Residual gases are completely mixed with traped air.
C      2) Residual gas fraction affect properties of unburned gas
C      RESIDUALS AT PREVIOUS COMBUSTION CYCLE:
C      H2O: XXH2O;   CO2: XXCO2;   O2: XXO2;   N2: XXN2.
C      SUM = XTOTAL=RHC/4+9.52*(1+RR)/EQVR.

C      No. of moles of intake air:
         NO2 = (MATRAP/28.97D0)*0.21D0
         NN2 = NO2*3.76D0
C      No. of moles of residuals:
         MWRES =
C         (XXCO2*MWCO2+XXH2O*MWH2O+XXO2*MWO2+XXN2*MWN2)/XTOTAL
         NRES = (FRES/(1-FRES))*(MATRAP/MWRES)
C      Total No. of moles of cylinder contents between IPC and BOI:
         NTOTU = NO2 + NN2 + NRES
C      PRINT*,'NO2=, NN2=, NRES=, ',NO2,NN2,NRES

C      ADD OXYGEN AND NITROGEN CONTENT IN RESIDUALS:
         NO2 = NO2 + NRES*XXO2/XTOTAL
         NN2 = NN2 + NRES*XXN2/XTOTAL
         NCO2 = NRES*XXCO2/XTOTAL
         NH2O = NRES*XXH2O/XTOTAL
         XO2 = NO2/NTOTU
         XN2 = NN2/NTOTU
         XCO2 = NCO2/NTOTU
         XH2O = NH2O/NTOTU
         WTMOLU = XO2*MWO2 + XN2*MWN2 + XCO2*MWCO2 + XH2O*MWH2O
         RU = 8.3143D0/WTMOLU
C      ****CALCULATE THE STORHC, STOROC AND STORNC AT STOICHIOMETRIC
C            COMPLETE COMBUSTION:
C      CHn + (1+n/4)(O2 + (XN2/XO2)N2 + (XH2O/XO2)H2O + (XCO2/XO2)CO2)
C      ---> (1+(1+n/4)*XCO2/XO2)CO2 + (n/2+(1+n/4)*XH2O/XO2)H2O
C            + ((1+n/4)*XN2/XO2)N2      (n = RHC)
C      STORHC is the hydrogen(H) to carbon (C) atomic ratio
C            at stoichiometric combustion.
C      STOROC is the oxygen (O) to carbon (C) atomic ratio
C            at stoichiometric combustion.
C      STORNC is the nitrogen (N) to carbon (C) atomic ratio
C            at stoichiometric combustion.

         BOTTOM = 1+(1+RHC/4)*XCO2/XO2
         STORHC = (RHC+2*(1+RHC/4)*XH2O/XO2)/BOTTOM
         STOROC = (1+RHC/4)*(2+XH2O/XO2+2*XCO2/XO2)/BOTTOM
         STORNC = 2*(1+RHC/4)*XN2/XO2/BOTTOM
```

```
        RFASTO =
      1    (12+RHC)/(1+RHC/4)/(MWO2+XN2*MWN2/XO2+XH2O*MWH2O/XO2
      2                +XCO2*MWCO2/XO2)
        IF (RFASTO1 .GT. RFASTO) GO TO 47
        A2 = DABS(RFASTO1-RFASTO)
        IF (A2 .LE. 0.001) GO TO 49
        RFASTO1 = RFASTO1 + A2/2
        J = J+1
        IF (J .LT. 50) GO TO 55
        GO TO 49
   47   A2 = DABS(RFASTO1-RFASTO)
        IF (A2 .LE. 0.001) GO TO 49
        RFASTO1 = RFASTO1 - A2/2
        J = J+1
        IF (J .LT. 50) GO TO 55
   49   PRINT*,'RFASTO=',RFASTO
        RETURN
        END

C*************************************************************
        SUBROUTINE UNBFUEL
C*************************************************************
        IMPLICIT REAL*8(A-H,O-Z)
        REAL*8 MWCO,MWCO2,MWNOX,MWO2,MWTHC,MWH2O,MWN2
        REAL*8 MWCH2,MWCH4,MWEXH
        REAL*8 MAIR,MDSL,MGAS,MEXH,MTOT,MUF
        COMMON/MASS/MTOT,MAIR,MDSL,MGAS
        COMMON/EMIS/YCO,YCO2,YNOX,YO2,YTHC,YH2O,UFRAT
        COMMON/PROPS/RDG,RHC,FRES,EQVR,RU
        COMMON/MW1/MWCO2,MWO2,MWH2O,MWN2,MWCH4,MWCH2
        COMMON/MW2/MWCO,MWNOX,MWTHC,MWEXH

        YCO = YCO/10000.D0
        YNOX = YNOX/10000.D0
        YTHC = YTHC/10000.D0
        YN2 = 100 - YCO - YCO2 - YNOX - YO2 - YTHC - YH2O
        FF =MWCH4*RDG/MWCH2
        FDSL = FF/(1+FF)
        MWTHC = FDSL*MWCH2 + (1-FDSL)*MWCH4
        SUMYMW = YCO*MWCO + YCO2*MWCO2 + YNOX*MWNOX + YO2*MWO2
      1          + YTHC*MWTHC + YH2O*MWH2O + YN2*MWN2
        MEXH = MAIR + MDSL + MGAS
        MUF = YTHC*MWTHC*MEXH/SUMYMW
        UFRAT = MUF/(MDSL+MGAS)
        MWEXH = SUMYMW/100
        RETURN
        END


C****************************************************************
        SUBROUTINE UNBURNED(TU,UU,CVU,VISC,L)
C****************************************************************
C  THIS SUBROUTINE IS USED TO COMPUTE THE THERMODYNAMIC PROPERTIES
```

```
C  OF UNBURNED AIR-RESIDUAL MIXTURE AT UNBURNED GAS ZONE, AND THE
C  THERMODYNAMIC PROPERTIES OF UNBRNED FUELS (CH4 AND CH2) AT
C  UNBURNED FUEL ZONE.

         IMPLICIT REAL*8(A-H,O-Z)
         REAL*8 MWO2,MWN2,MWCH4,MWCH2,MWH2O,MWCO2
         REAL*8 HFO2,HFN2,HFH2O,HFCO2
         REAL*8 DHO2,DHN2,DHH2O,DHCO2
         REAL*8 CPO2,CPN2,CPCH4,CPCH2,CPH2O,CPCO2
         COMMON/PROPS/RDG,RHC,FRES,EQVR,RU
         COMMON/MW1/MWCO2,MWO2,MWH2O,MWN2,MWCH4,MWCH2
         COMMON/MOLFRAC/XO2,XN2,XCO2,XH2O,WTMOLU

         HFO2  = 0.0D0
         HFN2  = 0.0D0
         HFH2O = -241827.D0
         HFCO2 = -393522.D0
         TDIM  = TU/100.0D0
         TDIMSQ = DSQRT(TDIM)
         TDIM2  = TDIM*TDIM
         TDIM3  = TDIM2*TDIM
         TDIM4  = TDIM3*TDIM
         TDIM14 = TDIM**0.25D0
         TDIM54 = TDIM**1.25D0
         TDIM74 = TDIM**1.75D0
         TDIM32 = TDIM**1.5D0
         TDIM52 = TDIM**2.5D0
         TDIM34 = TDIM**0.75D0

C *****Calculate molar enthalpy differences between 298K and TU,
         DHO2 = 3743.2D0*TDIM+0.80408D0*TDIM52+35714.0D0/
     1          TDIMSQ-23688.0D0/TDIM-23906.63D0
         DHN2 = 3906.0D0*TDIM+102558.0D0/TDIMSQ-107270.0D0/
     1          TDIM+41020.0D0/TDIM2-39673.0D0
         DHH2O = 14305.0D0*TDIM-14683.2D0*TDIM54+5516.73D0*
     1          TDIM32-184.95D0*TDIM2-11876.23D0
         DHCO2 = 6914.5D0*TDIM-40.265D0*TDIM74-40154.0D0*
     1          TDIMSQ+70704.0D0*TDIM14-43912.73D0

         IF(L .NE. 1) GO TO 10
C ****Calculate the internal energy of unburned air and residuals,
C       UU (kJ/kg):
         UU = (XO2*(HFO2+DHO2)+XN2*(HFN2+DHN2)+XH2O*(HFH2O+DHH2O)+
     1       XCO2*(HFCO2+DHCO2))/WTMOLU - RU*TU
         RETURN
  10     CONTINUE

         IF(L .NE. 2) GO TO 20
C ****Calculate the specific heat of unburned air and residuals,
C       CVU: CP (kJ/kmol-K) & CVU (kJ/kg-K)
         CPO2=37.432D0+0.020D0*TDIM32-178.57D0/TDIM32+236.88D0/TDIM2
         CPN2=39.060D0-512.79D0/TDIM32+1072.7D0/TDIM2-820.40D0/TDIM3
```

```
         CPH2O =
     1       143.05D0-183.54D0*TDIM14+82.751D0*TDIMSQ-3.6989D0*TDIM
         CPCO2 = 69.145D0-.70463D0*TDIM34-200.77D0/TDIMSQ+
     1           176.76D0/TDIM34
         CVU = (XO2*CPO2+XN2*CPN2+XH2O*CPH2O+XCO2*CPCO2)/WTMOLU - RU
  20     CONTINUE

         IF(L .NE. 3) GO TO 30
C  ****Calculate specific heat of CH4, CPG (kJ/kmol-K) & CVU
C     (kJ/kg-K):
         CPCH4 = -672.87D0+439.74D0*TDIM14-24.875D0*TDIM34+
     1           323.88D0/TDIMSQ
         CVU = (CPCH4 - 8.3143D0)/MWCH4
         RETURN
  30     CONTINUE

         IF(L .NE. 4) GO TO 40
C  ****Calculate specific heat of CH2, CPD (kJ/kmol-K) & CVU
C     (kJ/kg-K):
         CPCH2 = (104.18D0+46.55D0*TDIM)/12.D0
         CVU = CPCH2/MWCH2
         RETURN
  40     CONTINUE

C  ****Estimate the mean viscosity of  unburned air-residual
C     mixture:
         TM = TU**0.645D0
         VISC = (XO2*MWO2*5.09D0 + XN2*MWN2*4.57D0 +
     1       XH2O*MWH2O*3.26D0
     2       + XCO2*MWCO2*3.71D0)/WTMOLU*10.D0**(-7.D0)*TM
         RETURN
         END

C*******************************************************************
         SUBROUTINE BURNED(P,TB,VU,VM,UU,UM,VB,XMB,II)
C*******************************************************************
C     IN THIS SUBROUTINE XMB MEANS Mburned/MTOT, NOT THE FUEL
C     MASS-BURNED FRACTION. MTOT VARIES DURING THE FUEL INJECTION
C     PERIOD.

         IMPLICIT REAL*8(A-H,O-Z)
         REAL*8 D(3)
         COMMON/PROPS/RDG,RHC,FRES,EQVR,RU
         COMMON/BURN/UB
C
         IF(II .NE. 1) GO TO 10
         CALL TABLE(Q1,Q2,Q3,Q4,Q5,1)
         XMB = 0
         RETURN
  10     CONTINUE
C Find the linear relationship between UB and VB at the flame front
         IF( UM .NE. UU)GO TO 210
```

```
              A = -1.D0/P
              B = VU - A*UU
              GO TO 220
  210         A = (VM - VU )/(UM - UU )
              B = VU - A*UU
C     SOLVE FOR T,V,U JUST BEHIND FLAME AND MASS FRACTION X
  220         TB = 1000.D0
  230         D(1) = 0.D0
              D(2) = 0.D0
              D(3) = 0.D0
              M = 1
  240         TB = TB + 100.D0
  250         CALL TABLE(TB,P,SB,UB,VB,3)
              Y = VB - ( A*UB + B )
              IF( Y .GT. 0.D0) GO TO 252
              D(1) = TB
              GO TO 253
  252         D(2) = TB
  253         D(3) = D(1)*D(2)
              IF(TB .GT. 6000.D0 ) WRITE(10,261)
              IF(TB .GT. 6000.D0 ) go to 300
              IF( D(3) .EQ. 0.D0 ) GO TO 240
              M= M+1
              TB = 0.5D0*( D(1) + D(2) )
              IF(DABS(Y) .LE. 0.1D-7 ) GO TO 300
              IF( M .LT. 50) GO TO 250
              WRITE(10,260)
  260         FORMAT(1X,'NO CONVERGENCE ON FLAME TEMPERATURE IN 50
     1          TRIES')
  261         FORMAT(1X,'FLAME TEMPERATURE EXCEEDS 6000 K')
              RETURN
  300         CONTINUE
C  CALCULATE MASS FRACTION XMB CORRESPONDING TO ASSUMED PRESSURE
              XMB = (VM - VU )/(VB - VU)
  321         RETURN
              END


C**************************************************************************
                   SUBROUTINE TABLE(TBX,PBX,SBX,UBX,VBX,L)
C**************************************************************************
              IMPLICIT REAL*8(A-H,O-Z)
              REAL*8 PTAB(10),TBTAB(10)
              REAL*8 SBTAB(10,10),UBTAB(10,10),AMTAB(10,10)
              REAL*8 SBTAB1(10,10),UBTAB1(10,10),AMTAB1(10,10)
              REAL*8 SBTAB2(10,10),UBTAB2(10,10),AMTAB2(10,10)
              REAL*8 SP(10),UP(10),AMP(10),X(10),Y(10)
              REAL*8 EQREAD(6)
              COMMON/PROPS/RDG,RHC,FRES,EQVR,RU

              IF(L .NE. 1) GO TO 20
              PSTORE = -1000.D0
              DO 12 I = 1,10
```

```
            PTAB(I) = 0.D0
            SP(I) = 0.D0
            UP(I) = 0.D0
            AMP(I) = 0.D0
            TBTAB(I) = 0.D0
            DO 11 J = 1,10
            SBTAB(I,J) = 0.D0
            UBTAB(I,J) = 0.D0
            AMTAB(I,J) = 0.D0
   11       CONTINUE
   12       CONTINUE
C******************************************************************
C          READ TABLE OF BURNED GAS PROPERTIES
C  Reads files for different equivalence ratios; unit 11(0.2),
C  unit 12(0.4), unit 13(0.6), unit14(0.8), unit15(0.9),16(1)
C  THIS VERSION ASSUME THAT FOR DIESEL ENGINES THE BURNED GASES
C  ARE THE RESULT OF STOICHIOMETRIC COMBUSTION.
            DO 120 J = 1,10
            DO 110 I = 1,10
            DO 103 K = 6,6
            READ(K+10,*)TBTAB(I),PTAB(J),AMTAB1(I,J),VB,UBTAB1(I,J),
   1                    H,SBTAB1(I,J)
            READ(K+20,*)TBTAB(I),PTAB(J),AMTAB2(I,J),VB,UBTAB2(I,J),
   1                    H,SBTAB2(I,J)
  103       CONTINUE
            EQREAD(1) = 0.2D0
            EQREAD(2) = 0.4D0
            EQREAD(3) = 0.6D0
            EQREAD(4) = 0.8D0
            EQREAD(5) = 0.9D0
            EQREAD(6) = 1.0D0
C Set a burned-gas properties table for a given H to C ratio RHC
C by linearly interpolate the CH4 and CH2 tables at the same
C equivalence ratio EQVR.
            AMTAB(I,J)=AMTAB2(I,J)+(RHC-2)/2*(AMTAB1(I,J)-AMTAB2(I,J))
            UBTAB(I,J)=UBTAB2(I,J)+(RHC-2)/2*(UBTAB1(I,J)-UBTAB2(I,J))
            SBTAB(I,J)=SBTAB2(I,J)+(RHC-2)/2*(SBTAB1(I,J)-SBTAB2(I,J))
            PTAB(J) = PTAB(J)*101.325D0
            UBTAB(I,J) = UBTAB(I,J)*0.001D0
  109       FORMAT(1X,'TAB TB,P,AM,UB,SB=',5(1X,D10.4))
  110       CONTINUE
  120       CONTINUE
            PRINT*,'A table of proportional-model burned gas
   1          properties'
            PRINT*,'          for a given EQVR is formed'
            RETURN
C******************************************************************
C          GIVEN P AND SB OR TB
   20       IF(PBX .EQ. PSTORE) GO TO 160
            PSTORE = PBX
            NP = 10
            XSET = PBX
```

```
                DO 131 I = 1,10
                DO 130 J = 1,10
                X(J) = PTAB(J)
     130        Y(J) = UBTAB(I,J)
                CALL CUBICS(NP,X,Y,XSET,UP(I))
     131        CONTINUE
                DO 141 I = 1,10
                DO 140 J = 1,10
     140        Y(J) = AMTAB(I,J)
                CALL CUBICS(NP,X,Y,XSET,AMP(I))
     141        CONTINUE
                DO 151 I = 1,10
                DO 150 J = 1,10
     150        Y(J) = SBTAB(I,J)
                CALL CUBICS(NP,X,Y,XSET,SP(I))
     151        CONTINUE
     160        CONTINUE
                IF( L .NE. 2 ) GO TO 300
C*********************************
                XSET = SBX
                DO 230 I =1,10
                X(I) = SP(I)
     230        Y(I) = TBTAB(I)
                CALL CUBICS(NP,X,Y,XSET,TBX)
                DO 240 I = 1,10
     240        Y(I) = UP(I)
                CALL CUBICS(NP,X,Y,XSET,UBX)
                DO 250 I = 1,10
     250        Y(I) = AMP(I)
                CALL CUBICS(NP,X,Y,XSET,AMX)
                VBX = 8.3143D0/AMX*TBX/PBX
                RETURN
C*************************************
     300        XSET = TBX
                DO 330 I = 1,10
                X(I) = TBTAB(I)
     330        Y(I) = SP(I)
                CALL CUBICS(NP,X,Y,XSET,SBX)
                DO 340 I = 1,10
     340        Y(I) = UP(I)
                CALL CUBICS(NP,X,Y,XSET,UBX)
                DO 350 I = 1,10
     350        Y(I) = AMP(I)
                CALL CUBICS(NP,X,Y,XSET,AMX)
                VBX = 8.3143D0/AMX*TBX/PBX
                RETURN
                END


C*********************************************************
                SUBROUTINE CUBICS(NP,X,Y,XSET,YCALC)
C*********************************************************
C       NP IS NUMBER OF X,Y DATA PAIRS (I RUNS FROM 1 TO N)
```

```
          IMPLICIT REAL*8(A-H,O-Z)
          REAL*8 X(10),Y(10),D(10),E(10),F(10),G(10)
          M = NP -1
          MM = NP -2
C   CALCULATION OF SECOND DERIVATIVES G(I)
          G(1) = 0.D0
          G(NP) = 0.D0
          DO 100 I = 2,M
          D(I) = X(I) - X(I-1)
          E(I) = 2.D0*( X(I+1) - X(I-1) )
          F(I) = X(I+1) - X(I)
   100    G(I) = 6.D0/F(I)*(Y(I+1)-Y(I))+6.D0/D(I)*(Y(I-1) - Y(I))
          DO 1040 I = 2,MM
          FA = D(I+1)/E(I)
          E(I+1) = E(I+1) - FA*F(I)
          G(I+1) = G(I+1) - FA*G(I)
   1040   CONTINUE
          DO 1070 I = 2,M
          G(NP+1-I)=(G(NP+1-I)-F(NP+1-I)*G(NP+2-I))/E(NP+1-I)
   1070   CONTINUE
C   CALCULATION OF INTERPOLATED VALUE YCALC AT X=XSET
          D(NP) = X(NP) - X(NP-1)
          I = 1
   200    I = I + 1
          IF( XSET .GE. X(I) .AND. I .LT. NP) GO TO 200
          DELM = XSET - X(I-1)
          DELP = X(I) - XSET
          YCALC = G(I-1)/6.D0/D(I)*DELP**3 + G(I)/6.D0/D(I)*DELM**3
      1          +(Y(I-1)/D(I) -G(I-1)*D(I)/6.D0)*DELP
      2          +(Y(I)/D(I)   -G(I)*D(I)/6.D0  )*DELM
          RETURN
          END


C*********************************************************************
            SUBROUTINE CONVF(CFK)
C*********************************************************************
          IMPLICIT REAL*8 (A-H,O-Z)
       REAL*8 MAIR,MDSL,MGAS,MFUEL,MTOT,MEXH
       REAL*8 MFBMAX,NFBMAX,NBMAX,NEXH
       REAL*8 MWFUEL,MWTHC,MWEXH,MWCO,MWNOX
       COMMON/MASS/MTOT,MAIR,MDSL,MGAS
       COMMON/PROPS/RDG,RHC,FRES,EQVR,RU
       COMMON/MW2/MWCO,MWNOX,MWTHC,MWEXH
       COMMON/MOLFRAC/XO2,XN2,XCO2,XH2O,WTMOLU
       COMMON/AVGNO/XTBMAXAVG


C****Calculate the No. of moles of burned gas that burned at max.
C   temperature TBMAX:
C   MFBMAX is the mass of fuel (CHn) burned at max. temperature.
C   NFBMAX is No. of moles of fuel (CHn) burned at max. temperature.

       MFUEL = MDSL + MGAS
```

```
        MFBMAX = XTBMAXAVG*MFUEL
        MWFUEL = MWTHC
        NFBMAX = MFBMAX/MWFUEL
C  Combined fuel CHn complete combustion equation at max.
C  temperature is:
C        (NFBMAX)CHn + (NFBMAX)(1+n/4)[O2 + (XN2/XO2)N2
C        + (XH2O/XO2)H2O + (XCO2/XO2)CO2] ---->
C        (NFBMAX)[1+(1+n/4)(XCO2/XO2)]CO2
C        + (NFBMAX)[n/2+(1+n/4)(XH2O/XO2)]H2O +
C        (NFBMAX)(1+n/4)(XN2/XO2)N2
C  where RHC = n is the atomic ratio of hydrogen (H) to carbon (C)
C  in the fuel (CHn).
C  NBMAX is No. of moles of burned gas at max. temperature TBMAX.
        NBMAX = NFBMAX*(1 + RHC/2 + (1+RHC/4)*(XCO2+XH2O+XN2)/XO2)

C****Calculate the total No. of molea of engine exhaust and the
C     conversion factor for vonverting the equilibrium NO (ppm) to
C     tail-piper NO (ppm):
C  MEXH is the total mass of the engine exhaust per cycle.
C  NEXH is the total No. of moles of the engine exhaust per cycle.
        MEXH = MAIR + MDSL + MGAS
        NEXH = MEXH/MWEXH
        CFK = NBMAX/NEXH
        PRINT*,'CFK =',CFK
        RETURN
        END


C*****************************************************************
        SUBROUTINE PIKSR2(N,ARR,BRR)
C*****************************************************************
C  Sorts an array ARR of length N into ascending numerical order
C   by straight insertion. N is input; ARR is replaced on output
C   making the corresponding rearrangement of array BRR
C
        REAL*8 ARR(N),BRR(N)
        DO 12 J = 2,N
          A = ARR(J)
          B = BRR(J)
          DO 11 I = J-1,1,-1
            IF(ARR(I) .LE. A) GO TO 10
            ARR(I+1)=ARR(I)
            BRR(I+1)=BRR(I)
11        CONTINUE
          I = 0
10        ARR(I+1) = A
          BRR(I+1) = B
12      CONTINUE
        RETURN
        END


C*****************************************************************
        DOUBLE PRECISION FUNCTION ACYL(CA)
```

```
C*************************************************************
C Calculates the cylinder surface area for a given degree CA
        IMPLICIT REAL*8 (A-H,O-Z)
        COMMON/GEOM/BORE,STROKE,ROD,CLRH
C
        PI = 3.14159D0
        APSTON = PI/4.D0*BORE**2
        CAR = CA*PI/180.D0
        Z = ( 1.D0 + 2.D0*ROD/STROKE + DCOS(CAR)
       1    -DSQRT((2.D0*ROD/STROKE)**2+(DSIN(CAR))**2))*STROKE/2.D0
       2    + CLRH
        ACYL = Z*PI*BORE + 2.D0*APSTON
        RETURN
        END


C*************************************************************
        SUBROUTINE QWALL(TM1,V2,ASURF,AA,BB,DQWL)
C*************************************************************
C Calculates the heat transfer from the gas to the cylinder wall
C using Annand's and Woschni's correlation.
C
        IMPLICIT REAL*8 (A-H,O-Z)
        REAL*8 MTOT,MAIR,MDSL,MGAS,NU
        COMMON/GEOM/BORE,STROKE,ROD,CLRH
        COMMON/MASS/MTOT,MAIR,MDSL,MGAS
        COMMON/STATS/CABOI,RPM,N,NCYC,NCA
        COMMON/PROPS/RDG,RHC,FRES,EQVR,RU

        PISVEL = RPM * STROKE / 30.0
        DENS = MTOT / V2
        CALL UNBURNED(TM1,UU,CVU,VISC,2)
        RENUM = DENS * PISVEL * BORE / VISC
        NU = AA*RENUM**(BB)
        CPG = RU + CVU
        TRMLCO = CPG * VISC / 0.7D0
        H = AA * TRMLCO / BORE * RENUM**(BB)
C   The wall temperature is assumed to be constant
        TW = 450.0D0
        QCONV = -ASURF * H * (TM1-TW)
        QRAD = -(1.6E-12)*ASURF* ( TM1**4 - TW**4 )
        WRITE(9,26)RENUM,TRMLCO,H,NU
 26     FORMAT(1X,'RENUM=,TRMLCO=,H=,NU=,',4(E11.4,1X))
C       PRINT*,'RENUM=, TRMLCO=, ',RENUM,TRMLCO
        DQWL = (QCONV+QRAD)
        DQWL = DQWL * (60./RPM/360.)
        RETURN
        END
C*******************************************************
```